Characterization of Cyclic Adenosine Monophosphate/Protein Kinase A Signalling Networks in Blood Platelets.

Zaher Raslan

A thesis submitted for the degree of Doctor of Philosophy in Medical Sciences

The University of Hull and the University of York

Hull York Medical School (HYMS)

September 2012

Abstract

Platelet activation is a critical physiological event, whose main role is to prevent excessive blood loss and repair vessel wall injuries. However, platelet activation must be controlled to prevent unwanted and exaggerated responses leading to the occlusion of the blood vessel. The endothelial-derived inhibitors prostacyclin (PGI_2) and nitric oxide (NO) are known to play a critical role in the control of platelet activity, although the mechanism underlying their actions remains unclear beyond the triggering of cyclic nucleotides signaling pathways. The aim of this study was to improve our understanding of platelet regulation by cAMP signaling networks.

We observed differences in cAMP signaling depending on the agonists used. Using phosphorylation of PKA substrates as a marker of PKA activity, it was observed that PKA substrates were phosphorylated and dephosphorylated at different time points in a unique temporal pattern. Consistent with this observation we found that individual PKA isoforms, PKA I and II, were localized in distinct subcellular compartments, with PKA I being identified as a lipid raft protein. Our experimental data suggest that the localization of PKA I to lipid rafts is mediated by interaction with A-kinase anchoring proteins (AKAPs). Additionally, PKA signaling events were reversed when potential PKA type I interactions with AKAPs were disrupted with competitive peptides. Using this approach we found that the redistribution of PKA I to lipid rafts facilitated the phosphorylation of GPIbβ and the inhibition of von-Willebrand factor-mediated aggregation.

Our data also demonstrated for the first time that the chemical disruption of lipid rafts increased platelet sensitivity to PGI_2, through increased cAMP production and

PKA activity. The mechanism by which this occurs may involve sequestering a population of adenylyl cyclase 5/6 to a location remote from $G\alpha_s$.

In conclusion, data presented in this thesis suggest differential roles of PKA subtypes in the regulation of platelet activity. This involves, at least in part, the localisation of PKA I into specific subcellular compartments through an interaction with AKAPs. The potential presence of PKAII-AKAP interactions and the identification of specific AKAPs will be the main aim of future work.

Publications

Oral Presentation

The role of A-Kinase Anchoring Proteins in mediating the inhibitory effect of Protein Kinase A in blood platelets. 12th UK Platelet Meeting, Nottingham, UK (2010). (Winner of best oral presentation award).

Poster presentations

Raslan, Z., Aburima, A.A., Magwenzi, S.G., Tasken, K. & Naseem, K.M. Targeting of Type I Protein Kinase A to lipid rafts is required for platelet inhibition by the cAMP-signaling pathway. *4th British Pharmacological Society (BPS) Focussed Meeting on Cell Signalling. Leicester, UK (2012).*

Raslan, Z. & Naseem, K.M. The role of lipid rafts in the compartmentalisation of cAMP/PKA signalling in blood platelets. *13th UK Platelet Meeting. Cardiff, UK (2011).*

Raslan, Z. & Naseem, K.M. The role of lipid rafts in the compartmentalisation of cAMP/PKA signalling in blood platelets. *Northern Cardiovascular Research Group (NCRG) meeting, Hull, UK (2011).*

Table of Contents

Abbreviations

$\alpha_2\beta_1$	Integrin alpha 1 beta 2
$\alpha_{IIb}\beta_3$	Integrin alpha 2b beta 3
α-CD	Alpha-cyclodextrin
A_{2A}	Adenosin 2 A receptor
A_{2B}	Adenosin 2 B receptor
AA	Arachidonic acid
Ab	Antibody
ABP	Actin-binding protein
AC	Adenylyl cyclase
ACD	Acid-citrate dextrose
ADH	10-acetyl-3-7-dihydroxyphenoxazine
ADP	Adenosine diphosphate
AKAP	A-kinase anchoring proteins
AMP	Adenosine 5'-monophosphate
APS	Ammonium persulphate
Arg	Argenine
ATP	Adenosine triphosphate
BSA	Bovine serum albumin
Ca^{+2}	Calcium ion
cAMP	cyclic adenosine monophosphate
CBD	cAMP binding domain
cGMP	cyclic guanosine monophosphate
COX	cyclooxygenase
CRD	Cysteine-rich domain
DAG	Diacylglycerol
DIPEA	N,N-diisopropylethylamine
DMF	Dimethyl formamide
ECL	Enzyme chemiluminacense
ECM	Extra cellular matrix

EDRF	Endothelial-derived relaxing factor
EDTA	Ethylenediaminetetraacetic acid
EGTA	Ethylene glycol tetraacetic acid
EIA	Enzyme immunoassay
EPR	Prostaglandin E_1 receptor
ER	Endoplasmic reticulum
EXP	Exposure time
FRET	Fluorescence resonance energy transfer
Fsk	Forskolin
GDP	Guanosine diphosphate
GPCR	G-protein coupled receptors
GPIb-IX-V	Glycoprotein Ib-IX-V
GPVI	Glycoprotein VI
GSK3α	Glycogen synthase kinase 3 alpha
HBTU	2-(1H-Benzotriazole-1-yl)-1,1,3,3-tetramethyluronium hexafluorophosphate
HEK-293	Human embryonic kidney 293 cells
HEPES	N-(2-Hydroxyethyl)piperayine-N'-(2-ethanesulfonic acid)
HRP	Horseradish peroxidase
IB	Immunoblotting
IGF-1	Insulin-like growth factor 1
ILK	Integrin-linked kinase
IP	immunoprecipitation
IP_3R	Inositol 1, 4, 5-triphosphate receptor
IPR	Prostacyclin receptor
ITAM	immunoreceptor tyrosin-based activation motif
LASP	LIM and SH3 domain protein
LAT	Linker of Activated T cells
MAPK	mitogen-activated protein kinase
MAPKAPK	p38-activated MAP kinase
MβCD	Methyle-beta cyclodextrin

Mg^{+2}	Magnesium ion
MLC	Myosin light chain
MLCK	Myosin light chain kinase
NMR	Nuclear magnetic resonance
NO	Nitric oxide
NOS	Nitric oxide synthase
OCS	Open canalicular system
PAGE	Polyacrylamide gel electrophoresis
PAR	Protease-activated receptor
PBC	Phosphate-binding cassette
PBS	Phosphate-buffered saline
PDE	Phosphodiesterase
PGE_1	Prostaglandin E_1
PGG_2	Prostaglandin G_2
PGH	prostaglandin endoperoxide H
PGI_2	Prostaglandin I_2 (prostacyclin)
PGIS	Prostacyclin synthase
PIP_2	Phosphatidylinositol 4, 5-bisphosphate
PKA	Protein kinase A
PKA I	Protein kinase A type I
PKA II	Protein kinase A type II
PKB	Protein kinase B
PKC	Protein kinase C
PKG	Protein kinase G
PLB	Phospholamban
PLC	Phospholipase C
PLA	Phospholipase A
PMSF	Phenyl methyl solphonyl fluoride
PPP	Platelet poor plasma
PRP	Platelet rich plasma
PVD	Peripheral vascular disease

PVDF	Polyvinylidene fluoride
RI	PKA regulatory subunit type I
RIAD	RI-anchoring disruptor
RIAM	Rap1b interacting adaptor molecule
RII	PKA regulatory subunit type II
RNA	Ribonucleic acid
RP	RP-cAMPS
SD	Standard deviation
SDS	Sodium dodecyl sulphate
SEM	Standard error of the mean
Ser	Serine
sGC	Soluble guanylyl cyclase
SNARE	Soluble NSF Attachment Protein Receptors
SOCE	Store-operated extracellular calcium entry
St-Ht31	Stearic-Ht31
TAFI	Thrombin-activatable fibrinolysis inhibitor
TBS-T	Tris-buffered saline-tween20
TEMED	Tetramethylethylenediamine
TF	Tissue factor
Thr	Threonine
TPR	TxA_2 receptor
TPO	Thrombopoietin
TRPC	Transient receptor potential channel
TxA_2	Tromboxane
VASP	Vasodilator-stimulated phosphoprotein
VEGF	Vascular endothelial growth factor
VSMC	Vascular smooth muscle cells
vWF	von Willebrand factor
WCL	Whole cell lysate
WP	Washed platelets

List of tables

Chapter 1 – General Introduction

List of Figures

Chapter 1: General Introduction

Chapter 2: Materials and Methods

Acknowledgment

First and foremost, I would like to start by thanking God Almighty who, with his blessing, has given me the stamina to embark on this draining yet beautiful journey. It was only with his help that I was able to bounce back so many times especially every time I got knocked out by an unsuccessful lipid raft experiment.

This PhD would not have been possible without two people to whom I am grateful the most. Firstly, my dad (Abu Zaher), whose pockets I have absolutely drained and never once has he complained about it because, although he does not show it, I know he has always believed in me. I can never thank you enough Baba.

Secondly, my utmost gratitude goes to Prof. Khalid Naseem from whom I learned a great deal and who not only has been a great mentor but also a father and a friend to me. With his help and guidance I was able to hurdle all the obstacles, and God there were too many, to complete this journey.

A very big thank you to the two people I love the most in this world my Mum Hala for her constant prayers and my beautiful wife Almar, who stood by me and endured a great deal of winging and inexplicable grumpiness over the past three years.

Several heated scientific discussions as well as extensive 'shisha' sessions have culminated in gaining a new brother Dr. Ahmed Aburima to whom I look up and owe a great deal of gratitude.

Last but not the least, I would like to thank the rest of my colleagues Dr. Simbarashe Magwenzi for his help with the microscopy and flow experiments, Dr. Tanzeel Yousaf who adopted me when I first started my PhD (he always said "just stick with

me man"), Katie Wraith with whom I enjoyed sharing most of my ups and downs during this journey, Sreemoti Banerjee, Benjamin Spurgeon, Dr.Hassan Kahal, Dr. Myint Aye, Jonathan Wake and Dr. Wayne Roberts.

They say the best thing about a PhD is that "you only do it once in a lifetime"; I guess that's what makes it so special.

God bless Syria.

In deep gratitude

Zaher Raslan

Author's declaration

I confirm that this work is original and that if any passage(s) or diagram(s) have been copied from academic papers, books, the internet or any other sources these are clearly identified by the use of quotation marks and the reference(s) is fully cited. I certify that, other than where indicated, this is my own work and does not breach the regulations of HYMS, the University of Hull or the University of York regarding plagiarism or academic conduct in examinations. I have read the HYMS Code of Practice on Academic Misconduct, and state that this piece of work is my own and does not contain any unacknowledged work from any other sources.

Chapter 1: General Introduction

1.1 Introduction

Injury to the blood vessel wall initiates a complex physiological response to rapidly repair the damage and prevent blood loss. This highly complex system, termed haemostasis, involves proteins and cells of the blood vessel wall, a group of cryptic plasma enzymes and circulating platelets. Platelets are small anucleate cells (0.2 to 5µM in diameter) derived from bone marrow-residing megakaryocytes, whose only known role is to produce platelets and release them to the circulation (Deutsch and Tomer, 2006). The major biological role of blood platelets is the initial arrest of bleeding at sites of vascular damage thus playing a critical role in haemostasis. The dynamics of flowing blood push platelets to the edges of the blood stream, placing them in an ideal position to react rapidly and repair any injury in the vessel wall. Platelets circulate in a quiescent state maintained by a dynamic equilibrium that is imposed by the release of endothelium-derived antithrombogenic substances such as nitric oxide (NO) (Furchgott *et al*., 1984) and prostacyclin (PGI_2) (Moncada *et al*., 1976). These two inhibitors activate soluble guanylyl cyclase (sGC) and adenylyl cyclase (AC) respectively raising cyclic nucleotide levels (Schwarz *et al*., 2001). However, in the case of vascular injury, the equilibrium shifts towards platelet activation, but under a controlled manner to prevent occlusion of the blood vessel lumen.

Pathological conditions of the vasculature such as atherosclerosis are thought to result in a decrease in the antithrombotic properties of the endothelium (Ruggeri,

2002). Moreover, defects in cyclic nucleotide signalling in platelets, either arising from a pathological condition or an inherited mutation, have been linked with heart diseases (Chirkov and Horowitz, 2007, Van Geet *et al*., 2009). All these factors result in a disruption in the dynamic equilibrium controlling the growth of a platelet plug. Consequently, the chances of complete occlusion of the blood vessel increases and, depending on the organ affected, results in a stroke or a myocardial infarction. This chapter will review current understanding of blood platelets, in particular the mechanism of activation and how this is controlled by the cAMP/PKA signalling system.

1.2 Platelet formation

Platelets are generated from the cytoplasmic shedding of megakaryocytes in a process called thrombopoiesis. Megakaryocytes are large (50-100µM diameter) but rare (0.4% of bone marrow cells) cells that reside in the bone marrow. They evolve from heamatopoietic stem cells (HSCs) through a process called megakaryopoiesis, which involves a series of proliferation, differentiation and maturation stages (Patel *et al*., 2005). Mature megakaryocytes undergo nuclear and cytoplasmic maturation followed by formation of membrane extensions called proplatelets. Megakaryocyte organelles then travel from the cytoplasm into the peripheral proplatelet extensions. At this stage of thrombopoiesis, matured megakaryocytes start expressing platelet surface markers such CD42 and GPVI. They then migrate into the bone marrow sinusoids where they get released and enter the blood stream (Patel *et al*., 2005). Each megakaryocyte produces approximately 200-5000 platelets (Italiano *et al*., 1999, Long, 1998). The average adult produces 1 x 10^{11}

platelets per day, which circulate in the blood for approximately 7 to 10 days, to maintain a normal platelet count of 150 x 10^9 to 400 x 10^9 per litre (Kaushansky, 2005). Platelet production rate is mainly regulated by thrombopoietin (TPO), a glycoprotein produced in the liver, kidneys and the bone marrow. When circulating unbound to its *c-Mpl* receptor on platelets, TPO triggers thrombopoiesis (Kaushansky, 2005).

1.3 Platelet structure

Platelets circulate in the blood stream in an inactive discoid shape. Upon activation, through interaction with the blood vessel wall, the inactive shape of platelets undergo fundamental morphological changes featured by transforming into a flat spread shape to cover the largest possible part of the injury. In addition, membrane protrusions, known as lamellipodia and filopodia, emerge and serve to bind and recruit more platelets to the site of the injury (Figure 1.1). The structure of each discoid platelet can be divided into a membrane and submembrane area, a sol-gel zone, which contains a meshwork of microtubules and actin filaments, and an organelle system (Hartwig, 2006).

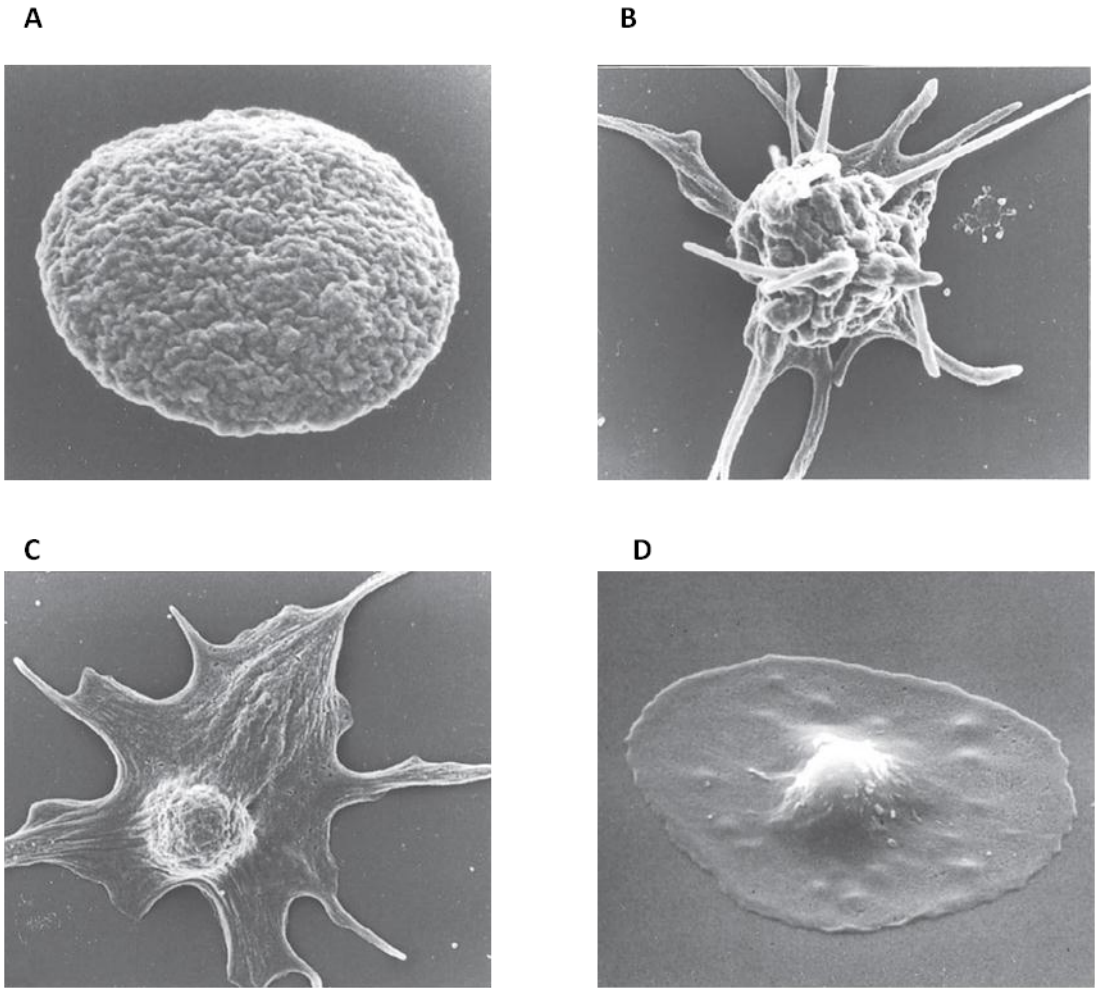

Figure 1. 1: Electron microscopic images of platelet shape change

(A) Discoid platelets imaged in the low-voltage high-resolution electron scanning microscope (LVHR-SEM). The wrinkled appearance of the outside of the cell resembles the surface of the brain. **(B)** A platelet at the early stage of activation (early dendritic platelet) imaged by LVHR-SEM. Surface of pseudopods is smooth compared with the wrinkled surface of the central body. **(C)** Early spread platelet. The wrinkles of the central body have started to disappear as the cytoplasm is spreading to fill the gaps between the pseudopods. **(D)** A fully spread platelet. Images and legend are adapted from figures in reference (White, 2007).

1.3.1 Platelet membrane

The first contact point on platelet surface with the vascular wall is a very dynamic structure termed the glycocalyx. It is covered with various adhesive receptors and glycoproteins such as GPIb-IX-V and $\alpha_{IIb}\beta_3$, which enables platelets to react quickly once an injury has been detected. The glycocalyx sits on a lipid bilayer which has tiny folds known as the open canalicular system (OCS). This lipid bilayer is incompressible and unable to stretch. Therefore, the OCS plays an important role by contributing to the extra membrane surface needed for platelet shape change and spreading. The OCS also facilitates the entrance of small molecules to platelet cytoplasm (White, 1988). Underneath the membrane is a very important submembrane area that contains a thin filament system composed of proteins such as filamin and cytoplasmic tails of different receptors. This filament system facilitates signal transduction downstream platelet receptors by linking them with their cytoplasmic substrates and effectors. It also ensures the translocation of receptor complexes to the exterior surface of platelets (White, 1987).

1.3.2 Platelet cytoskeleton

Platelet cytoskeleton is a network of “rods and girders” that define and maintain the discoid shape in resting platelets and facilitates shape change and spreading when they are activated (Hartwig and DeSisto, 1991). From the membrane inwards the platelet cytoskeleton is composed of a spectrin-based membrane skeleton, which directly supports the cytoplasmic side of the membrane, then a microtubule coil that lines the perimeter of the platelet disc, and then finally, a firm network of crosslinked actin filaments that fills the cytoplasm. Myosin heads lean on actin

filaments and render them barbed leaving the other ends, with no myosin on them, pointed. The barbed ends are the only place in the cell where actin monomers can assemble. The pointed ends, however, has a low affinity towards actin monomers and therefore are the actin filament disassembly points (Carlier, 1993). These barbed ends are where the cytochalasin compounds bind and inhibit actin filament elongation (Hartwig and Stossel, 1979). When platelets encounter a vascular injury, they respond rapidly by disassembling the cytoskeleton structure that supports the inactive discoid shape and replacing it with a new structure that supports the spread active shape to seal off the damage (Hartwig, 2006).

1.3.3 Platelet organelles.

Platelets possess several secretory granules that have a very important role in establishing a repairing microenvironment at the site of the vascular injury. Examples of these granules are the α-granules and the dense granules, which can be distinguished according to their contents and their appearance under an electronic microscope. α-granules originate from megakaryocytes by homotypic fusion of trans-Golgi vesicles as well as heterotypic fusion of these vesicles with others obtained through endocytosis (Harrison *et al*., 1989, Harrison and Cramer, 1993). Therefore, α-granules contain molecules that have a very wide array of functions. An elegant mass spectrometry study identified more than 280 molecules in these granules. Most importantly, they have adhesive molecules such as von Willebrand factor, P-selectin and thrombospondin, plasma-derived proteins such as fibrinogen, fibrinolytic molecules that are important for clot remodelling such as PAI-1 and TAFI in addition to mitogens and growth factors such as IGF-1 and VEGF,

which play an important role in wound healing and angiogenesis (Reed, 2004). Recently, α-granules have been reported to participate in platelet non-heamostatic functions by releasing chemokines and some cytokines, which recruit an immune response into the site of the injury (Ren *et al*., 2008).

Whereas α-granules contain a very versatile cargo, the contents of the dense granules support recruitment of remote platelets and the amplification of platelet activatory signal (See 1.4.3). They mainly release small molecules such as serotonin, ATP, ADP and Ca^{++} (Ren *et al*., 2008) (McNicol and Israels, 1999). In addition platelets also contain a number of more generic granules that are required for cellular homeostasis and energy production.

1.4 Platelet activation

When patrolling platelets in the blood lumen encounter a vascular injury, they become exposed to pro-thrombogenic extracellular matrix proteins such as collagen, von Willebrand factor (vWF) and laminin. These proteins act to arrest platelets through the binding of the proteins to various platelet surface receptors.

Collagen and vWF have the capacity to activate platelets leading the synthesis or release of soluble platelet agonists, which act to propagate this activation response. These pathways converge on the activation of the key platelet receptor integrin $\alpha_{IIb}\beta_3$ leading to platelet aggregation, which in turn facilitates the formation of a haemostatic plug at the site of the injury (Figure 1.2) (Broos *et al*., 2011).

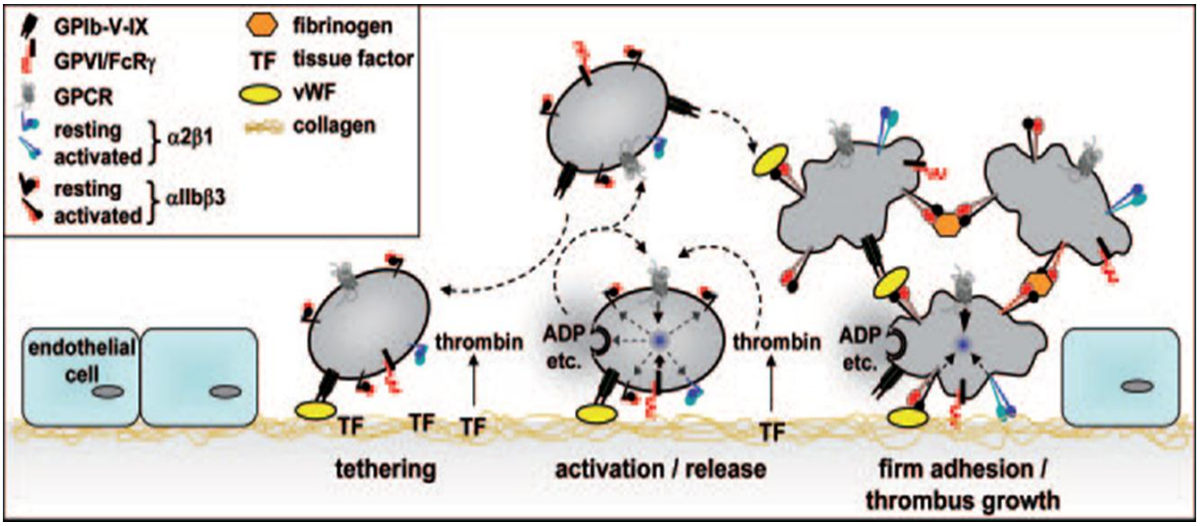

Figure 1. 2: Platelet adhesion and aggregation on the extracellular matrix (ECM).

GPIbα-vWF interactions allow GPVI to interact with collagen, which triggers inside-out signalling leading to the release of soluble agonists such ADP and TxA_2 and the deployment of remote platelets to the site of the injury. Concomitantly, tissue factor (TF) triggers thrombin formation, which also activates platelets. Figure and legend are adapted from (Varga-Szabo *et al*., 2008).

1.4.1 Platelet adhesion to the vessel wall

Under normal conditions and when the vasculature is intact, platelets almost never interact with the endothelium. However, at sites of vascular damage, platelets come into contact with a wide array of thrombotic components of the extracellular matrix (ECM) such as collagen, von Willebrand Factor (vWF), fibronectin and laminin to which they adhere. Platelet adhesion is the first step in platelet activation and is a coordinated process that involves tethering, rolling, activation and then stable adhesion. The outcome of platelet adhesion is the formation of a single layer of spread and activated platelets on the site of the injury, which in turn start releasing their granules to recruit remote inactive platelets and enlarge the growing thrombus (Varga-Szabo *et al*., 2008, Ruggeri and Mendolicchio, 2007). Numerous mechanisms are involved in platelet adhesion depending on the shear rate and the adhesive substrate that platelets come into contact with.

At high shear rate (>1000 s^{-1}) found in small arteries and stenotic vessels, platelet adhesion relies largely on the interaction of the A1-domain of vWF (exposed on collagen or in ECM) with its receptor GPIb-IX-V (GPIbα), which plays a key role in slowing down the fast flowing platelets, which facilitates collagen receptor binding (Huizinga *et al*., 2002). The absence of vWF and GPIbα are associated with von Willebrand disease and Bernard-Soulier syndrome, respectively, which confirm their importance in haemostasis (Salles *et al*., 2008, De Meyer *et al*., 2009).

At lower shear rate (<1000 s^{-1}) found in veins and larger arteries, interaction of platelets with collagen is more favoured. Platelets express several collagen

receptors on the surface, with the two best characterised of these are GPVI (Moroi *et al*., 1989) and the integrin $\alpha_2\beta_1$ (Santoro, 1986). The differential role in platelet adhesion of these two receptors is a subject of intense debate (Nieswandt and Watson, 2003). The structure of GPVI is shown in figure 1.3. Through its transmembrane domain, GPVI is physically associated with the FcRγ chain that has an immunoreceptor tyrosin-based activation motif (ITAM) for signal transduction (Gibbins *et al*., 1996). Despite its critical role in platelet activation, this receptor has a low affinity to collagen and hence cannot, by itself, mediate stable adhesion (Verkleij *et al*., 1998). The reversible interaction between GPVI and collagen is still sufficient to induce signalling events activating integrin $\alpha_2\beta_1$, which then through its high affinity to collagen stabilises platelet adhesion and allows GPVI to trigger signal transduction (Moroi *et al*., 2000, Watson *et al*., 2000).

Recent elegant studies showed the existence of a synergistic cooperation not only between $\alpha_2\beta_1$ and GPVI but also between $\alpha_2\beta_1$ and GPIbα (Pugh *et al*., 2010). Despite its proposed inability to mediate stable adhesion on its own, the importance of GPVI in platelet activation is evident from experiments performed with GPVI-knockout mice whose platelets are unable to mediate stable adhesion (Nieswandt *et al*., 2001).

The final step in platelet adhesion is the activation of $\alpha_{IIb}\beta_3$, through GPVI inside-out signalling (See 1.4.2). The activated form of $\alpha_{IIb}\beta_3$ mediates platelet firm adhesion to the ECM through its interaction with vWF. Furthermore, platelets can adhere to

immobilized fibrinogen, thrombospondin, laminin and other adhesive molecules (Hindriks *et al*., 1992, Savage *et al*., 1996, Jurk *et al*., 2003).

Regardless of the agonist, platelet activation proceeds through the interaction of the ECM proteins with constitutively expressed receptors. These receptors, once ligated, activate signalling cascades that cause several key events to be initiated including (a) activation of integrin receptors, (b) shape change, and (c) secretion of granules, all of which are required for stable platelet adhesion and aggregation.

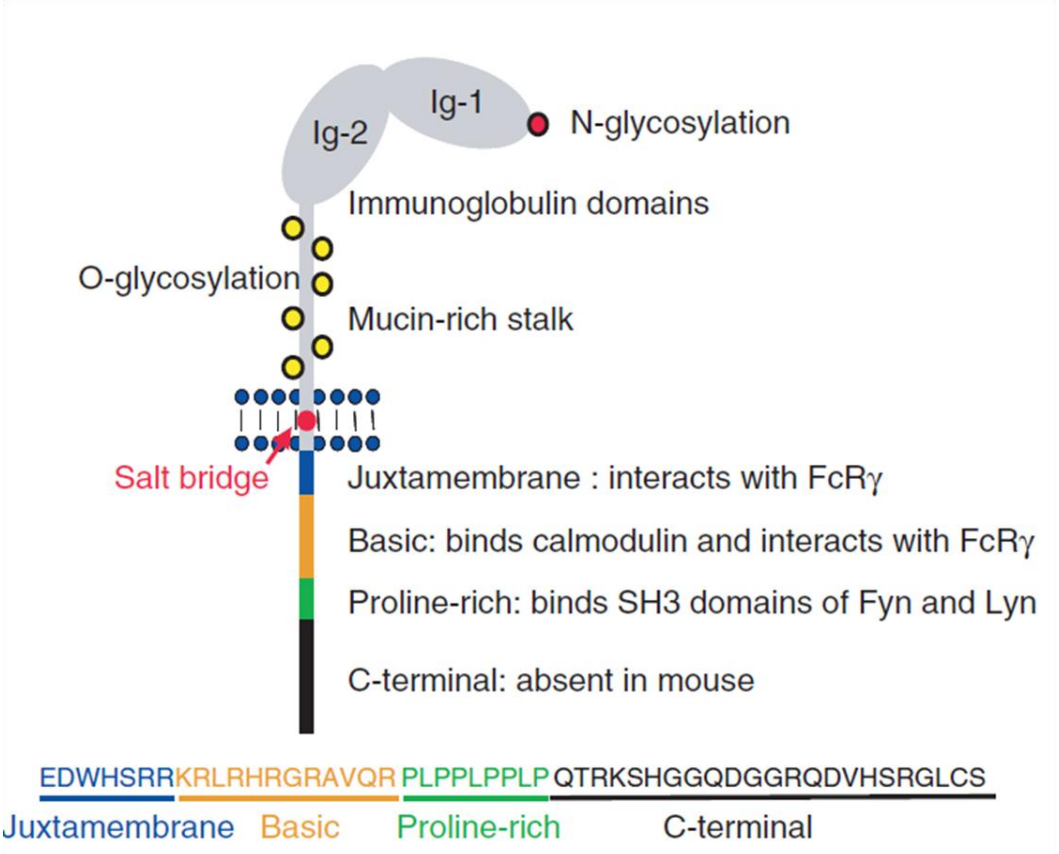

Figure 1. 3: The structure of GPVI.

The extracellular part of GPVI is comprised of two immunoglobulin domains which are carried by a mucine-like stalk which is rich in α-glycosylation sites. The GPVI cytoplasmic tail has a juxtamembrane region that interacts with FcRγ through its salt bridge, a basic region, a proline-rich region that attracts Src kinases and a C-terminal. Figure and legend are modified from (Watson *et al*., 2005).

1.4.2 Platelet signal transduction

1.4.2.1 Tyrosine kinase-mediated signalling

This signalling pathway is triggered downstream several platelet receptors such as GPVI in response to collagen (Gibbins, 2004a), GPIb in response to vWF (Du, 2007) and CLEC2 by podoplanin (Watson *et al*., 2010). Tyrosine kinase signal transduction after activation of blood platelets involves a series of phosphorylation events that are spatially and temporally regulated and mediated by a plethora of kinases and scaffolding proteins (Figure 1.4).

Glycoprotein VI exists in platelets as a multi-protein complex in which it is non-covalently associated with Fc Receptor–γchain (FcRγ) (Gibbins *et al*., 1997). The significance of this receptor in platelet function is well established in the literature with some *in vivo* and *ex vivo* studies (Kato *et al*., 2003, Massberg *et al*., 2003). The binding of GPVI to collagen leads to GPVI clustering followed by the phosphorylation of the FcRγ at the ITAM by Src-family kinases Lyn and Fyn, which are physically associated with the cytoplasmic tail of GPVI by their Src homology 3 domain (SH3) (Gibbins *et al*., 1996, Briddon and Watson, 1999). The phosphorylation of FcRγ provides a docking site for the Src-homology 2 (SH2) domains of Syk, which is phosphorylated and consequently activated (Shiue *et al*., 1995). Activated Syk will phosphorylate its adaptor protein LAT (Zhang *et al*., 1998a). LAT is the second docking site in this signalling cascade. This docking site attracts and activates several kinases such as phospho inositide 3-kinase (PI3K) and phospholipase C-γ2 (PLCγ2) (Gibbins *et al*., 1998, Gross *et al*., 1999) and as a result

places them in a close proximity with their substrates. PI3K generates phosphatidylinositol (3,4)-bisphosphate (PIP_2) and phosphatidylinositol (3,4,5) tris-phosphate (PIP_3). PI3K activates other downstream enzymes including Akt (PKB), integrin-linked kinase (ILK) and PDK1 (Barry and Gibbins, 2002), although their roles in platelet activation are still unresolved. Critically the activated PLCγ2 generates two important messengers in platelet activation (Quek *et al*., 1998, Oda *et al*., 2000). The first is inositol (1,4,5)-trisphosphate (IP3), which will mediate calcium release from intracellular stores, a process that is followed by the opening of storage-operated calcium channels allowing the influx of extracellular calcium (Varga-Szabo *et al*., 2009). The second is diacylglycerol (DAG), which activates the protein kinase C (PKC). PKC isoforms mediates platelet secretion and integrin activation, although the precise roles of individual isoforms remain unclear. In summary, tyrosine phosphorylation signal transduction in response to platelet activation results in elevation of intracellular calcium and activation of PKC. Both outcomes are important for platelet shape change, integrin activation and the release of various granule contents to the blood stream (Figure 1.4) (Hathaway and Adelstein, 1979, Shattil and Brass, 1987).

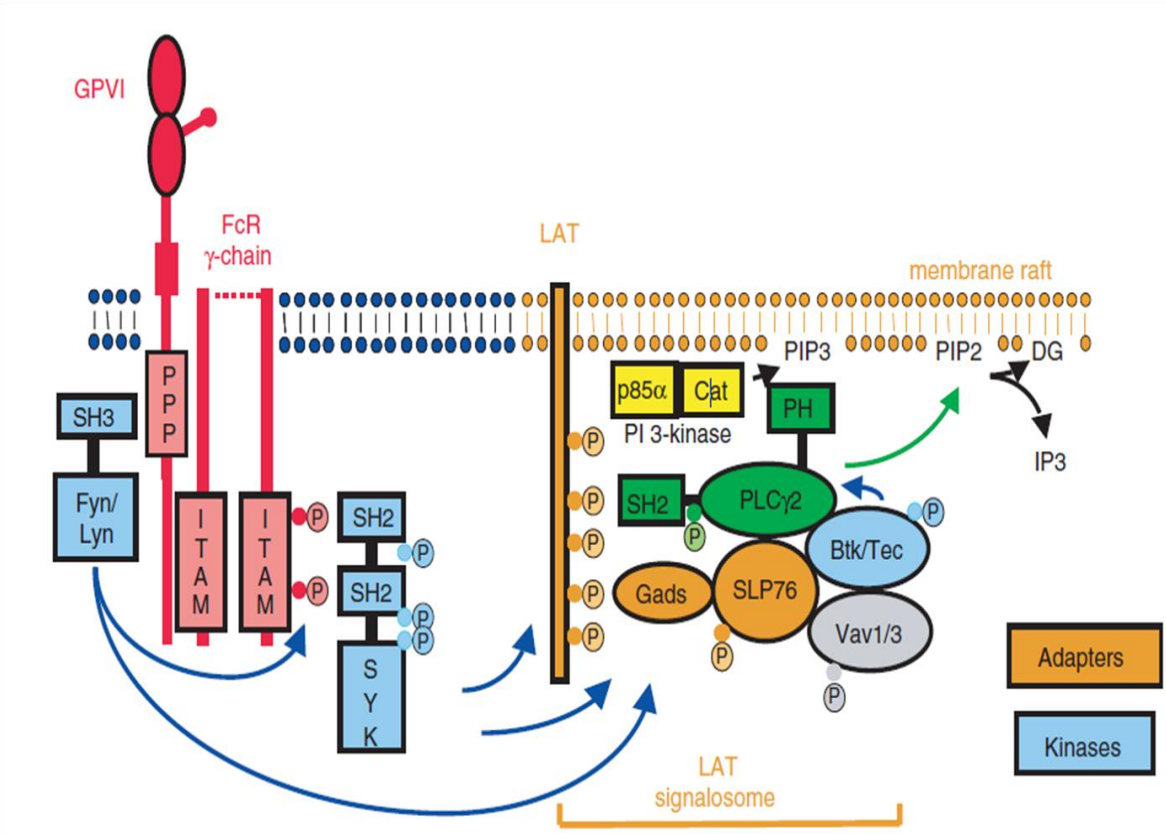

Figure 1. 4: Signalling cascade downstream GPVI.

Upon the cross-linking of GPVI by collagen, the ITAMs of the FcRγ chain are tyrosine-phosphorylated by the Src kinases Fyn and Lyn, which are constitutively bound to the proline-rich domain of GPVI. Consequently, a Syk-dependent signal is triggered, which results in the formation of a LAT signalosome and the activation of PLCγ2 with the latter event being supported by Vav and Tec families. PLCγ2 is associated with Gads, SLP76 and PIP3. The outcome of PLCγ2 activation is the production of DAG and IP_3. Figure and legend are modified from (Watson *et al*., 2005).

1.4.2.2 Platelet activation through the activation of G-protein coupled receptors

Platelets express multiple G-protein coupled receptors, which trigger both activatory as well as inhibitory signalling pathways (Offermanns, 2006). Heterotrimeric G-proteins are composed of an α subunit that in the resting state is bound to GDP and associated with a β and a γ subunit. Upon activation, the α subunit-associated GDP is substituted with GTP and concomitantly with the dissociation of β and γ subunits. The activation of G-proteins is terminated by intrinsic GTPase activity of the α subunit.

Thromboxane receptors TP, the ADP receptor $P2Y_1$ (Murugappan *et al*., 2004) and thrombin receptors PAR-1 and PAR-4 (Brass, 2003) are all linked to Gq proteins, whose main effector is PLCβ2 (Figure 1.5). Similar to PLCγ2, the activation of PLCβ2 results in the production of IP_3 and DAG, which increase intracellular calcium levels (Offermanns, 2006). In addition to Gq, TP and PAR receptors are bound to $G_{12/13}$ proteins, whose activation result in triggering the calcium-independent Rho/Rho-kinase pathway, which regulates myosin phosphatase and results in the phosphorylation of myosin light chain (MLC) (Brass, 2003, Murugappan *et al*., 2004). The phosphorylation of MLC is thought to be critical to driving platelet shape change (Daniel *et al*., 1984). Moreover, other GPCRs such as $P2Y_{12}$ are coupled to the inhibitory G protein Gi, which inhibits adenylyl cyclase (AC) and as a result blocks cAMP production (Dorsam and Kunapuli, 2004). The βγ complex of Gi has been reported to activate PI3Kβ, which activates a variety of downstream effectors such as Akt (PKB) and Rap1b (Garcia *et al*., 2010).

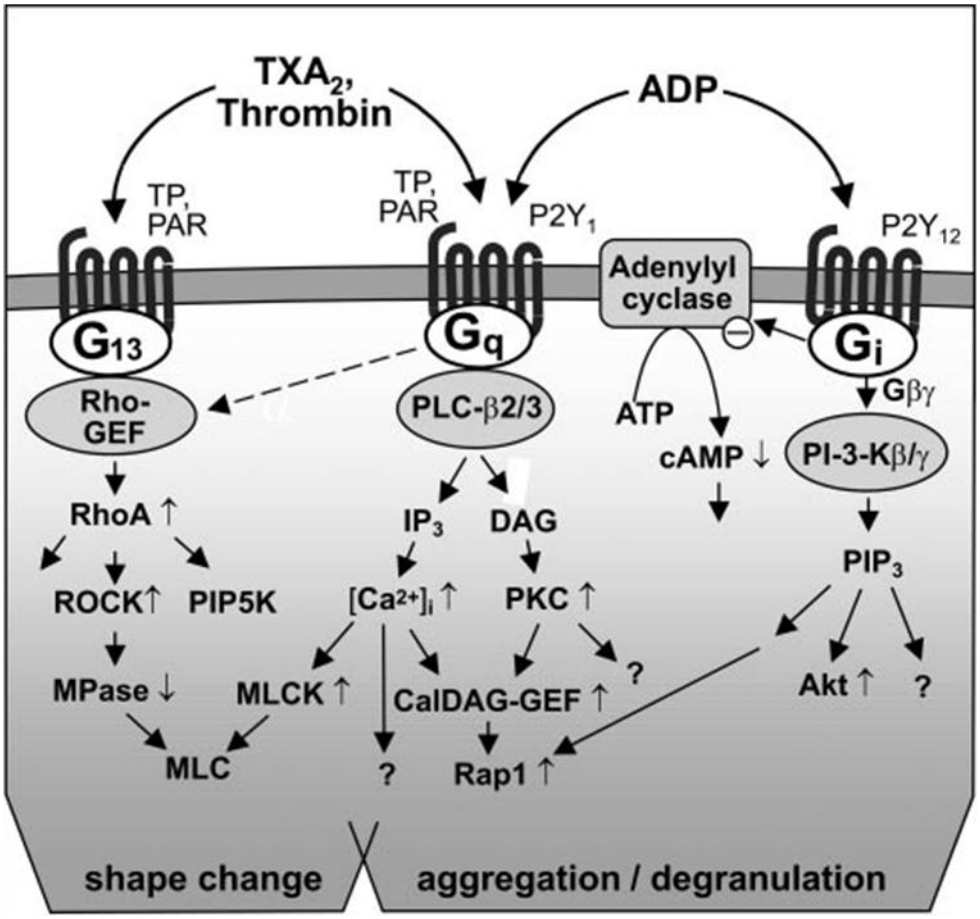

Figure 1. 5: Platelet signalling pathways induced by GPCRs

Shown are signalling cascades downstream of TxA_2**,** thrombin, ADP receptors that are coupled to G_{13}, G_q and G_i proteins. Signalling downstream these receptors results in shape change, integrin activation, granule secretion and aggregation of platelets through Ca^{+2}-dependent and independent pathways. Figure and legend are modified from (Offermanns, 2006).

1.4.2.3 Inside-out signalling and activation of integrin $\alpha_{IIb}\beta_3$

The common outcome of platelet stimulatory signalling pathways is the activation of integrin $\alpha_{IIb}\beta_3$ in a process termed the inside-out signalling (Ma *et al*., 2007). The main purpose of inside-out signalling events is to change the confirmation of integrin $\alpha_{IIb}\beta_3$, which under non-activatory conditions is unable to bind its substrates fibrinogen and vWF. The inactive conformation of integrin $\alpha_{IIb}\beta_3$, which keeps the extracellular domains "bent", is maintained through an interaction between the membrane proximal cytosolic regions of α and β subunits. The outcome of platelet activatory signalling events is an increase in calcium levels and the production of DAG. This activates the calcium and DAG-regulated guanine nucleotide exchange factor I (CalDAG-GEFI). This complex activates Rap1b, which plays an important role in integrin activation through the formation of "integrin activation complex". This complex contains Rap1b, Rap1b interacting adaptor molecule (RIAM) and talin. In its turn talin binds the β subunit of the integrin, which leads to the disruption of its interaction with the α subunit and results in a conformational change that renders the integrin, in a switchblade-like motion, active and capable of binding its substrates (Luo *et al*., 2007). Another protein that has been recently linked with the activation of integrin $\alpha_{IIb}\beta_3$ is kindlin3. Impaired integrin activation has been proposed to be associated with the absence and dysfunction of this protein in mice and in patients, respectively (Moser *et al*., 2008, Malinin *et al*., 2009). The indispensable role of $\alpha_{IIb}\beta_3$ is evident in Glanzmann's thrombasthenia disease where integrin $\alpha_{IIb}\beta_3$ is either missing or dysfunctional (Bellucci and Caen, 2002). Once "activated" $\alpha_{IIb}\beta_3$ is able to bind fibrinogen, which

acts as a molecular bridge between platelets facilitating aggregation. The ligation of $\alpha_{IIb}\beta_3$ triggers a series of signalling events termed outside-in signalling which result in secondary secretion and platelet spreading (Shattil and Newman, 2004).

1.4.3 Amplification of platelet activation

After the first layer of activated platelets have been formed by directly binding to exposed ECM components, remote inactive platelets are recruited to the site of the vascular injury to extend the growth of the thrombus. Amplification of platelet signalling is an autocrine/paracrine process that involves the release of platelet granule cargo such as ADP, fibrinogen and vWF as well as the synthesis of soluble agonists such as thromboxane A_2 (TxA_2).

Following platelet primary activation, the increase in intracellular calcium combined with the activation of PKC drive platelet organelles into the cellular membrane where they release their contents through exocytosis, enriching the site of injury with a multitude of bio-active molecules. Membrane fusion of platelet granules is facilitated by a family of proteins called Soluble NSF Attachment Protein Receptors (SNAREs) (Ren *et al*., 2008). Interactions of two types of SNAREs govern this process as membrane target-SNAREs or t-SNAREs attract their matching counterpart expressed on the vesicle, which are called vesicle-SNAREs or v-SNAREs (Ren *et al*., 2008). The release of α-granule contents is facilitated by the SNARE syntaxin-4 (Flaumenhaft *et al*., 1999) whereas syntaxin-2 act on dense granules (Chen *et al*., 2000). As stated previously in section 1.3.3 α-granule secretion provides a localised source of fibrinogen and vWF to drive aggregation and a number of other factors that promote both wound healing (eg, platelet-derived growth factor) and

coagulation (eg, FV and FVIIa). On the other hand, the release of dense granule contents such as ADP and serotonin mainly trigger signals downstream of several GPCRs, which drive further secretion and aggregation (See 1.4.2.2).

ADP binds to two GPCRs, $P2Y_1$ and $P2Y_{12}$, which are coupled to Gq and Gαi respectively (Ohlmann *et al*., 1995, Offermanns *et al*., 1997). Dense granule-secreted ADP induces all activation events including Ca^{++} release, shape change, cytoskeleton reorganization, secretion, protein phosphorylation and platelet aggregation (Gachet *et al*., 2006). $P2Y_1$ is involved in shape change and aggregation as it was demonstrated on $P2Y_1$ knockout mice, which had defective shape change and aggregation in response to low doses of ADP (Leon *et al*., 1999). $P2Y_{12,}$ on the other hand, is responsible for potentiating platelet aggregation triggered by ADP through $P2Y_1$, but has no effect on shape change as demonstrated in $P2Y_{12}$ deficient mice (Foster *et al*., 2001). In putting together, a complementary role for these two receptors has been suggested where $P2Y_{12}$ amplifies the activation process that has been initiated by $P2Y_1$ (Jin and Kunapuli, 1998, Gachet *et al*., 2006).

Another important secondary platelet agonist is thromboxane A_2 (TxA_2), which plays a crucial role in amplification of platelet activatory signals by acting in autocrine and paracrine manner on its TP receptor. TxA_2 is produced by activated platelets after the activation of phospholipase A_2 (PLA_2) in response to agonist-induced calcium mobilisation. PLA_2 releases arachidonic acid from membrane phospholipids, which is then converted by cyclo-oxygenase-1 (COX-1) into prostaglandin cyclic endoperoxides PGG_2 and PGH_2. In platelets, the latter is converted by thromboxane synthase into TxA_2 (Samuelsson *et al*., 1978, Needleman

et al., 1976). TXA_2 binds to TP receptor, which is coupled into Gαq and $G_{12/13}$ proteins inducing platelet shape change, secretion and aggregation (Offermanns *et al*., 1994, Kinsella *et al*., 1997). TP knockout mice showed impaired platelet aggregation (Thomas *et al*., 1998).

1.4.4 Platelet aggregation

Platelet aggregation is the ability of platelets to clump together forming a stable fibrinogen-rich thrombus at the site of vascular injury. It is a dynamic and a complex process that involves platelets with many receptors and their ligands (Jackson, 2007). Adhesion and aggregation are two faces of the same coin, and like adhesion; the mechanism of aggregation to some extent depends on the rheological conditions at the site of the vascular injury. There are three proposed mechanisms that govern platelet aggregation *in vivo*.

Under low shear rates (<1000 s^{-1}) found in venules and large veins, stable aggregation takes place after agonist-mediated activation of $\alpha_{IIb}\beta_3$, which then binds to fibrinogen (Takagi et al., 2002). The closest simulation of these conditions *in vitro* is in flow chambers when platelets are subjected to low shear rates. Although *in vitro* studies suggested the predominance of $\alpha_{IIb}\beta_3$-fibrinogen interactions on platelet aggregation under these conditions (Savage et al., 1998), *in vivo* studies showed that vWF plays an important role (Brill et al., 2011).

At shear rate between 1000-10000 s^{-1}, aggregation has been suggested to occur in a two-step process. The first step is reversible and is mediated by interactions of vWF

on immobilised platelets and GPIbα on free circulating platelets whereas the second one is irreversible and is reliant on $\alpha_{IIb}\beta_3$ (Kulkarni *et al*., 2000). At the reversible step and under high shear rate, membrane protrusions called membrane tethers are formed. Interestingly, the formation of these tethers is independent of any platelet activation or any soluble agonists such as ADP, TxA_2 or thrombin. They are indeed the result of the hemodynamic dragging forces imposed on platelets by the high shear rate. A key feature of these tethers is to slow down platelets, which not only allows sustained contact with thrombus surface, but also create a protective environment for the accumulation of soluble agonists that leads to full platelet activation and then the formation of stable aggregates (Brass *et al*., 2005). Several studies *in vivo* confirmed the presence of a complementary mechanism between GPIb-IX-V and $\alpha_{IIb}\beta_3$ and their ligands in mediating platelet aggregation under these conditions (Suh *et al*., 1995, Denis *et al*., 1998, Ni *et al*., 2000). One study showed that thrombus formation in both vWF- and fibrinogen-knockouts was impaired but not absent. Interestingly, the same study showed that vWF- and fibrinogen-double knockouts were still able to form a thrombus suggesting the participation of other players such as fibronectin in this complex process (Ni *et al*., 2000).

Finally, a fully activation-independent mechanism mediated exclusively by GPIbα-vWF interactions facilitates platelet aggregation in stenotic arteries, where shear rate can be more than 10000 s^{-1}, has been reported, although the physiological relevance of this is unclear (Ruggeri *et al*., 2006, Jackson, 2007). All the aggregation models under all these different conditions are summarised in figure 1.6.

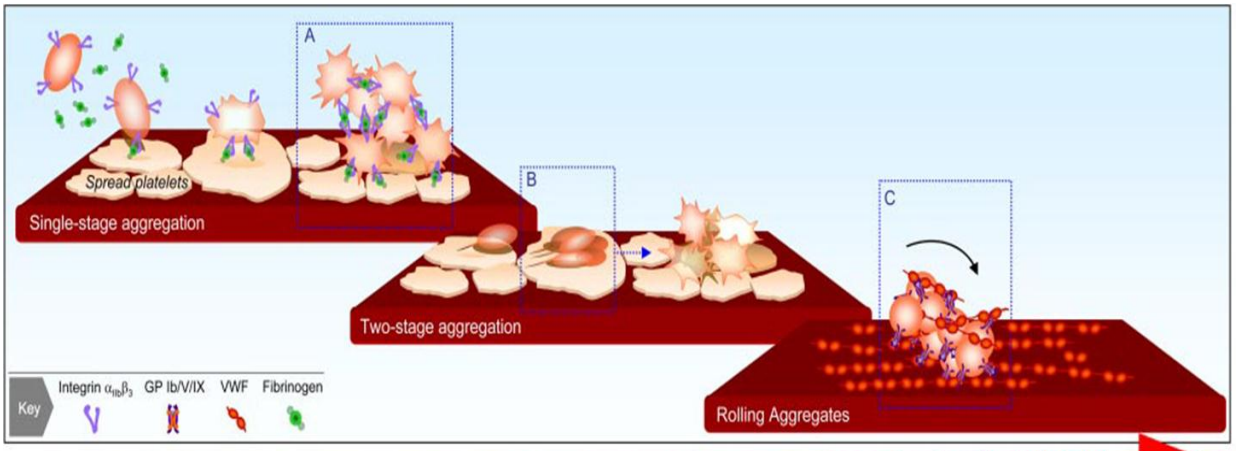

Characteristic Features:	A	B	C
Adhesion Receptor	Integrin $\alpha_{IIb}\beta_3$	Integrin $\alpha_{IIb}\beta_3$, GP Ib/V/IX	GP Ib/V/IX
Activation-dependent	Yes	Yes	No
Tether formation	No	Yes	Yes
Ligand	Fibrinogen	VWF, Fibrinogen, Fibronectin	VWF
Platelet Morphology	Sphere and filopodia	Discoid	Smooth Spherical

Figure 1. 6: Mechanisms mediating platelet aggregation under different shear rates.

(A) Under low shear rate <1000 s^{-1}, platelet aggregation is predominantly mediated by fibrinogen-integrin $\alpha_{IIb}\beta_3$ interactions where platelet get activated, change shape and then stably form thrombi. **(B)** Under high shear rate between 1000-10000 s^{-1}, platelet aggregation takes place via the distinct two-step process which requires membrane tethers and is dependent on both vWF-GPIbα and fibrinogen- integrin $\alpha_{IIb}\beta_3$ interactions. Stable aggregation under these conditions requires platelet activation by soluble agonists. **(C)** At shear rate of >10000 s^{-1} aggregation is independent of fibrinogen-$\alpha_{IIb}\beta_3$ interactions and is exclusively reliant on membrane tethers and vWF-GPIbα interaction. Figure and legend are adapted from (Jackson, 2007).

1.5 Platelet regulation by the endothelium

The endothelium is an anti-thrombogenic cell layer that lines the vessel to isolate platelets from various thrombogenic components of the extracellular matrix (ECM) (de Nucci *et al*., 1988). Platelets in the circulation remain dormant while the endothelium is physically as well as biochemically intact. Spontaneous and sustained platelet activation is prevented at all times to avoid the occlusion of blood lumen and consequently ischemia. When platelets encounter a vascular injury, the endothelium also responds to control, limit or even reverse platelet activation in a process called "endothelial thromboregulation" (Marcus and Safier, 1993). This process is primarily mediated by two endothelium-derived factors (1) prostacyclin (PGI_2) and (2) nitric oxide (NO).

1.5.1 The regulation of platelet function by nitric oxide

NO is a free radical gas that is constitutively released by the endothelium (Ignarro *et al*., 1987) in response to the pulsatile flow of blood. It was first identified as the endothelium-derived relaxing factor (EDRF), whose main role is to regulate the vascular tone (Furchgott *et al*., 1984). Shortly after that, Radomski and colleagues discovered that NO can inhibit platelet function (Radomski *et al*., 1987b). Furthermore, animal studies confirmed later that NO is the main regulator of vascular homeostasis (Huang *et al*., 1995). For review see (Naseem, 2005).

NO synthesis is triggered by an enzymatic reaction that mediates the conversion of L-arginine in the presence of molecular oxygen into a NO molecule and L-citrulline (Radomski *et al*., 1990). A family of enzymes called nitric oxide synthase (NOS)

mediate the synthesis of NO from its precursor (Bruckdorfer, 2005). Three distinct isoforms of this enzyme have been identified, inducible NOS (iNOS), neuronal NOS (nNOS) and endothelial NOS (eNOS). These isoforms differ in their expression, distribution and their regulation. In the vasculature, pulsatile blood flow continually activates the calcium-dependent eNOS, which leads to the release of NO into the blood lumen where it exerts its effect on platelets and vascular smooth muscle cells.

The ability of NO to target several platelet activatory signalling pathways enables it to inhibit different aspects of platelet activation (Schwarz *et al*., 2001) including platelet adhesion (Williams and Nollert, 2004), calcium flux (Cavallini *et al*., 1996), degranulation and aggregation (Tsikas *et al*., 1999). Not only does NO regulate haemostasis, it also plays a protective role in atherosclerosis as it inhibits leukocyte recruitment into the activated endothelium, vascular smooth muscle proliferation and scavenges lipid radicals (Naseem, 2005). In fact, dysfunctional NO production, either arising from eNOS uncoupling or from reduced NO bioavailability, has been associated with atherothrombosis (Munzel *et al*., 2005).

NO exerts its inhibitory effects on platelet function by diffusing through platelet membrane and activating its intracellular receptor soluble guanylyl cyclase (sGC) (Figure 1.8). The activation of sGC results in the production of cyclic guanine-monophosphate (cGMP) from Mg^{2+}-GTP. Intracellular cyclic nucleotide levels in platelets are modulated by the hydrolysing activity of a family of enzymes called phosphodiesterase (PDE) (Omori and Kotera, 2007). In platelets, cGMP has many

effectors such as protein kinase G, phosphodiesterase 3 (PDE3) and ion gated channels (Naseem and Roberts, 2011). However, the main effects of NO on platelet functions are mediated by PKG, as exemplified by PKG-deficient mice, which showed enhanced platelet adhesion and aggregation in vivo and loss of NO sensitivity in vitro (Massberg *et al*., 1999). PKG is a member of the AGC kinase family. It is a serine/threonine protein kinase and exists as two isoforms in mammalian cells PKG-I and PKG-II (Lohmann and Walter, 2005) with only the former expressed in platelets (Antl *et al*., 2007). PKG modulates platelet function through targeting a multitude of substrates in platelets such as VASP (Halbrugge *et al*., 1990), MLC-Kinase (Nishikawa *et al*., 1984), PI3-Kinase (Pigazzi *et al*., 1999), PKC (Gopalakrishna *et al*., 1993) and thromboxane A_2 receptor (Reid and Kinsella, 2003). Phosphorylation of these proteins and others, or potentially enzymes that regulate them, are proprosed to modulate platelet activation (Walter and Gambaryan, 2009, Schwarz *et al*., 2001).

1.5.2 The regulation of platelet function by prostacyclin

1.5.2.1 Prostacyclin synthesis and structure

Prostaglandin I_2 (PGI_2) or prostacyclin was discovered by John Vane's laboratory in 1976 as a potent vasodilator and a powerful inhibitor of platelet function (Moncada *et al*., 1976). Prostacyclin is a highly labile prostanoid, whose half-life in the blood is only about 3 minutes after which it is broken down in the plasma into the ineffective 6-keto-prostaglandin $F_{1\alpha}$, which can be detected in the urine (Dusting *et*

al., 1978). Therefore, PGI_2 is normally protected from degradation by its binding to serum albumin (Tsai *et al*., 1991). Moreover, serum albumin enhances the binding of PGI_2 to its receptor on platelets (Tsai *et al*., 1991). Not very long after its discovery, stable PGI_2 analogues were developed to enable the study of the role of this compound in various aspects of the vascular system and particularly platelet function (Whittle and Moncada, 1985, Armstrong, 1996).

PGI_2 is a member of the prostanoid family of lipids that are synthesised almost in all cell types and have various physiological and pathological roles. It is a 20-carbon unsaturated carboxylic acid with a cyclopenton ring. The key players in prostanoids production (Figure 1.8) are the fatty acid arachidonic acid (AA), and the enzymes phsospholipase A_2 (PLA_2) and cyclooxygenase (COX) (Moncada, 1982b, Parente and Perretti, 2003).

Arachidonic acid, also known as 5,8,11,14-eicosatetraenoic acid, is a C-20 member of the polyunsaturated omega-6-fatty acids (ω-6) that is constitutively esterified to form part of membrane phospholipids. AA is cleaved from membrane phospholipids by PLA_2, which is activated in response to increased intracellular Ca^{+2}. Firstly, through its cyclooxygenase activity, COX converts AA into prostaglandin G_2 (PGG_2). Secondly, the same enzyme, this time through its hydroperoxidase activity, mediates the reduction of PGG_2 into the unstable prostaglandin endoperoxide H (PGH). The outcome of the following step in AA metabolism is determined by the type of enzyme expressed in each cell type. For example, in endothelial cells, PGH is converted into PGI_2 by prostacyclin synthase (PGIS) (Weksler *et al*., 1977, Moncada,

1982a). Prostacyclin is then released from the endothelium to exert its effects on neighbouring vascular smooth muscle cells (VSMCs), or on platelets, located on the luminal side of the endothelial cells (Armstrong, 1996). In platelets, however, where PGI_2 synthase is not present, PGH is converted to thromboxane A_2 (TxA_2) by thromboxane A_2 synthase (Needleman *et al*., 1976). In contrast to PGI_2, TXA_2 is a platelet activator and vasoconstrictor (Samuelsson *et al*., 1978). There is a general consensus that platelet-produced TXA_2 and endothelium-produced PGI_2 work in concert to maintain vascular homeostasis.

The role of COX in prostaglandins' production is very crucial as evidenced by the award of the Nobel prize in Physiology and Medicine to John Vane in 1982 for his discovery of the role of aspirin as a COX inhibitor. Aspirin at low dose (75mg), irreversibly inhibits COX, which in platelets cannot be replaced for the whole lifetime of these enucleate cells whereas the nucleated endothelial cells can still produce COX and, as a result, PGI_2. This tips the balance between TXA_2 and PGI_2 towards the latter, which then results in an antithrombogenic effect. There are two isoforms of this enzyme COX-1 and COX-2. The former is, like eNOS, a constitutive isoform and is known to play a housekeeping role whereas the latter is, like iNOS, inducible and its expression and activity is associated with inflammations and infections. Platelets' exclusive expression of COX-1 is well established (Vane *et al*., 1998, Reiter *et al*., 2001). By contrast, there is a debate about what isoform of COX is expressed in endothelial cells (Mitchell and Warner, 2006b) with some reports suggesting the presence of COX-2 (McAdam *et al*., 1999, Parente and Perretti,

2003) whereas others argue that COX-1 is the predominant isoform (Mitchell and Warner, 2006a, Mitchell et al., 2008).

The synthesis of PGI_2 takes place in the endoplasmic reticulum (ER), where PGIS and COX colocalise (Liou *et al*., 2000). In response to increased intracellular Ca^{+2}, PLA_2 also translocates into the ER, where it releases arachidonic acid from membrane phospholipids (Schievella *et al*., 1995). Similar to NO, PGI_2 production is also triggered by physiological shear stress through upregulation of PGIS and COX enzymes (Frangos *et al*., 1985). The nonphysiological "turbulent" shear stress found at sites of atherogenic lesions, however, is unable to enhance PGI_2 production in endothelial cells (Topper *et al*., 1998). Interestingly, activated platelets, through the release of arachidonic acid-containing microparticles upon stimulation, have also been shown to upregulate COX and, as a result, enhance PGI_2 production providing a negative feedback loop to control thrombus growth (Barry *et al*., 1999).

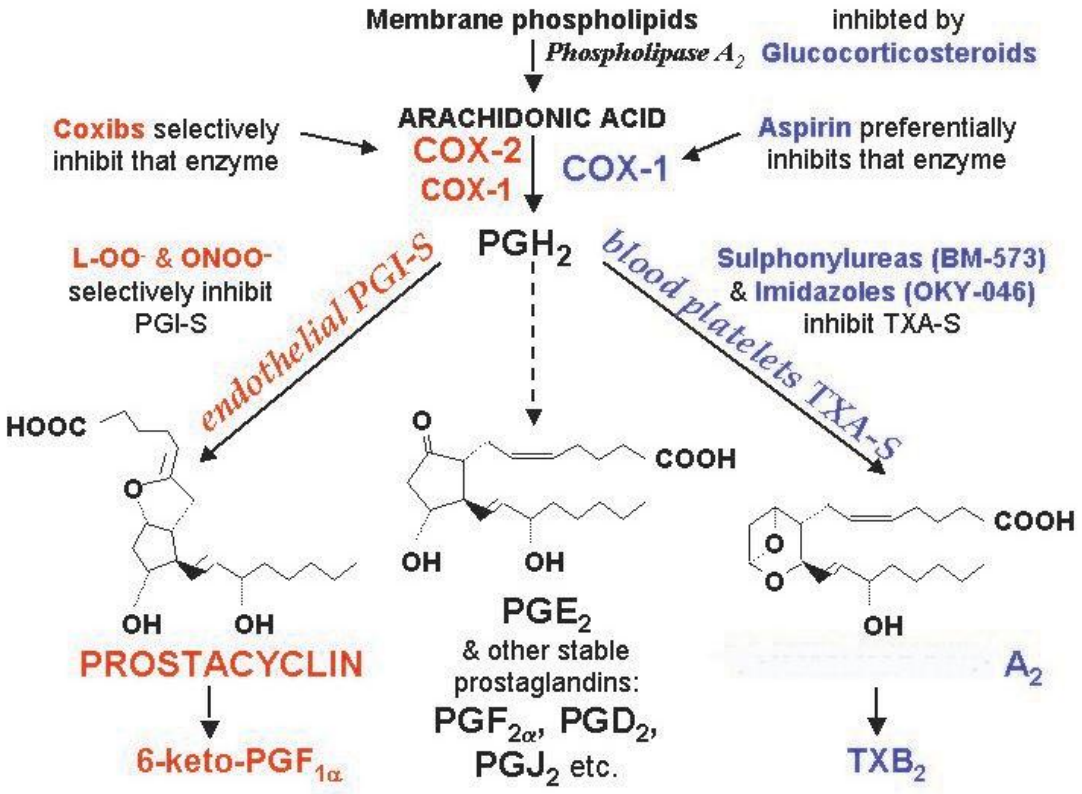

Figure 1. 7: Pharmacological interference into Arachidonic acid cascade.

PLA_2 releases Arachidonic acid from membrane phospholipids. Arachidonic acid is then oxidised by COX into PGH2 which is then reduced by the same enzyme into PGG2. Depending on the cell type, PGG2 is converted into PGI_2 and TxA_2 by PGI-S and TXA-S which are expressed in endothelial cells and platelets, respectively. PGI_2 and TxA_2 are quickly degraded into 6-keto-$PGF_{1\alpha}$ and TxB_2, respectively. Figure is from (Gryglewski, 2008).

1.5.2.2 Prostacyclin and the vasculature

PGI_2 is a local hormone that affects proximal environment rather than a conventional circulating one that affects distal target cells (Blair *et al*., 1982). Plasma levels of the stable PGI_2 metabolite 6-keto-prostaglandin $F_{1\alpha}$ are about 3ng per litre (Blair *et al*., 1982). After production, it either diffuses to the abluminal side of the endothelium causing relaxation of VSMC or is released to the blood lumen where it exerts anti-aggregatory effects on blood platelets (Moncada, 1982a, Vane and Corin, 2003). Animal studies have shown that PGI_2 plays a regulatory role by controlling the vasculature's response to local stimuli such as prevention of vasospasm and thrombosis in response to TxA_2 (Murata *et al*., 1997). This means that, unlike NO (Huang *et al*., 1995), PGI_2 does not play a role in maintaining vascular homeostasis. However, it has been found that PGI_2 plays a protective role in the vasculature by inhibiting the proliferation and migration of VSMCs and maintaining their differentiated state (Fetalvero *et al*., 2007). Moreover, PGI_2 has a protective role against atherogenesis, which is evident by its ability to enhance the activity of cholesterol-lowering enzymes in VSMCs, inhibit accumulation of cholesterol esters by macrophages and sequester the release of growth factors that cause thickening of vessel walls (Willis *et al*., 1986). Clinical studies showed that PGI_2 deficiency is associated with pathogenesis of vascular diseases such as peripheral vascular diseases (PVD) (Group, 2000). Moreover, arterial infusion of PGI_2 analogues in patients with atherosclerotic lower limb PVD showed significant improvements in their health (Szczeklik *et al*., 1980). In addition, a clinical trial showed recently that the use of selective COX-2 inhibitors such as rofecoxib, in

patients with genetic predisposition of heart disease, resulted in increased thrombosis, onset and progression of atherosclerosis and hypertension (Wang *et al*., 2005).

1.5.2.3 Prostacyclin receptor

Unlike NO, it was observed that PGI_2 agonists have membrane binding sites on target tissues. This was the first clue of the presence of PGI_2 receptors through which this prostanoid could exert its effects on target cells (Armstrong *et al*., 1989). Human prostacyclin receptor, called the IP receptor, was first cloned from lung cDNA library in 1994 (Nakagawa *et al*., 1994, Boie *et al*., 1994). IP is a member of the prostanoid receptor subfamily, which is a member of the seven transmembrane-domain GPCR superfamily (Armstrong, 1996). The PGI_2 analogue iloprost has the highest affinity to the IP receptor followed by PGI_2 then PGE_1 (Nakagawa *et al*., 1994, Boie *et al*., 1994).

The receptor undergoes several post-translational modifications including phosphorylation (Smyth *et al*., 1996, Smyth *et al*., 1998), isoprenylation (Hayes *et al*., 1999) and glycosylation (Zhang *et al*., 2001). Mutagenesis studies suggested a role for IP glycosylation in membrane translocation, ligand binding and downstream signalling (Zhang *et al*., 2001). A PKC phosphorylation site (serine-328) has been identified on human IP receptor (hIP). In HEK293 cells expressing the hIP, basal PKC-mediated phosphorylation was detected. PKC phosphorylation increased upon agonist stimulation of IP and was associated with desensitization mechanisms (Smyth *et al*., 1996, Smyth *et al*., 1998). Mice mutagenesis studies confirmed that

cysteine-414 is the isoprenylation site on the mouse IP receptor. These studies showed that isoprenylation is indispensable for cAMP accumulation and inhibition of $[Ca^{+2}]_I$ mobilisation (Hayes *et al*., 1999).

The transmembrane domain of the IP receptor contains a PGI_2 binding pocket. This binding pocket accommodates the cyclopentane ring at the first to second transmembrane domain and the side chain at the seventh transmembrane domain (Kobayashi *et al*., 1997, Kobayashi *et al*., 2000). hIP receptor is mainly coupled to $G\alpha_s$, which leads to stimulation of AC and consequently production of cAMP (Armstrong, 1996). However, in VSMCs it might be coupled to other isoforms of Gα proteins, which results in cAMP-independent effects upon agonist stimulation (Vane and Corin, 2003).

As mentioned above, hIP is phosphorylated by PKC at serine-328 and like all GPCRs this phosphorylation is associated with receptor desensitization and internalization. There are some discrepancies, across different cell types, in reports addressing the rate of IP receptor desensitization after agonist binding with one report suggesting that it happens within minutes in HEK239 (Smyth *et al*., 1998) and another suggesting that it happens within hours in human fibroblasts (Nilius *et al*., 2000) after agonist stimulation. Internalization kinetics of platelet hIP receptor were investigated using [^{3}H]-labelled iloprost (Giovanazzi *et al*., 1997). This study suggests that the IP receptor is internalized in response to preincubation with the PGI_2 analogue in a time-dependent manner, which results in desensitization to

subsequent treatment with the same analogue. IP receptor desensitization has been reported to be reversible in vitro (Fisch *et al*., 1997).

Interestingly, IP knockout mice were normotensive and had normal bleeding time (Murata *et al*., 1997). This provided strong evidence that PGI_2 is not the main regulator of vascular homeostasis and maybe rather works on demand when required. This is supported by data from the same study suggesting $IP^{-/-}$ mice has more tendency to form occlusive thrombi upon vascular injury with $FeCl_3$ compared with the mural thrombi in wild type mice. These data are in contrast with others obtained from animals lacking endothelial nitric oxide synthase. Those mice were hypertensive suggesting a more dominant role for NO in regulating vascular homeostasis compared with PGI_2 (Huang *et al*., 1995). Thus, even though both NO and PGI_2 are vasodilators and platelet inhibitors it is possible that they play slightly different physiological roles allowing complementary and overlapping effects.

1.6 Platelet inhibition by cAMP/PKA signalling pathway

Platelet function is regulated by two cyclic nucleotide inhibitory pathways cyclic adenosine monophosphate (cAMP) and cyclic-guanosine monophosphate (cGMP) pathways (Figure 1.8). These two pathways are physiologically triggered by two endothelium-derived platelet inhibitors PGI_2 and NO, respectively. NO and PGI_2 trigger the production of platelet cyclic nucleotides through the activation of soluble guanylyl cyclase (sGC) and adenylyl cyclase (AC), respectively. This is followed by activation of their respective protein kinases, PKG and PKA which induce phosphorylation events modulating different aspects of platelet activation

such as calcium mobilisation, adhesion, fibrinogen binding and platelet aggregation (Smolenski, 2011, Schwarz *et al*., 2001). This section will review current findings about the regulation of platelet function by cAMP-mediated signalling pathway. Comprehensive reviews on cGMP and platelets are available (Schwarz *et al*., 2001, Walter and Gambaryan, 2009).

cAMP/PKA signal transduction is triggered in platelets under physiological conditions by endothelium derived PGI_2 and PGE_1 which bind to their respective $G\alpha_s$-coupled receptors on platelets (Armstrong, 1996). In addition, in response to injury/inflammation adenosine is produced and then binds to its A_{2A} receptor which is also expressed on platelets and coupled to $G\alpha_s$ proteins (Johnston-Cox *et al*., 2011). Genetic defects in the cAMP/PKA signalling pathway have been linked with various hemostasis disorders (Van Geet *et al*., 2009). For instance, gain of function mutations in $G\alpha_s$ proteins result in platelet hypersensitivity to cAMP increasing agents whereas other mutations, which result in reduced cAMP levels render the platelets hyperactive. Commercially available forms of different physiological cAMP increasing agents can be used as tools to study the whole signalling pathway, whereas other nonphysiological agents such as forskolin, a direct AC activator (Seamon *et al*., 1981), and cAMP analogues, direct PKA activators, can be used to study only parts of the pathway.

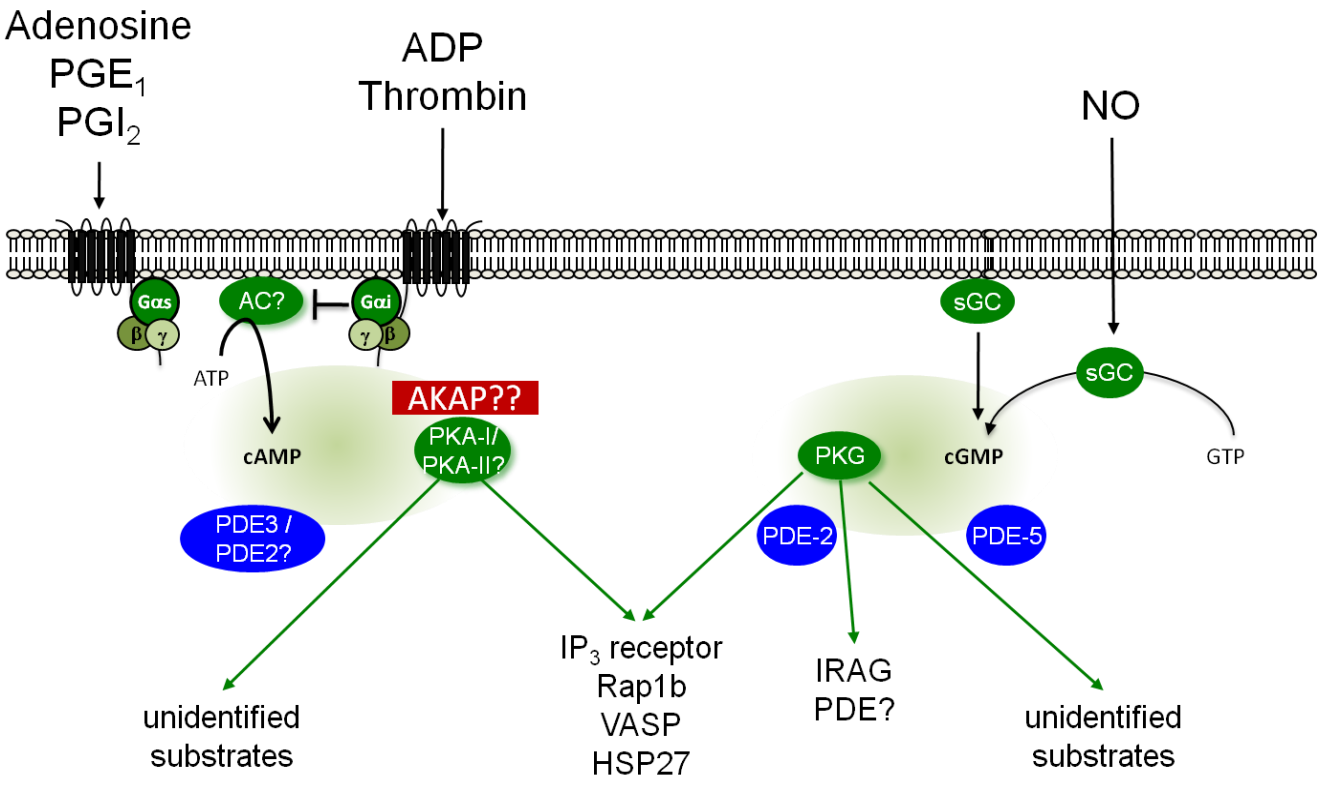

Figure 1. 8: Cyclic nucleotide signalling in blood platelets.

Prostaglandins bind to their $G\alpha_s$-PCRs and activate AC which mediates the production of cAMP and activation of PKA. PKA then mediates the phosphorylation of different substrates which regulate various aspects of platelet function. NO on the other hand diffuses into the cell activating sGC which mediates the production of cGMP and the activation of PKG. PKG phosphorylates different substrates some of which are also targets for PKA. Question marks (?) represent unknown isoforms.

1.6.1 cAMP synthesis by adenylyl cyclase in blood platelets

cAMP levels in platelets and in all cell types increase through the activation of adenylyl cyclase (AC), which converts ATP into cAMP (Hanoune and Defer, 2001, Cooper and Crossthwaite, 2006). Nine AC isoforms have been cloned to date and are differentially distributed in a cell type-dependent manner (Hanoune and Defer, 2001). Low expression levels and unreliability of isoform-specific antibodies combined with low levels of mRNA found in platelets, has made definitive confirmation of what AC isoforms are expressed in platelets difficult. One review suggested the presence of AC isoform 2 along with the ubiquitously expressed 6 and 7 (Hanoune and Defer, 2001). An elegant platelet transcriptome study suggested the potential presence of AC3, 6 and 7, with AC3 is the most abundant (Rowley *et al*., 2011). However, direct confirmation through immunoblotting or proteomics is still lacking.

Different isoforms of AC have distinct regulatory properties and may be differentially localised in the cell (Hanoune and Defer, 2001, Cooper and Crossthwaite, 2006). For example, AC3 resides in lipid rafts and is negatively regulated by $G\alpha_i$ but positively regulated by Ca^{2+}. AC6 and 7 are both negatively regulated by Ca^{2+} and $G\alpha_i$, but the former is localised in rafts whereas the latter is excluded from rafts. All known AC isoforms in platelets are activated by GTP-bound $G\alpha_s$ proteins, which are coupled to receptors such as IP, EP, A_{2A} and A_{2B} (Armstrong, 1996, Johnston-Cox *et al*., 2011). The AC stimulating activity of $G\alpha_s$ is switched off by its intrinsic GTPase activity, which is induced in platelets by regulator of G-protein signalling 2 (RGS2) (Noe *et al*., 2010). On the other hand, $G\alpha_i$ activation

through $G\alpha_i$-coupled platelet receptors, like $P2Y_{12}$ and α2 receptors, will result in the inhibition of AC and thus a decrease in cellular cAMP levels (Dorsam and Kunapuli, 2004). However, it seems that $G\alpha_i$ does not influence basal cAMP but prevents those that are stimulated by $G\alpha_s$ (Dorsam and Kunapuli, 2004). Thus it is likely that this mechanism is designed to reduced cAMP signalling specifically in areas of vascular injury, where factors such as ADP could accumulate.

AC is a transmembrane enzyme that is composed of two transmembrane domains, TM_1 and TM_2, and two cytoplasmic domains, C_1 and C_2 (Figure 1.9) (Krupinski *et al*., 1989). The two transmembrane domains are in tandem and separated by the C_1 domain. The interaction between C_1 and C_2 domains forms the catalytic core. The process of cAMP production from ATP by AC is still poorly understood. Briefly, AC has three nucleotide binding sites and one Mg^{2+} binding site that are required for the conversion of ATP into cAMP upon activation. In order to capture the ATP molecule, Lys-923 and Asp-1000 on the C_2 domain, interact with N-1 and N-6 from the purine ring of the ATP molecule (Liu *et al*., 1997a). Point mutation studies revealed that these residues allow the AC to specifically interact with ATP rather than GTP (Sunahara *et al*., 1998). Two Mg^{2+} ions are, most likely, required for the production of one cAMP molecule. The first one facilitates a nucleophilic attack on the 3'-hydroxyl group of the ATP molecule, after mediating its deprotonation. A second Mg^{+2} ion helps stabilize a transient ATP conformation that resulted from the nucleophilic attack. After that, three residues, Asn1007, Arg1011 and Lys1047 approach the phosphate moieties in the ATP molecule and mediate the release of a

pyrophosphate group and the production of a cAMP molecule (Zimmermann *et al*., 1998, Hurley, 1999).

Forskolin, which is a ditrepene isolated from an Indian plant called *Forskohlii*, is a very potent activator of all types of AC except AC9 (Seamon *et al*., 1981). Forskolin fits into the ventral cleft that forms the catalytic core "gluing" the two cytoplasmic domains together and consequently activating the enzyme (Tesmer *et al*., 1997, Liu *et al*., 1997b). $G\alpha_s$ activates AC through binding to a crevice formed by the outside of the C_2 domain and the N terminal part of the C_1 domain and therefore activates the enzymatic activity by linking the two C domains. $G\alpha_s$ does not compete with forskolin for the binding to AC but rather works with it synergistically (Tesmer *et al*., 1997, Yan *et al*., 1997). Gαi, on the other hand, binds to a groove whose location has been suggested to be psudosymmetrical to that of the $G\alpha_s$ which enables it to work in opposition (Tesmer *et al*., 1997, Yan *et al*., 1997).

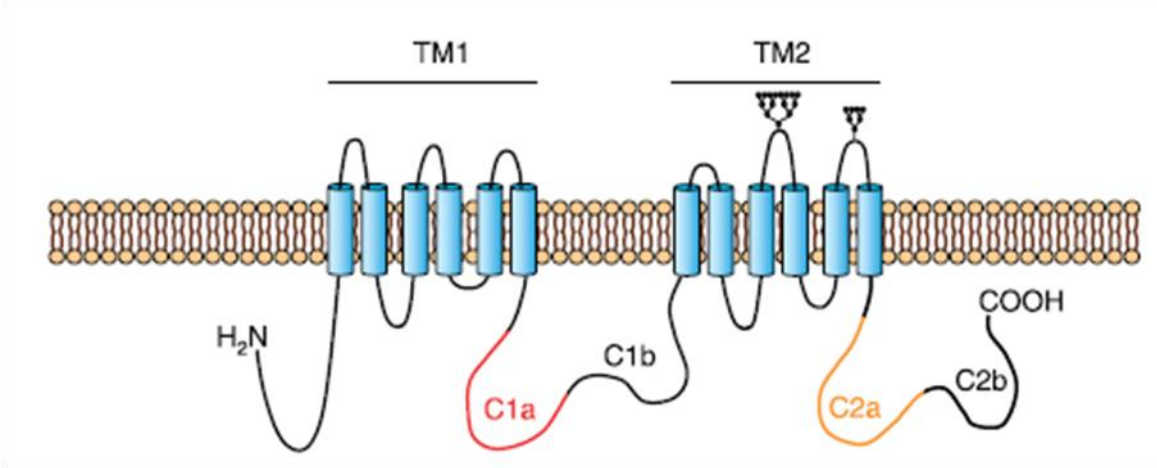

Figure 1. 9: The general structure of adenylyl cyclase.

ACs have 5 major domains: the NH_2 terminus, the first transmembrane cluster (TM1, blue cylinders), the first catalytic loop comprised of C1a (red) and C1b (black), the second transmembrane domain (TM2, blue cylinders), the second catalytic loop containing C2a (orange) and C2b (black). The dimerization of C1a and C2b upon $G\alpha_s$ activation forms the catalytic core. Figure and legend are modified from (Willoughby and Cooper, 2007).

1.6.2 cAMP degradation by phosphodiesterases in blood platelets

Phosphodiesterases (PDEs) are crucial to the control of the cAMP/PKA signalling pathway, by acting to terminate signal transduction. They play a critical role in regulating the intensity of the cAMP signal as well as its duration. Eleven families of those phosphodiesterases have been identified to date (Omori and Kotera, 2007). They mediate the degradation of cyclic nucleotides by hydrolyzing the 3'-phosphoester bond and converting the 3'-cyclic nucleotide into an inactive 5'-nucleotide (Omori and Kotera, 2007). Three of the eleven PDE isozymes have been identified in platelets, including PDE2A, PDE3A and PDE5A (Haslam *et al*., 1999, Ito *et al*., 1996, Weishaar *et al*., 1986). PDE2 is a cGMP-stimulated and it has two allostreric binding sites for cGMP on the regulatory domain (Stroop and Beavo, 1991). It has a similar binding affinity for both cAMP and cGMP (Omori and Kotera, 2007). PDE3, on the other hand, is inhibited by cGMP, which competes with cAMP for its binding sites, although it has a higher affinity towards cAMP (Degerman *et al*., 1997). PDE5 is exclusively activated by cGMP and it has a very high affinity for the hydrolysis of cGMP (Hagiwara *et al*., 1984, Ito *et al*., 1996, Omori and Kotera, 2007) and acts as a feedback loop for regulating cGMP signalling.

The exact role and the relative contribution of each PDE isoform to the regulation of platelet function are still poorly understood. Manns and colleagues suggest that PDE3 has a more dominant role in regulating platelet function. They showed that inhibiting PDE3, but not PDE2, leads to inhibition of agonist–induced platelet aggregation as well as calcium mobilization. Moreover, inhibition of PDE3 resulted in increased PKA activity represented by enhanced phosphorylation of VASP[157]

(Manns *et al*., 2002). Similar findings were produced by Feijge and colleagues who suggested an interesting role for PDE3. They suggest that, in platelets, cAMP is persistently produced in a $G\alpha_s$-independent manner and PDE3 keeps it at a low equilibrium level that imposes a low cAMP-regulated threshold for platelet activation (Feijge *et al*., 2004). In the light of the these report there is a growing body of evidence suggesting that PDE3 contribute more to platelet regulation than PDE2 does. But there is some ambiguity around the regulation of its activity. Whereas one report suggests that thrombin activates PDE3 in an Akt-dependent manner (Zhang and Colman, 2007), another group suggests that this happens through phosphorylation by PKC not Akt (Hunter *et al*., 2009). However, regardless of the mechanism, it would seem logical that platelet agonists would activate PDE3 as a mechanism to inhibit cAMP signalling and thereby activates platelets.

The ability of PDE2 and PDE3 to hydrolyze both cGMP and cAMP and to be independently regulated by cGMP, allows for crosstalk between both cyclic nucleotides in platelets. The crosstalk between cGMP and cAMP in platelets was the main interest of many research groups. It has been reported that both cAMP and cGMP participate in NO-mediated inhibition of platelet aggregation (Jang *et al*., 2002). A more prominent role for cAMP was suggested by Jensen and colleagues, who suggest that NO-mediated inhibition of platelet shape change was associated with increased cAMP levels and $VASP^{157}$ phosphorylation; an effect that was mimicked only with PDE3 inhibitors but not with cGMP analogues or PDE2 inhibitors (Jensen *et al*., 2004). The exact mechanism that triggers the involvement of cAMP in NO-mediated inhibition of blood platelets is still not well-established.

Work by Murice and Haslam showed that cGMP potentiates cAMP production through inhibiting PDE3 in platelets (Maurice and Haslam, 1990). Later the same group reported that, in the presence of cGMP, PDE2 plays an essential role in the hydrolysis of low cAMP concentrations and limits the increase in cAMP production attributed to cGMP-dependent inhibition of PDE3 (Dickinson *et al*., 1997). Similar findings showed that a low concentration of sildenafil combined with NO resulted in diminished agonist-induced platelet secretion, which was concomitant with increased cAMP levels due to inhibition of PDE3. Increasing the concentration of the same PDE5 inhibitor, however, neither had an effect on platelet secretion nor on cAMP levels due to activation of PDE2 (Dunkern and Hatzelmann, 2005).

1.6.3 Protein kinase A in platelets

In most cells cAMP has several downstream effectors including the exchange proteins activated by cAMP (Epac) (de Rooij *et al*., 1998), cyclic-nucleotide gated ion channels (Nakamura and Gold, 1987) and Protein kinase A. However, in platelets PKA is the only known effectors of cAMP signalling (PKA) (Schwarz *et al*., 2001).

PKA is a heterotetramer composed of two inactive catalytic subunits (C) which are kept in an inactive state through binding to two regulatory subunits (R). The binding of four cAMP molecules releases the C subunits which mediate the kinase activity (Figure 1.10) (Potter and Taylor, 1979). Two types of the regulatory subunit have been identified RI and RII giving rise to two isoforms of PKA type I (PKA I) and type II (PKA II) (Corbin *et al*., 1975b). PKA I is classically known to be cytosolic whereas PKA II tends to localize with organelles and specific cellular structure (Skalhegg and

Tasken, 2000). To further add to the complexity, molecular cloning studies identified more R isoforms namely RIα, RIβ, RIIα and RIIβ and more C subunits namely Cα, Cβ, and Cγ. These isoforms differ in their biochemical and physical properties as well as their tissue distribution (Scott, 1991). In platelets, it has been reported that PKA types RIβ and RIIβ are the major isoforms expressed in platelets (Schwarz *et al*., 2001). But recent platelet transcriptome studies (Rowley *et al*., 2011) suggests that equal RNA levels for Cα and Cβ subunits are present in platelets. In addition, they suggest that among all R isoforms, RIIβ has the highest RNA levels in platelets followed by RIα and the RIβ. Only traces of RIIα RNA were detected under their conditions. The differential role and relative contribution of these PKA isoforms to the inhibition of platelet function is still vague and requires further investigation. PKA knockout studies are still lacking in platelets, but a platelet microRNA study showed that the absence of PKA RII subunit from mouse platelets led to significantly diminished activation by a combination of adrenalin and PAR4-activating peptide compared to wild type (Nagalla *et al*., 2011).

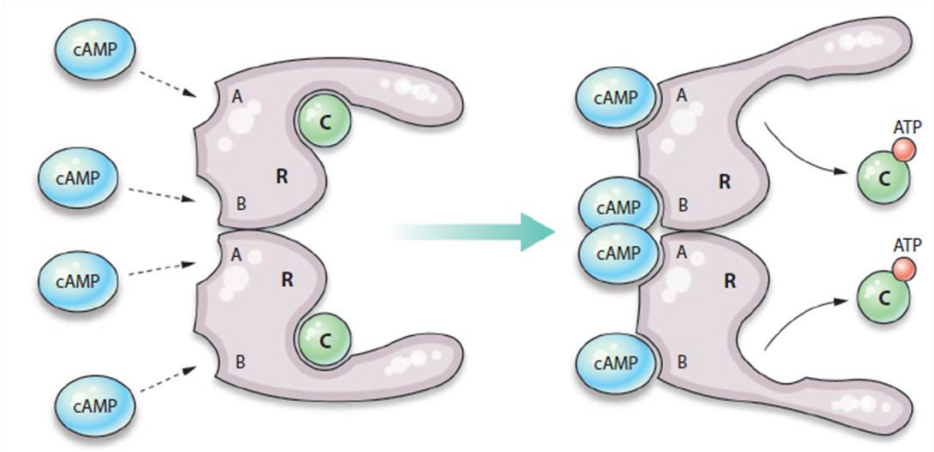

Figure 1. 10: Activation of PKA by cAMP.

In its inactive state, PKA consists of two regulatory subunits (R) bound to two catalytic subunits (C). Each regulatory subunit has two cAMP binding sites (A and B). The binding of four cAMP molecules to the four cAMP binding sites result in the release of the catalytic subunits which bind to ATP molecules and consequently phosphorylates adjacent PKA substrates. Figure and legend are adapted from (Murray, 2008).

1.6.4 Protein kinase A structure and activation

The regulatory subunit (R) of PKA is not only the main receptor for cAMP molecules, but is also a highly dynamic multi-domain protein that can interact with and bind to a variety of proteins (Figure 1.11) (Taylor *et al*., 2005, Taylor *et al*., 2008). Although there are multiple isoforms of the R subunit, they share the same general architecture with a dimerization/docking domain (D/D domain) at the N terminus, followed by a hinge region that contains an inhibitory site and then two tandem and highly homologous cAMP binding domains (CBDs), designated A and B. Each CBD has a Phosphate Binding Cassette (PBC) to which the ribose phosphate of the cAMP molecule binds (Taylor *et al*., 2008). Whereas the D/D domain and the CBDs are highly conserved in all R isoforms (Canaves and Taylor, 2002), the inhibitor site is very variable in length and in sequence (Vigil *et al*., 2004). The inhibitor site contains an autophosphorylation site in RII and a pseudophosphorylation site in RI (Martin *et al*., 2007). The spontaneous binding of the substrate-resembling motif of the autophosphorylation site of the RII subunit (Rangel-Aldao and Rosen, 1976, Diskar *et al*., 2007, Zhang *et al*., 2012) and the allosteric binding of the pseudophosphorylation site of the RI (Dostmann and Taylor, 1991, Herberg and Taylor, 1993, Diskar *et al*., 2007) to their C subunits ensure the stabilisation of the inactive confirmation of the holoenzyme.

The catalytic subunit (C), or the kinase core, is comprised of an N-lobe, which is a small and very dynamic amino terminal. The N-lobe is followed by a short linker connected to a large helical carboxy terminal called the C-lobe, where the catalytic machinery and the docking sites sit. The C- and the N-lobe are flanked by a C-tail

and an N-tail respectively. The main function of these two tails is to position the catalytic core in an active conformation that supports the catalysis (Taylor *et al*., 2008).

In the inactive holoenzyme, the con formation of the R subunits only allows the CBD-B to be exposed to cAMP molecules. Upon the binding of a first cAMP molecule to this site, a conformational change takes place and results in the exposure of the CBD-A, which allows another cAMP molecule to bind. The occupation of the CBDs changes the conformation of the R subunit, particularly the hinge region, reducing its affinity for the C subunit. This results in dissociation of the active site on the C subunit from the inhibitory site on the R subunit and subsequent release of the C subunit. The outcome of all these conformational changes is an R dimer, which is occupied by four cAMP molecules and two catalytically active C monomers. The catalytically active C subunit is now able to phosphorylate proximal targets that possess a PKA consensus motif (Arg-Arg-X-Ser/Thr, Arg-Lys-X-Ser/Thr, Lys-Arg-X-Ser/Thr or Lys-Lys-X-Ser/Thr) (Taylor *et al*., 2008). The reassociation of the R and C subunits after activation is a very poorly understood process. But it has been reported that proximal phosphatases such as calcinerium, which is activated by elevated calcium and is anchored by AKAPs (see 1.8), might dephosphorylate the RII subunit, a process that is believed to mediate the regeneration of the holoenzyme (Oliveria *et al*., 2007). An AKAP- and phosphatase-independent model, however, has been suggested to mediate the regeneration of the PKA I holoenzyme. This model suggests that RI binds and activates PDE, which in its turn hydrolyses RI-bound cAMP molecules resulting in

reassociation with the C subunit and the termination of the signal (Moorthy *et al*., 2011). Recently, a cAMP-independent activation of the C subunit has been reported in platelets, where stimulation with thrombin or collagen led to the release of the PKA C subunit from a complex with NFκB-IκB complex and the phosphorylation of PKA substrates (Gambaryan *et al*., 2010).

The variability in cAMP affinity provides the individual PKA subtypes with distinct biochemical properties. For example PKA I is known to be more sensitive to cAMP than PKA II with an activation constant (K_{act}) of 50-100nM and 200-400nM of cAMP, respectively (Cadd *et al*., 1990, Gamm *et al*., 1996). These properties combined with the differential cellular localisation of PKA I and PKA II are believed to contribute to the specificity of the cAMP/PKA signalling pathway, an issue that is yet to be addressed in blood platelets.

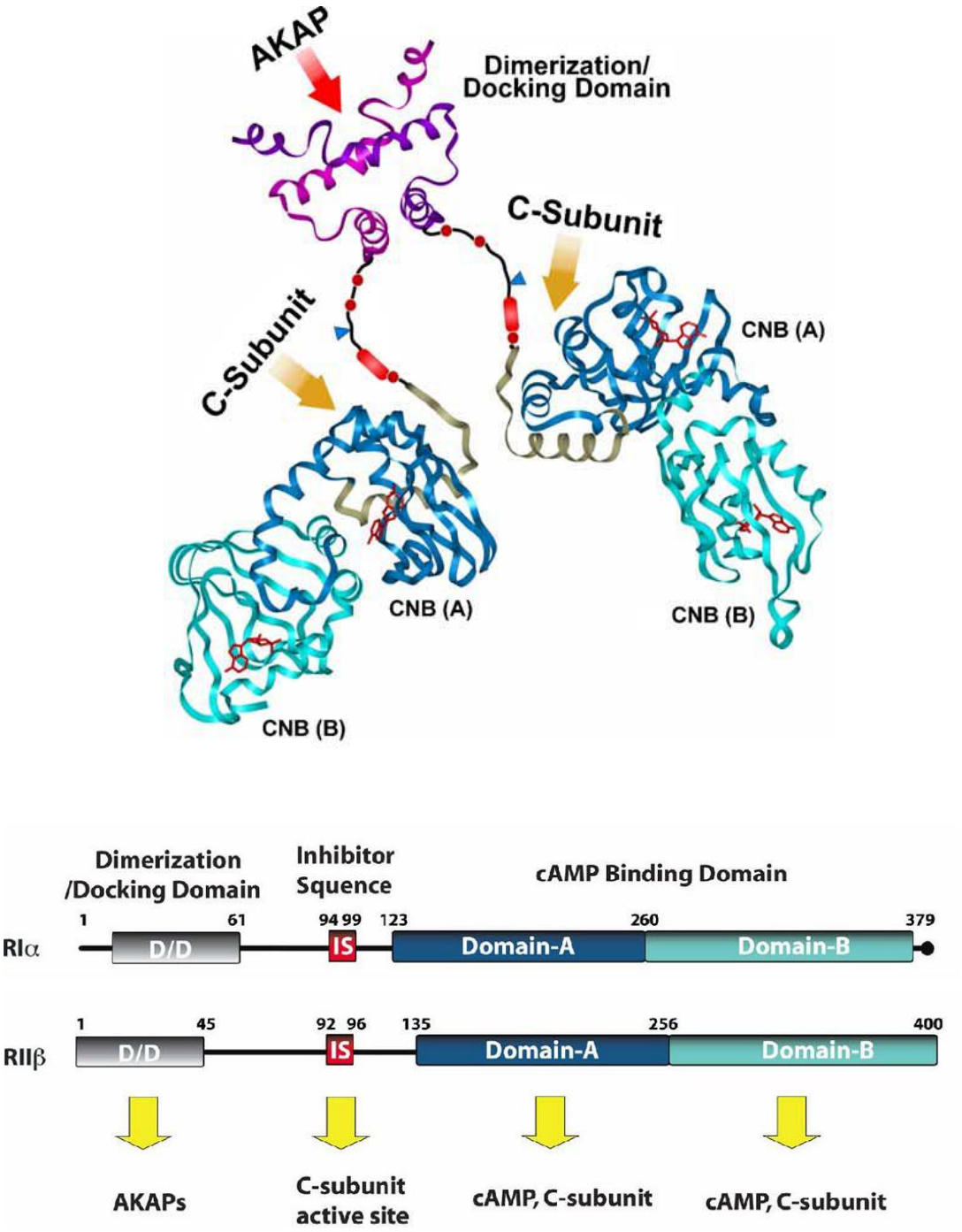

Figure 1. 11: Organisation of the regulatory subunits of PKA.

The top figure shows an NMR-solved model of RIα showing its structure and its different domains. The bottom figure is a cartoon showing the domain organisation of regulatory subunits RIα and RIIβ. Figure and legend are modified from (Taylor *et al*., 2005, Taylor *et al*., 2008).

1.6.5 Protein kinase A substrates in blood platelets

Platelet inhibition induced by PGI_2 or any other cAMP elevating agents is thought to be mediated by PKA, through the phosphorylation of distinct substrates involved in different stages in the process of platelet activation (Table 1.1). This includes the inhibition of cytoskeletal reorganization, intracellular calcium elevation and platelet secretion (Schwarz *et al*., 2001). However, the physiological relevance of these substrates is unclear as many of the studies have identified the substrate through in vitro experimentation. Nevertheless they do provide a framework with which we can begin to examine cAMP/PKA signaling affects platelets.

1.6.5.1 Cytoskeletal reorganization

Vasodilator-stimulated phosphoprotein (VASP) was first isolated from platelets in 1989 (Halbrugge and Walter, 1989) and then later was identified as a common substrate for both PKA and PKG (Halbrugge *et al*., 1990). The main two phosphorylation sites on VASP are ser^{157} and ser^{239} with PKA having a preference for the former and PKG for the latter. PKA-mediated phosphorylation of VASP on ser^{157} causes a mobility shift in SDS-PAGE changing the apparent molecular weight from 46 to 50kDa (Butt *et al*., 1994). In platelets and other cell types, VASP is involved in cytoskeletal reorganization through the regulation of actin bundling and polymerization (Reinhard *et al*., 2001). VASP-deficient mice showed enhanced platelet adhesion (Massberg *et al*., 2004). NO-mediated inhibition of platelet adhesion was also impaired in these mice (Massberg *et al*., 2004). The functional relevance of VASP phosphorylation in platelets is still not fully understood. One report suggested that cGMP analogue- and NO-mediated phosphorylation of VASP

at ser^{239} is predominantly mediated by PKA (Li *et al*., 2003). It has been suggested that phsophorylation of VASP at ser^{157} negatively regulates the activation of fibrinogen receptor $\alpha_{IIb}\beta_3$ (Horstrup *et al*., 1994). *In vitro* studies showed that the phosphorylation of VASP by PKA leads to the inhibition of actin nucleation as well as actin filament bundling (Harbeck *et al*., 2000). Recently, VASP phosphorylation has been branded with a protective role in ischemia-reperfusion injury through its inhibition of platelet-neutrophil interactions (Kohler *et al*., 2011). In addition to its phosphorylation by PKA, ser^{157} has been found to be phosphorylated by Rho kinase as well as PKC in response to platelet stimulation with thrombin (Wentworth *et al*., 2006). This raises some questions on the reliability of this phosphorylation event on its own as a PKA activity marker in platelets. GPIbβ is a subunit of the vWF platelet receptor complex GPIb-V-IX. This receptor mediates initial platelet adhesion, activation (Andrews and Berndt, 2008) and is also a link between actin filaments and membrane glycoproteins (Fox, 1985). PKA phosphorylates GPIbβ on ser^{166} in platelets both basally and in response to cAMP elevating agents; an event that was found to be associated with inhibition of collagen-induced actin polymerization, platelet binding to vWF and vWF-induce platelet agglutination (Wardell *et al*., 1989, Bodnar *et al*., 2002). The basal phosporylation of GPIbβ was observed in an elegant phosphoproteome study of resting human platelets (Zahedi *et al*., 2008).

Another protein that is phosphorylated by PKA in platelets is Filamin-A (Actin-binding protein (ABP)). Filamin-A is an important component of the membrane contractile cytoskeleton and plays a significant role in stabilizing actin filaments. Upon platelet activation ABP undergoes proteolytic cleavage induced by calpain,

which leads to cytoskeletal reorganization (Hartwig and DeSisto, 1991). The phosphorylation of Filamin-A at ser^{2152} by PKA inhibits this proteolytic cleavage and maintains the stability of the cytoskeleton (Chen and Stracher, 1989). Caldesmon is another actin-binding protein that mediates the formation of the actin-caldesmon-myosin complex, and subsequantly enhances the binding of myosin to the cytoskeleton upon platelet activation (Hemric *et al*., 1994). *In vitro* studies identified two phosphorylation sites for PKA on platelet-purified caldesmon (Hettasch and Sellers, 1991), but the functional consequence of this phosphorylation event is unknown. Several proteins in platelets, involved in agonist-induced cytoskeletal reorganization, have been proposed to be substrates for both PKA and PKG. Among those proteins is the heat shock protein 27 (Hsp27), which upon stimulation leads to actin polymerization (Lavoie *et al*., 1993). Hsp27 has two phosphorylation sites. The first one is stimulatory and is targeted by the p38 MAP-activated MAPKAPK-2. The other phosphorylation site is inhibitory and is targeted by both PKA and PKG (Butt *et al*., 2001). Although the phosphorylation of Hsp27 by PKG has been shown in intact platelets, only *in vitro* data are available for its PKA phosphorylation. LIM and SH3 domain protein (LASP) is an actin-binding protein that is phosphorylated by both PKA and PKG at ser^{146} in human platelets. This phosphorylation has been suggested to inhibit LASP binding to F-actin; a finding that is yet to be confirmed in platelets (Butt *et al*., 2003). *In vitro* studies showed that the calmodulin-induced myosin light chain kinase (MLCK) is a dual substrate for both PKA and PKG. MLCK phosphorylates MLC, which leads to myosin filament formation and contractility that mediate platelet shape change

(Schoenwaelder and Burridge, 1999). Cyclic nucleotides-mediated phosphorylation of MLCK is believed to decrease its affinity to calmodulin (Nishikawa *et al*., 1984). But these are only in vitro observations that require confirmation in intact platelets.

1.6.5.2 Intracellular calcium mobilization

Another platelet aspect that is known to be regulated by PKA signaling is the elevation of intracellular calcium (Schwarz *et al*., 2001). Calcium release in platelets is involved in various steps of cellular activation such as the activation of integrins, shape change and granule secretion (Varga-Szabo *et al*., 2009). The increase in intracellular Ca^{+2} in platelets comes from two consecutive events, the release from intracellular stores (ER) and then the store-operated extracellular calcium entry (SOCE) or calcium influx, reviewed in (Varga-Szabo *et al*., 2009). Inositol-1,4,5-triphosphate receptors (IP3-R) are Ca^{+2} permeable channels that operate calcium release from the ER. IP3-R are present in 3 isoforms, type I, type II and type III all of which are expressed in platelets. PKA has been reported to phosphorylate all IP3-R isoforms (El-Daher *et al*., 2000, Cavallini *et al*., 1996). However, the functional outcome of this phosphorylation is controversial. One report suggested an inhibitory effect of IP3-R phosphorylation by PKA (Supattapone *et al*., 1988), whereas another suggested the opposite (Nakade *et al*., 1994). Transient receptor potential channel (TRPC) are the main mediators of SOCE in platelets facilitated by the coupling of TRPC with IP_3-R, an event that follows the release of intracellular calcium (Varga-Szabo *et al*., 2009). Seven subfamilies of TRPC have been identified

so far, two of them have been found in platelets TRPC1 and TRPC6 (Hassock *et al*., 2002). Only TRPC6 has been found to be phosphorylated by PKA but the functional consequence of this phosphorylation is not very clear (Hassock *et al*., 2002).

1.6.5.3 G-proteins and G-protein-coupled receptors

G proteins or guanyl nucleotide-binding proteins are a family of proteins whose main function is to transfer signals, generated at the plasma membrane, from receptors (GPCRs) to their respective cellular effectors. They exert their effect through their ability to release GDP and exchange it for GTP upon receptor activation. G proteins are then switched off as a result of their internal GTPase activity. For review see (Neves *et al*., 2002).

Rap1b is a small GTPase of the Ras family. The exact role of Rap1b in platelets is not fully understood, but platelets from Rap1b -/- mice showed impaired platelet aggregation, defective integrin $\alpha_{IIb}\beta_3$ activation and prolonged tail bleeding. Rap1b is phosphorylated at ser^{179} by both PKA as well as PKG (Siess *et al*., 1990, Lapetina *et al*., 1989, Danielewski *et al*., 2005). The functional outcome of this phosphorylation is elusive. Rap1GAP2 was identified as a GTPase-activating protein for Rap1b in platelets (Schultess *et al*., 2005). Rap1GAP2 is activated by ADP- and/or thrombin-induced binding of the 14-3-3 protein. This event is inhibited by PKA- and PKG-mediated phosphorylation of Rap1GAP2, which in turn leads to the inhibition of Rap1b function in platelets (Schultess *et al*., 2005, Hoffmeister *et al*., 2008). The thromboxane A_2 receptor TP is a seven transmembrane domain

receptor that is linked to G_q, G_{12} and G_{13} proteins (See 1.4.2.2). Signaling through G_{12} and/or G_{13} proteins is involved in platelet shape change by activating RhoA/Rho-kinase pathway which inhibits, MLC phosphatase and leads to an increase in MLC phosphorylation (Klages *et al*., 1999). PKA was found to phosphorylate the TP-linked G_{13} protein in platelets, which blocks the thromboxane A_2-induced signaling (Manganello *et al*., 1999). Finally, a role for PKA in switching off its own signal has been reported as it phosphorylates and activates the cGMP-inhibited PDE3 (Macphee *et al*., 1988, Grant *et al*., 1988).

The number of identified platelet PKA substrates is very modest compared with that of putative physiological substrates reported in other cells, which now numbers 100 substrates (Anja Ruppelt, 2010). In addition, the functional outcome of some PKA-mediated phosphorylation events in platelets is still unknown. Moreover, the identification of some of these substrates relied on in *vitro* approaches that are yet to be verified *in vivo*. Furthermore no data exists on which PKA isoform targets these individual substrates. A recent phosphoproteomic study performed on resting human platelets suggested the presence of 23 putative PKA substrates including 12 that have not been reported before the most important of which is GPIbα (Zahedi *et al*., 2008). More work is needed to verify these observations and to further investigate the role of PKA basal activity in platelets. In addition, similar work is needed to identify more novel PKA substrates under PKA stimulatory conditions.

Table 1.1: Identified PKA substrates with their molecular weights and the proposed outcome of phosphorylation on platelet function.

PKA Substrate	Molecular Weight (kDa)	Confirmation	Proposed role of phosphorylation in platelets	Reference
Rap1b	22	Platelets	Unknown	(Lapetina *et al*., 1989, Altschuler and Lapetina, 1993)
Glycoprotein 1b β	24	Platelets	Inhibits actin polymerisation and platelet-vWF binding	(Wardell *et al*., 1989, Bodnar *et al*., 2002, Fox *et al*., 1987)
HSP27	27	*In vitro*	Unknown	(Butt *et al*., 2001)
LASP	37	Platelets	Unknown	(Butt *et al*., 2003)
$G\alpha_{13}$	44	Platelets	inhibits TxA_2-induced aggregation	(Manganello *et al*., 1999)
VASP	46/50	Platelets	Inhibition of integrin $\alpha_{IIb}\beta_3$	(Halbrugge and Walter, 1989)
Caldesmon	82	*In vitro*	Unknown	(Hettasch and Sellers, 1991)
MLCK	100	*In vitro*	Unknown	(Hathaway *et al*., 1981)
TRPC	100	Platelets	Unknown	(Hassock *et al*., 2002)
ABP	240	Platelets	Inhibition of cytoskeleton reorganisation during activation	(Chen and Stracher, 1989)
IP3R	260	Platelets	Unknown	(El-Daher *et al*., 2000, Cavallini *et al*., 1996)
PDE3A	110	Platelets	Activation of PDE3	(Macphee *et al*., 1988)

1.7 Compartmentalisation of cAMP/PKA signalling in platelets and other cell types

The concept of the parallel signalling cascades and the idea of molecules randomly floating in a homogenous cytoplasm are now obsolete. A more realistic concept of signal transduction describes cellular signalling cascades as a complex web of events that are sophisticatedly regulated in time and space. This means that at a specific moment of time in the cell, some signals are being initiated, others are being reduced or amplified and while others are being terminated. Moreover, structurally similar molecules can be anchored to different subcellular compartments where they mediate diverse signalling events resulting in different biological and functional responses.

GPCRs are a large family of receptors that is comprised of hundreds of members with each cell type expressing a multiplicity of them. Despite the expression of many GPCRs in one cell type, each GPCR still triggers a specific signal that regulates a specific biological function (Hermans, 2003). A large subset of these GPCRs is coupled to $G\alpha_s$ proteins, which activate different isoforms of AC and generate cAMP. The simplistic linear cAMP signalling pathway has been replaced by a more sophisticated yet realistic one (Steinberg and Brunton, 2001). The proposed system of cAMP signalling relies on the presence of an intricate network of signalling pathways within which a tight spatial and temporal regulatory mechanism governs the propagation and the transduction of a signal along unique branches of this network depending on the extracellular stimulus (Steinberg and Brunton, 2001). Such a sophisticated model has been suggested after observing that, in some cell types, cAMP mediates different biological functions depending on the stimulus. For

example, in cardiomyocytes both PGE_1 and isoproterenol induce cAMP production, but each one of them has a different functional outcome on the cell (Hayes *et al*., 1979). Moreover, PKA subsets are confined in different subcellular compartments with each subset being activated in response to a distinct stimulus. The specificity of any cAMP signal has been attributed to compartmentalisation of different components of the cAMP signalling pathway (Pidoux and Tasken, 2010, Zaccolo, 2011). The first line of cAMP signal compartmentalisation is the plasma membrane. The plasma membrane is heterogeneous containing different compartments with different lipid and protein composition characterised by raft and non-raft microdomains (Simons and Toomre, 2000, Marguet *et al*., 2006). Some $G\alpha_s$PCRs such as βAR as well as some AC isoforms such as AC3 and 6 are localised into lipid rafts whereas others are excluded (Willoughby and Cooper, 2007, Pontier *et al*., 2008). The differential localisation of receptors and AC, to membrane raft or non-raft domains, creates physical barriers that can separate distinct cAMP signalling networks, which can be simultaneously triggered in a specific cell type (Figure 1.12) (Cooper and Crossthwaite, 2006, Willoughby and Cooper, 2007). In addition to the physical confinement by lipid rafts, the diffusion of cAMP through the cytoplasm is controlled by the hydrolysing activity of specifically localised PDEs resulting in distinctively compartmentalised pools of cAMP (Zaccolo and Pozzan, 2002, Stangherlin and Zaccolo, 2012). The presence of these pools in many cell types has been confirmed by live cell imaging and fluorescence resonance energy transfer techniques (FRET) (Zaccolo and Pozzan, 2002). It has been also reported in other cell types that specific PDE isoforms are compartmentalised with specific PKA

isoforms (Tasken and Aandahl, 2004). For example in platelets, work published by Mann *et al* and Jensen *et al* who showed that inhibiting different PDE isoforms had different impacts on cAMP signalling pathway suggesting nonredundant roles for PDE2 and PDE3 and postulating the presence of specific cAMP pools into which specific cAMP components are compartmentalised (Manns *et al*., 2002, Jensen *et al*., 2004). Furthermore, an elegant chemical proteomic study in platelets showed recently that triggering GPVI-mediated signalling affect specific localised cAMP and cGMP pools with other pools not affected (Margarucci *et al*., 2011). More work is needed to confirm these hypotheses.

It has been shown in many cell types that the localisation of these cAMP pools also dictates the localisation of PKA isoforms (Tasken and Aandahl, 2004). The specific compartmentalisation of PKA isoforms has been proposed through observations that a particulate or a cytosolic fraction of PKA can be activated in response to different stimulus resulting in different outcomes (Brunton *et al*., 1981, Buxton and Brunton, 1986). Further studies using biochemical techniques aimed to study protein-protein interaction revealed that PKA is anchored to distinct subcellular compartments by a family of proteins called A-Kinase Anchoring proteins (Figure 1.12) (Carr and Scott, 1992).

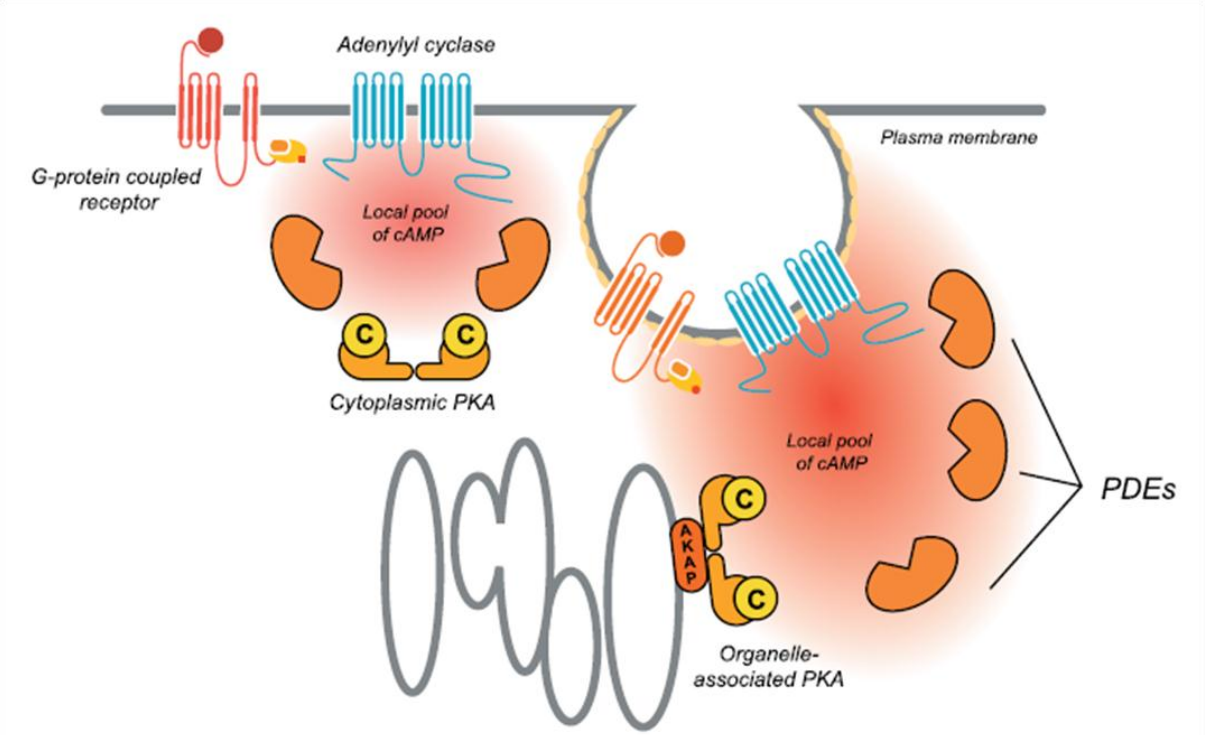

Figure 1. 12: The compartmentalisation of the cAMP/PKA signal.

Different G protein-coupled receptors are physically confined to different membrane domains. GPCRs, stimulated by different stimulus, activate proximal ACs and generate pools of cAMP. The concentration and the distribution of cAMP gradients are determined by PDEs. The physically confined receptors and ACs can associate with specific subcellular organelles or the cytoskeleton. These organelles can also harbour a specific PKA isoform through its binding to an A-kinase anchoring protein. This results in the limitation and the assembly of the cAMP pathway to a defined area of the cell where specific PKA substrates reside and can trigger a distinct biological effect. Figure and legend are from (Tasken and Aandahl, 2004).

1.8 A-Kinase Anchoring Proteins

A-kinase anchoring proteins or AKAPs are a family of structurally diverse yet functionally similar proteins that mediate the localisation of PKA into a close proximity with its substrates as well as signal terminating enzymes (Pidoux and Tasken, 2010, Smith *et al*., 2006). To date more than 50 members of this family including splice variants have been identified (Tasken and Aandahl, 2004). The important role of AKAPs further involves targeting PKA into specific subcellular compartments where cAMP pools, PKA substrates and PKA signal modulating enzymes reside. This provides spatial and temporal (spatiotemporal) regulation for PKA-mediated signalling events (Tasken and Aandahl, 2004). Each AKAP has a unique targeting domain that determines the localisation of the anchored PKA and despite the diversity in their structure, they all have a highly homologous PKA-binding domain (Tasken and Aandahl, 2004). This PKA-binding domain is comprised of 14-18 amino acid residues that form an amphipathic helix with hydrophobic residues are present on one face and charged ones on the other (Carr *et al*., 1991). The integrity of this amphipathic helix is critical for the binding to PKA (Figure 1.13). In fact, proline substitutions resulting in defects in the helical structure of this domain, compromises the binding to PKA (Carr *et al*., 1991). The dimerisation/docking domain of the regulatory homodimer of the PKA holenzyme has a unique docking site for AKAPs (Gold *et al*., 2006, Newlon *et al*., 2001, Leon *et al*., 1997). This docking site is an X-type four helix bundle which results from the dimerisation of two antiparallel polypeptides, at the N-terminus of each R subunit, in a helix-turn-helix motif (Figure 1.13). The AKAP docking site on PKA I and PKA II

are conformationally similar. In PKA II, it starts from residue 1 to 44 on and is slightly shifted on PKA I as it starts from residue 12 to 61 of the R subunit (Figure 1.11) (Leon *et al*., 1997). According to their affinity to each regulatory subunit of PKA, AKAPs are either PKA II-specific or PKA I and PKA II dual-specific (Tasken and Aandahl, 2004). Recently, a new entirely PKA I-specific AKAP has been identified (Means *et al*., 2011). RII has higher affinity to AKAPs compared to that of the RI (Herberg *et al*., 2000).

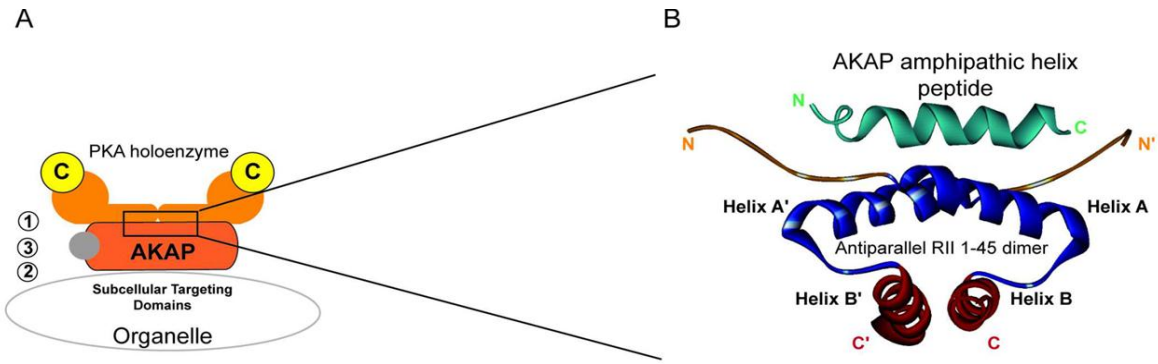

Figure 1. 13: The structure of PKA-AKP complex.

(A) A cartoon showing AKAP properties: 1) a conserved PKA binding domain binds PKA, 2) a unique targeting domain targets the complex into a specific subcellular compartment and 3) additional binding domains which can bind other signalling proteins such as other kinases or phosphatases. **(B)** An NMR-solved representation of the RII 1-45 diemer (yellow, blue and red) and the conserved AKAP amphipathic helix (green) which binds PKA. Figure and legend are modified from (Pidoux and Tasken, 2010).

Various techniques have been utilised to determine the functional role of PKA-AKAP interactions such as the use of inhibitory peptides, siRNA-mediated knockdown, expression of mutant AKAPs, generation of mutant mice and expression of compartment-specific AKAPs. Inhibitory peptides that can compete with AKAPs for binding to the D/D domain of PKA are one of the simplest and most widely used tools to determine the functional relevance of PKA-AKAP interactions (Figure 1.15). The first peptide to be developed was Ht31 which mimics the PKA binding domain of AKAP-Lbc, one of the earliest AKAPs to be characterised (Carr *et al*., 1991, Rosenmund *et al*., 1994). Ht31 has been shown to disrupt interactions of AKAPs with both PKA isoforms (Herberg *et al*., 2000). In order to delineate the specific outcomes of PKA I anchoring as opposed to that of PKA II, scientists have developed inhibitory peptides that can specifically block the interactions between either PKA I and AKAPs or PKA II and AKAPs. An example of the former is the RI-anchoring disruptor or RIAD (Carlson *et al*., 2006) and of the latter is SuperAKAP-*IS* (Gold *et al*., 2006).

In addition to their ability to bind and target PKA, AKAPs have been described as multienzyme scaffolding proteins. Enzymes such as the phosphotase PP2B (Coghlan *et al*., 1995), PKC (Klauck *et al*., 1996) and some PDEs (Dodge *et al*., 2001) have been reported to be also anchored by AKAPs. This can potentially create a macromolecule that not only regulates cAMP/PKA signal transduction positively but also negatively.

The presence of AKAPs in platelets has not been confirmed yet. However, some reports have already suggested that a spatial regulation mechanism for PKA activity might exist in platelets. El-Daher *et al* demonstrated that PKA substrates are differentially distributed in platelets, a finding which suggests that there must be a mechanism that facilitates the translocation of PKA into a close proximity with these substrates (El-Daher *et al*., 1996). Another report by the same group shows that PKA targets all three isoforms of the IP3-R, which they found to be distributed in different subcellular compartments (El-Daher *et al*., 2000). Chemical proteomic and RNA transcriptome data have shown that AKAPs are present in platelets (Margarucci *et al*., 2011, Rowley *et al*., 2011). However, validation of these findings by immunoblotting techniques and establishment of the functional relevance of their presence is still lacking.

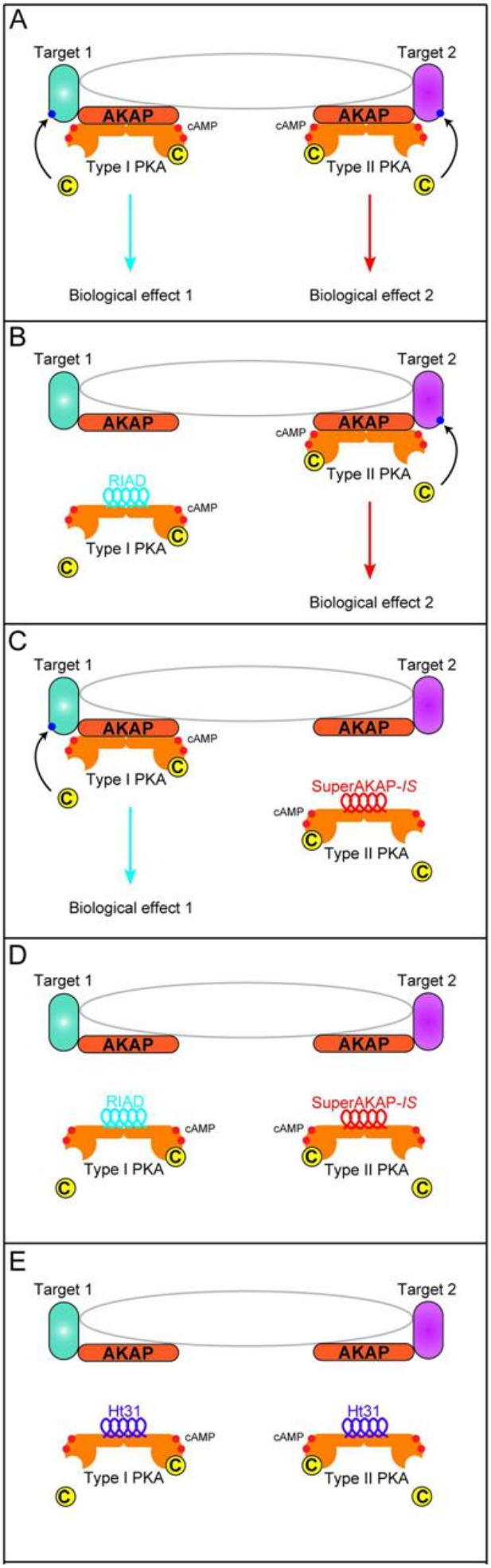
A
Target 1
Target 2
AKAP
cAMP
Type I PKA
Type II PKA
C
Biological effect 1
Biological effect 2
B
RIAD
C
Biological effect 2
D
SuperAKAP-IS
E
Ht31

Figure 1. 14: A schematic illustration of the effect of different PKA-AKAP disrupting peptides.

(A) A cartoon showing PKA-I and PKA-II anchored by AKAPs into different cellular compartments, where target 1 and 2 are localised, and mediating biological effect 1 and 2, respectively. **(B)** Shows how the RI-anchoring disruptor (RIAD) competes with the interaction of AKAP with **PKA-I** which blocks **only** biological effect **1**. **(C)** Shows how SuperAKAP-*IS* disrupts the interaction of AKAP with **PKA-II** which blocks **only** biological effect **2. (D)** Shows that when using both RIAD and SuperAKAP-*IS*, it blocks **both** biological effect **1** and **2**. **(E)** Shows the effect of the non-specific PKA-AKAP disruptor Ht31 which also results in blocking **both** biological effects **1** and **2**. Figure is from (Pidoux and Tasken, 2010).

1.9 Aims of this study

Platelet activation is critical for repairing vessel wall injuries and preventing excessive blood loss. Modulation of platelet activity, on the other hand, is equally important as it prevents unwanted activation and controls the growth of the clot to avoid vessel occlusion. Platelets are primarily regulated by PGI_2 and NO, which exert their effect through cAMP and cGMP signalling pathways, respectively (Schwarz *et al*., 2001, Smolenski, 2011). Compared with platelet activation, very little is known about the molecular mechanisms of platelet modulation by cyclic nucleotides.

cAMP is a second messenger that mediates a large variety of biological effects in response to different stimuli. The effects of cAMP are mediated by its main effector PKA, which phosphorylates specific substrates localised in different subcellular compartments. The specificity of cAMP signalling is achieved in a single cell through an intricate network of coexisting pathways that function under a precise spatial and temporal control (Stangherlin and Zaccolo, 2012).

Little is known about the regulation of cAMP/PKA signalling in platelets as opposed to other cell types. Platelets, like many other cell types, express different isoforms of every component of the cAMP/PKA signalling pathway (Rowley *et al*., 2011). But the differential contribution of these isoforms is very much elusive. Moreover, the spatial and temporal regulation of cAMP/PKA signalling cascade in platelets needs to be dissected. More work also needs to be done to clarify the precise functional role of various established PKA substrates as well as some putative ones, reported

in proteomic and transcriptome studies (Rowley *et al*., 2011, Zahedi *et al*., 2008), in modulating platelet activity.

We hypothesise that a precise spatiotemporal regulation among different cAMP signalling networks is present in platelets in order to achieve an adequate and specific inhibitory response. This study aims to investigate the mechanisms that govern this spatiotemporal regulation.

The aims of this study were,

- To characterize and compare the inhibitory dynamics as well as the potency of different cAMP elevating agents.
- To determine the role of platelet lipid rafts in the compartmentalization of cAMP signaling in blood platelets.
- To dissect the differential contribution of each PKA isoforms in platelets.
- To ascertain the presence of a spatial-temporal regulation of PKA signalling through AKAPs.

Chapter 2: Materials and methods

2.1 Materials

A detailed list of all the buffer composition and equipments which have been used throughout the study can be found in appendix I. A list of the main platelet agonists and inhibitors used in this study can be found in appendix II. All other general chemicals were bought from Sigma Aldrich and Fisher Scientific.

2.2 Methodologies used in the preparation of human blood platelets.

2.2.1 Procurement of human blood:

Blood was obtained by trained phlebotomists from healthy consented volunteers, who confirmed they were not taking any medication that interfered or might affect platelet function such as aspirin, anti-histamines and some non-steroidal anti-inflammatory drugs.

The venepuncture of the ante-cubital vein was performed using a 21G-butterfly needle. The first 2ml were discarded to avoid any artificial activation of the platelets. Subsequently, blood was collected in 20ml-syringes containing pre-warmed acid citrate dextrose (ACD) anticoagulant (see appendix I) at a ratio of 1:5.

2.2.2 Isolation of platelets from whole blood by lowering of blood pH.

This method was used throughout the study as an alternative to the classical prostacyclin method reported by Vargas *et al* (Vargas *et al*., 1982). The "pH method" was adapted from Mustard *et al* (Mustard *et al*., 1989), where pH of the plasma is reduced to 6.4 thereby preventing platelet activation during centrifugation. This method was used to avoid activating PKA signaling cascade which would potentially lead to misinterpretation of our data

Whole blood was centrifuged at 200g for 20 minutes room temperature (RT) to obtain platelet rich plasma (PRP). The PRP was transferred into a sterile 15ml centrifugation tubes and the plasma pH reduced to 6.4, by the addition of citric acid (0.3M) at ratio of 1:50. The PRP was then centrifuged at 800g for 12 minutes at RT to obtain platelet pellet and platelet poor plasma (PPP). The PPP was discarded, while the pellet was re-suspended in 5ml of washing buffer (see appendix I). The resuspended platelets were centrifuged again at 800g for 12 minutes at 20^{o}C to remove any residual plasma. The final pellet was resuspended in 1ml of modified Tyrode's buffer (see appendix I).

2.2.3 Quantification of platelet numbers.

Platelet quantification was performed manually using a haemocytometer**.** Isolated washed platelets (WP) were diluted at 1:100 with ammonium oxalate (1%w/v), to fix the platelets, and then applied to the double-chambered haemocytometer. The addition of a glass cover slip and the resulting confined space holds a defined volume of cell suspension 0.1mm above the grids. Platelets were then left to settle in the chambers by leaving them at a horizontal position for 10 minutes before they were visualized and counted under a converted light microscope (x40 magnification) (Figure 2.1). Dilution and volume corrections were applied to the count which was expressed as platelets/mL. Platelets were then diluted to the desired count depending on the experiment.

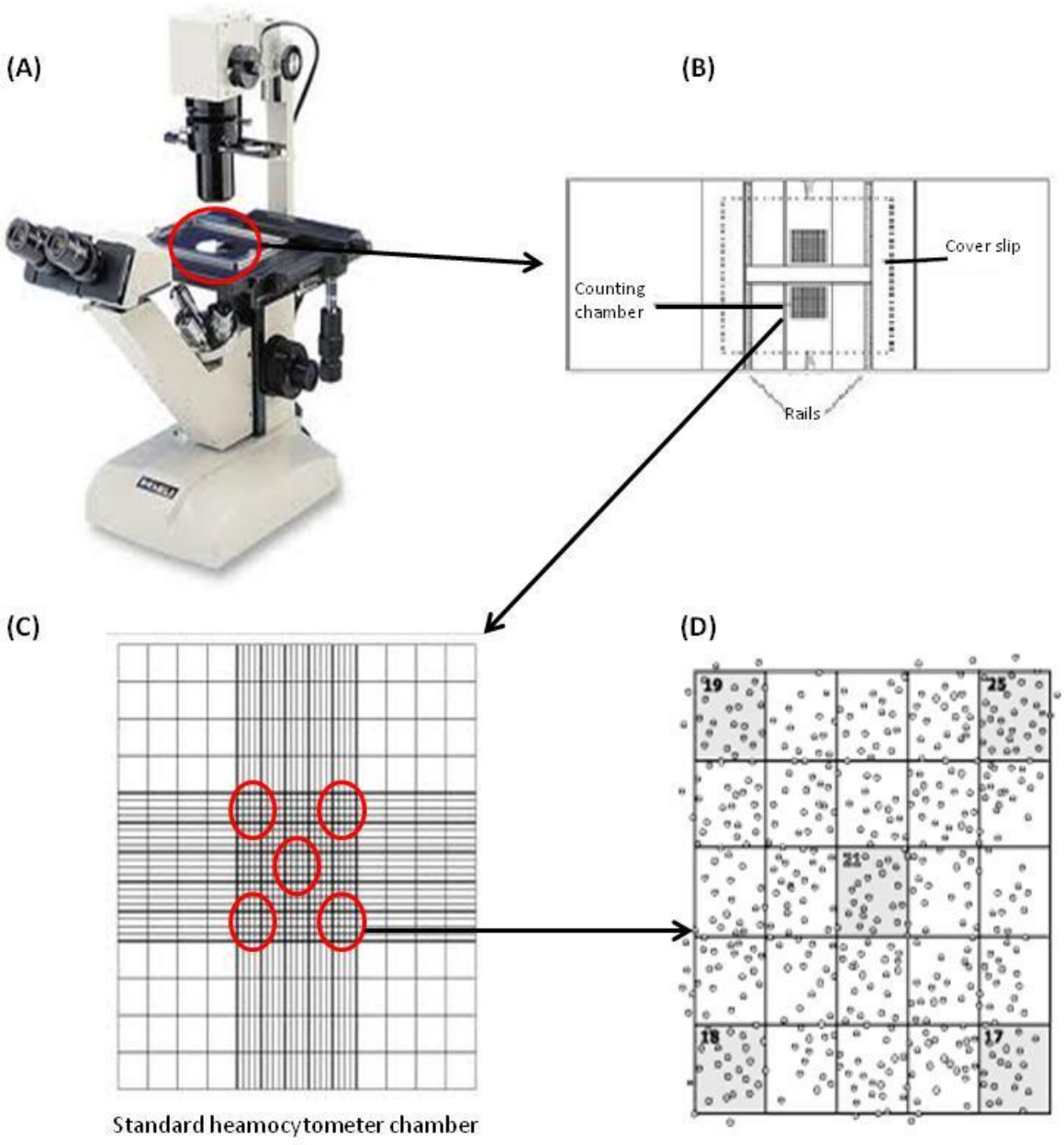

Figure 2. 1: Schematic representation of the platelet count technique.

(A) An inverted light microscope.

(B) A diagram representing a haemocytometer

(C) A diagram representing a single chamber with red circles representing where platelets are normally counted.

(D) A diagram representing a single square containing platelets.

2.3 Assessment of platelet functions

2.3.1 Platelet aggregation

Platelet aggregation is the final stage of series of chemical and biophysical events that take place in platelets after being activated with a specific stimulus. Although it can be considered a rather late index of platelet activity, this assay is still one of the most sensitive *in vitro* assays, which determines the functional viability of platelets in suspension. Light transmission aggregometery was developed by Born in 1962 and is based on changes in light scattering through a platelet suspension which is detected by a photocell (Born, 1962). It is assumed that when using small volumes with stirring that resting platelets are uniformly distributed in suspension. A homogenous platelet suspension would scatter the light. However, the addition of a platelet agonist activates platelets resulting in the formation of aggregates and hence the disruption of the homogeneity of suspension. This allows more light to go through the tube depending on the size of those aggregates which in turn is dependent on the level of activation. The extent of light transmission is proportional to the level of platelet aggregation which is in turn dependent on the degree of platelet activation**.** Prior to aggregation platelets undergo a shape change which can be observed on the trace as a momentary decrease in light transmission (Figure 2.2).

Washed platelets ($2.5x10^8$platelets/ml) were incubated with stirring (1000rpm) for 1min at 37^oC to allow for temperature equilibration. After the addition of a stimulus (collagen, Thrombin or vWF/Ristocetin) platelet aggregation would be monitored for 4 minutes with stirring (1000rpm) using a multi-channel Chronolog

aggregometer. In some cases platelet were treated with inhibitors such as PGI_2 prior to the addition of the agonist. The aggregometer is calibrated for every sample using untreated WP as 0% aggregation and modified Tyrode's buffer as 100%. The conditions of the individual experiments are described in detail in each of the subsequent chapters.

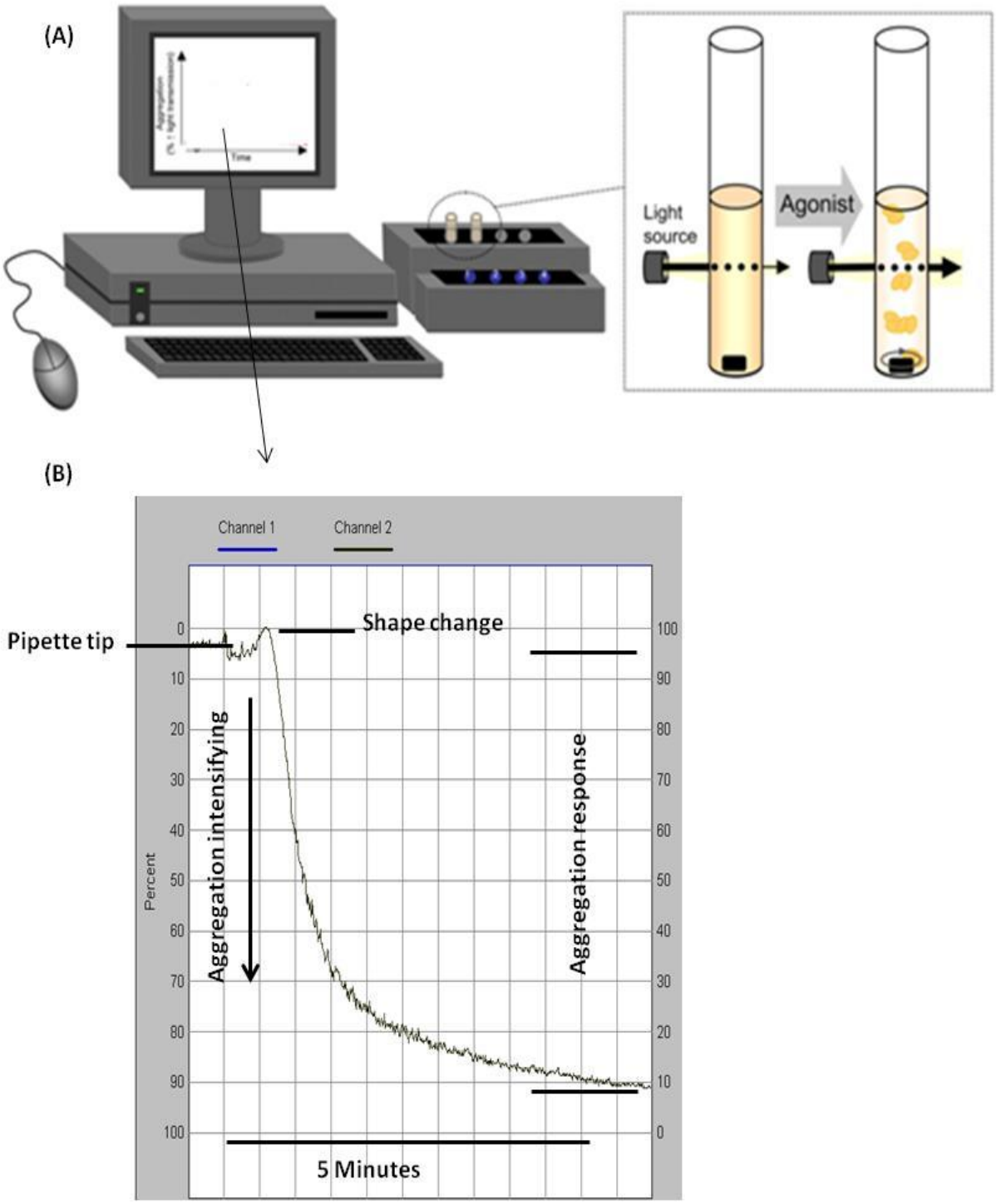

Figure 2. 2: A schematic discription of platelet aggregation assay.

(A) A schematic representation of the principle of aggregation, adapted from (Jackson, 2007). **(B)** A representative aggregation trace.

2.3.2 Measurement of platelet dense granule secretion

ATP release as a result of platelet activation was chosen to be an index to study platelet dense granule secretion. This assay relies on a luminescence reaction of the firefly extract luciferin with the enzyme luciferase. This reaction is ATP-dependent which is obtained, in this case, from platelets' dense granules as a result of activation (Feinman *et al*., 1977). The emission of light is detected by a specific light path in a Chrono-Log lumi-aggregometer and is translated in real time into a developing curve. In addition, aggregation is measured simultaneously so the temporal relationship between platelet aggregation and dense granule secretion can be evaluated.

Treated or untreated platelets, in aggregation tubes, are pre-incubated with the luciferin-luciferase mixture (chronolume; see appendix I) for two minutes, with stirring (1000rpm), before the addition of collagen (5 µg/mL). Secretion and aggregation levels are then monitored for 4 minutes. Secretion levels are then determined by the comparison to an ATP standard.

2.4 Methodologies used in the analysis of platelet proteins

Throughout this study platelet signaling proteins were analyzed by solubilising cellular membranes and then separating proteins according to their mass using a one-dimential, dissociating and discontinuous polyacrylamide gel electrophoresis system followed by different immunochemical detection techniques.

2.4.1. Immunoprecipitation

Immunoprecipitation is a method used to isolate a protein from a mixture such as a cell extract (figure 2.3)**.** An antibody selective for a target protein is added to the mixture to form antibody-antigen complexes. The complexes are then precipitated by adsorbing the antibodies to an insoluble matrix such as agarose or sepharose beads conjugated to protein A or G. The latter two proteins derive from bacteria and are stably bound by antibody constant regions. The isolated protein may be studied further using SDS-PAGE and Western blotting.

2.4.1.1 Immunoprecipitation methodology

Samples were prepared as described in section 2.4.2.1, with the exception that the reactions were terminated by the addition of IP lysis buffer (see appendix I) in the presence of protease and phosphatase inhibitor cocktails (1:200). All samples were transferred into eppendorfs and put on ice until the beads were ready.

A 50% (w/v) suspension of either protein A or G sepharose beads in TBS-T was prepared (slurry). Equal aliquots of the slurry were either incubated with the appropriate amount of the antibody of interest or with the same amount of normal IgG control to account for protein-antibody nonspecific bindings. The antibody and the slurry were allowed to bind for at least one hour with agitation at 4^{o}C. Meanwhile, the cell lysate (300-500µg of proteins) was precleared by incubating with the slurry. The beads were then pelleted by centrifugation at 8500*g* for 1min. The supernatant was transferred into a clean eppendorf, to ensure the elimination of any potential nonspecific bindings with the beads. The antibody-bound beads were then incubated with precleared lysate overnight with agitation at 4^{o}C before centrifugation for 1min at 8500*g*. The resultant supernatant was discarded whereas the pellet washed sequentially, once with IP lysis buffer and twice with TBS to remove residual proteins. The beads were then boiled in Laemmli buffer to release the proteins of interest from the beads (Figure 2.3). The beads were pelleted through centrifugation for 1min at 8500*g* and the liberated proteins separated by SDS-PAGE and analysed by Western blotting.

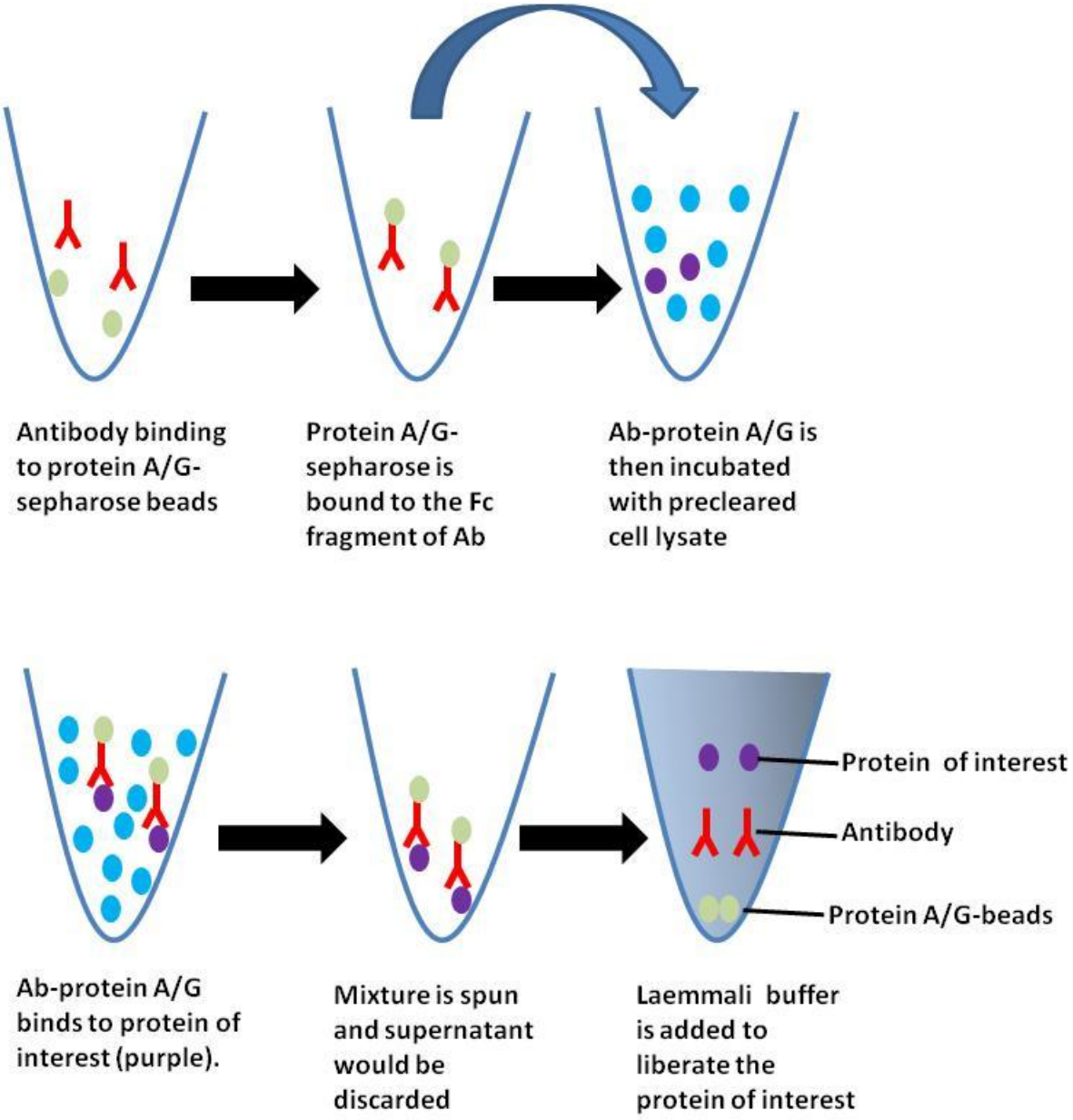

Figure 2. 3: A schematic summary of the immunoprecipitation method.

2.4.2 Sodium dodecyl sulphate -polyacrylamide gel electrophoresis (SDS-PAGE)

One-dimensional sodium dodecyl sulphate-polyacrylamide gel electrophoresis is used to separate charged macromolecules in an electric field. When applied to a porous matrix such as a gel it can be used to separate molecules based on their size and charge. The main principal of this technique is to combine the properties of negatively charged SDS, a polyacrylamide gel and electrophoresis.

SDS is an anionic detergent that binds and denatures proteins leaving them with similar, rod-shaped tertiary structure. Furthermore, it confers equal negative charge per unit protein mass (1.4g SDS per 1g protein). This protein binding affinity results in neutralizing all positively charged amino acids and giving all peptides a constant negative charge at an equal charge/unit length ratio. This allows the proteins to migrate from the anode towards the cathode depending on their molecular weight.

SDS-Polyacrylamide Gel Electrophoresis (PAGE), uses a combination of SDS and the polyacrylamide gels to separate proteins according to their molecular masses by electrophoretic migration. Acrylamide molecules polymerise into long linear chains which are cross-linked by bisacrylamide. This polymerisation is accelerated by the presence of free radicals. Hence, ammonium persulphate (APS) is added when casting gels as it decomposes to release SO_4^- ions. Tetramethylethylenediamine (TEMED) is also included to catalyse the decay of APS. The percentage of the acrylamide used in these solutions determines the pore size and therefore the relative separation of the proteins within the mixture.

Throughout this study a dissociating-discontinuous buffer system was used in all SDS-PAGE experiments. The dissociating system utilizes the denaturing properties of SDS and a reducing agent so proteins can run in a primary structure. The discontinuous buffer system depends on loading samples on a low-percentage stacking gel at pH 6.8, which allows the proteins to be concentrated and then enter the resolving gel all at the same time. Conversely, the resolving gel has higher percentage at pH 8.8 to allow protein separation according to size.

.

2.4.2.1 Sample preparation for SDS-PAGE

Sample preparation performed based on the method described by Laemmli (Laemmli, 1970), which uses a denaturing agent (SDS) and a reducing agent (2-mercaptoethanol) in order to lyse the cells and reduce all proteins to their primary structure. All platelet samples for SDS-PAGE and immunoblotting were prepared at 37^{o}C under stirring at (800rpm). In some cases platelets were incubated with EGTA (1mM), apyrase (1U/mL) and indomethacin (10µM) to create non-aggregatory conditions. When pre-treating samples with reagents that require more than 2 minutes incubation, they would only be stirred for 30 seconds and then left at 37^{o}C for the required incubation time. Platel*et al*iquots (200µl) were stimulated with different agonists and/or inhibitors and the reaction was terminated by the addition of an equal amount of x2 laemmli buffer (see appendix I). . Samples were then stored at -20^{o}C. Before analyzing those samples by SDS-PAGE and immunobloting, they were boiled for 3 minutes to ensure denaturation of all proteins.

2.4.2.2 Quantification of platelet protein concentrations

Protein concentration was determined using the Bio-Rad *DC* Protein Assay kit according to the manufacturer's protocol. It is based on the well-established Lowry assay (Lowry *et al*., 1951) that is applied on detergent-solubilized cell lysates. This assay measures the intensity of a characteristic blue colour, at 750nm, that develops as a result of a reaction between proteins with copper in an alkaline medium and the subsequent reduction of a Folin reagent. The main residues that are involved in this interaction are tyrosine and tryptophan residues. The more blue colour is produced the more protein there is in the sample. BSA solutions of defined concentrations were used to calculate sample protein concentration. Each sample and standard was diluted 1:2 in protein assay buffer (see appendix) and was assayed in triplicate in a 96-well plate. Light absorption at 750nm was obtained using a multiplate reader.

2.4.2.3 Sodium dodecyl sulphate-polyacrylamide gel electrophoresis methodlogy

In this study a 7.5 or 10% polyacrylamide gel were used depending on the protein under investigation, (see Appendix). For phospho-PKA substrate as well as tyrosine phosphorylation protein profiles, 10-18% gradient gels were used. Each gel is composed of acrylamide monomers with cross linking agent (bisacrylamide) to enhance the polymerization of these monomers. Furthermore, ammonium persulphate (APS) and tetramethylethylenediamine (TEMED) are also added in order to initiate and accelerate the polymerization reaction respectively. A 1.5mm resolving gel was poured either directly or with the help of a peristaltic pump. This

was followed by direct pouring of the 3% stacking gel. For gradient gels, an aliquot of 10% and another for 18% were consecutively poured into the channels of a gradient mixer and then were poured using a peristaltic pump that was connected to the mixer. Wells within the gel were loaded with aliquots of protein samples (20µg) along with a biotinylated protein standard (see appendix I). Fixed percentage gels were subjected to 120V for 90 minutes, while gradient gels were subjected to the same voltage but for 2.5 hours.

2.4.3 Immunoblotting

Western blotting is a powerful and commonly used method to indirectly detect and quantify a protein or a group of proteins in a mixture (Towbin *et al*., 1979). This involves transferring the proteins from a gel to an adhesive matrix such as nitrocellulose or polyvinylidene difluoride (PVDF) membranes under an electric field. Once transferred, the membranes are probed with specific primary antibodies against target proteins. This is followed by incubation with an enzyme-conjugated secondary antibody, usually horseradish peroxidase (HRP). Detection of antigen-bearing proteins is facilitated by enhanced chemiluminescence (ECL) through which a signal can be produced as a result of an interaction between hydrogen peroxide and luminol in the presence of horseradish peroxidase. The outcome of this interaction is an excited product, which decays to a lower energy state and simultaneously luminesces at 425nm that can be captured and visualized on x-ray films.

2.4.3.1 Western blotting methodology for detection of platelet proteins

After separation of the protein mixtures by SDS-PAGE, separated proteins were transferred into a methanol-pre-activated PVDF membrane at 100V for 2.5 hours. The correct order of the gel and membrane in the cassette as well as the orientation of the cassette in the tank ensures the migration of the negatively charged proteins on the gel towards the anode, which results in their capture by the membrane (Figure 2.4). The membrane was then blocked, to inhibit nonspecific protein-membrane interactions, by incubation with bovine serum albumin (BSA; 10% w/v) (see appendix I) or skimmed dry milk (5% w/v) in TBS-T for 30 minutes at room temperature with agitation . After blocking, the membrane was incubated with the primary antibody (1:1000 in 2% BSA/TBS-T unless otherwise is stated) overnight at 4^{o}C with agitation. After two TBS-T washing steps, membranes were incubated for 1 hour at room temperature with an HRP-conjugated anti-rabbit or anti-mouse secondary anti-body (1:10000 in TBS-T). This was followed by six washing steps of 15 minutes with TBS-T. When using milk for blocking, the same protocol was followed except that all washing steps were carried out with the milk-based blocking buffer and primary and secondary antibodies were made with 1% w/v skimmed dry milk solutions in TBS-T. Membranes were then incubated with enhanced chemiluminescence solutions (ECL1 and ECL2; see appendix I) and the produced signal was captured on an x-ray film which was visualized using developer and fixer solutions (see appendix I).

In some cases antibodies were stripped by incubating membranes with Restore^{TM} western blotting stripping buffer (Thermo Scientific, UK) with agitation. Here,

membranes were incubated for 20 minutes at room temperature, followed by two washing steps, with TBS-T and re-blocking with BSA/TBS-T (10% w/v) for 30 minutes. Membranes were then reprobed with anti-β-tubulin antibody (1:1000) overnight at 4^{o}C to check for equal loading of protein in each lane.

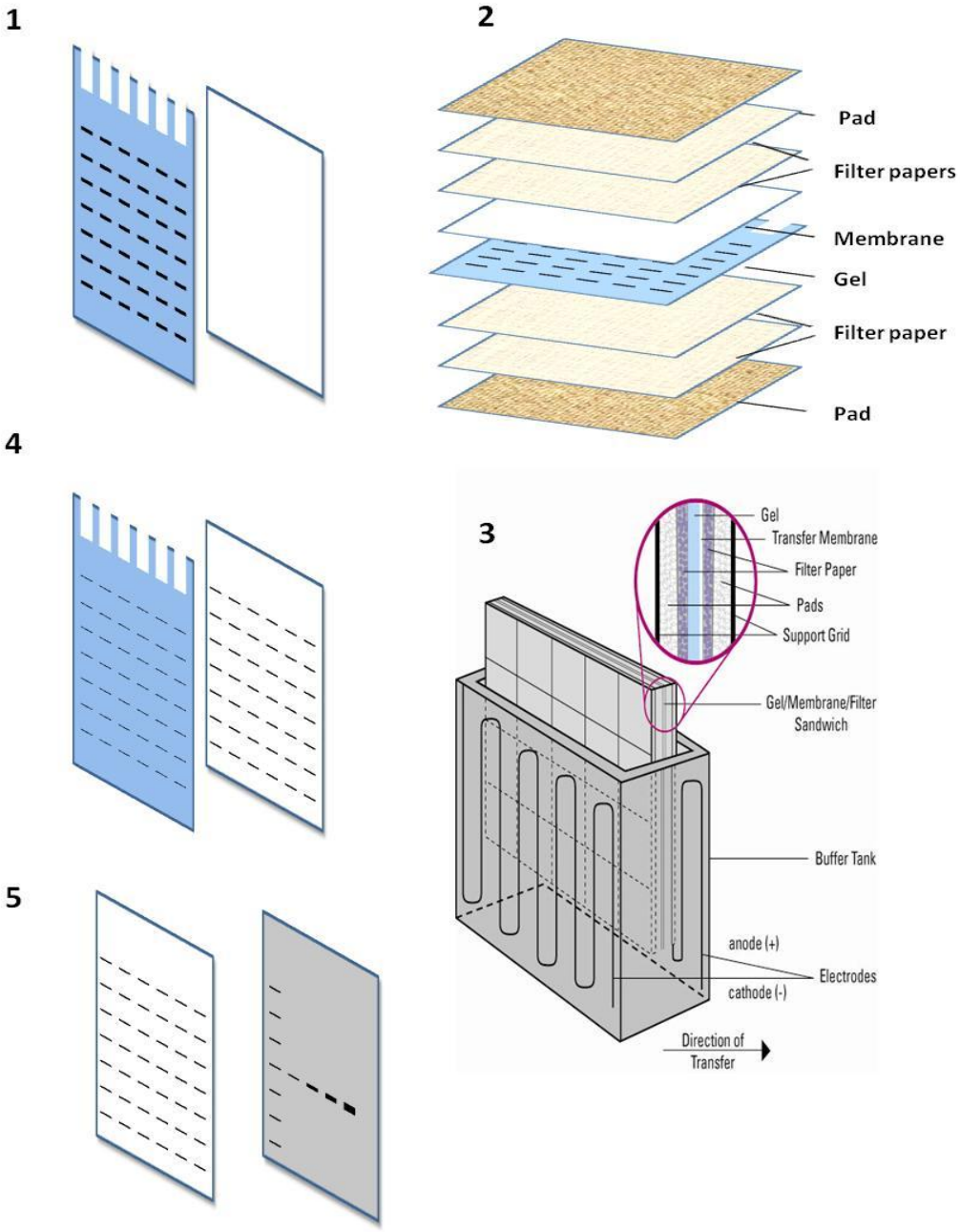

Figure 2. 4: A schematic summary of the western blotting method.

Proteins are first resolved via SDS-PAGE (1), the western blot sandwich is then prepared (2), followed by western blot apparatus assembly (3), protein transfer then takes place (4) and finally membrane is developed on a photographic film after probing the membrane with antibody of protein of interest (5).

2.5 Isolation of platelet lipid rafts

Lipid rafts are dynamic assemblies enriched in cholesterol and sphingolipids forming islands of lipids that exist in a liquid-ordered state discrete from the bulk of the membrane lipids that exist in a liquid-disordered state. It is well established in the literature now that lipid rafts play an important role as platforms of signal transduction (Simons and Toomre, 2000). This is fulfilled by bringing different signaling molecules, either raft-based or non-raft-based, into close proximity which focuses the signal and ensures its specificity. Lipid raft isolation methods exploit two essential characteristics of those liquid-ordered membrane assemblies. Firstly, lipid rafts are resistant to low temperature non-ionic detergent solubilization. Secondly, their relative low density allows them to float into 5-30% sucrose gradients following ultracentrifugation (Hooper, 1999). These characteristics were used to isolate lipid raft membrane fractions in blood platelets.

2.5.1 Lipid raft isolation by sucrose ultracentrifugation.

This method was adapted from Lee *et al* (Lee *et al*., 2006). Platelet samples (450µl; $1x10^9$ platelets/ml) were treated as described in 2.4.2.1, with the reaction terminated by the addition of x2 lipid raft lysis buffer (see appendix I) in the presence of protease and phosphatase inhibitor cocktails (1:200). All samples were transferred into eppendorfs and placed on ice for 30 minutes to induce solubilization. Cell lysates were then transferred into an Ultra-ClearTM tube (Beckman Coulter, UK) and a sucrose gradient created. An 80% w/v sucrose solution (900µl) was added at the bottom of the tube and mixed with the solubilized cells to generate a 40% sucrose layer. A second 30% w/v sucrose solution (5 mL), followed by a third 5% w/v sucrose solution (5 mL) were carefully layered sequentially on top of the initial layer. All sucrose solutions were made with x1 lipid raft lysis buffer. The sucrose density gradient containing platelet lysates were ultracentrifuged at 200,000g for 18h at 4^oC using a SW41-Ti rotor. Twelve fractions of 1ml were then removed from the top of the tube (Figure 2.5). These fractions were subjected to SDS-PAGE and immunoblotting after the addition of equal amounts of laemmli buffer. LAT and β3 were used as markers for lipid rafts and soluble fractions, respectively.

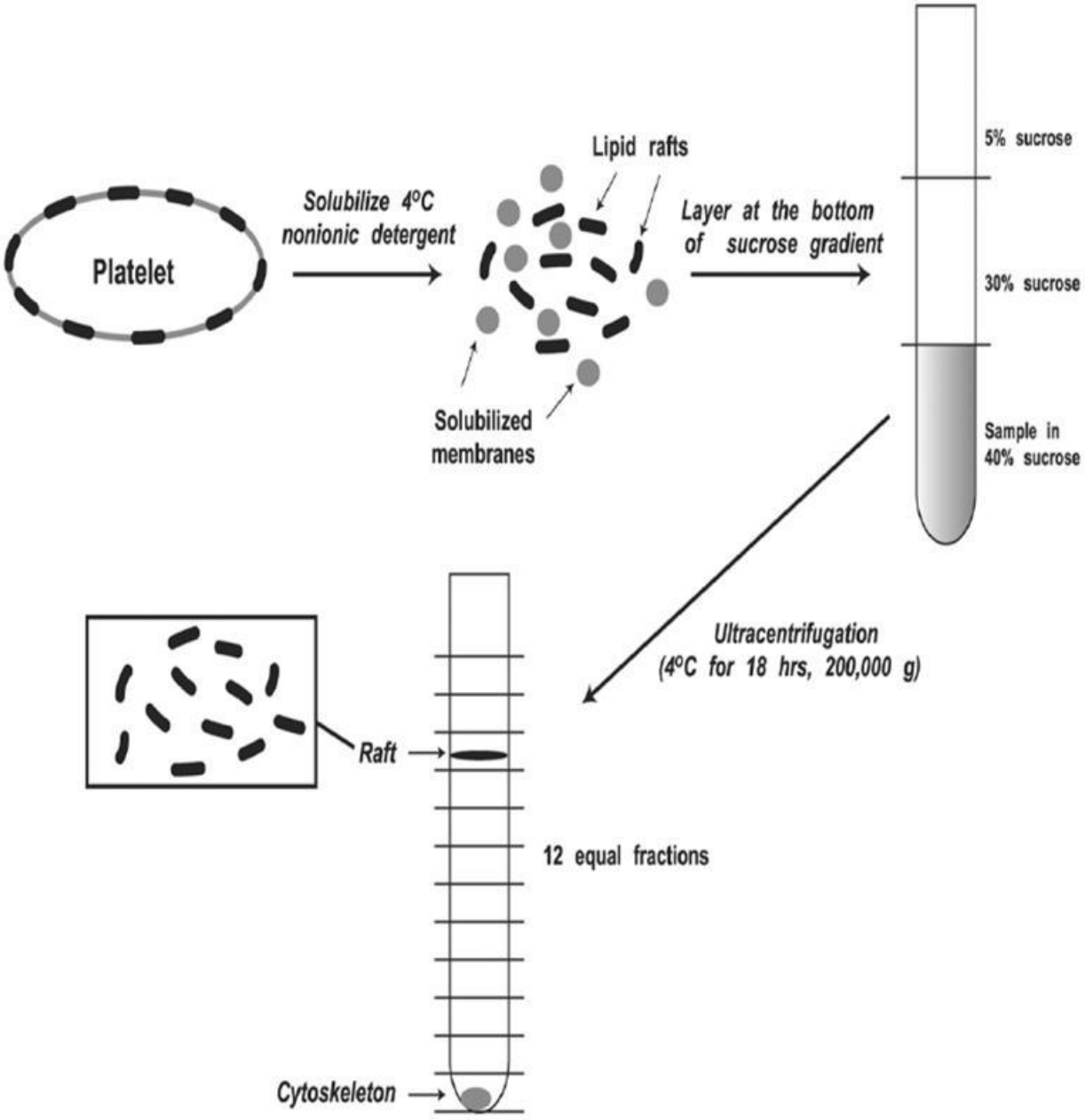

Figure 2. 5: A schematic representation of the lipid raft isolation method.

Diagram is taken form (Gibbins, 2004b)

2.6 Determination of cAMP levels

cAMP levels were determined using a well-established enzyme-immuno assay (EIA) kit (Cayman Chemical Company) according to the manufacturer's protocol. This assay is based on the competition between free cAMP and acetylcholinesterase-conjugated cAMP (cAMP tracer), to occupy a limited number of cAMP binding sites on a cAMP-specific rabbit antibody. The amount of free cAMP is variable depending on sample treatment whereas the amount of cAMP tracer is constant in every assay. Therefore, the amount of cAMP tracer bound to the cAMP rabbit antibody is inversely proportional to the amount of free cAMP in the sample. The rabbit antibody-cAMP complex, either free or conjugated, binds to a mouse anti-rabbit IgG with which the plate has been previously coated.

cAMP standards, samples, cAMP tracer and the cAMP rabbit antibody are all added to the mouse anti-rabbit IgG-precoated plate. The mixture is then left for 18 hours to allow the binding. After washing, the acetylcholinesterase's substrate is added to induce an enzymatic reaction that results in a coloured product, which can be read between 405-412 nm (Figure 2.6). The intensity of the colour determines how much cAMP tracer is bound to the antibody, which is inversely proportional to the amount of free cAMP that is competitively bound to the same antibody.

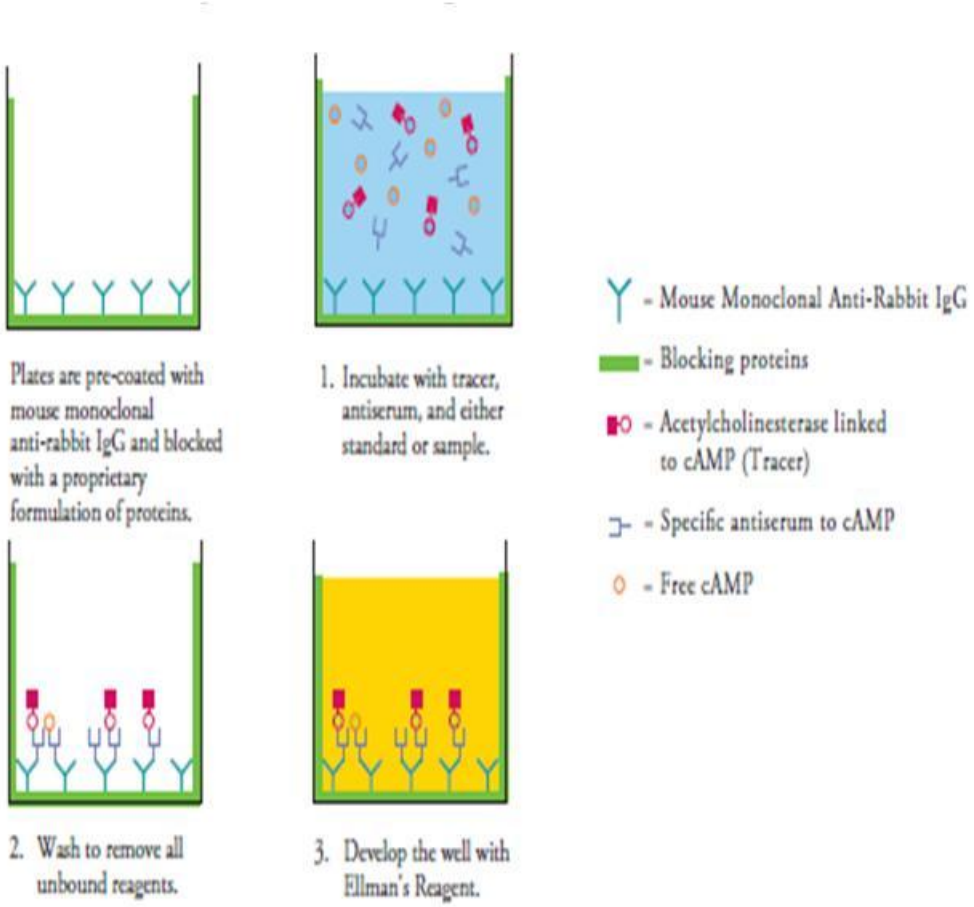

Figure 2. 6: A schematic representation of cAMP EIA (courtesy of Cayman Chemicals).

2.6.1 Sample preparation for cAMP EIA

Washed platelets were treated as usual and then sample media was removed as recommended by the manufacturer to minimize any potential interference with the assay.

Platelets (200µl; $2x10^8$ platelets/ml) were treated with PGI_2 (50nM) for 30 seconds. Following treatments, samples were transferred into clean eppendorf tubes and then centrifuged at 1000*g* for 10mins. The supernatant was discarded whereas the pelleted cells were lysed with 200µl 0.1M HCl for 20 min on ice. The samples were centrifuged again at 1000*g* for 10mins to pellet cell debris. Supernatant was then diluted with the EIA assay buffer at a ratio of 1:4. Following sample preparation, cAMP standards (0.078-10 pmol/mL) were prepared following the manufacturer's protocol to generate a standard curve.

In order to increase the sensitivity of the assay, an acetylation protocol was used. Since cyclic nucleotides are not immunogenic molecules, cAMP antibodies are normally raised against the conjugate and hence their affinity towards free cAMP is quite low. However, acetylation of cyclic nucleotides with potassium hydroxide and acetic anhydride results in a structure that mimics the immunogenic structure of the conjugate and consequently enhances the affinity of the antibody towards cAMP molecules.

All samples and standards were acetylated according to the manufacturer's protocol before carrying out the assay. All wells were read at 405 nm using a Thermo Scientific multiplate reader. Raw data were processed then analysed according to the manufacturer's protocol and using their automated analysis tool at

www.myassays.com or their computer spreadsheet at www.caymanchem.com/analysis/eia.

2.7 Determination of cholesterol concentrations

Platelet cholesterol concentrations following lipid raft fractionation were determined for each fraction using a commercially available cholesterol assay kit (Cayman chemical company). The assay relies on an enzymatic reaction that can detect both free and esterised cholesterol. Cholesteryl esters are firstly hydrolised by cholesterol esterase to free cholesterol. Total free cholesterol is then oxidized by cholesterol oxidase to yield hydrogen peroxide and the corresponding ketone. The addition of horseradish peroxidase (HRP) in the presence of ADH (10-acetyl-3-7-dihydroxyphenoxazine), which is a stable and sensitive probe for hydrogen peroxide, results in the production of a highly fluorescent resorufin (Amundson and Zhou, 1999). The produced fluorescence can be read using excitation wavelengths of 530-580 nm and emission wavelengths of 585-595 nm.

Cholesterol contents of every fraction were determined after preparing cholesterol standards. The assay and raw data analysis were carried out according to the manufacturer's protocol and final data were expressed as µM cholesterol.

2.8 Investigation of potential AKAP-PKA interactions in platelets.

In order to establish the functional relevance of AKAP-PKA interactions in different cellular processes, a number of synthetic peptides has been developed that can compete with AKAPs for PKA binding. These peptides contain an amino acid sequence that mimic the PKA binding domain of an AKAP allowing them to form an amphipathic helix. The permeability of these peptides is normally enhanced through attachment with molecular carriers such as polyarginine tails or stearic acid. The first peptide to be identified as an AKAP-PKA inhibitor was the Ht31, which disrupts interaction of AKAPs with both PKA I and PKA II (Carr *et al*., 1991). Recently more specific peptides have been developed in order to isolate cellular processes that are regulated by individual PKA isoforms. Examples of these specific peptides is the development of the RI-anchoring disruptor also known as RIAD (Carlson *et al*., 2006) and SuperAKAP-*IS* (Gold *et al*., 2006), which target PKA I-AKAP and PKA II-AKAP interactions, respectively. Throughout this study both RIAD-Arg_{11} and st-Ht31 were used to study the functional relevance of AKAP-PKA interactions in blood platelets.

2.8.1 R-I Anchoring Disruptor (RIAD) synthesis and determination of loading conditions

RIAD is an inhibitory peptide than has been developed by Prof. John Scott's group in 2006 (Carlson *et al*., 2006). This peptide binds competitively to the docking and dimerization domain of protein kinase A inhibiting the binding of this domain to PKA binding domain on an AKAP. This results in uncoupling of the PKA from AKAPs

allowing the study of the importance of this interaction. In addition, this peptide is highly specific to PKA-I specific AKAPs (AKAP-I) as has been reported by the same group (Carlson *et al*., 2006).

RIAD was kindly supplied to us throughout this study by Prof. Kjetil Tasken (University of Oslo, Norway). The regular peptide (RIAD: LEQYANQLADQIIKEATEK) and the scrambled negative control (scRIAD: IEKELAQQYQNADAITLEK) were synthesized and tagged with an 11 residue long arginine tail to enhance cellular permeability (Nakase *et al*., 2008). The cellular uptake of the PKA-AKAP inhibiting peptide was determined by conjugating the peptide to fluorescein then carrying out a standard static adhesion experiment following a well-established protocol optimized by our group (Oberprieler *et al*., 2007).

2.8.2 RIAD-Arg_{11} conjugation with fluorescein

The peptide was labeled with fluorescein, which is a fluorophore whose absorption maximum is at 495nm and emission maximum is at 521nm. Fluorescein was conjugated to RIAD at a molar ratio of 5:1 (fluorescein:RIAD). Briefly, the fluorescein was firstly dissolved in dimethyl formamide DMF and then the peptide was added to the solution. A catalyzing mixture of 0.5 M N,N-diisopropylethylamine (DIPEA) and 1M 2-(1H-Benzotriazole-1-yl)-1,1,3,3-tetramethyluronium hexafluorophosphate (HBTU) was added to the DMF-dissolved mixture to catalyze the condensation reaction of fluorescein with RIAD. The mixture was then left for 1 hour at room temperature to allow the conjugation. The DMF was then removed by precipitating the peptide with ice-cold ether. The mixture was then freeze-dried overnight to remove the residual ether. The peptide was then dissolved with water and subsequently used with washed platelets. For platelet visualization method please see section 2.10.1.

2.9 Data representation and statistical analysis

Aggregation data with platelet inhibitors were represented as percent inhibition of maximum aggregation.

$$\% \text{ inhibition of aggregation} = \frac{\boldsymbol{aggregation\ max - aggregation\ after\ treatement}}{\boldsymbol{aggregattion\ max}} \times \mathbf{100}$$

For Western blotting, a representative blot of three independent experiments was shown. In some cases densitometry analysis was carried out on scanned blots using *Image J* software.

cAMP data were presented as fmol cAMP/10^7 platelets. In some cases they were expressed as percent increase in cAMP over basal levels.

$$\% \text{ increase of cAMP levels} = \frac{\boldsymbol{cAMP\ levels\ after\ treatment - basal\ cAMP\ levels}}{\boldsymbol{basal\ cAMP\ levels}} \times \mathbf{100}$$

Results for experiments that have been carried out at least three times were expressed as means $\pm$ SEM for the number of experiments indicated (n). Data were checked for normality and then analysed by t-test or analysis of variance (ANOVA) using Statistical Package for Social Sciences (SPSS, version 15) and Microsoft Office Exel (2007). Data with $p \leq 0.05$ were considered significant.

2.10 Supplementary methods

The following experiments were carried out by Dr. Simbarashe Magwenzi.

2.10.1 Visualization of RIAD uptake by adhered platelets

Unstained platelets ($5x10^7$platelets/ml) were incubated with the fluorescein-conjugated peptide (1µM) for different time points at 37^{o}C. Platelets were then washed with platelet washing buffer two times. After that, platelets were left to adhere for 30 minutes at 37^{o}C on a glass slide. Two washing steps with PBS were carried out after incubation, to remove unbound platelets, followed by fixation with 4% w/v paraformaldehyde for 30 minutes. Slides were then visualized with an Olympus 1X71 fluorescence microscope equipped with an XM10 CCD camera (Olympus, Japan). Images were captured under an x60 oil emersion objective lens and analysed using ImageJ software from the National institute of Health (NIH, USA).

2.10.2 Platelet aggregation under flow

This method was adapted from Kulkarni *et al* (Kulkarni *et al*., 2007). Platelets ($4x10^8$ platelets/ml) were incubated with either RIAD-Arg_{11} or scRIAD-Arg_{11} (10µM) for 1h at 37^{o}C then treated with PGI_2 (100nM) for 2min. The platelets were subsequently fluorescently labeled with DIOC6 (1µM) at 37^{o}C for 10min and reconstituted with autologous washed red blood cells (50% v/v). Reconstituted blood was perfused through glass microslide capillary tubes (Camlab; Cambridge, UK), coated with von Willebrand's Factor (vWF, 100µg/mL) for 12h at 4^{o}C and blocked with BSA

(10mg/mL) for 1h. Perfusion was carried out at a constant shear rate of $1000s^{-1}$ for 4min followed by flushing with PBS for 4min at equivalent shear to leave only stably adherent platelets. Images of adhered platelets were captured under ×60 magnification of an IX71 fluorescence microscope equipped with an XM10 CCD camera (Olympus, Japan) and analysed using ImageJ software (NIH). Data are presented as surface area coverage (%), since the software could not fully discriminate between single platelets and platelet aggregates (Kulkarni *et al*., 2007).

Chapter 3: Characterization of platelet inhibition by agents that activate Protein kinase A

3.1 Introduction

Under physiological conditions, platelets circulate in a quiescent state that is maintained by the non-thrombogenic environment imposed by the endothelium. The undamaged endothelium releases anti-thrombogenic agents into the blood, which both limit platelet activation and control their activity once they have encountered a vascular injury. The major endothelial-derived anti-thrombogenic agents include nitric oxide (NO) (Mellion *et al*., 1981) and at least two prostanoids including prostacyclin (PGI_2) (Moncada *et al*., 1976) and prostaglandin (PGE_1) (Kloeze, 1970). Prostacyclin has been considered the main physiological cAMP-dependent platelet inhibitor (Tateson *et al*., 1977).

These physiological platelet inhibitors exert their effects by triggering two different cyclic nucleotide-dependent signalling pathways, cyclic adenosine monophosphate- and cyclic guanine monophosphate-dependent signalling pathways. This thesis will particularly focus on the former, which is physiologically triggered in platelets by prostacyclin (PGI_2) and prostaglandin (PGE_1). PGI_2 bind to its Gs-protein-coupled receptor, the IP receptor. This binding leads to the activation of the transmembane embedded adenyl cyclase (AC), which results in the elevation of cAMP concentrations (Dutta-Roy and Sinha, 1987). Protein kinase A (PKA) is the main effector of cAMP in blood platelets. It is a serine/threonin kinase that phosphorylates different target proteins and this leads to the regulation of several

aspects in the process of platelet activation (Smolenski, 2011). In this thesis, understanding the mechanisms of how the cAMP/PKA signalling system regulates platelet function is the overarching aim. To achieve this, a number of different tools were used including agents that target the cAMP/PKA signalling cascade at different levels. Therefore, it was important to characterise these agents.

Physiological agents such as PGI_2 and PGE_1 were used to stimulate the whole pathway downstream of different receptors. On the other hand, nonphysiological agents such as forskolin and cAMP analogues were used to trigger the pathway downstream of GPCR and AC, respectively.

Therefore, it was very important to characterize each of these agents in terms of their ability to activate the cAMP/PKA signalling pathway and inhibit platelet function before they were used to study the molecular regulation of this pathway in the successive chapters.

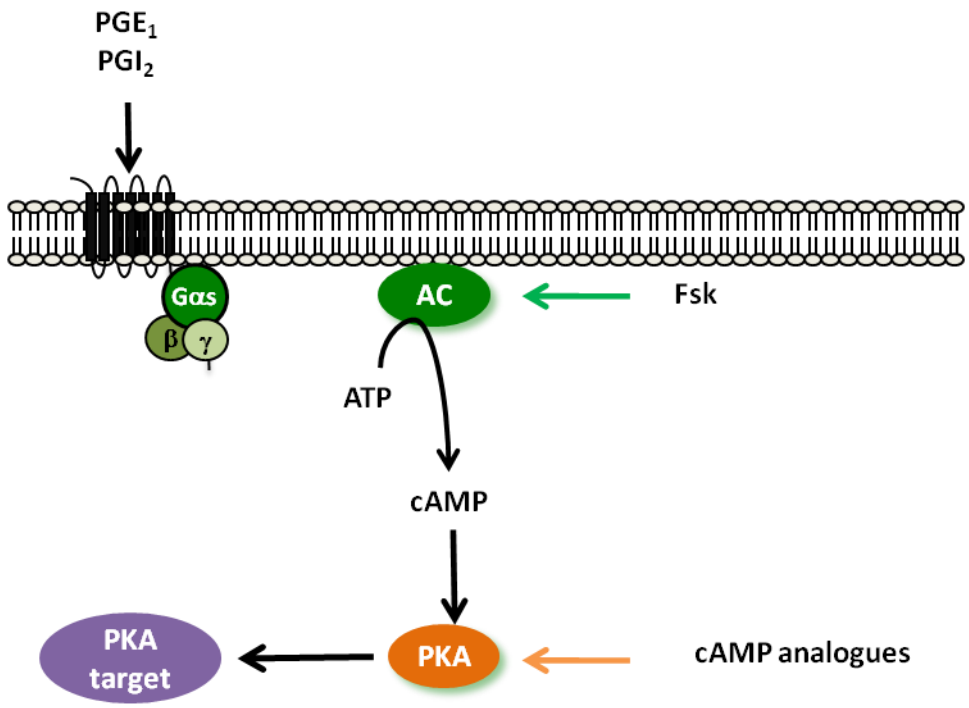

Figure 3. 1:A schematic representation of cAMP/PKA signalling pathway

The diagram shows the main elements of this pathway and highlights what part of the pathway physiological (PGI_2 and PGE_1) and nonphysiological (Fsk and cAMP analogues) agents activate.

Aims and objectives

The aim of this chapter is to establish the parameters for the tools that would be used in future chapters and standardise their conditions. More specifically the objectives were to:

- Characterise the inhibitory effects and the potency of different cAMP/PKA activating agents on washed platelets.
- Characterise the inhibitory dynamics of these agents through producing time-course curves.
- Characterise different PKA activity markers in platelets. This would be established using immunoblotting techniques with different antibodies.

3.2 Validation of platelet isolation method

Many studies isolate blood platelets using methods adapted from "prostaglandin washing procedure" where platelets are inhibited in PRP with PGE_1 (Vargas *et al*., 1982). This method produces isolated platelets that are very sensitive to platelet activation, probably because it relies on a physiologically relevant inhibitory pathway. The prostaglandin washing method could not be used when studying cAMP signalling as the added PGE_1 leads to activation of the cAMP/PKA signaling pathway, which could potentially result in a misinterpretation of the data. Thus, throughout this study platelets were isolated by the well-established pH method (Mustard *et al*., 1989). This method relies on lowering the pH of the PRP to 6.4 at which platelets cannot be activated. It is a robust and reproducible method for isolation of blood platelets. However, it was important to validate this method of platelet isolation by assessing the functional and signaling responsiveness of the isolated platelets.

3.2.1 Assessment of platelet functional response

Washed platelets isolated by the pH method were tested for their functional response to collagen. A concentration-dependent increase in light transmission was observed starting with a threshold response at 0.1µg/ml and reaching near maximal response when using 10µg/ml. All aspects of the platelet aggregation trace could be observed including shape change (Figure 3.2). Data from this experiment show that platelets isolated by pH method are functional.

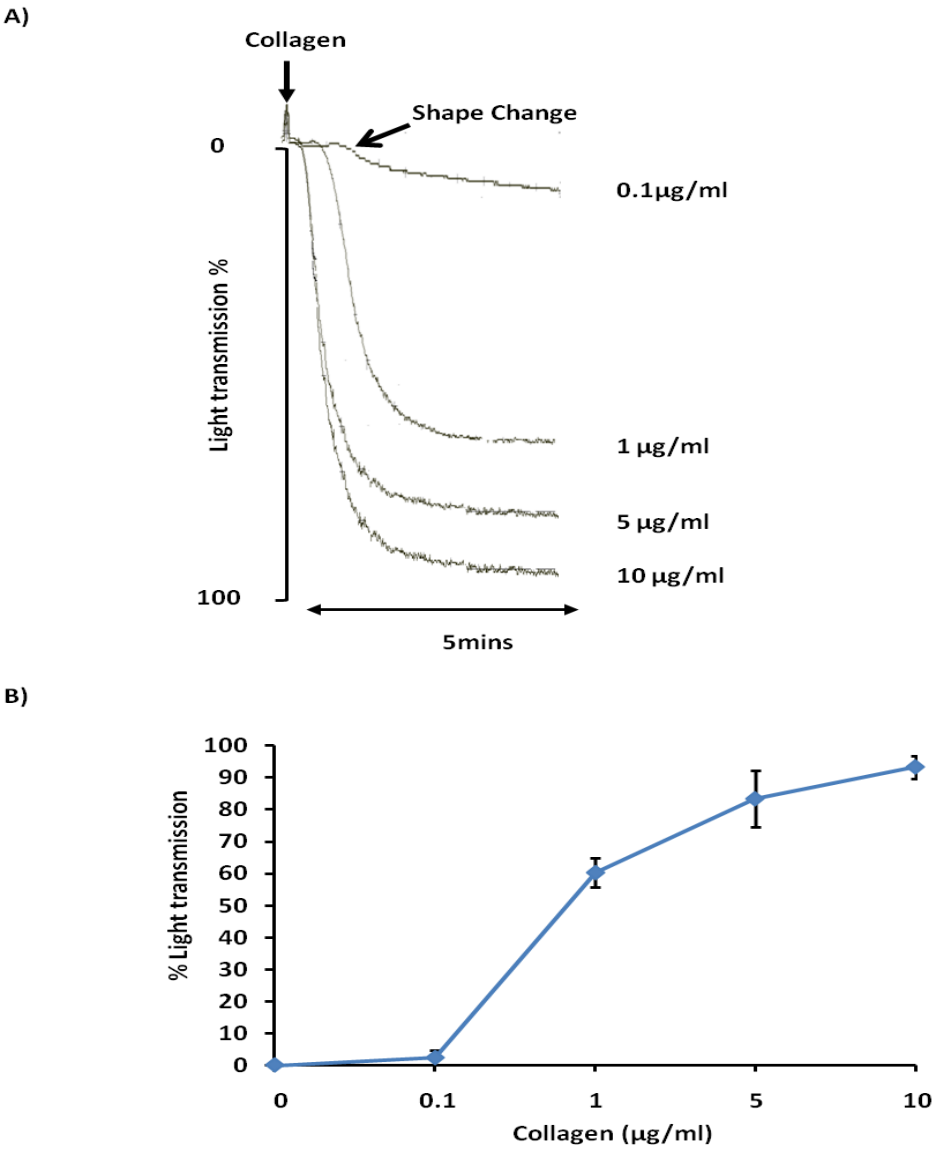

Figure 3. 2: The responsiveness of washed platelets isolated by the pH method as assessed by collagen-induced platelet aggregation.

WP ($2.5x10^8$ platelets/mL) were isolated by the pH method as described in chapter 2. After prewarming for 2mins, platelets were stimulated with increasing concentrations of collagen (0-5µg/mL) and aggregation was monitored for 5min under constant stirring (1000rpm) at 37^{o}C using a chrono-log dual channel light transmission aggregometer. **(A)** Shows representative aggregation traces generated by aggreo/link computer software (chrono-log, USA). **(B)** Shows data from 3 independent experiments with separate blood donors represented as means ± SEM.

3.2.2 Assessment of tyrosine phosphorylation of platelet proteins in response to collagen

Having established that WPs isolated by pH method were functionally responsive, their ability to trigger activatory signaling events had to be examined. A well-established and a sensitive signaling marker for platelet activation is tyrosine phosphorylation of platelet proteins. Here platelets were stimulated with increasing concentrations of collagen (0 – 50 μg/mL) and tyrosine phosphorylation in whole cell lysates was assessed by SDS-PAGE and immunoblotting. Figure 3.3 shows lightly phosphorylated proteins with molecular weights of 27, 30, 40, 60, and 140 kDa and a heavily phosphorylated one with molecular weight of 65 kDa under basal conditions. Stimulating platelets with collagen leads to a concentration-dependent increase in phosphorylation of the basally phosphorylated proteins and the appearance of several other bands with apparent molecular weights of 45, 90 and 100 kDa (Figure 3.3 top panel). The bottom panel shows β-tubulin as an evidence for equal protein loading in all lanes. These data from figure 3.2 and 3.3 suggest that washed platelets isolated by the pH method retain their ability to aggregate and trigger tyrosine phosphorylation events in response to collagen. The responses that we obtained are comparable to those obtained by other people who used the classic prostaglandin method of platelet isolation (Hers *et al*., 2000) (Dhanjal *et al*., 2007) (Tomlinson *et al*., 2007).

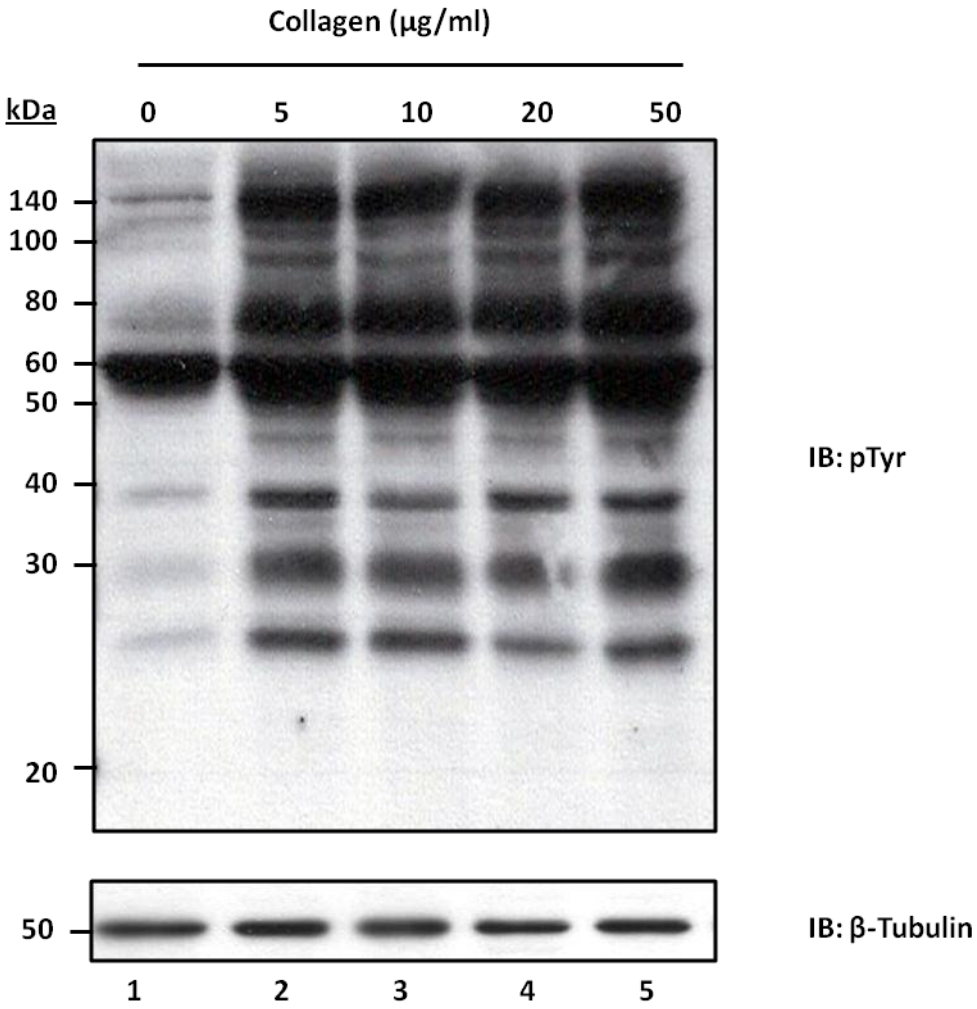

Figure 3. 3: The responsiveness of washed platelets isolated by the pH method as assessed by collagen-induced phosphorylation events.

WP ($5x10^8$ platelets/mL) were isolated using the pH method as described in chapter 2. Platelets were prewormed for 2mins then stimulated with increasing concentrations of collagen (0-50µg/mL) under non-aggregatory conditions for 90secs. Platelet lysates (20µg/well) were loaded onto a 10-18% gradient polyacrylamide gel and then resolved by SDS-PAGE for 2.5h at 120V. Proteins were then transferred onto a PVDF membrane for 2.5h at 100V. Membranes were then blocked and immunoblotted with anti-phospho-tyrosine mouse antibody (top) overnight at 4^oC. Following that membranes were stripped and then reprobed with anti-β-tubulin mouse antibody (bottom) overnight at 4^oC to check for equal loading. Blots are representative of two independent experiments with two separate donors

3.3 Prostacyclin inhibits collagen-induced platelet aggregation in a dose-dependent manner

One of the criticisms of many studies examining cAMP/PKA signalling in platelets is the use of unphysiological agents that act as global activators of AC or PKA. One of the main aims of this study was to characterise cAMP/PKA signalling networks in blood platelets under more physiological conditions in order to better understand how the pathway works. Since the main physiological cAMP activating agent (Moncada *et al*., 1976) is prostacyclin it was important to fully characterise its effects on a number of aspects of platelet function before examining its downstream biochemical pathways.

In the first instance the inhibitory effect PGI_2 could have on a platelet function was tested. Increasing concentrations of PGI_2 (0-100nM) were preincubated with WP for 1 min before stimulating with collagen (5µg/mL). A threshold inhibitory effect was observed with 10nM giving an inhibitory effect of 6±2%, while 100nM of the prostanoid almost abolished the aggregation response with an inhibitory effect of 88±14% and 50% inhibition was achieved with 49±8nM (Figure 3.4).

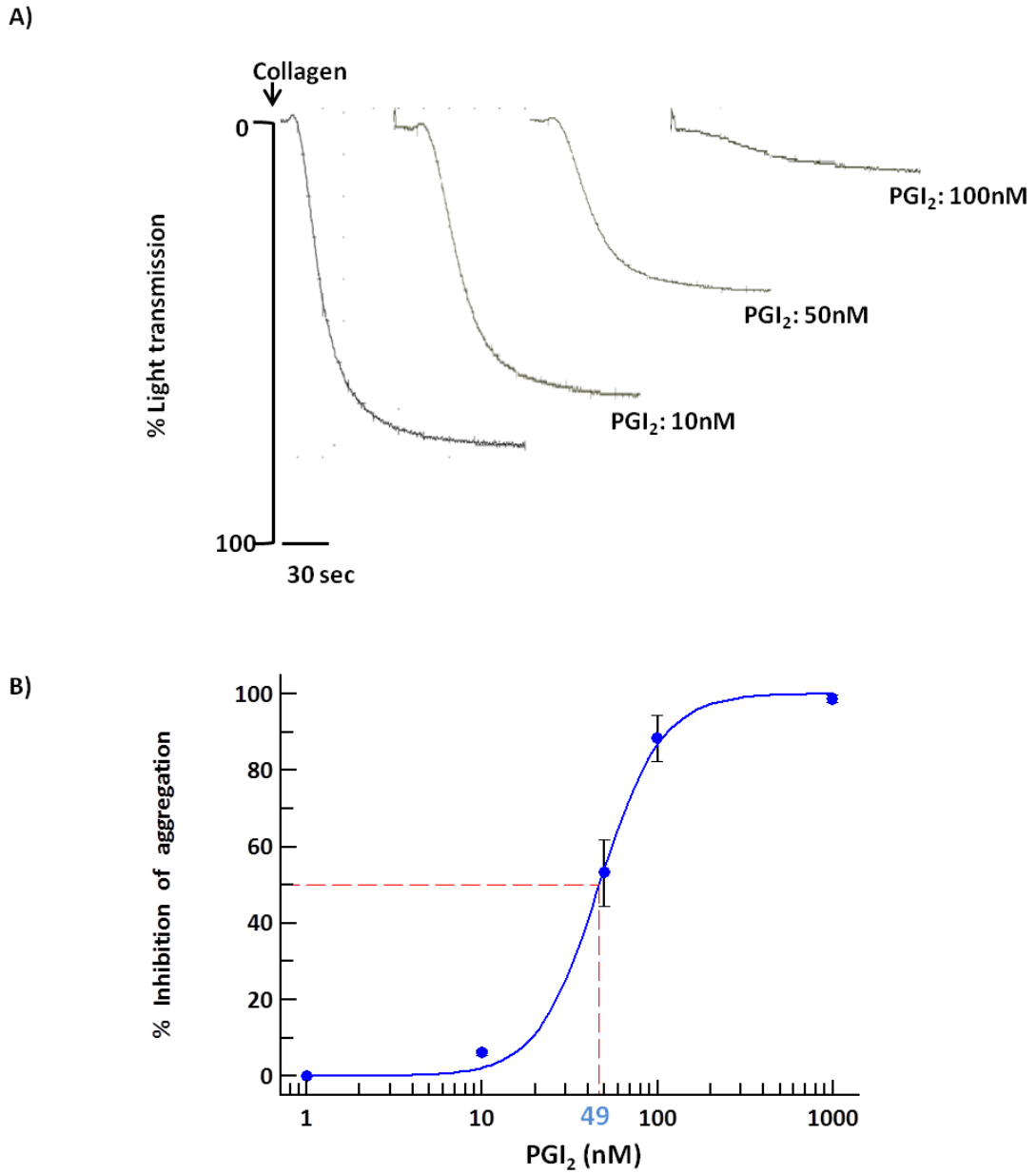

Figure 3. 4: Prostacyclin (PGI_2) inhibits collagen-induced platelet aggregation in a dose dependent manner.

WP ($2.5x10^8$ platelets/mL) were pre-treated with increasing concentrations of PGI_2 (1-100nM) for 1min then were stimulated with collagen (5µg/mL). Aggregation was monitored for 4mins under constant stirring (1000rpm) at 37^oC using a chrono-log dual channel light transmission aggregometer. **(A)** Shows representative aggregation traces generated by aggreo/link computer software (chrono-log, USA). **(B)** A dose response fit showing the relationship between PGI_2 concentration and % inhibition of aggregation. Data are from 5 independent experiments with separate blood donors and expressed as means ± SEM.

3.4 The inhibitory effect of prostacyclin on platelet aggregation is reversible

Having confirmed that PGI_2 inhibits collagen-induced platelet aggregation, the temporal nature of the inhibitory effect was explored. Here PGI_2 (100nM) was incubated with platelets for increasing time points (0-30min) before stimulating with collagen (5µg/mL). PGI_2 induced a rapid inhibitory response on platelet aggregation with 87±4% inhibition observed just after 15 sec. This level of inhibition was maintained for 5 minutes post PGI_2 treatment before the inhibitory response rapidly decayed such that at 30 min only 17±17% inhibition was observed (Figure 3.5). These data illustrate a rapid and reversible effect of PGI_2 on platelet aggregation. In the light of these observations 1min incubation time was selected for all aggregation experiments with PGI_2.

A)

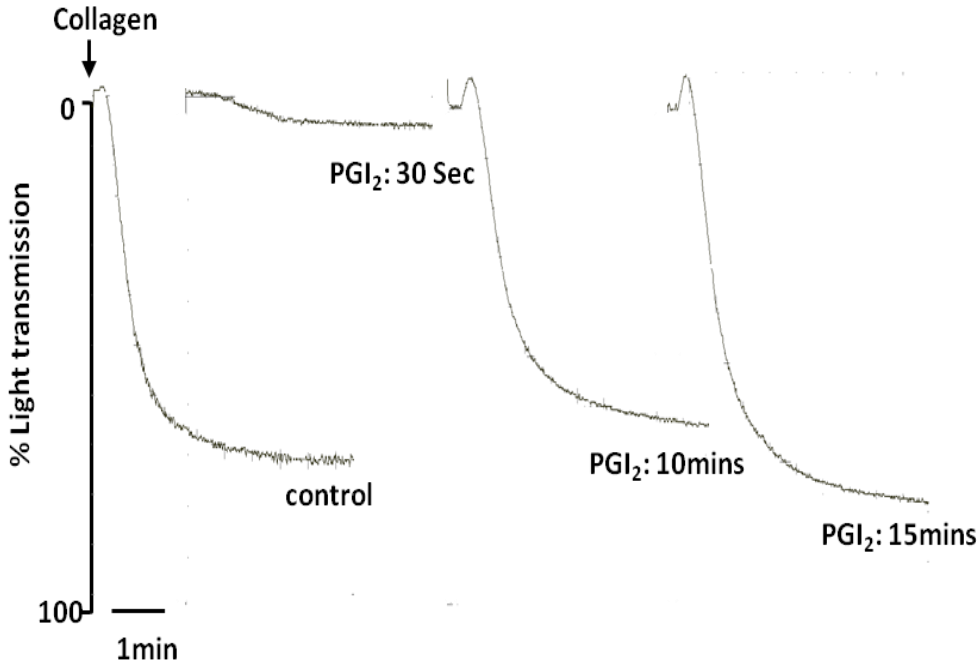
Collagen
0
100
% Light transmission
1min
control
PGI2: 30 Sec
PGI2: 10mins
PGI2: 15mins

B)

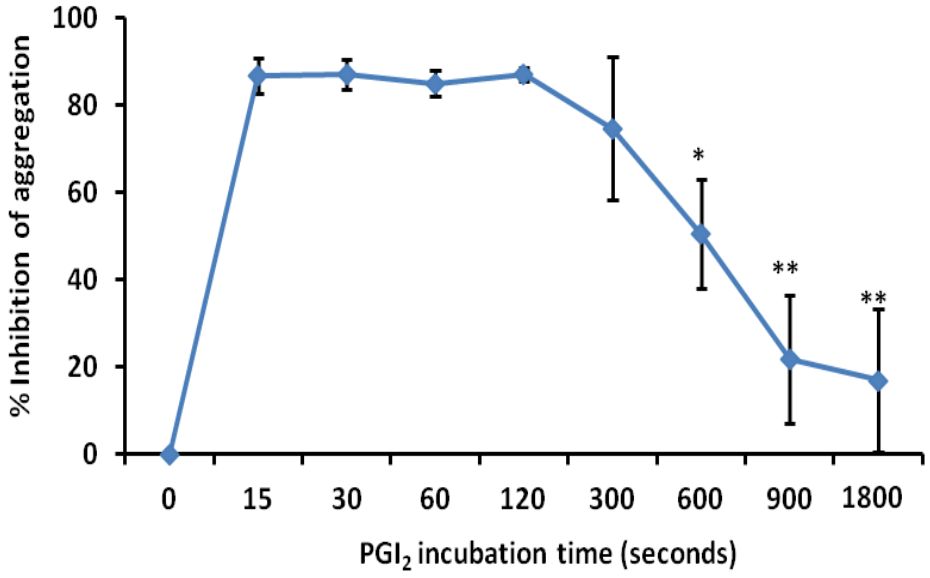
% Inhibition of aggregation
100
80
60
40
20
0
0
15
30
60
120
300
600
900
1800
*
**
**
PGI2 incubation time (seconds)

Figure 3. 5: The inhibitory effect of prostacyclin (PGI_2) on platelet aggregation is reversible.

WP ($2.5x10^8$ platelets/mL) were pre-treated with PGI_2 (100nM) for an increasing periods of time (0-30min) then were stimulated with collagen (5µg/mL). Aggregation was monitored for 4mins under constant stirring (1000rpm) at 37^oC using a chrono-log dual channel light transmission aggregometer. **(A)** Shows representative aggregation traces generated by aggreo/link computer software (chrono-log, USA). **(B)** Shows data from 3 independent experiments represented as % inhibition of aggregation and expressed as means ± SEM (*: $p<0.05$, **: $p<0.01$ when compared with 60 seconds).

3.5 Prostacyclin inhibits thrombin-induced platelet aggregation in a concentration-dependent manner

Having characterised the inhibitory properties of PGI_2 on platelet aggregation induced by the stimulation of an immunoglobulin receptor (GPVI) by collagen, the ability of PGI_2 to modulate platelet aggregation induced by stimulation of a GPCR was tested. In this case the effect of PGI_2 on platelet aggregation induced by thrombin was examined.

Consistent with the previous observations with collagen, incubating WP with increasing concentrations of PGI_2 (0-1000nM) for 1min inhibited platelet aggregation induced by thrombin (0.02U/mL) in a concentration-dependent manner. We observed a threshold inhibitory effect with 10nM giving an inhibitory effect of 18±7%, and 100nM of PGI_2 inducing almost complete inhibition of aggregation 84±13% (Figure 3.6). The PGI_2 concentration that caused 50% inhibition at this concentration of thrombin was 52±18nM. These data confirm the ability of PGI_2 to inhibit G-protein-mediated platelet aggregation induced by thrombin, which suggests that PGI_2 targets aspects of platelet function that are common to different agonists.

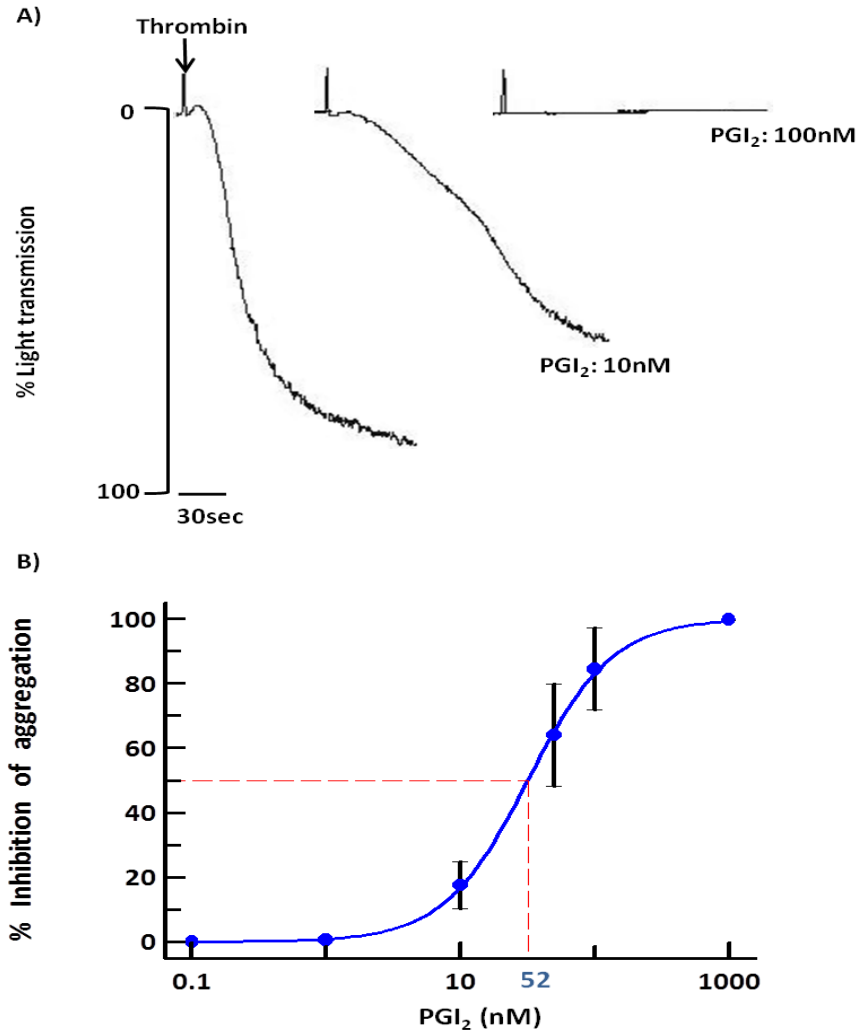

Figure 3. 6: Prostacyclin (PGI2) inhibits thrombin-induced platelet aggregation in a dose dependent manner.

WP ($2.5x10^8$ platelets/mL) were pre-treated with increasing concentrations of PGI_2 (0.1-100nM) for 1min then were stimulated with thrombin (0.02 U/mL). Aggregation was monitored for 4mins under constant stirring (1000rpm) at 37^oC using a chrono-log dual channel light transmission aggregometer. (A) Shows representative aggregation traces generated by aggreo/link computer software (chrono-log, USA). (B) Data are represented as a dose response fit showing the relationship between PGI_2 concentration and % inhibition of thrombin-induced aggregation. Data are from 4 independent experiments with separate blood donors and expressed as means ± SEM.

3.6 Prostacyclin has a more potent inhibitory effect on platelet aggregation than prostaglandin E1

In this experiment the inhibitory effect of PGI_2 on thrombin-induced platelet aggregation was compared with PGE_1. A comparison between these two physiological inhibitors was performed on the same donor, on the same day and under the same conditions to exclude any experimental or donor variations. Furthermore, the same concentration for each of the inhibitors was tested successively to minimize any changes in platelet activity over time.

Consistent with its description as a regulator of platelet function, PGE_1 induced a concentration dependent inhibition of thrombin induced platelet aggregation. We observed a threshold inhibitory effect with 10nM giving an inhibitory effect of 9±4%, with 1000nM of PGE_1 inducing almost complete inhibition of aggregation 93±4% (Figure 3.7). We next compared these inhibitory effects with those of PGI_2. In Figure 3.7 two concentration-response curves representing % inhibition of platelet aggregation for increasing concentrations of PGI_2 and PGE_1 are presented. The concentration that caused 50% inhibition of aggregation was 52±18nM and 178±45nM for PGI_2 and PGE_1, respectively ($p<0.05$). This rightward shift in the curve representing PGE_1 data in comparison to the one representing PGI_2 confirm that PGI_2 is the more potent cAMP-dependent physiological inhibitor when tested on thrombin-induced platelet aggregation.

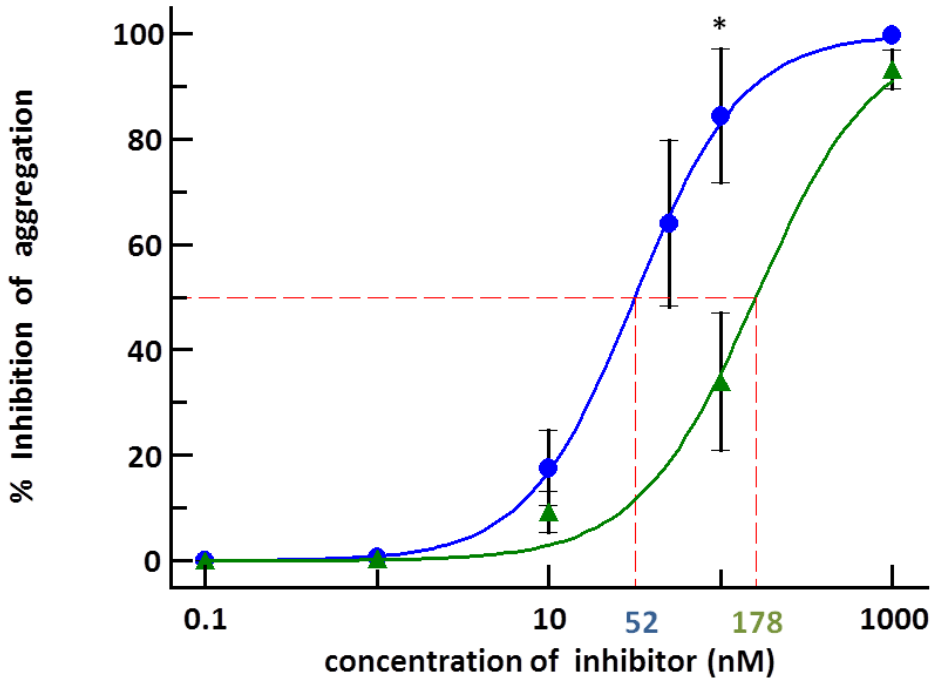

Figure 3. 7:Prostacyclin (PGI_2) has a more potent inhibitory effect than prostaglandin E1 (PGE1) as assessed by platelet aggregation.

WP ($2.5x10^8$ platelets/mL) were pre-treated with increasing concentrations of PGI_2 (0.1-1000nM, Blue fit) or similar concentrations of PGE_1 (green fit) for 1min then were stimulated with thrombin (0.02 U/mL). Aggregation was monitored for 4mins under constant stirring (1000rpm) at 37°C using a chrono-log dual channel light transmission aggregometer. Data are displayed as scatter plots with best fits showing the relationship between inhibitor concentration and % inhibition of thrombin-induced aggregation. Data are from 4 independent experiments with separate blood donors and expressed as means ± SEM (*: $p \leq 0.05$ when compared with PGE_1 treatment).

3.7 Characterisation of the inhibitory effects of forskolin on platelet aggregation

In addition to PGI_2, the physiological cAMP-dependent platelet inhibitor that was mainly used in this study, we also used forskolin as a direct activator of AC. Forskolin (Fsk) is a ditrepene that can be isolated from an Indian plant called *Forskohlii* and was first discovered by Seamon *et al* (Seamon *et al*., 1981). Forskolin has been used widely as a tool to increase cAMP levels in a receptor-independent manner (Seamon *et al*., 1981). Fsk activates all AC isoforms except AC9 by slipping into the ventral cleft of the active domain allowing its two cytoplasmic tails to glue together through a combination of hydrophobic and hydrogen-binding interactions (Zhang *et al*., 1997). Throughout this study Fsk was used to characterise global cAMP signalling networks compared with that activated by the IP receptor.

Here the inhibitory effects of Fsk on collagen-induced platelet aggregation were characterised and the optimal conditions for its use determined. In the first instance, a time-course experiment was performed to determine the optimal incubation time and whether any inhibitory effects were reversible. Inhibition by Fsk (10µM) peaked at 5min reducing aggregation from 64%, when WP were treated with collagen alone, to 25%. This was maintained for up to 15 min before declining back to basal by 30 min (Figure 3.8 A). Consequently, 5min incubation was chosen as a standard incubation time for Fsk.

In the second instance, a Fsk concentration-response curve was generated. Increasing concentrations of Fsk (0.1-20µM) were incubated for 5min with WP prior to addition of collagen (5µg/mL) and aggregation was monitored. Fsk (2µM) had a

threshold inhibitory effect on aggregation causing an 8±2% inhibition, whereas 10µM showed a more pronounced inhibitory effect causing 51±2% inhibition (figure 3.8 B). Full inhibition of aggregation was never attained even at the maximal concentration tested: Fsk (20µM) caused 67% inhibition. Data from this experiment suggest that 5 min incubation with Fsk inhibits collagen-induced platelet aggregation in a concentration-dependent and reversible manner.

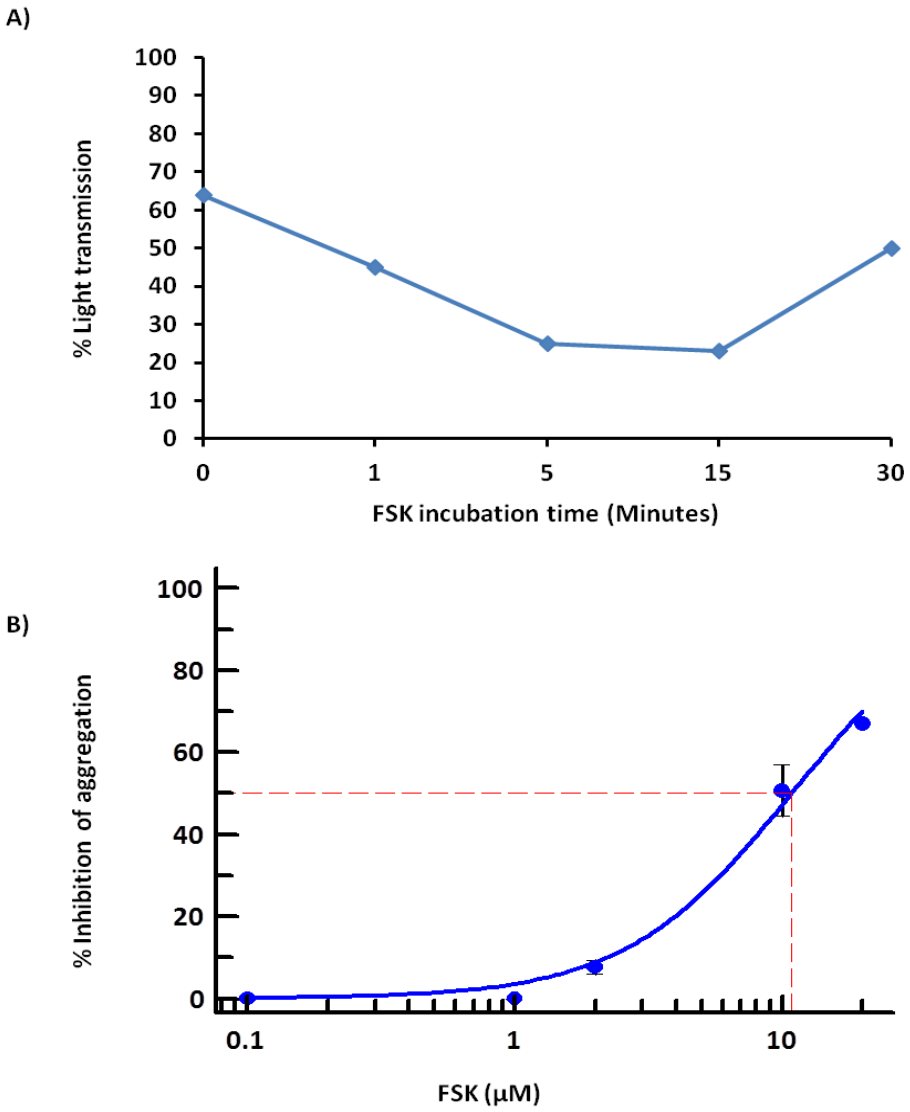

Figure 3. 8: Characterization of the inhibitory effect of forskolin (Fsk) on platelet aggregation induced by collagen.

WP ($2.5x10^8$ platelets/mL) were pre-treated with Fsk then were stimulated with collagen (5µg/mL). Aggregation was monitored for 4mins under constant stirring (1000rpm) at 37°C using a chrono-log dual channel light transmission aggregometer. **(A)** Fsk (10µM) was pre-incubated with WP for increasing time points (0-30mins) before stimulating with collagen. Data are from 1 experiment and represented as % Light transmission. **(B)** Increasing concentrations of Fsk (0.1-20µM) were pre-incubated with WP for 5mins before stimulating with collagen. Data are from 4 independent experiments (except 1 and 20µM), expressed as % inhibition of aggregation and represented as means ± SEM.

3.8 Characterisation of the inhibitory effects of cAMP analogues on blood platelets

In addition to PGI_2 and Fsk, we used cell-permeable direct PKA activators that can bypass the receptor and AC and therefore wanted to optimise them under our conditions. A number of cell-permeable cAMP analogues have been developed that can act as direct activators of PKA. They are also often resistant to hydrolysis by cytoplasmic PDEs leading to long term activation of PKA. They have been developed as a tool to study biological responses that are dependent exclusively on the activation of PKA. There is a wide range of these cAMP analogues commercially available that vary in their lipophillicity and their specificity towards a specific element of the cyclic nucleotide signal transduction. 8-CPT-cAMP is a cAMP analogue that is synthesised by adding a chlorophenylthiol moiety to position 8 of the cAMP molecule. This compound has been shown to have a high affinity for all cAMP binding sites both on PKA I and PKA II (Schwede *et al*., 2000). But in platelets, this compound showed some nonspecific effects on PKG as well as low membrane permeability when compared with other cAMP analogues (Sandberg *et al*., 1991). It has been found however that the substitution of a hydrogen atom at position 6 of the cAMP molecule with an aromatic ring such as a phenyl ring enhances the specificity of cAMP analogues towards PKA as well as their membrane permeability (Christensen *et al*., 2003). Therefore, 8-CPT-6-Phe-cAMP was chosen as an activatory cAMP analogue to be used throughout this study.

To determine the optimal conditions under which this cAMP analogue could be used, time-course and concentration response pilot experiments were performed

on WP to study its inhibitory effect on collagen-induced platelet aggregation. Maximal inhibition of collagen-induced platelet aggregation occurred after 5 min incubation with 8-CPT-6-Phe-cAMP (40µM), where aggregation was reduced from 83% to 33%. This was maintained for 10mins, which was the longest time tested and therefore, 5min was considered the optimal incubation time for further experiments. In addition, 8-CPT-6-Phe-cAMP (1-100µM) inhibited collagen-induced aggregation in a concentration-dependent manner with a threshold inhibitory effect at 10µM with 11±3% inhibition and reaching to 77±5% inhibition at 100µM (Figure 3.9 B). The chosen concentrations and time points were similar to those used by Sandberg *et al* when they tried similar compounds on platelets (Sandberg *et al*., 1991). The 8-CPT-6-Phe-cAMP concentration that caused 50% inhibition under these conditions was 30±6µM. Data from this experiment suggest that 8-CPT-6-Phe-cAMP can inhibit platelet aggregation induced by collagen in a concentration-dependent manner.

A)

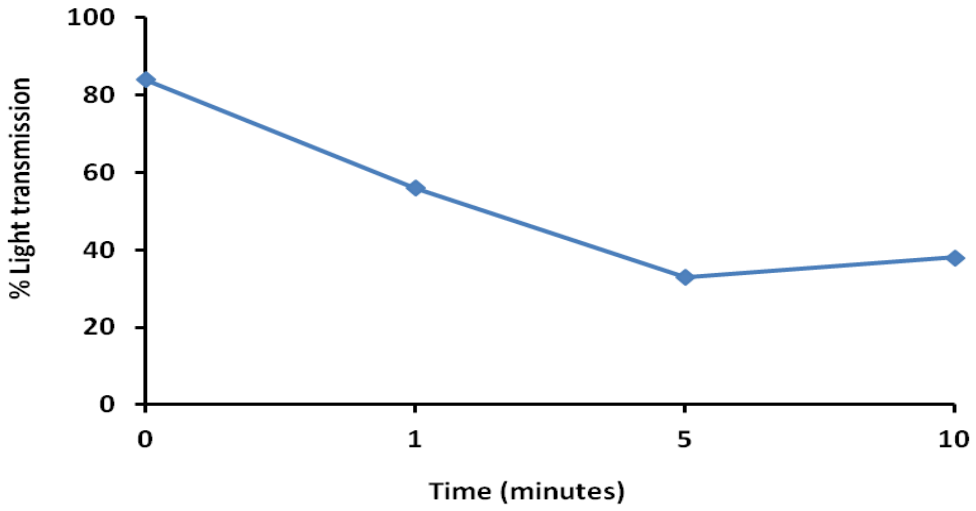

B)

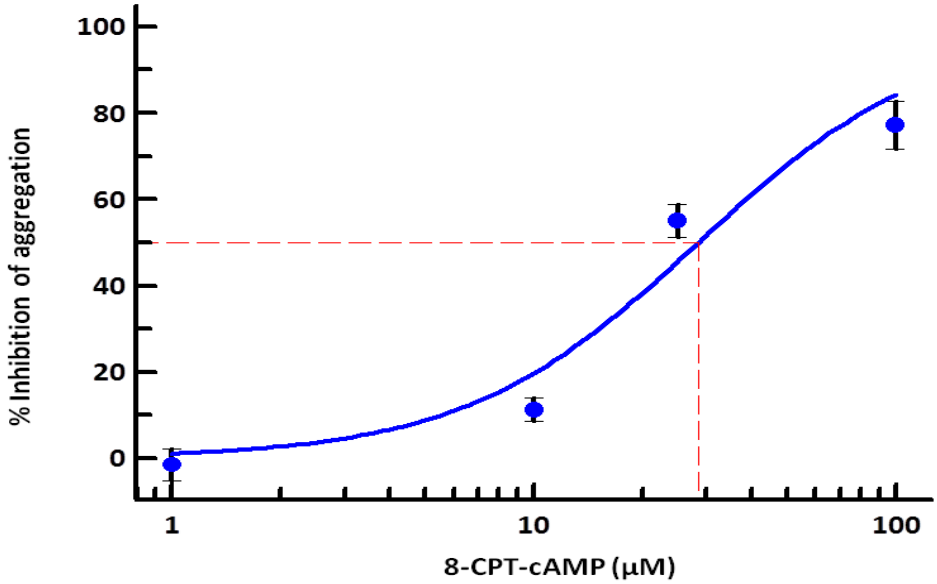

Figure 3. 9: Characterization of the inhibitory effect of the cAMP analogue 8-CPT-6-Phe-cAMP on platelet aggregation induced by collagen.

WP ($2.5x10^8$ platelets/mL) were pre-treated with 8-CPT-6-Phe-cAMP then were stimulated with collagen (5µg/mL). Aggregation was monitored for 4mins under constant stirring (1000rpm) at 37°C using a chrono-log dual channel light transmission aggregometer. **(A)** 8-CPT-6-Phe-cAMP (40µM) was pre-incubated with WP for increasing time points (0-10mins) before stimulating with collagen. Data is from 1 experiment and is represented as % Light transmission. **(B)** Increasing concentrations of 8-CPT-6-Phe-cAMP (1-100µM) were pre-incubated with WP for 5 min before stimulating with collagen. Data are from 3 independent experiments with separate donors, expressed as % inhibition of aggregation and represented as means ± SEM.

3.9 Characterisation of adenylyl cyclase activity in response to prostacyclin and forskolin

In the next set of experiments we wanted to investigate AC activity for PGI_2 and other cAMP–elevating agents that were used in this study. The mechanism by which PGI_2 exert its inhibitory effect is through raising cAMP levels (Tateson *et al*., 1977) in response to its binding to the Gs-protein coupled IP receptor (Kennedy *et al*., 1982). In contrast, Fsk diffuses through the membrane and directly activates AC (Seamon *et al*., 1981). Therefore, assessing AC activity represented by measuring cAMP levels is a very important tool in studying cAMP/PKA signalling pathway in platelets.

In this experiment cAMP levels were measured using an EIA-based method in response to increasing concentrations of PGI_2 and Fsk. Washed platelets maintain a basal level of cAMP 198$\pm$16 fmol cAMP/10^7 platelets (n=3), which does not decrease with time (data not shown). Stimulating platelets with increasing concentrations of PGI_2 led to increased AC activity in a concentration-dependent manner (Figure 3.10A). PGI_2 (10nM) only slightly increased AC activity over basal levels producing 222±27 fmol cAMP/10^7 platelets (p=0.24 compared with basal) whereas 100nM, which normally abolishes platelet aggregation (see figure 3.4), raised cAMP levels up to 450±31 fmol cAMP/10^7 platelets (p<0.001 compared with basal). The highest concentration of PGI_2 we measured was 1000nM which produced 691±208 fmol cAMP/10^7 platelets (p<0.05 compared with basal).

After that we stimulated WP with PGI_2 (100nM) for increasing time points (0.5-10 min). Data from this experiment showed that PGI_2-mediated AC activity peaked after 1 min with 511 fmol cAMP/10^7 platelets and then started to dip reaching 327 fmol cAMP/10^7 platelets after 10 min which was the longest time measured in our experiment (Figure 3.10 B, n=2).

Similar to PGI_2, Fsk caused an increase in AC activity in a concentration-dependent manner elevating cAMP levels from 198$\pm$16 up to 436±59 fmol cAMP/10^7 platelets (p<0.05 when compared with basal) when WP were treated with Fsk (20µM) (Figure 3.10 C). Data from this experiment confirm that PGI_2 and Fsk increase AC activity in a dose-dependent manner and the effect of PGI_2 on platelet AC activity is reversible.

.

A)

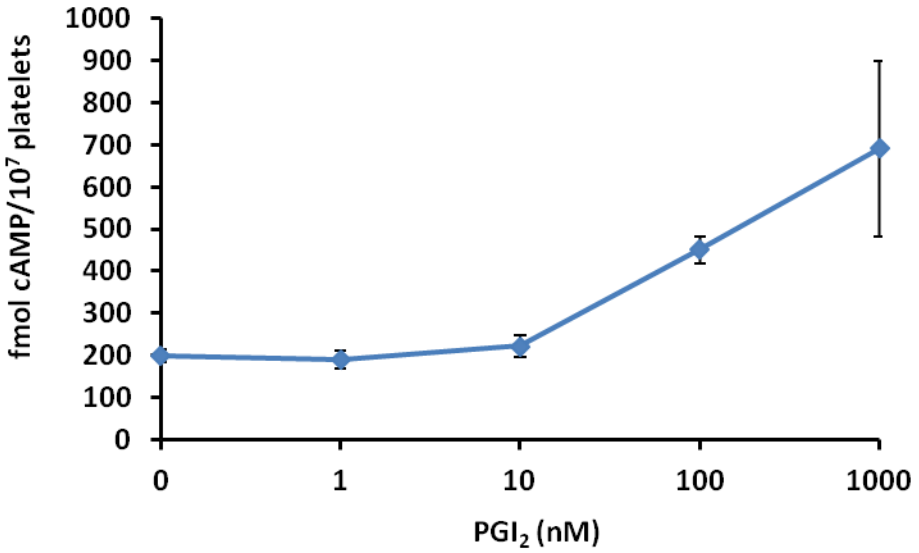
fmol cAMP/10^7 platelets
1000
900
800
700
600
500
400
300
200
100
0
0
1
10
100
1000
PGI2 (nM)

B)

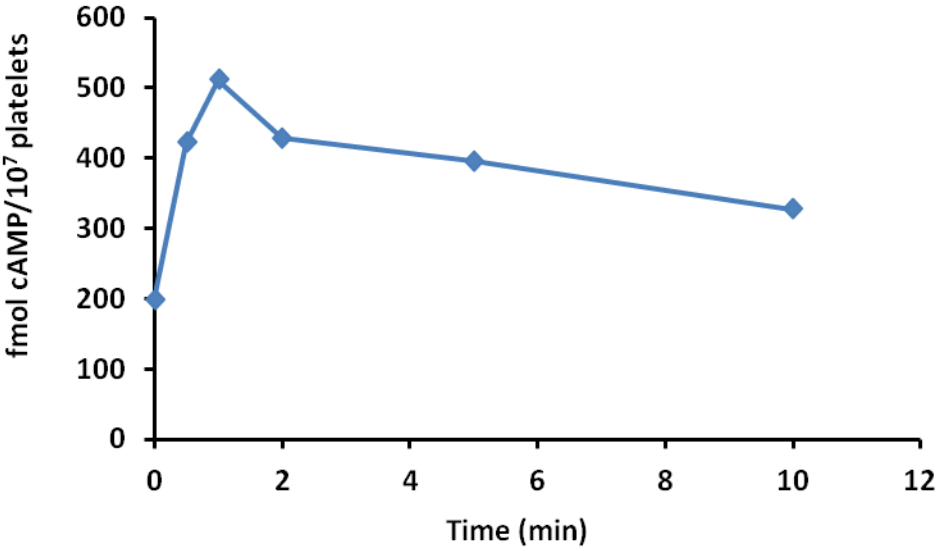
fmol cAMP/10^7 platelets
600
500
400
300
200
100
0
0
2
4
6
8
10
12
Time (min)

C)

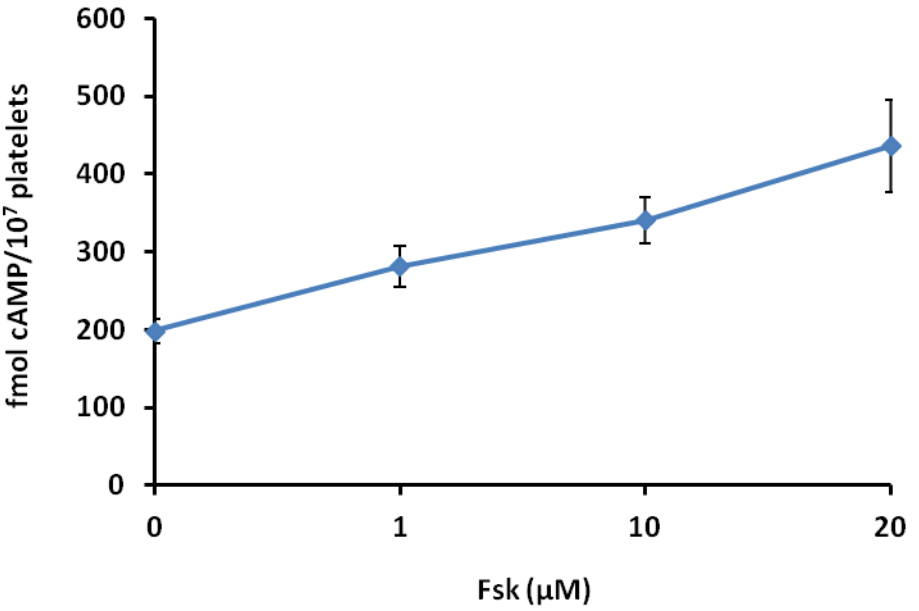
fmol cAMP/10^7 platelets
600
500
400
300
200
100
0
0
1
10
20
Fsk (µM)

Figure 3. 10: Prostacyclin and forskolin induce AC activity in a dose dependent manner.

(A) WP ($2x10^8$ platelets/mL) were stimulated with increasing concentrations of PGI_2 (0-1000nM) for 30 sec at 37^oC under constant stirring using a chrono-log dual channel light transmission aggregometer. Samples were then processed as described in chapter 2. Data are representative of 3 independent experiments from separate donors and expressed as means ± SEM. **(B)** As in A except that WP were treated with a constant concentration of PGI_2 (100nM) for increasing time points (0.5-10 min). Data are from 2 independent experiments with separate donors and expressed as means. **(C)** As in A but WP were treated with Fsk (0-20µM) for 5 min. Data are representative of 3 independent experiments from separate donors and expressed as means ± SEM.

3.10 Studying PKA-mediated phosphorylation events in blood platelets

Assessment of PKA-mediated phosphorylation events by immunoblotting is an important marker for PKA activity. After increasing the basal activity of AC and triggering the production of cAMP by several agents, these cAMP molecules bind to an inactive tetrameric PKA holoenzyme. This binding leads to dissociation of the catalytic subunit and subsequently phosphorylation of several PKA substrates. These phosphorylation events result in blunting various aspects of platelet activity (Schwarz *et al*., 2001).

In order to assess PKA signalling events in platelets we employed two PKA signalling markers. The first one is an antibody that can detect the phosphorylation of the cytoskeletal protein VASP at serine^{157}, which is a well-established PKA target in platelets (Halbrugge *et al*., 1990) (Horstrup *et al*., 1994). This antibody produces a band at an apparent molecular weight of 50kDa on SDS-PAGE representing phospho-VASP^{ser157}. Secondly, we used an antibody that detects a range of PKA-phosphorylated proteins through its ability to recognise phosphorylated PKA consensus sequences (-Arg-Arg-X-Ser/Thr-X) on different cellular proteins. Therefore, two cellular markers would be used in studying PKA-dependent phosphorylation events phospho-VASP^{ser157} and phospho-PKA substrate protein profile.

Under basal conditions we observed that PKA substrates with apparent molecular weights of 16, 44 and 55 were heavily phosphorylated. These bands were always present. But other bands such as those at ~35, 70, 130 and 240 were only mildly

phosphorylated under basal conditions and their presence depended on the transfer as well as the film exposure time (compare figure 3.11, 12, 13 and 14). Interestingly we observed that basal phosphorylation was milder when WP were left for 60 min between preparation and lysis.

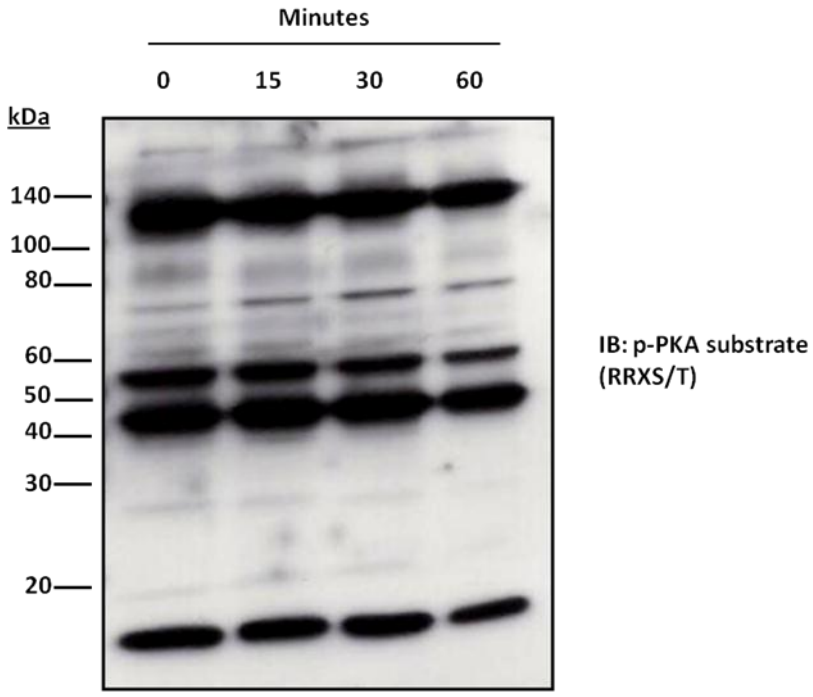

Figure 3. 11: Characterization of basally phosphorylated proteins detected by phospho-PKA substrate antibody.

WP ($2.5x10^8$ platelets/mL) were isolated using the pH method as described in chapter 2. They were then lysed with Laemmli buffer after different time points since resuspending with modified Tyrode's buffer. Platelet lysates (20µg/well) were loaded onto a 10-18% gradient polyacrylamide gel and then resolved by SDS-PAGE for 2.5h at 120V. Proteins were then transferred onto a PVDF membrane for 2.5h at 100V. Membranes were then blocked and immunoblotted with anti-phospho-PKA substrate rabbit antibody (1:1000) overnight at 4^oC. Blot is representative of one experiment.

3.10.1 Characterisation of PKA phosphorylation events induced by prostacyclin

Having characterised the effects of PGI_2 on AC activity, we next wanted to determine the subsequent PKA-mediated signalling events. In this set of experiments the effects of PGI_2 on the phosphorylation of $VASP^{ser157}$ and other proteins, represented by the phospho-PKA substrate protein profile, were examined.

WP were stimulated with increasing concentrations of PGI_2 (0-100nM) resulting in a concentration-dependent increase in the phosphorylation of different PKA substrates (Figure 3.12A, top panel, lanes 1-4). Robust phosphorylation was observed when stimulating with 100nM of PGI_2 (lane 4). This blot showed an increase in the phosphorylation of basally phosphorylated proteins at molecular weights of 16, 35 and 240kDa. Furthermore, some new phosphoproteins were visible that corresponded to molecular weights of 27, 32, 48 and 66kDa. On the other hand, we observed a decrease in the phosphorylation of the band at 44kDa. The specificity of this antibody to PKA activity was checked using different combinations of PKA inhibitors (Figure 3.12A top panel, lanes 5, 6). The rationale behind using combination of different PKA inhibitors is the well documented unspecificity of these inhibitors (Murray, 2008). We used the PKA inhibitor KT 5270 (10µM) in combination with either H89 (20µM) or Rp-8-CPT-6-Phe-cAMPS (500µM). Both KT 5270 and H89 act as competitive antagonists for ATP at its binding domain on the catalytic subunit of PKA (Engh *et al*., 1996) (Kase *et al*., 1987) whereas Rp-cAMPS compound is an inactive cAMP analogue that can compete with endogenous cAMP molecules at the cAMP binding domain on the regulatory subunit (de Wit *et*

al., 1984). The phosphorylation of VASP^{ser157} followed a similar trend and this phosphorylation was almost abolished when platelets were pretreated with KT 5720 and H89 (Figure 3.12 A, middle panel). Equal loading was checked using β-tubulin (figure 3.12 A, bottom panel).

Next we explored the temporal pattern of the phosphorylation of these PKA substrates. This was achieved by incubating WP with a constant concentration of PGI_2 (50nM) for increasing time points (0-60 min). In order to pick up as many bands as possible, proteins were transferred using a new transfer system (Trans-Blot Turbo, Bio-Rad) and films, for this experiment, were overexposed. Data from this experiment showed that phosphorylation of different PKA targets followed a distinct temporal pattern (Figure 3.12 B).

The majority of the bands peaked at 5 min but decayed at different time points. For example the bands at ~240, 82 and 24 kDa appeared at 15 to 30 sec, peaked at 5 min and then started to decay until they disappeared after 60 min. Similarly the band at 27 kDa peaked at 5 min however it disappeared relatively quicker at 30 min. Moreover, the band at 35 kDa was slightly phosphorylated basally then it peaked at 5 min and started to decay until it got back to basal levels at 60 min.

On the other hand, the bands at ~66 and 48 kDa emerged and peaked notably quickly after 15-30 sec and were maintained for 5 min then started to decay gradually until they disappeared after 60 min.

In contrast, other bands underwent a rather delayed temporal pattern such as the band at 22 kDa which emerged at 1 min, peaked after 5 min and then started to decay quickly and disappeared completely at 60 min.

Surprisingly, the band at 44 kDa, which was heavily phosphorylated under basal conditions, started to decay straight after stimulation with PGI_2 and reached its lowest levels after 30 min and then it went up slightly after 60 min.

The phosphorylation of VASP also followed a distinct temporal pattern with a rapid phosphorylation at 15 sec, a peak at 5 min then a gradual decrease until it got back to basal levels at 15 min (Figure 3.12 B, middle panel).

These data suggest that stimulating platelets with PGI_2 triggers PKA-mediated phosphorylation events which are temporally regulated. In addition, based on those data 1min was chosen to be the optimal stimulating time when studying PGI_2-induced signalling events.

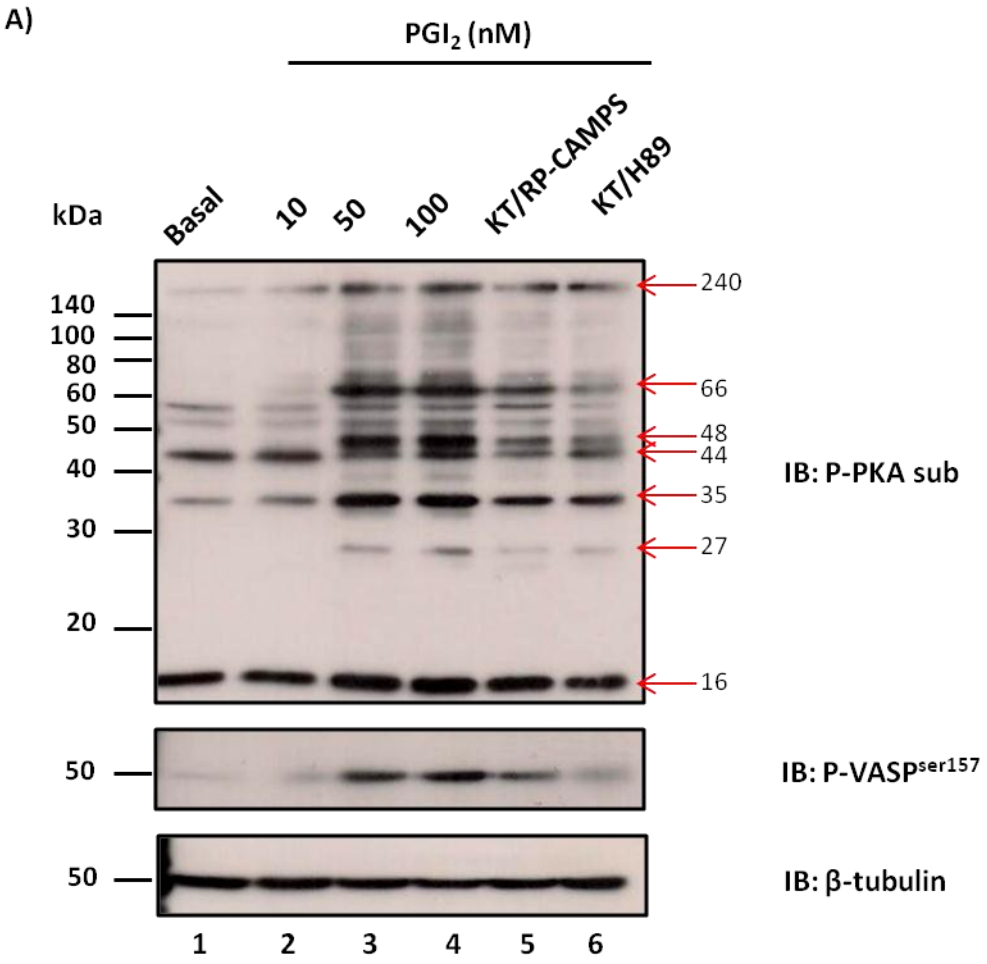
A)
PGI2 (nM)
kDa
Basal
10
50
100
KT/RP-CAMPS
KT/H89
140
100
80
60
50
40
30
20
240
66
48
44
35
27
16
IB: P-PKA sub
50
IB: P-VASPser157
50
IB: β-tubulin
1 2 3 4 5 6

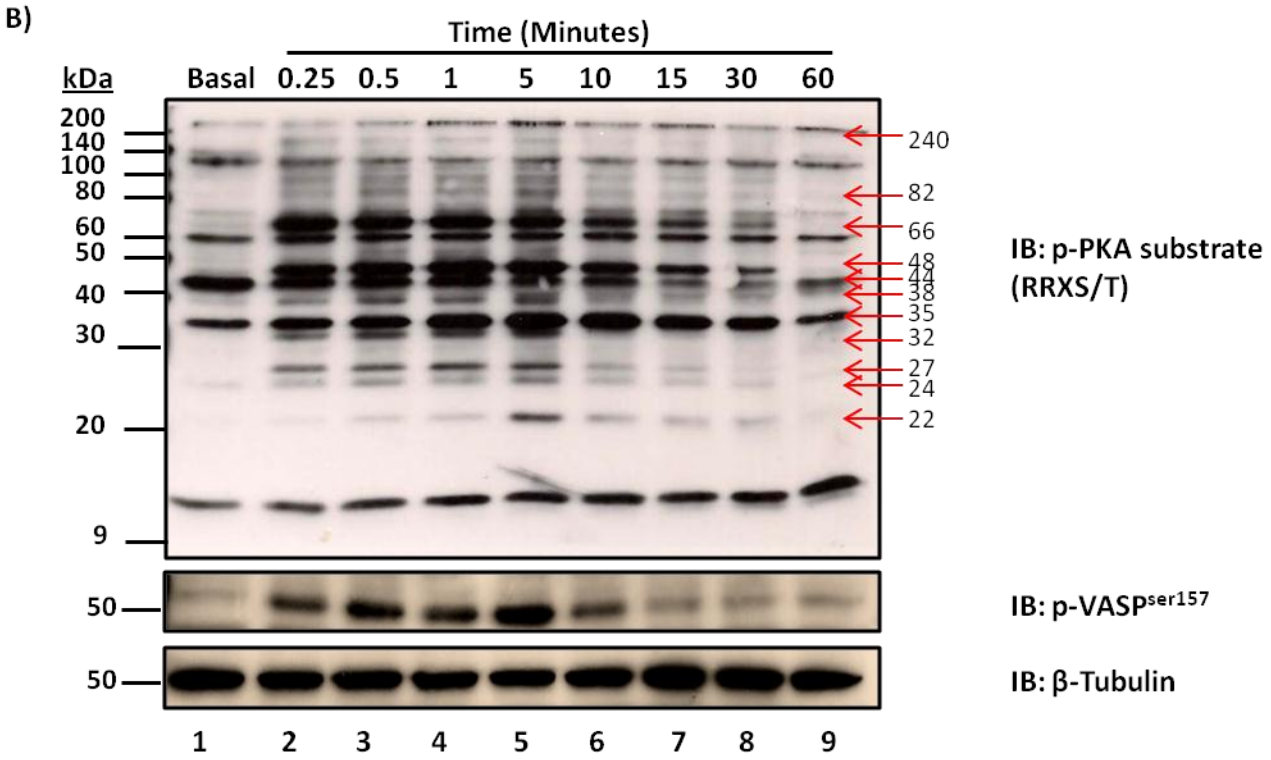
B)
Time (Minutes)
kDa
Basal
0.25
0.5
1
5
10
15
30
60
200
140
100
80
60
50
40
30
20
9
240
82
66
48
44
38
35
32
27
24
22
IB: p-PKA substrate (RRXS/T)
50
IB: p-VASPser157
50
IB: β-Tubulin
1 2 3 4 5 6 7 8 9

Figure 3. 12: Characterization of prostacyclin-induced phosphorylation events in blood platelets.

(A) WP ($2.5x10^8$ platelets/mL) were isolated using the pH method as described in chapter 2. Platelets were pre-warmed for 2 min then stimulated with increasing concentrations of PGI_2 (0-100 nM) for 1 min (lanes 1-4). PKA inhibitors (KT 5270: 10µM, H89: 20µM and Rp-8-CPT-6-Phe-cAMPS: 500µM) were incubated with WP for 20 min prior to stimulating with PGI_2 (100nM) (lanes 5, 6). **(B)** As in A, but WP were stimulated with a constant concentration of PGI_2 (50nM) for increasing time points (0.25-60mins). Platelet lysates (20µg/well) were loaded onto a 10-18% gradient polyacrylamide gel and then resolved by SDS-PAGE for 2.5h at 120V. Proteins were then transferred onto a PVDF membrane for 2.5h at 100V. Membranes were then blocked and immunoblotted with anti-phospho-PKA substrate rabbit antibody (1:1000) (top panels) overnight at 4^oC. Membranes were then stripped and reprobed with anti phospho-$VASP^{ser157}$ rabbit antibody overnight at 4^oC (middle panels). Membranes were finally immunoblotted for anti-β-Tubulin mouse antibody (bottom panels) overnight at 4^oC to check for equal loading. Red arrows indicate bands of interest. Blots are representative of three independent experiments with three separate donors.

3.10.2 Characterisation of PKA phosphorylation events induced by forskolin and cAMP analogues

Since other nonphysiological cAMP/PKA activating agents were used throughout this study, it was important to characterise the signalling events associated with these agents. Therefore, in this set of experiments we sought to characterise the phosphorylation events induced by the AC activator Fsk and the cAMP analogue 8-CPT-6-Phe-cAMP.

Stimulating washed platelets with increasing concentrations of Fsk resulted in dose-dependent increase in the intensity of phosphorylation of PKA substrates as well as $VASP^{ser157}$ (Figure 3.13 A). Phosphorylation peaked with 10µM Fsk and after 5 min incubation (Figure 3.13 A, lane 7) which is consistent with the aggregation data (Figure 3.8). The phospho-PKA substrate profile was similar to that observed with PGI_2 with Increased phosphorylation observed with proteins at apparent molecular weights of 16, 22, 35, 48, 66, 100 and the basally phsphorylated protein at 240 kDa (Figure 3.13 A, see red arrows).

On the other hand, the time course experiment showed a less obvious temporal pattern in the phosphorylation signal when compared with that of PGI_2 (See figure 3.12 B) as only the band at 66 kDa appears to be temporally regulated in this blot. This band emerged after 1 min, peaked at 5 min and went down after 30 min (Figure 3.13 A top panel). Similarly to what we observed with PGI_2, a decrease in the phosphorylation of the basally phosphorylated protein at 44kDa could also be

observed (Figure 3.13 A top panel). The phosphorylation of $VASP^{ser157}$ also underwent no obvious temporal regulation (figure 3.13 A, middle panel).

Finally, we looked at the phosphorylation profile induced by stimulating PKA with the cAMP analogue 8-CPT-6-Phe-cAMP. We observed that increasing concentrations of 8-CPT-6-Phe-cAMP (0-50µM) also caused a gradual increase in the phosphorylation signal detected by phospho-PKA substrate and phospho-$VASP^{ser157}$ antibodies (figure 3.12 B). The phospho-PKA substrate profile was also similar to that observed with PGI_2 and Fsk with Increased phosphorylation observed with proteins at apparent molecular weights of 16, 35, 48, 66, 100 and 240 kDa (Figure 3.13 B, see red arrows).

Data from those experiments show that both Fsk and 8-CPT-6-Phe-cAMP can trigger PKA-dependent phosphorylation events similar to that of PGI_2. But the temporal pattern was less obvious.

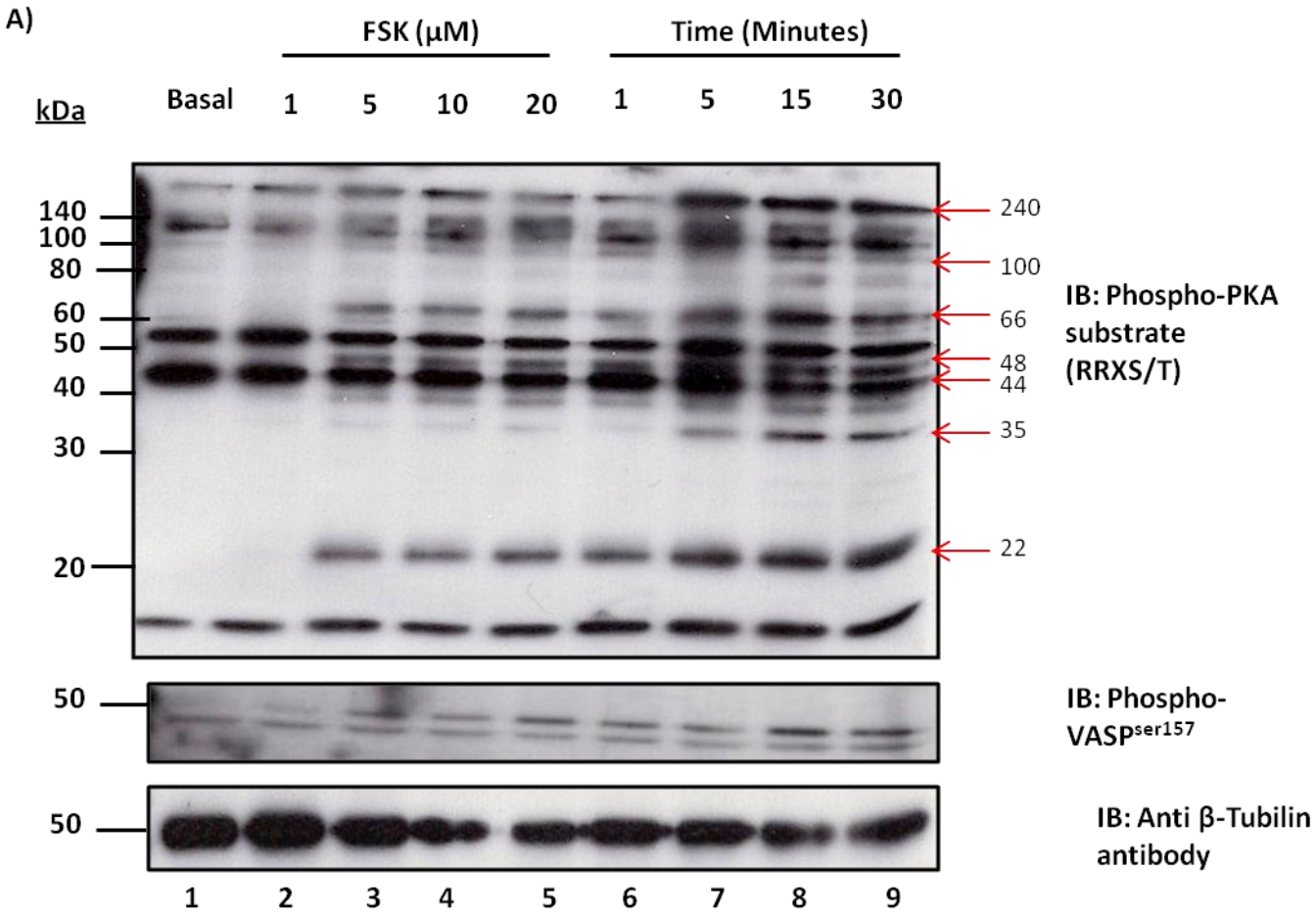
A)
FSK (µM)
Time (Minutes)
kDa
Basal
1
5
10
20
1
5
15
30
140
100
80
60
50
40
30
20
240
100
66
48
44
35
22
IB: Phospho-PKA substrate (RRXS/T)
50
IB: Phospho-VASPser157
50
IB: Anti β-Tubilin antibody
1
2
3
4
5
6
7
8
9

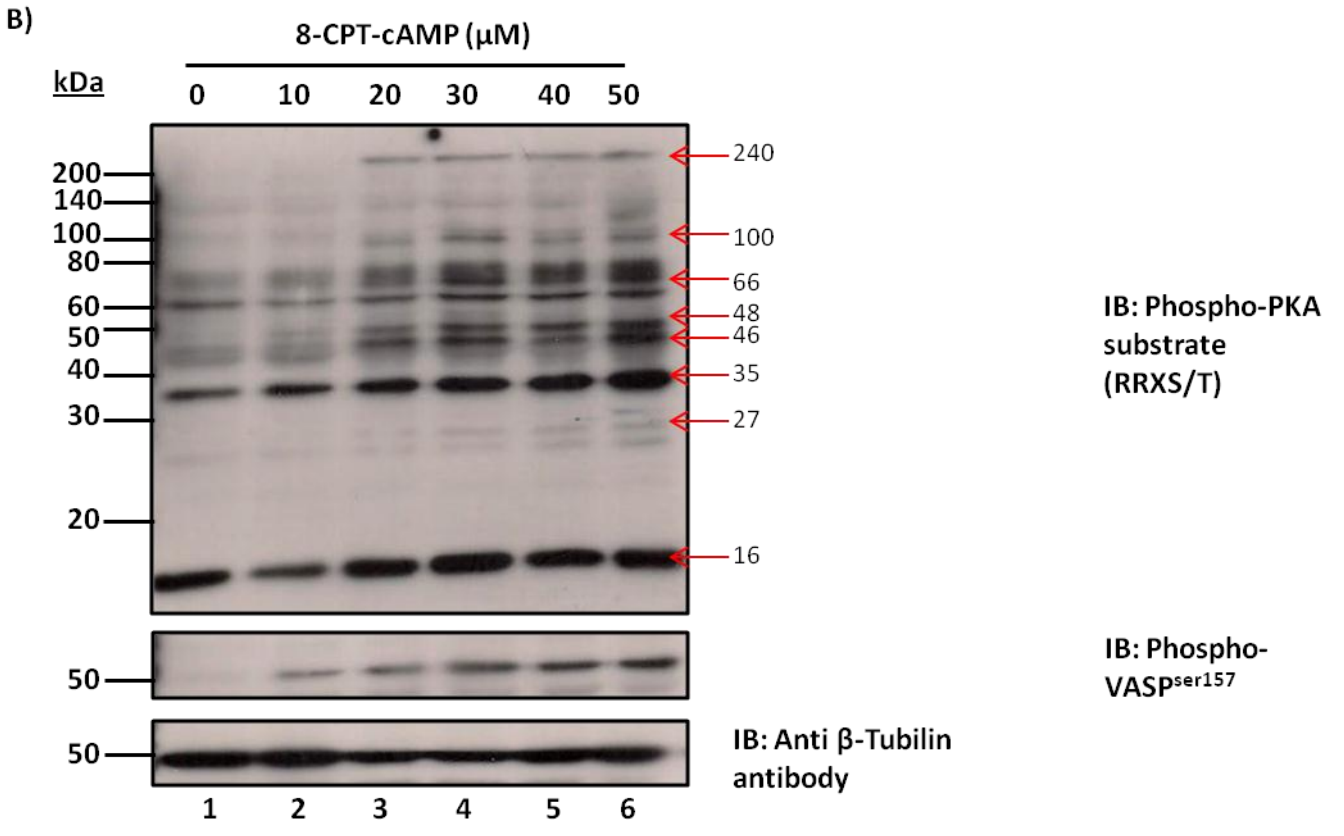
B)
8-CPT-cAMP (µM)
kDa
0
10
20
30
40
50
200
140
100
80
60
50
40
30
20
240
100
66
48
46
35
27
16
IB: Phospho-PKA substrate (RRXS/T)
50
IB: Phospho-VASPser157
50
IB: Anti β-Tubilin antibody
1
2
3
4
5
6

Figure 3. 13: Characterization of forskolin- and 8-CPT-6-Phe-cAMP-induced phosphorylation events in blood platelets.

WP ($2.5x10^8$ platelets/mL) were isolated using the pH method as described in chapter 2. **(A)** Platelets were pre-wormed for 2mins then stimulated with increasing concentrations of Fsk (0-20µM) for 1min (lanes 1-5) or they were stimulated with a constant concentration of Fsk (10µM) for increasing time points (1-30mins) (lanes 6-9). **(B)** As in (A) but platelets were stimulated with increasing concentrations of 8-CPT-6-Phe-cAMP (0-50µM) for 5min. Platelet lysates (20µg/well) were loaded onto a 10-18% gradient polyacrylamide gel and then resolved by SDS-PAGE for 2.5h at 120V. Proteins were then transferred into a PVDF membrane for 2.5h at 100V. Membranes were then blocked and immunoblotted with anti-phospho-PKA substrate rabbit antibody (top panel) overnight at 4^oC. Membranes were then stripped and reprobed with anti phospho-$VASP^{ser157}$ rabbit antibody overnight at 4^oC (middle panel). Membranes were finally immunoblotted for anti-β-Tubulin mouse antibody (bottom panels) overnight at 4^oC to check for equal loading. Red arrows indicate bands of interest. Blot represents one independent experiment.

3.10.3 Characterisation of the effect of platelet agonists on PKA-mediated phosphorylation events

In the circulation, platelets are constantly exposed to endothelium-derived inhibitors to keep them circulating in a quiescent state. But when platelets encounter a vascular injury they come into contact with components of the thrombogenic subcellular matrix, whose effect outweighs the anti-thrombogenic effects of the endothelium and induces platelet activation.

Therefore, in attempt to mimic what happens in the vasculature, we wanted to investigate the effect of platelet agonists such as collagen and thrombin on PKA signalling events under basal and PGI_2-treated conditions. In this experiment, WP were stimulated with collagen (5µg/mL) or with thrombin (0.02 U/mL) under nonaggregatory conditions in the presence or absence of PGI_2 (50nm). After that, the phosophorylation profile of PKA was examined (Figure 3.14). We observed a robust increase in the phosphorylation 44kDa phosphoprotein when platelets were stimulated with collagen and thrombin alone. Consistently with our data, stimulating WP with PGI_2 (50nM) led to an increase in the PKA phosphorylation profile and a decrease in the phosphorylation of the basally phosphorylated band of 44kDa. Interestingly, stimulating WP with collagen following the treatment with PGI_2 had no clear effect on the phosphorylation profile with the exception of the band at 44kDa whose phosphorylation increased significantly. Similar treatment with thrombin however, had a less significant effect on the band at 44kDa but a more pronounced effect on the whole of the PKA phosphorylation profile.

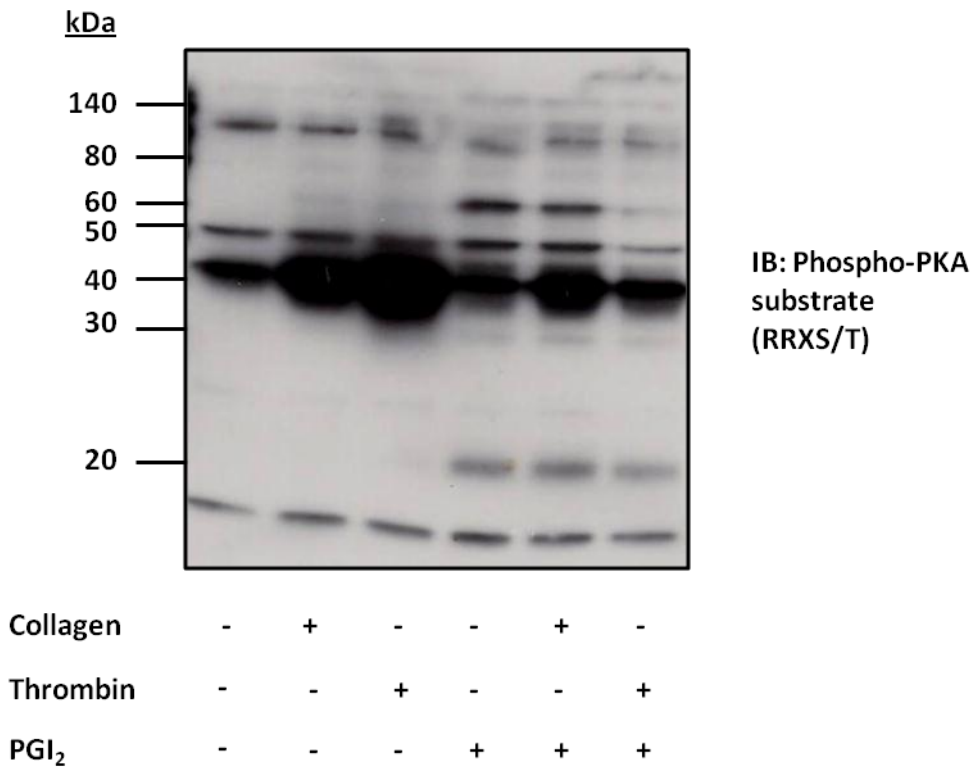

Figure 3. 14: The effect of platelet agonists on the phospho-PKA substrate profile.

WP ($2.5x10^8$ platelets/mL) were isolated using the pH method as described in chapter 2. Platelets were pre-wormed for 2 min under nonaggregatory conditions then either stimulated directly with platelet agonists (collagen: 5µg/mL or thrombin: 0.02 U/mL) for 90 sec or pretreated with PGI_2 (50nM) for 1 min before they were stimulated with the same agonists under the same conditions. Platelet lysates (20µg/well) were loaded onto a 10-18% gradient polyacrylamide gel and then resolved by SDS-PAGE for 2.5h at 120V. Proteins were then transferred into a PVDF membrane for 2.5h at 100V. Membranes were then blocked and immunoblotted with anti-phospho-PKA substrate rabbit antibody overnight at 4^oC. The blot is representative of two independent experiments with separate donors.

3.11 Discussion

The discovery of cAMP as a second messenger goes back to 1957 (Sutherland and Rall, 1958) whereas its role in inhibiting platelets in response to PGE_1 was identified later in the 1960s (Marquis *et al*., 1969). After that, prostacyclin was identified as the main cAMP-dependent platelet inhibitor (Moncada *et al*., 1976, Tateson *et al*., 1977). The importance of this pathway is exemplified by various pathological conditions that are associated with defects in the cAMP signalling pathway such as various bleeding disorders and atherosclerosis. For instance, reduced sensitivity to prostacyclin results in platelet hyperactivity, which is a major player in atherosclerosis and thrombosis (Van Geet *et al*., 2009). Conversely, platelet hypersensitivity to prostacyclin, attributed to a gain-of-function mutation in a Gs protein, gives rise to different bleeding phenotypes (Van Geet *et al*., 2009). This highlights the importance of understanding cAMP signalling networks in platelets, which are still after nearly five decades of research poorly understood. Throughout this study the main aim was to improve our understanding of cAMP/PKA signalling networks in blood platelets.

Work presented in this chapter aimed to characterise the inhibitory properties of various physiological and nonphysiological cAMP elevating agents under our own experimental conditions. The first step in this process was selecting an appropriate method for isolating platelets. The use of the classic prostaglandin method (Vargas *et al*., 1982) would potentially lead to misinterpretation of data as a result of adding prostaglandin to plasma, which would trigger the cAMP/PKA signalling pathway leading to residual effects of cAMP and receptor desensitisation. An available

alternative for this method relied on lowering the plasma pH to 6.4 without having to add any inhibitors (Mustard *et al*., 1989). Therefore, it was important to validate this method under our conditions. Data from figure 3.2 and 3.3 showed that platelets isolated by this method respond normally to agonists by assessing their aggregability and signalling responsiveness.

Since prostacyclin is the main physiological cAMP-dependent platelet inhibitor it was chosen to be our tool to explore the cAMP/PKA signalling cascade. We began by testing the inhibitory effect of PGI_2 on platelet aggregation mediated by different agonists. Data from figure 3.4 showed that PGI_2 can inhibit collagen-induced platelet aggregation in a concentration-dependent manner with 50% inhibition achieved with 49±8nM. In addition to inhibiting collagen-induced platelet aggregation, we showed that PGI_2 can inhibit thrombin-induced platelet aggregation with 50% inhibition achieved using 52±18nM (Figure 3.6). These data suggest that PGI_2 is a universal inhibitor of platelet functions, which is consistent with other reports in which the effect of PGI_2 was tested on multiple platelet agonists (Radomski *et al*., 1987a) (Fisher *et al*., 1987). Moreover, a direct comparison with PGE_1 was made and we found that PGI_2 is effective at a lower concentration than that of PGE_1 (Figure 3.7). The difference in potency between these two inhibitors, which supposedly trigger the same signalling pathway and were in the past thought to act through the same receptor (Schafer *et al*., 1979), is yet very much elusive. Data from this experiment highlighted the great potency of PGI_2, which agrees with earlier reports that compared the potency of PGI_2 with both PGE_1 and NO (Radomski *et al*., 1987a) (Tateson *et al*., 1977).

We also characterised the temporal dynamics of the inhibitory effects of PGI_2. Our data showed that the inhibitory effect of PGI_2 on aggregation is reversible (Figure 3.4). This is important physiologically as platelets need to retain their ability to aggregate when they encounter a vascular injury despite being constitutively exposed to PGI_2 released from the endothelium (Moncada, 1982b). These temporal dynamics fit in with time course experiments carried on PGI_2-induced AC activity as well as PKA phosphorylation events.

Our cAMP data showed that both PGI_2 and Fsk trigger concentration-dependent AC activity. But interestingly, we observed that comparable inhibitory effects of these two agents required different levels of cAMP. This was observed when PGI_2 (50nM) and Fsk (10µM) both induced 50% inhibition of aggregation through production of 237±39 and 340±29 fmol cAMP/10^7 platelets, respectively. In addition, we showed that PGI_2-induced AC activity is reversible although this experiment was only performed twice. Despite that, these cAMP data agree with early reports from Gorman and colleahues, which suggested that cAMP levels produced by PGI_2 peaked after 30 seconds and were maintained for two minutes then they started to decline reaching basal levels within 30 minutes (Gorman *et al*., 1977). These kinetics also agree with our proposed temporal regulation of PKA signalling events (Figure 3.12). This report also suggests that in contrast to PGI_2, elevation of cAMP levels induced by PGE_1 starts to fall after 30 seconds, which might help interpret our observations that PGI_2 is the most potent inhibitor of the two prostanoids. But this also begs another question that is: why is the temporal regulation of the AC activity triggered by two GsPCR different? A possible explanation for this phenomena has

been suggested by Zaccolo and colleagues who suggest that specific PDE isoforms are compartmentelised downstream a specific GsPCR (Stangherlin and Zaccolo, 2012).

Due to the low number of confirmed PKA substrates in platelets combined with the lack of specific phospho-antibodies for these substrates, we only used two different markers for PKA activity. The first one was the well-established PKA-mediated phosphorylation of VASP^{ser157} (Halbrugge *et al*., 1990) (Horstrup *et al*., 1994) whereas the other one was phosphorylation of PKA substrate profile. The use of phospho-PKA substrate as an additional PKA activity marker not only confirmed data obtained from using p-VASP^{ser157} but also allowed us to simultaneously look at multiple PKA substrates (Patel *et al*., 2010, Biton and Ashkenazi, 2011, Moir *et al*., 2006), and assess their differential regulation in response to various stimulating conditions. Within these experiments, especially the time-course experiments, the blots were deliberately overexposed to increase the number of bands. Although the majority of the bands were observed across all experiments, a small minority could not be observed in some occasions. This could be due to various reasons such as variation across different donors, inefficient transfer of proteins onto the PVDF membrane or maybe insufficient separation of bands with close molecular weights when using small gels. Transfer issues were later overcome by using the new Trans-Blot Turbo system from Bio-Rad (see figure 3.12 B) after which more bands were transferred onto the PVDF membrane and with a better resolution.

We showed that PGI_2 induced the phosphorylation of $VASP^{ser157}$ and several other substrates as detected by the phospho-PKA substrate antibody. The apparent molecular weight of most of these substrates was consistent with molecular weights reported by others (El-Daher *et al*., 1996) (Waldmann *et al*., 1987). The temporal regulation of VASP phosphorylation followed a trend that agreed with the aggregation data (Figure 3.12). In addition, the phosphorylation of PKA substrates was also reversible and in general followed a trend similar to that of phospho-$VASP^{157}$. But the temporal regulation for individual bands followed an astonishing distinct pattern with bands coming up, peaking and disappearing at different time points (Figure 3.12). The reversibility of PKA phosphorylation events in platelets has been reported by El-Daher *et al* although they used a cAMP analogue in their study instead of PGI_2. Some of their observations were similar to ours as they suggested that most phophosphorylation events peaked within 2.5 min and started to decay after 5 min with the exception of the band at 22kDa whose phosphorylation persisted for an hour (El-Daher *et al*., 1996). We observed basal phosphorylation of several bands such as those at 16, 44, 55 and 130kDa. Bands with similar apparent molecular weights were observed basally by both Sandberg and El-Daher when phosphorylation was detected by autoradiograph (El-Daher *et al*., 1996) (Waldmann *et al*., 1987). The basal PKA activity is important and can be interpreted as a natural result of basal AC activity resulting from constitutive exposure of platelets to PGI_2 in circulation in order to maintain their dormant state. We showed that stimulation with PGI_2 increased the phosphorylation of the basally phosphorylated proteins in addition to some new substrates. The basally phosphorylated band at 44kDa was an

exception whose phosphorylation rather went down in response to PGI_2 but increased in response to platelet agonists (Figure 3.14) which is consistent with early reports (Waldmann *et al*., 1987). This band has been suggested to be inositol triphosphate 5`-phosphomonoesterase (Waldmann *et al*., 1987). Although the identity of the phosphoproteins recognised by the phospho-PKA substrate antibody is yet to be established, some of the previously-reported PKA substrates in platelets match the apparent molecular weights of substrates reported in this study (see table 3.1). Mass-spectrometric analysis of those bands can potentially identify and confirm their identity.

The inhibitory properties of other nonphysiological cAMP-dependent agents were characterised. These agents allow different parts of the PKA pathway to be activated independently and therefore can be used as tools to dissect the regulation of the pathway at different levels. Firstly, the inhibitory effects of the direct AC activator Fsk, were assessed. Fsk inhibited collagen-induced platelet aggregation in a concentration-dependent manner, but with lower potency than physiological inhibitors as 50% inhibition was achieved with 10±4µM. Even 20µM of Fsk did not completely abolish the aggregation response (Figure 3.8). Higher concentrations of Fsk should be used to achieve full inhibition of platelet aggregation. The inhibitory effect of Fsk on aggregation was also reversible, which is consistent with early reports when Fsk was first identified (Seamon *et al*., 1981). Fsk also induced PKA-mediated phosphorylation events with a significantly less pronounced temporal pattern compared with PGI_2 (Figure 3.13 A). It has to be

mentioned here that all Fsk time course experiments were performed only twice and more experiments are needed to consolidate these findings.

The inhibitory effects of a cAMP analogue used to directly activate PKA in an AC-independent manner were also tested. The analogue that we used was derived from 8-CPT-cAMP, which has no preference to any PKA isoform (Schwede *et al*., 2000). This was important to us in order to avoid biased activation of a specific PKA isoform, which would make the comparison with other PKA activators irrelevant. 8-CPT-6-Phe-cAMP (Biolog, Germany) was the cAMP analogue of choice throughout this study mainly for its high membrane permeability attributed to the inclusion of a phenyl ring (Christensen *et al*., 2003). This compound showed a good concentration-dependent inhibitory effect with 50% inhibition achieved using 30±6μM, which only required 5 min preincubation when tested on collagen-induced platelet aggregation (Figure 3.9). It also stimulated PKA-mediated signalling events represented by phosphorylation of PKA substrate profile and $VASP^{ser157}$ (Figure 3.13 B).

Data from these experiments showed that the potency of PGI_2 is greater than that of the other nonphysiological PKA activators tested. These data also suggest that PGI_2 is more efficient than the other nonphysiological PKA-dependent inhibitors. This was observed when comparable inhibitory effects (50%) were achieved with lower cAMP levels produced with PGI_2 when compared with the concentration of the cAMP analogue that was used and the levels of cAMP produced by Fsk. We postulate that this is due to temporal and spatial regulation of the IP receptor-

triggered signal, which directs the signal into specific cellular compartments where it is needed the most. We hypothesise that this specificity would be compromised when nonphysiological agents were used and hence more cAMP would be needed to achieve the same level of inhibition.

In conclusion, data in this chapter described the inhibitory properties of different cAMP/PKA activating agents. The conditions for these agents to inhibit platelet aggregation, trigger PKA-mediated signalling and induce cAMP production were optimised. We also utilised a new PKA activity marker which is an antibody that can detect PKA-phosphorylated proteins. All the parameters that have been optimised in this chapter would be subjected to various experimental conditions in successive chapters in order to try to unravel spatial and temporal regulation of cAMP/PKA signalling networks in blood platelets.

Chapter 4: The role of A-kinase anchoring proteins in platelet inhibition by cAMP/PKA signalling.

4.1 Introduction:

PGI_2 plays an important role in controlling the growth of a platelet plug at the site of a vascular injury and thereby controls thrombosis. The mechanism by which PGI_2 exerts its biological effects in platelets occurs through elevating intracellular cAMP levels (Tateson *et al*., 1977). Increased cAMP in platelets is associated with inhibition of Ca^{+2} mobilisation (Cavallini *et al*., 1996), platelet dense granule secretion (Feinstein and Fraser, 1975), $\alpha_{IIb}\beta_3$ activation, aggregation (Graber and Hawiger, 1982) as well as accrual of platelets at the site of a vascular injury (Sim *et al*., 2004). However, the molecular mechanism by which cAMP-regulated molecules inhibit platelet function is still poorly understood.

Protein kinase A (PKA) is the main effector of cAMP signalling in blood platelets. The inactive PKA holoenzyme is a heterotetramer composed of two regulatory (R) holding two catalytic (C) subunits. Two isoforms of PKA have been identified, PKA I and PKA II (Corbin *et al*., 1975a). These isoforms differ in their regulatory subunits (RI and RII). In their turn both R and C subunits exist in different isoforms (RIα, RIβ, RIIα, RIIβ, Cα, Cβ, Cγ), which adds to the complexity. In platelets, isoforms RIα, RIβ, RIIβ, Cα and Cβ are expressed giving rise to PKA I and PKA II holoenzyme (Rowley *et al*., 2011). However, the differential roles, localisation and the relative contribution of these two isoforms to the inhibition of platelet function is still very much elusive.

The spatio-temporal regulation of a cellular signal is a relatively new term that has emerged to refer to the initiation and termination of a signal at a distinct subcellular compartment and at a specific time point. In this "compartment" the components of signalling machinery are present in close proximity to focus on particular substrates that regulate a specific cellular function. The spatio-temporal regulation of cAMP/PKA signalling in other cell types has been attributed to the effect of a structurally diverse yet functionally similar family of proteins called A-kinase anchoring proteins (AKAPs). These AKAPs bind to the D/D domain of the PKA regulatory subunits through an amphipathic helix that is characteristic of all AKAPs (Carr *et al*., 1991). The function of AKAPs further involves targeting PKA into specific subcellular compartments through a unique targeting domain that is characteristic of every AKAP. To date 48 AKAPs have been identified, most of which are PKA II-specific and the rest are dual-specific (Tasken and Aandahl, 2004). An entirely PKA I-specific AKAP has been identified recently (Means *et al*., 2011).

Spatio-temporal regulation of cAMP/PKA signalling networks is yet to be reported in blood platelets. However, early findings by El-Daher *et al* demonstrated a differential distribution of various PKA substrates in different subcellular compartments (El-Daher *et al*., 1996), suggesting potential compartmentalisation of signalling. In addition, a recent quantitative chemical proteomic study and an RNA-seq analysis of human platelet transcriptomes reported the presence of cAMP pools and some potential AKAPs in platelets (Margarucci *et al*., 2011, Rowley *et al*., 2011). While the components of these signalling pools were not identified, these studies suggest that compartmentelisation of cAMP/PKA signalling in platelets might exist.

The distinct biochemical properties as well as the differential localisation of the two PKA isoforms provide the rationale for potential non-redundant roles. However, this is yet to be established in blood platelets.

Aims and objectives

In this chapter the potential spatio-temporal regulation of cAMP/PKA signalling networks in platelets was explored. More specifically the objectives were:

- To determine the differential localisation of PKA isoforms in platelets.
- To determine functional relevance of PKA I-AKAP interactions in platelets.
- To identify a potential subcellular compartment to which PKA I localises in an AKAP-dependent mechanism and establish a functional relevance for this localisation.
- To identify a PKA I-specific substrate whose phosphorylation is regulated by AKAPs.

4.2 The presence of both PKA isoforms in blood platelets

To date, two isoforms of PKA have been identified, PKA-I and PKA-II, which are distinguished according to their regulatory subunits RI and RII, respectively. In the first instance the presence of the two PKA isoforms in platelets was confirmed.

Increasing amounts of protein (1-40μg) from untreated platelet whole-cell lysate were separated by SDS-PAGE and immunoblotted for PKA-RI, PKA-RII and PKAc using specific antibodies. The blots demonstrate clearly the presence of PKA-RI, PKA-RIIβ and PKAc in platelet lysates (Figure 4.1). The antibody used to probe for RI recognises both RIα and RIβ and so we were unable to differentiate the expression of the two individual regulatory units.

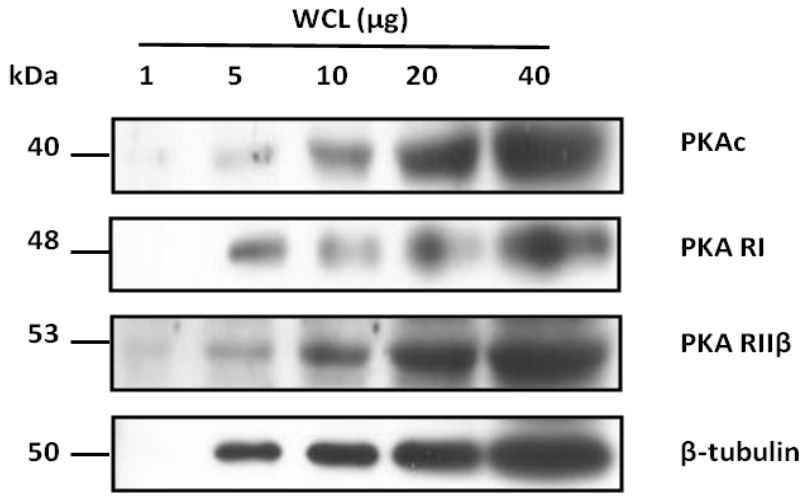

Figure 4. 1: All PKA subunits are expressed in platelets.

WP (2-5x10^8 platelets/mL) were isolated using the pH method as described in chapter 2. They were then lysed with Laemmli buffer under basal levels. Platelet lysates (1-40µg/well) were loaded onto a 10% polyacrylamide gel and then resolved by SDS-PAGE for 1.5h at 120V. Proteins were then transferred onto a PVDF membrane for 2.5h at 100V. Membranes were then blocked and immunoblotted with anti-PKA RI, anti-PKA RIIβ or anti-PKAc mouse antibodies (1:1000) overnight at 4^{o}C. Membranes were then stripped and re-probed for anti-β-tubulin antibody. Blot is representative of two independent experiment.

4.3 PKA isoforms are differentially expressed in platelet lipid rafts

Having proven the presence of both PKA isoforms in platelet lysate, we next wanted to determine their differential localisation into platelet lipid rafts. Lipid rafts are areas of the cellular membrane that are enriched in cholesterol and sphingolipids, which are distinct from the non-raft parts of the membrane that are enriched in glycerophospholipids. Lipid rafts play an important role in signal transduction both in platelets and other cell types (Simons and Toomre, 2000, Lopez *et al*., 2005). More specifically lipid rafts have been reported to play a critical role in cAMP signalling in numerous cell types (Willoughby and Cooper, 2007). For these reasons, platelet lipid rafts appealed to us as a potential cAMP/PKA platelet subcellular compartment to explore.

4.3.1 Validation of platelet lipid raft isolation technique

Lipid rafts are resistant to solubilisation with a non-ionic detergent, which is why they are called the detergent resistant membranes (DRM) (Simons and Toomre, 2000). In this study, cold extraction of lipid rafts using Triton X-100-based lysis buffer followed by sucrose gradient ultracentrifugation was the method of choice (see methods for details).

Initial validation of the methodology included analysis of different lipid raft lysis buffers with varying concentrations of Triton X-100 were used to extract platelet lipid rafts. LAT was used as a well-established lipid raft marker (Zhang *et al*., 1998b) whereas integrin β3 was used as a non-raft marker. The quality of lipid raft isolation using this method and the fore-mentioned markers is normally assessed by the

ability to obtain two distinctive populations of LAT, at the buoyant fractions between 5-30% and at the heavy fractions 40% of the sucrose gradient, and one population of integrin β3 localised at the heavy fractions. Excessive or insufficient amounts of the detergent, leads to impaired isolation of lipid rafts and as a result the lack of distinctive populations of LAT or β3. Figure 4.2 A shows that 0.065% v/v Triton X-100 in the lipid raft lysis buffer was sufficient to solubilise all non-raft fractions, but low enough to allow the lipid rafts to remain intact. A population of LAT in lanes 4, 5 and 6 can be observed which corresponds to detergent resistant fractions and may represent lipid rafts. A second population of LAT can be observed in lanes 10, 11 and 12. In addition, a single population of β3 is observed in lanes 10 to 12 corresponding to detergent-soluble or non-raft fractions. In contrast, the distinctive two populations of LAT were less clear, when using 0.045 and 0.1%v/v of Triton X-100 in the lysis buffer. To determine which of the fractions were the peak raft fraction the concentration of cholesterol in each fraction was measured. Fraction 5, which had the highest amount of the raft marker LAT, also had the greatest cholesterol content compared with the rest of the fractions (figure 4.2 B). From these data 0.065% v/v Triton X-100 in lipid raft lysis buffer was used for the isolation of lipid rafts from human platelets.

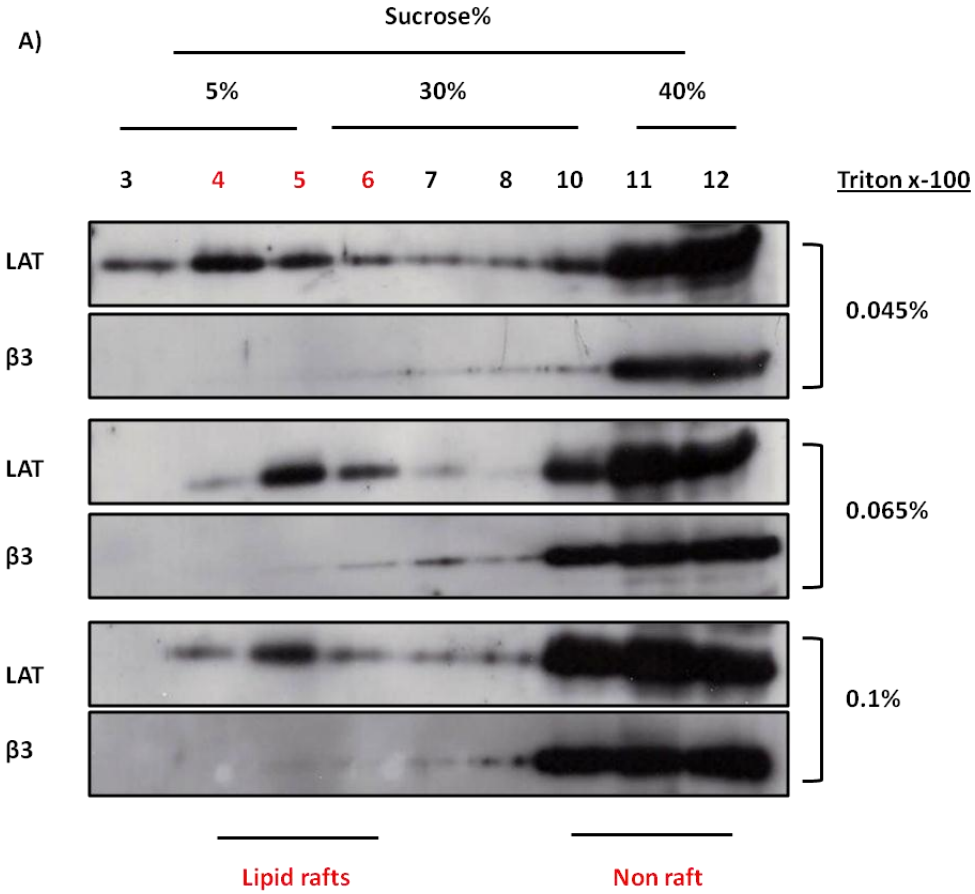
A)
Sucrose%
5%
30%
40%
3
4
5
6
7
8
10
11
12
Triton x-100
LAT
β3
0.045%
LAT
β3
0.065%
LAT
β3
0.1%
Lipid rafts
Non raft

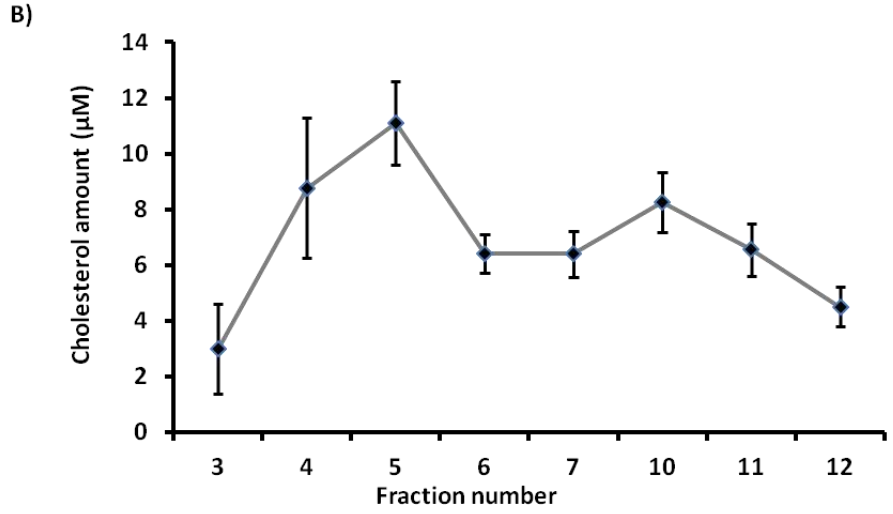
B)
Cholesterol amount (µM)
0
2
4
6
8
10
12
14
3
4
5
6
7
10
11
12
Fraction number

Figure 4. 2: Optimisation of platelet lipid raft isolation technique.

Washed platelets ($1x10^9$ platelets/mL) were lysed with lipid raft lysis buffer containing 0.045, 0.065 or 0.1% Triton X-100 for 30 min on ice. Lipid rafts were isolated using sucrose gradient ultracentrifugation as described in methods. **(A)** Aliquots of fractions (45µl) were then analysed by 10% SDS-PAGE for 1.5h at 120V followed by immunoblotting for 2.5h at 100V. Membranes were then blocked and then probed with LAT (1:1000 rabbit) and integrin β3 (1:1000 rabbit) overnight at 4^oC to identify raft and non-raft fractions, respectively. Data are representative of 2 independent experiments. **(B)** Cholesterol content of the loaded fractions was determined using a fluorescence assay as described in methods. Data are representative of 4 independent experiments.

4.3.2 PKA isoforms are differentially distributed into platelet lipid rafts

In many cell types, PKA isoforms are found in distinct cellular locations allowing them to perform specific functions in response to distinct stimuli. In light of the critical role that lipid rafts play in regulating cAMP signaling in numerous cell types (Tasken and Ruppelt, 2006, Willoughby and Cooper, 2007), we examined the presence of PKA isoforms in the these cholesterol and sphingolipid enriched microdomains.

Platelet fractions were isolated by ultracentrifugation and then analysed by SDS-PAGE followed by immunoblotting. Under basal conditions PKA was distributed into two pools, a very small amount was observed in the lipid raft (fraction 5)(Figure 4.3 A, third panel from top), with the vast majority localised in the non-raft fraction. In contrast, under the same conditions PKA-RII was found exclusively in the non raft fraction (Figure 4.3 A, bottom panel). Upon stimulation of platelets with PGI_2 (100nM) there was a significant redistribution of PKA-RI into the detergent-resistant fractions (figure 4.3 B, top panel) raising its presence there by nearly two folds ($p<0.05$) (figure 4.3 C). Interestingly, PGI_2 stimulation did not redistribute PKA-RII into lipid rafts and rather remained exclusively in non-raft fractions. The lipid raft marker LAT was detected in fractions 4 and 5 whereas the non-raft marker β3 was observed in fractions 10,11 and 12 (figure 4.3 A, top two panels). These data suggest that only PKARI is present in lipid rafts, and that its movement is a dynamic process that is associated with increased cAMP levels.

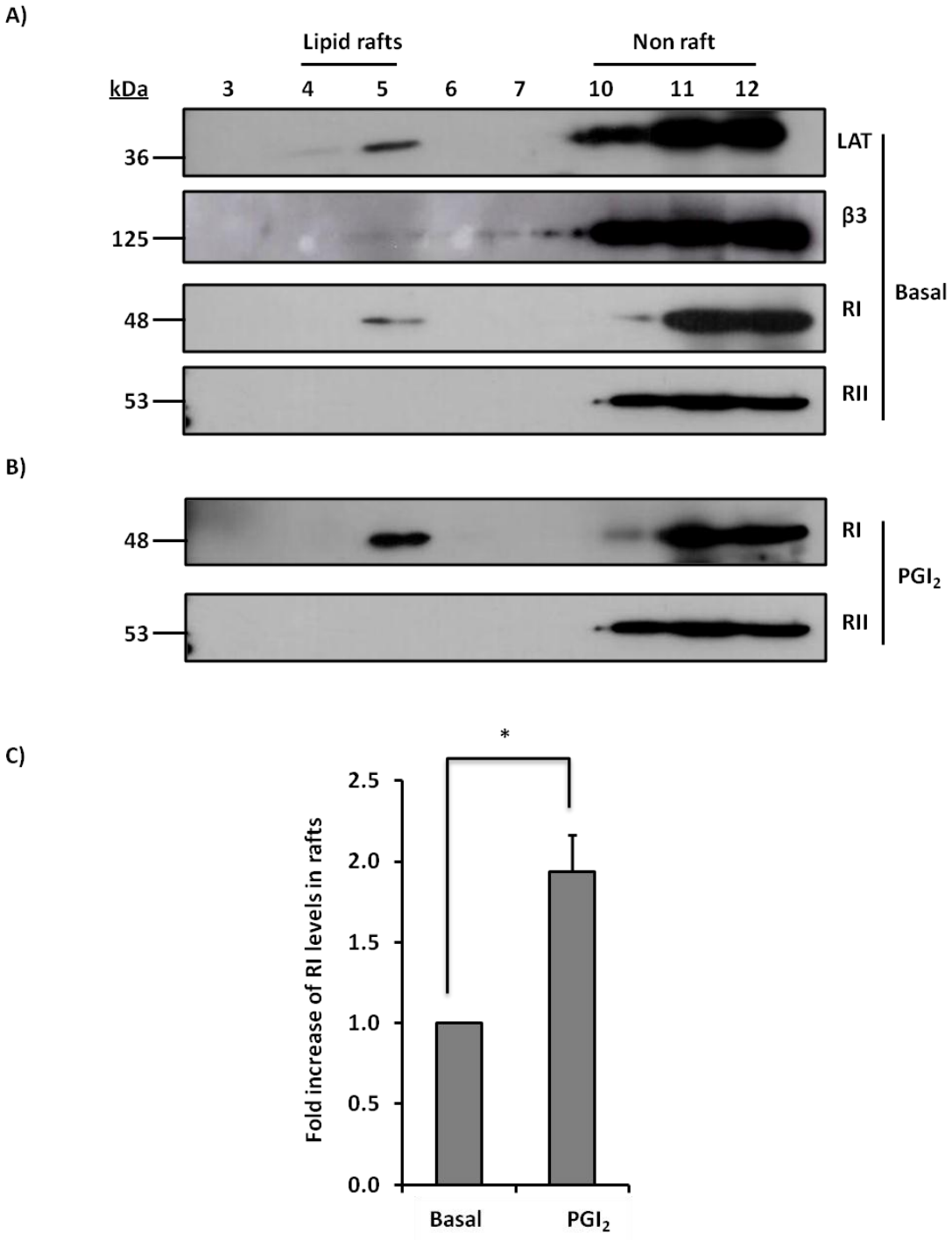
A)
Lipid rafts
Non raft
kDa
3
4
5
6
7
10
11
12
36
125
48
53
LAT
β3
RI
RII
Basal
B)
48
53
RI
RII
PGI2
C)
*
Fold increase of RI levels in rafts
2.5
2.0
1.5
1.0
0.5
0.0
Basal
PGI2

Figure 4. 3: PKA isoforms are differentially distributed into lipid rafts.

Platelets ($1x10^9$ platelets/mL) were either left untreated (A) or stimulated with PGI_2 (100nM) for 1 min at 37^oC (B). Platelets were then lysed with lipid raft lysis buffer containing 0.065% Triton X-100 for 30 min on ice. Lipid raft and non-raft fractions were then separated by sucrose gradient ultracentrifugation. Aliquots of fractions (45µl) were then analysed by 10% SDS-PAGE for 1.5h at 120V followed by immunoblotting for 2.5h at 100V. Membranes were then blocked and firstly probed with LAT (1:1000 rabbit) and integrin β3 (1:1000 rabbit) to identify raft and non-raft fractions, respectively. Membranes were then probed with either PKA-RI (1:1000 mouse) or PKA-RII (1:1000 mouse). Blots are representative of 4 independent experiments. (C) Fold increase of RI levels in lipid rafts normalised against basal levels. Data are from 4 independent experiments with 4 separate blood donors and are expressed as means ± SEM (*: $p \leq 0.05$ compared with basal).

4.4 Characterisation of the RI-Anchoring Disruptor (RIAD)

The spatio-temporal regulation of cAMP/PKA signalling can be mediated by AKAPs in numerous cell types (Tasken and Aandahl, 2004). A major tool used to study the biological relevance of AKAPs in other cell types is the use of cell-penetrating inhibitory peptides. These peptides mimic the PKA binding domain of AKAPs, and competitively block the interaction between PKA R subunits and their AKAPs. Numerous AKAP-PKA disruptor peptides have been developed, which differ in their specificity towards an individual PKA isoforms (Pidoux and Tasken, 2010).

In the present study a number of different peptides were used in order to ascertain the type of AKAPs present. The peptide Ht31 was used as an established disruptor of dual-specificity AKAPs and PKA. This was then supplemented by the use of a newly developed RI Anchoring Disruptor (RIAD-Arg_{11}), which was specific for PKA I-AKAPs (AKAP-I). This peptide was synthesised with a poly-Arg tail, which has been shown previously to aid in the cell penetration of peptides (Nakase *et al*., 2008). The scrambled partner (ScrRIAD-Arg_{11}) was used as a negative control to rule out nonspecific effects (see Methods for details about peptide and its scrambled analogue).

4.4.1 Optimisation of conditions for cell penetration of RIAD-Arg_{11}

An important first step in examining the role of platelet PKA-AKAP interactions was to determine the conditions for the use of our PKA-AKAP disrupter. To be confident that the inhibitor peptide was being internalised, RIAD-Arg_{11} was labelled with fluorescein prior to incubation with washed platelets for different time points (5-60 minutes) at 37^{o}C. Platelets were adhered for 30 min on glass slides before being examined by a fluorescence microscope. Here, only platelets that were incubated with the peptide for 60 minutes produced a fluorescence signal suggesting that the peptide needs 60 minute incubation at 37^{o}C to penetrate the cell (Figure 4.4). Shorter incubation times showed no fluorescence suggesting that the peptide was not simply interacting with the cell surface.

From this figure we can conclude that the peptide needs at least 60 minute incubation at 37^{o}C before it gets into the cell and in order to observe its functional effects on various biological processes.

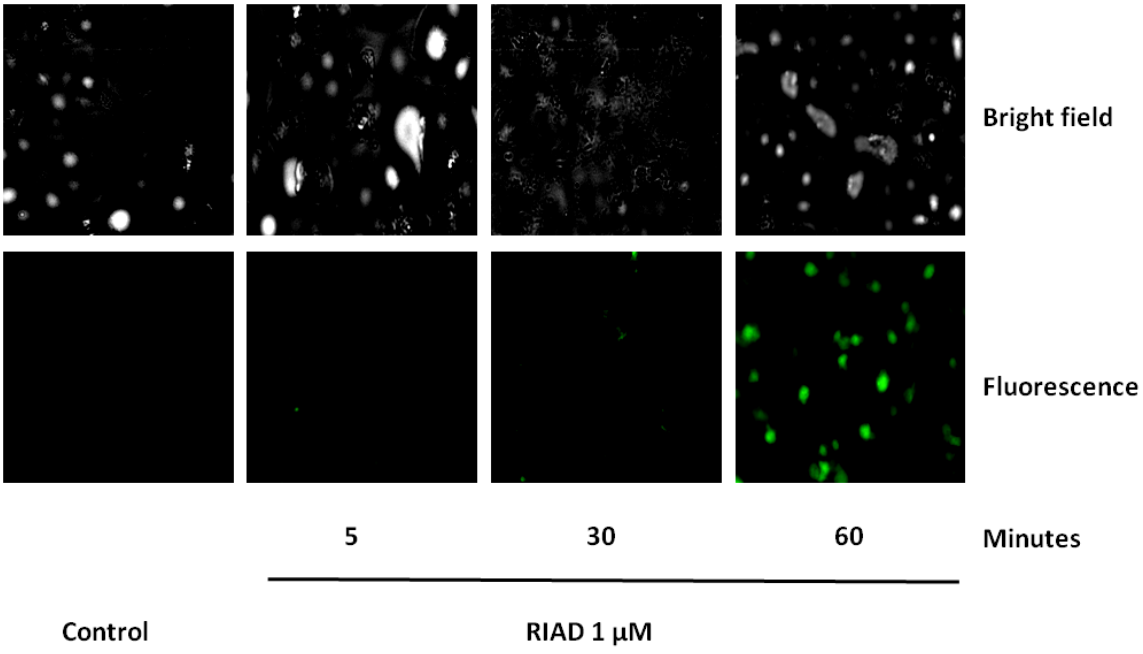

Figure 4. 4: Optimisation of RIAD-Arg11 incubating conditions with blood platelets.

Platelets ($5x10^7$plts/ml) were left to adhere on glass slides for 30 minutes at 37^oC after being incubated with fluorescein-conjugated RIAD-Arg_{11} (1µM) for increasing time points (0, 5, 30 and 60 minutes). Platelets were then visualized under an Olympus fluorescence microscope. Images are representative of 2 independent experiments. Experiment was carried out in collaboration with Dr. Simbarashe Magwenzi.

4.5 cAMP-mediated inhibition of platelet aggregation requires AKAP-RI interactions

Having established the optimal conditions for use of RIAD-Arg_{11} with platelets, we wished to investigate whether or not the potential interactions of AKAPs with PKA I could impact on platelet sensitivity to cAMP-mediated inhibition of platelet functions. The rationale for this approach was that if AKAP-PKA I interactions were important, then the presence of RIAD-Arg_{11} would prevent or reduce the inhibitory actions of cAMP elevating agents.

4.5.1 Inhibition of platelet aggregation by PGI_2 requires AKAP-RI interactions

Initial experiments were designed to examine whether the inhibitory effect of the most physiologically relevant cAMP-dependent platelet inhibitor, PGI_2, was reliant on AKAP-RI interactions.

Treating platelets with PGI_2 (50nM) caused a 76±3% inhibition of collagen-induced platelet aggregation ($P<0.001$). Pretreating platelets with increasing concentrations of RIAD-Arg_{11} (0.1-10µM) resulted in a concentration-dependent reversal of PGI_2-mediated inhibition of aggregation, although this reversal effect was not complete. A significant reversal was observed with 1µM of the RIAD-Arg_{11} where the inhibitory effect of PGI_2 dropped from 76±3% down to 44±5% ($p\leq0.0001$ when compared with PGI_2 alone, figure 4.5). A further decrease in PGI_2-mediated inhibitory effect was observed when RIAD-Arg_{11} was used at a concentration of 10µM but that decrease was not statistically significant when compared with 1µM. In control experiments the scrambled analogue of the peptide ScrRIAD-Arg_{11} (1µM)

failed to cause any reversal of the inhibitory effect of PGI_2 on collagen-induced aggregation (figure 4.5). In further experiments we tested the effects of St-Ht31, as another PKA-AKAP inhibitor to cross validate our findings with RIAD-Arg_{11}. St-Ht31 is a nonspecific PKA-AKAP inhibitor that can disrupts the binding of both PKA I and PKA II to AKAPs. Similar to RIAD-$Arg_{11,}$ pretreatment of platelets with St-Ht31 (5µM) for 1 hour decreased PGI_2-mediated inhibition of platelet aggregation from 76±3% to 49±5% ($P<0.05$, Figure 4.5 B and C).

Data from this experiment suggest that inhibition of collagen-induced platelet aggregation by PGI_2 is significantly reversed in the presence of RIAD-Arg_{11}, which could be attributable to disruption of AKAP-PKA I interactions.

The observation that both St-Ht31 and RIAD-Arg_{11} could reverse the inhibitory effect of cAMP on platelet aggregation induced by collagen suggested a role for a type 1 AKAP in platelets. Consequently, we focussed our work on the use of RIAD to delineate the role of PKA I functions in platelets.

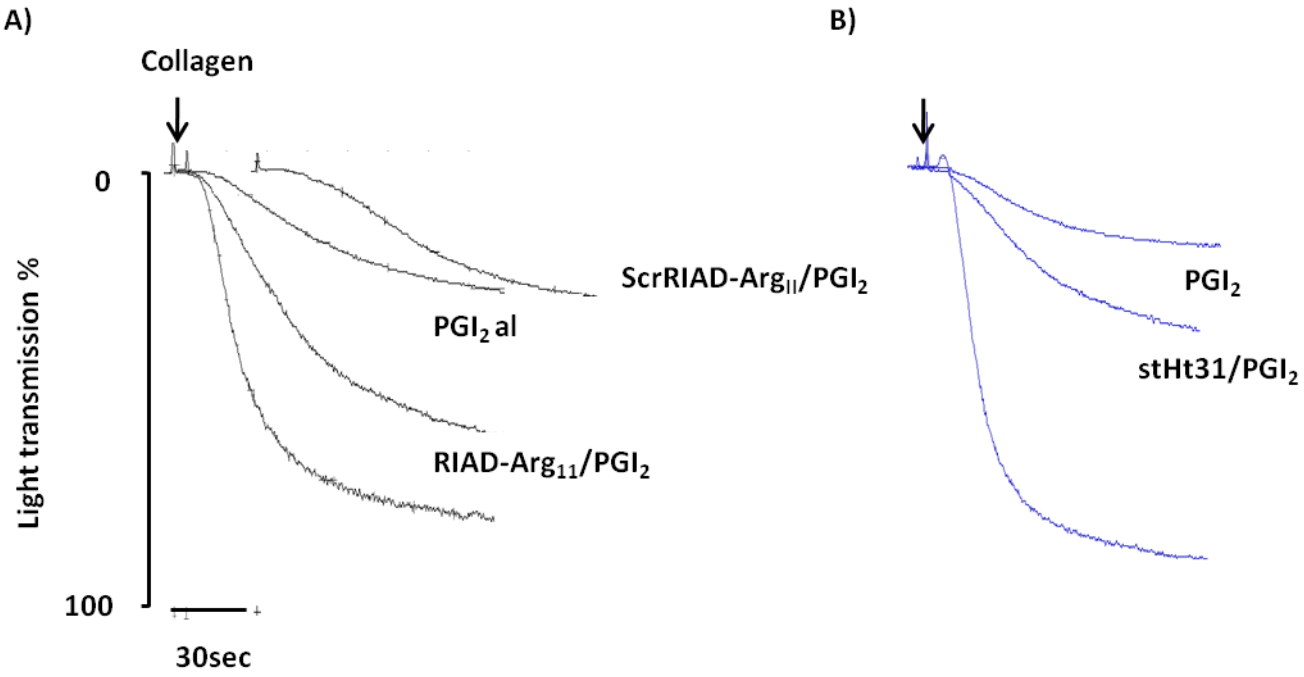
A)
Collagen
0
100
Light transmission %
30sec
ScrRIAD-Arg$_{II}$/PGI$_2$
PGI$_2$ al
RIAD-Arg$_{11}$/PGI$_2$
B)
PGI$_2$
stHt31/PGI$_2$

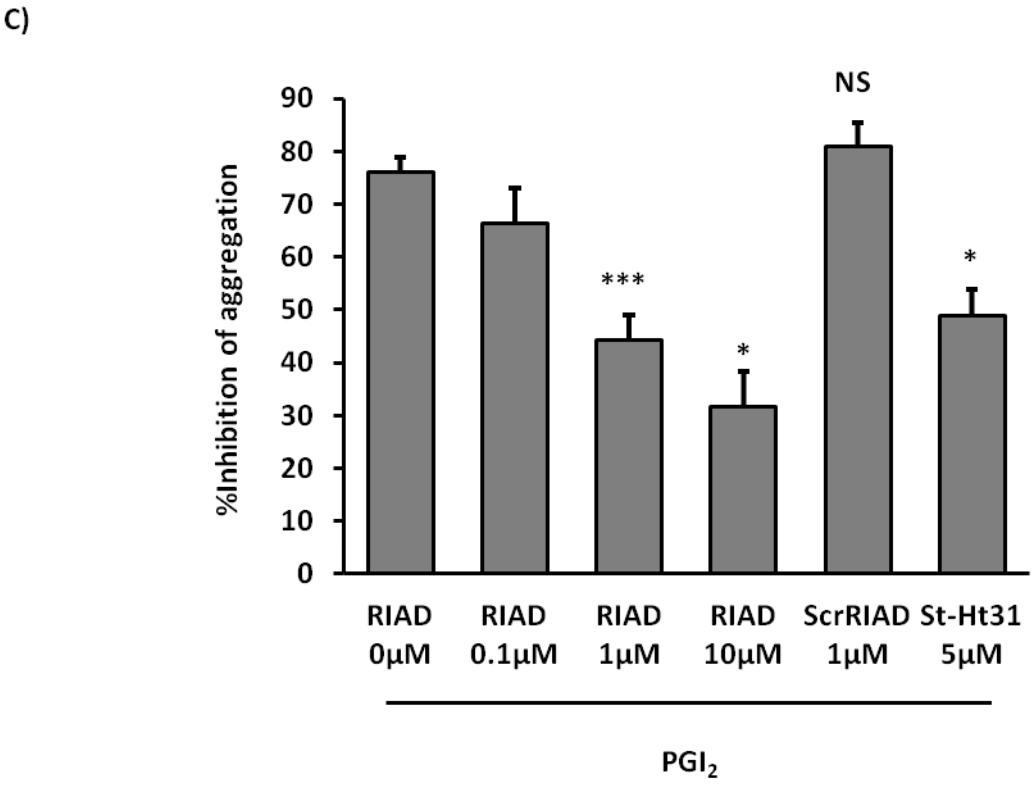
C)
%Inhibition of aggregation
90
80
70
60
50
40
30
20
10
0
NS
***
*
*
RIAD 0µM
RIAD 0.1µM
RIAD 1µM
RIAD 10µM
ScrRIAD 1µM
St-Ht31 5µM
PGI$_2$

Figure 4. 5: RIAD reverses the inhibitory effect of PGI2 on collagen-mediated aggregation.

WP ($2.5x10^8$ platelets/mL) were either stimulated with collagen (5µg/mL) or pre-incubated with **(A)** RIAD-Arg_{11} (0.1-10µM), ScrRIAD-Arg_{11} (1µM) or vehicle for 1 hour or **(B)** St-Ht31 (5µM) for 30 min at 37°C. After treatment with peptides, platelets were then treated with PGI_2 (50nM) for 1 min before stimulating with collagen. Aggregation was monitored for 4 min under constant stirring (1000rpm) at 37°C using a chrono-log dual channel light transmission aggregometer and aggregation traces were generated by aggreo/link computer software (Chrono-log, USA). **(B)** Data expressed as means ± SEM of %inhibition of aggregation represent 8 independent experiments (except RIAD 10µM and st-Ht31 data, N=3) from separate donors (* : $p \leq 0.05$, *** : $p \leq 0.0001$ when compared with PGI_2 alone).

4.5.2 Inhibition of platelet aggregation by Fsk requires AKAP-RI interactions

Having established that potential disruption of PKA-AKAP interactions influenced platelet sensitivity to PGI_2, it was important to determine whether this was specific to PGI_2 or a more generic effect. Hence the effects of RIAD on Fsk-mediated platelet inhibition were examined.

Treating platelets with Fsk (10μM) caused an inhibitory effect of 53±9% of collagen-induced aggregation. However, this inhibitory effect dropped to 27±10% ($P<0.05$ when compared with Fsk alone) when platelets were pre-incubated with RIAD-Arg_{11} (1μM) for 1 hour before treatment with Fsk (Figure 4.6). In contrast control experiment with ScrRIAD-Arg_{11} used under the same conditions had no significant effect on Fsk-mediated platelet inhibition (Figure 4.6).

Data from this experiment confirm that the effect of RIAD-Arg_{11} is not specific to PGI_2 and suggest that inhibiting platelet aggregation through directly raising cAMP levels might also require AKAP-PKA I interactions.

One possible explanation for the reduced sensitivity to cAMP signalling in the presence of RIAD is that the peptide itself stimulates or potentiates platelet aggregation. In order to exclude the possibility that RIAD-Arg_{11} is potentiating platelet aggregation rather than reversing the inhibitory effect by PGI_2, we tested its effect on aggregation with two agonists. Firstly, the influence of RIAD-Arg_{11} on collagen-induced aggregation was tested. RIAD-Arg_{11} (1μM) did not influence the rate or extent of aggregation induced by either high concentration (5μg/mL) or low dose (0.25μg/mL) of collagen (Figure 4.7 A, B). Similarly, no potentiating effect was observed when the same test was carried out on thrombin (0.02U/mL) (Figure 4.7

C). These data suggest that RIAD-Arg_{11} affects cAMP signalling rather than activating or potentiating platelet aggregation by an agonist.

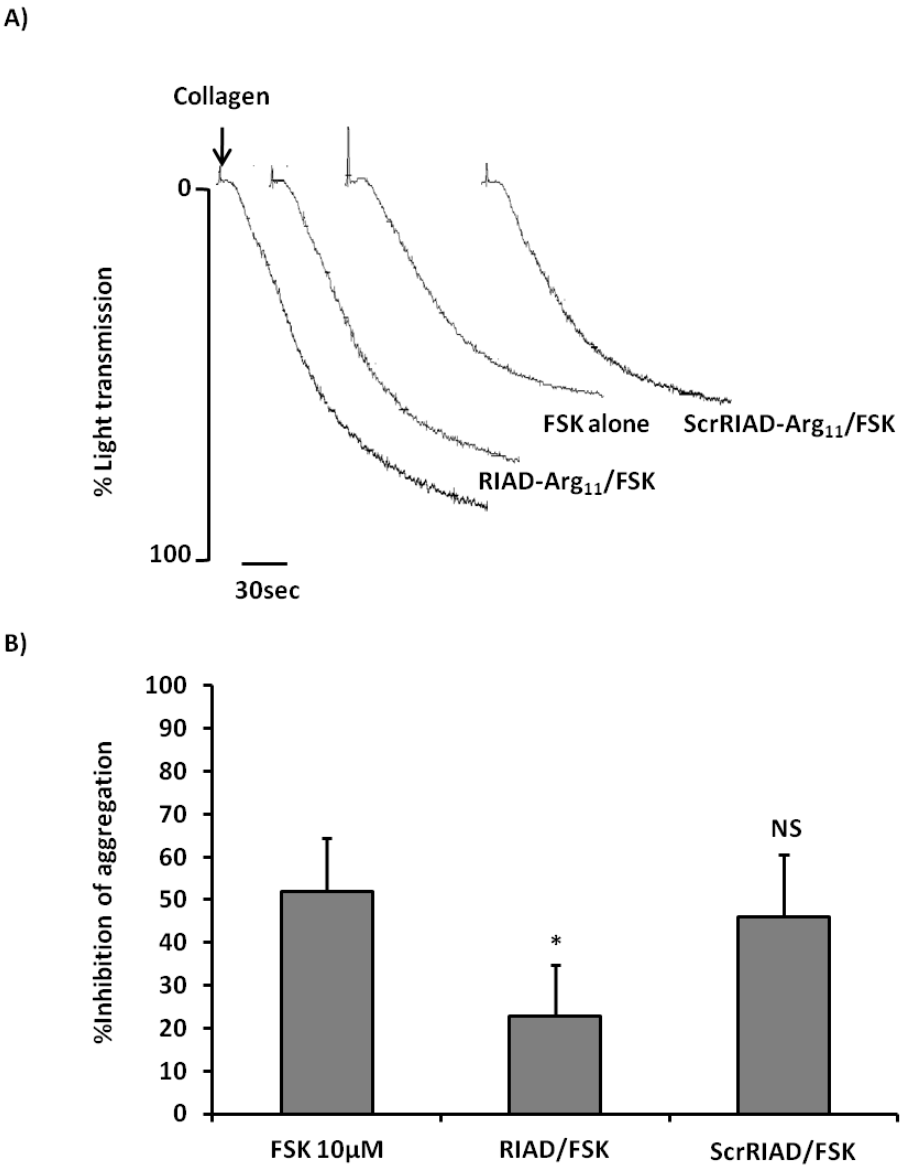

Figure 4. 6: RIAD reverses Fsk-mediated inhibition of platelet aggregation.

(A) WP ($2.5x10^8$ platelets/mL) were either stimulated with collagen (5µg/mL) or pre-incubated with RIAD-Arg_{11} (1µM), ScrRIAD-Arg_{11} (1µM) or vehicle for 1 hour at 37^oC. Platelets were then treated with Fsk (10µM) for 5 min before stimulating with collagen.. Aggregation was monitored for 4 min under constant stirring (1000rpm) at 37^oC using a chrono-log dual channel light transmission aggregometer and aggregation traces were generated by aggreo/link computer software (chrono-log, USA). **(B)** Aggregation data were expressed as means ± SEM of 5 independent experiments with separate donors (* : $p \leq 0.05$ when compared with PGI_2 alone).

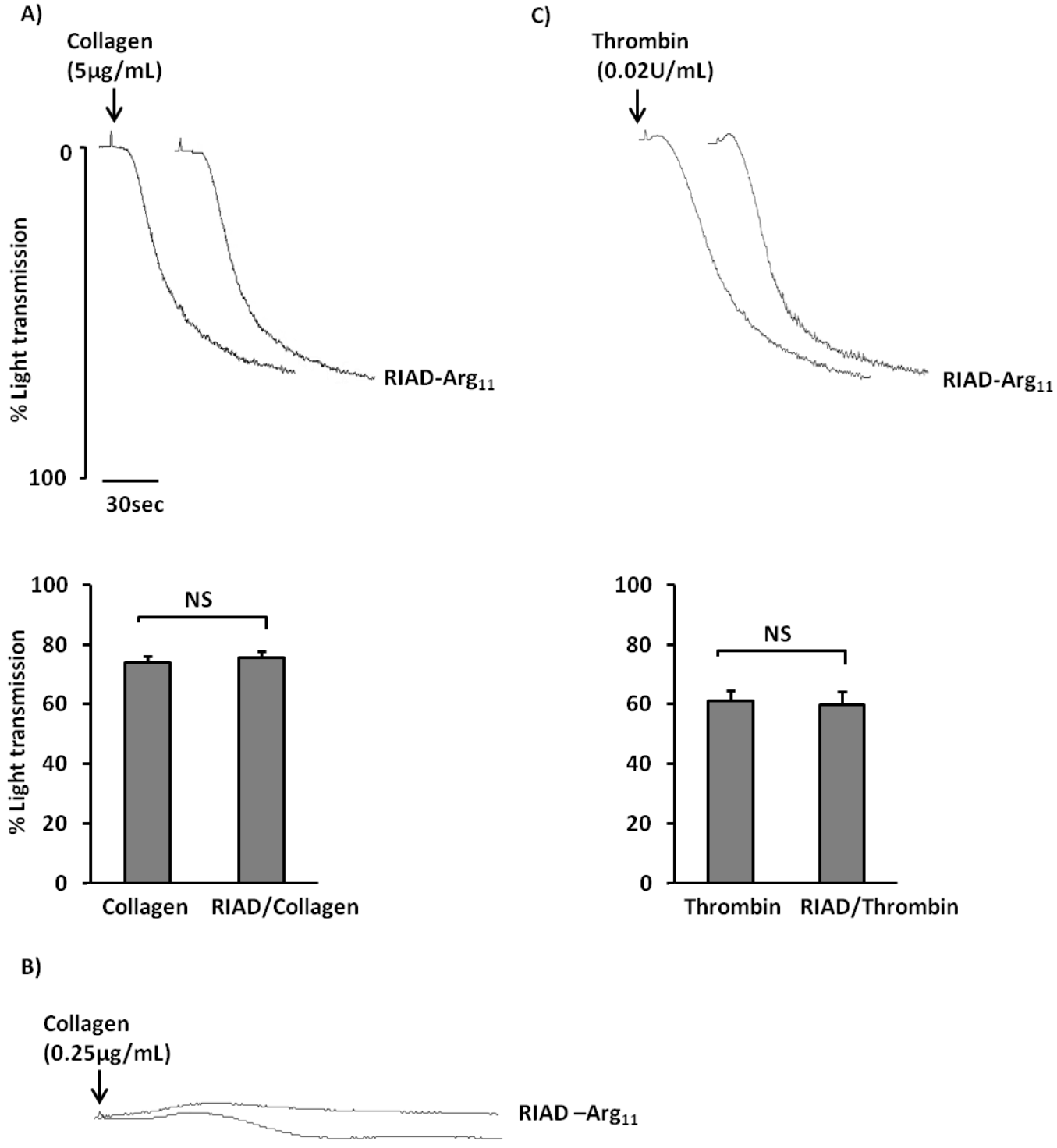
A)
Collagen
(5µg/mL)
0
100
% Light transmission
30sec
RIAD-Arg11
C)
Thrombin
(0.02U/mL)
RIAD-Arg11
100
80
60
40
20
0
% Light transmission
NS
Collagen
RIAD/Collagen
NS
Thrombin
RIAD/Thrombin
B)
Collagen
(0.25µg/mL)
RIAD –Arg11

Figure 4. 7: RIAD does not potentiate platelet aggregation.

(A) WP ($2.5x10^8$ platelets/mL) were pre-incubated with RIAD-Arg_{11} (1µM) or vehicle for 1 hour at 37^oC then were stimulated with high dose of collagen (5µg/mL). Aggregation was monitored for 4 min under constant stirring (1000rpm) at 37^oC using a chrono-log dual channel light transmission aggregometer and aggregation traces were generated by aggreo/link computer software (chrono-log, USA). **(B)** As in (A) except WP were stimulated with low dose of collagen (0.25µg/mL). **(C)** As in (A) except WP were stimulated with thrombin (0.02U/mL). Data are representative of 3 independent experiments with 3 separate donors.

4.5.3 RIAD-Arg_{11} has no effect on the inhibitory effect of cAMP analogues on platelet aggregation

PGI_2 and Fsk inhibit platelets through the generation of cAMP and activation of PKA. In this context it was important to understand how RIAD was influencing this signalling cascade. To begin to understand this mechanism the influence of RIAD on platelets that are inhibited by cAMP analogues was investigated.

To achieve this, platelets were pre-treated with 8-CPT-6-Phe-cAMP (25µM) before they were stimulated with collagen (5µg/mL). The cAMP analogue induced an inhibitory effect of 55±4%. Strikingly, when platelets were pre-incubated with RIAD-Arg_{11} (1µM) for 1 hour, the inhibitory effect remained unaltered (54±4%, figure 4.8). This data would suggest that RIAD might influence signalling prior to cAMP binding to PKA.

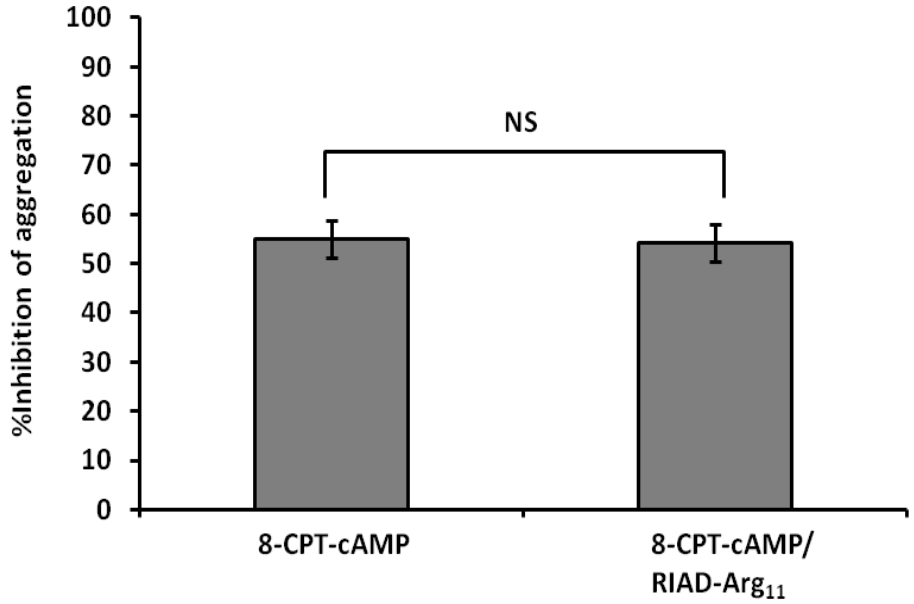

Figure 4. 8: RIAD does not reverse the inhibitory effect of cAMP analogues.

Platelets ($2.5x10^8$ platelets/mL) were pre-incubated with RIAD (1µM) or vehicle for 1 hour at 37^oC then were treated with 8-CPT-6-Phe-cAMP (25µM) for 5 min before stimulating with collagen (5µg/mL). Aggregation was monitored for 4 min under constant stirring (1000rpm) at 37^oC using a chrono-log dual channel light transmission aggregometer and aggregation traces were generated by aggreo/link computer software (chrono-log, USA). Data are representative of 3 independent experiments and expressed as means ± SEM.

4.6 RIAD-Arg_{11} reverses the inhibitory effect of PGI_2 on collagen-induced dense granule secretion

Having determined the effect of RIAD-Arg_{11} on platelet aggregation, we then wanted to examine other platelet functions. Platelet activation involves a complicated series of events one of which is the release of dense granule contents. The contents of these granules such as ADP play a pivotal role in recruiting dormant remote platelets into the site of the injury. Dense granule secretion is one of the main platelet activation processes that have been reported to be regulated by elevated cAMP levels (Feinstein and Fraser, 1975). In the light of this, we examined whether the modulation of platelet dense granule secretion by cAMP requires any AKAP-PKA I interactions.

Stimulating platelets with collagen (5µg/mL) resulted in the release of 1003±229pmol of ATP. Pre-treatment with PGI_2 (50nM) had a profound effect on dense granule secretion with ATP levels reduced to 140±87pmol ($P<0.0001$). Consistent with the aggregation data, pre-incubation with RIAD-Arg_{11} (1µM) for 1 hour before treating with PGI_2, significantly reversed its inhibitory effect on collagen-induced dense granule secretion. Here ATP secretion increased to 545±129pmol of ATP ($p\leq0.05$ when compared with PGI_2 alone, figure 4.9). Control experiments showed that ScrRIAD-Arg_{11} (1µM) did not have a significant effect on PGI_2-mediated inhibition of platelet dense granule secretion under the same conditions.

These data suggest that inhibition of platelet dense granule secretion by PGI_2 require AKAP-PKA I interactions.

A)

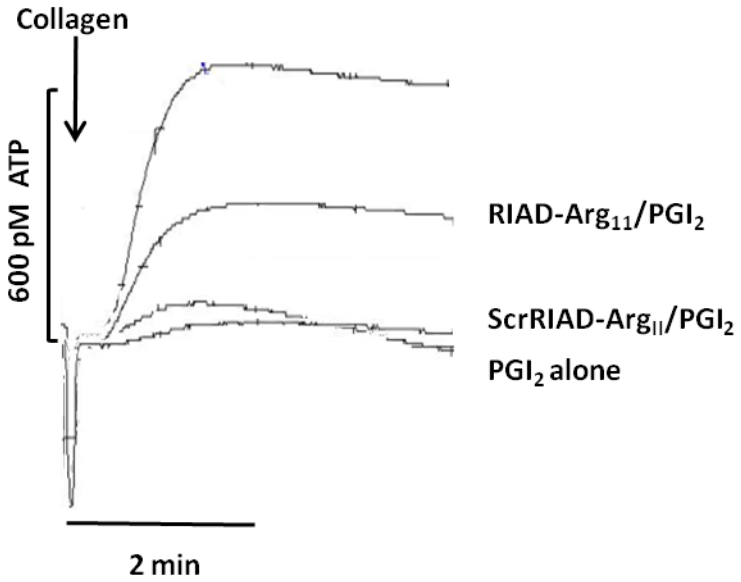
Collagen
600 pM ATP
RIAD-Arg11/PGI2
ScrRIAD-Arg11/PGI2
PGI2 alone
2 min

B)

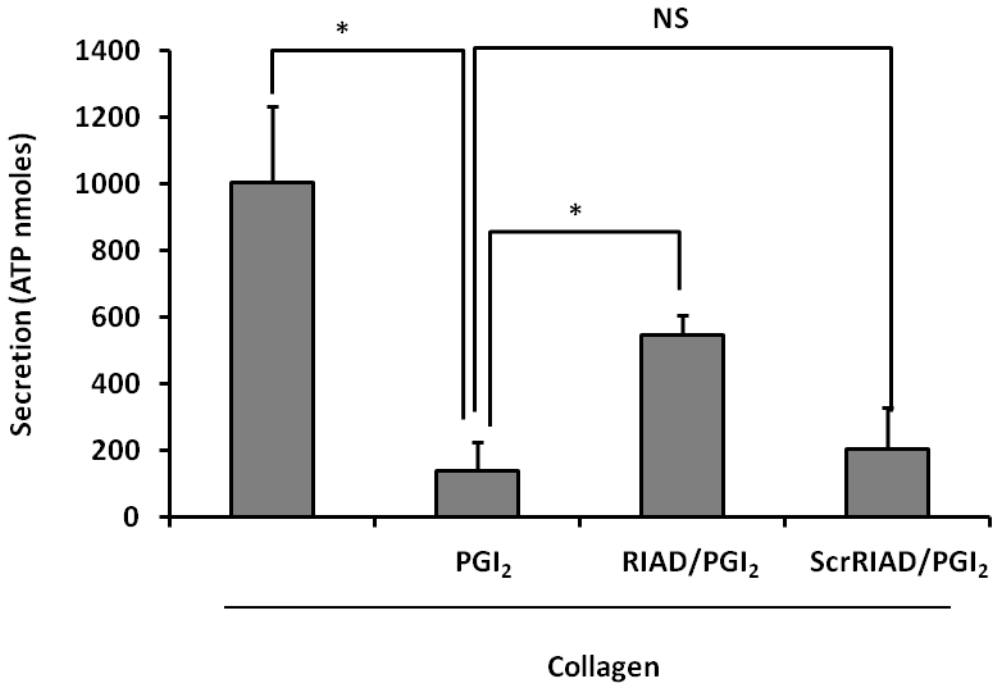
*
NS
*
1400
1200
1000
800
600
400
200
0
Secretion (ATP nmoles)
PGI2
RIAD/PGI2
ScrRIAD/PGI2
Collagen

Figure 4. 9: RIAD reverses PGI2-mediated inhibition of platelet dense granule secretion.

WP ($2.5x10^8$ platelets/mL) were either stimulated with collagen (5µg/mL) or pre-incubated with RIAD-Arg_{11} (1µM), ScrRIAD-Arg_{11} (1µM) or vehicle for 1 hour at 37^oC. Platelets were then treated with PGI_2 (50nM) for 1 min before stimulating with collagen. ATP secretion was monitored for 4 min under constant stirring (1000rpm) at 37^oC using a chrono-log Lumi-aggregometer and secretion traces were generated by aggreo/link computer software (chrono-log, USA). **(B)** Secretion data were expressed as means ± SEM of 4 independent experiments with separate donors (*: $p \leq 0.05$).

4.7 RIAD-Arg_{11} does not inhibit PGI_2-induced AC activity

The binding of PGI_2 to its Gs-coupled receptor (IPR) activates AC and results in an increase in intracellular cAMP levels. The elevated cAMP then binds to and activates PKA. Therefore, it was possible that RIAD was exerting its effects through modulating cAMP concentrations and hence it was important to investigate this possibility.

In all platelet preparations, basal concentrations of 87±37 fmol cAMP/10^7 platelets were found. Pre-incubating platelets with RIAD-Arg_{11} or ScrRIAD-Arg_{11} (1µM for 60min) had no significant effect on basal cAMP concentrations which were 70±24 and 112±11 fmol/10^7 platelets, respectively (Figure 4.10 A, gray bars).

Treatment of platelets with PGI_2 (50nM) increased cAMP concentrations to 150±52 fmol/10^7 platelets ($p<0.05$ when compared with basal levels). Pre-incubating platelets with similar concentrations (1µM) of RIAD-Arg_{11} or ScrRIAD-Arg_{11} before stimulating with PGI_2 did not have a significant effect on cAMP levels which remained at 153±38 and 177±25 fmol/10^7 platelets, respectively (Figure 4.10 A, black bars). These data provide a 'snap-shot" of the effects of the cell penetrating peptides on cAMP synthesis. The experiments were repeated in the presence of the PDE3-specific inhibitor milrinone (10µM) (Figure 4.10 B), which allowed the examination of total cAMP accumulation over a finite period of time. Under these conditions, PGI_2 stimulated cAMP concentrations were significantly higher than in the absence of milrinone consistent with the prevention of cyclic nucleotide hydrolysis. The peptides failed to affect cAMP concentration, either basally or that induced by PGI_2. Thus RIAD-ARg_{11} has no effect cAMP concentrations under the

conditions tested. This is in agreement with its proposed effect as an inhibitor of PKA I-AKAP interactions.

A)

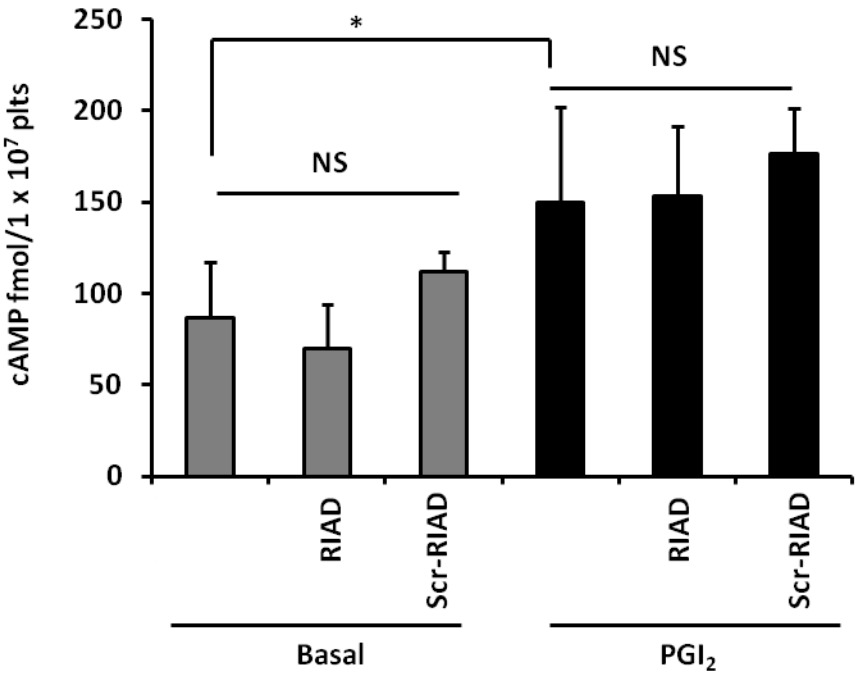

No milrinone

B)

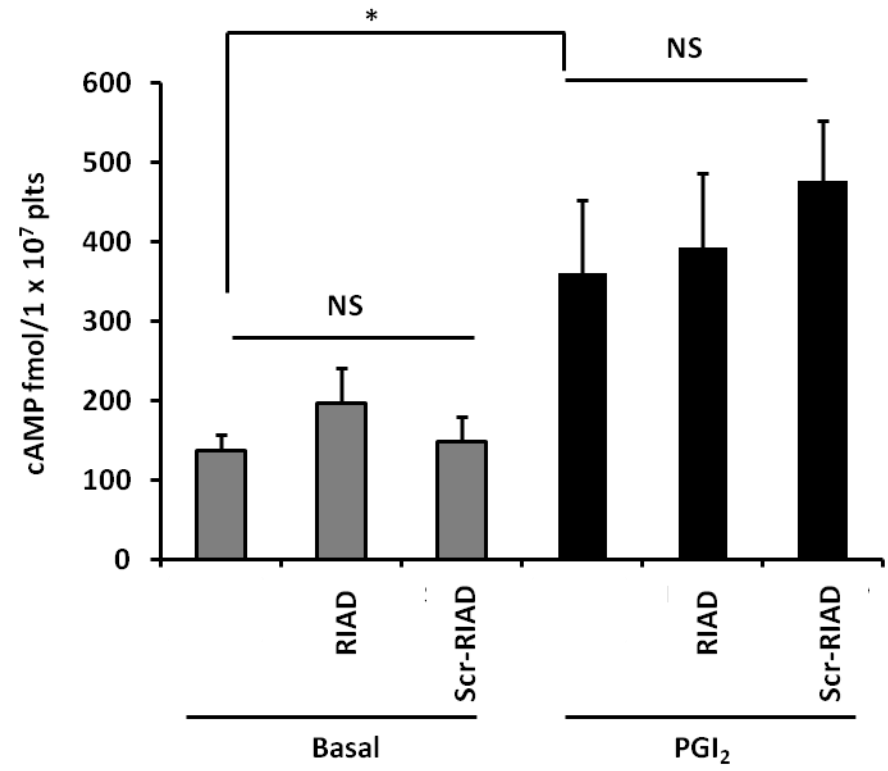

With milrinone

Figure 4. 10: RIAD does not affect cAMP synthesis.

(A) For measuring cAMP levels under non-stimulatory (grey bars) conditions, WP (2x108 platelets/mL) were pre-incubated with RIAD-Arg11 (1µM), scrRIAD-Arg11 (1µM) or vehicle for 1 hour then cAMP levels were measured. For measuring cAMP levels under stimulatory conditions (black bars), platelets were stimulated with PGI2 (50nM) for 30 sec either directly or after pre-incubation with the peptides under the same conditions. (B) As in (A) except that platelets were treated with milrinone (10µM) for 20 min before stimulation with PGI2. Data are representative of 3 independent experiments with different donors and were expressed as means ± SEM (*: P≤0.05).

4.8 PKA-AKAP disruptor peptides diminish PGI_2-mediated signalling events

Having shown that RIAD-Arg_{11} modulated platelet inhibition by PGI_2, it was important to try to understand the underlying effects on PKA signalling events. PGI_2-induced cAMP synthesis results in the activation of PKA, which releases its catalytic subunit in response to the binding of cAMP molecules to the regulatory subunits. PKAc then mediates the phosphorylation of several cellular substrates which blunts various aspects of platelet activation (Schwarz *et al*., 2001).

Platelets were stimulated with PGI_2 in the presence or absence of RIAD-Arg_{11} and then PKA activity was studied using Western blotting for several PKA signalling markers. Firstly, we examined phosphorylation of numerous potential PKA substrates in whole cell lysates using phospho-PKA substrate antibody. We found that proteins with apparent molecular weights of 55 and 60kDa were mildly phosphorylated, while proteins of 16, 44 and 130kDa were heavily phosphorylated under basal conditions. Stimulation of AC with PGI_2 (50nM) increased phosphorylation of basally phosphorylated PKA substrates of 60 and 130kDa and induced the phosphorylation of substrates with apparent molecular weights of 24, 27, 35, 48, 66, 82, 90, 140 and 240 kDa (Figure 4.11 A, top panel, lane 2). The majority of these molecular weights are consistent with those previously reported by el-Daher *et al* as proteins phosphorylated in response to cAMP (El-Daher *et al*., 1996). In the presence of RIAD-Arg_{11} (1µM), the phosphorylation of these proteins was reduced, but not abolished (Figure 4.11 A, top panel, lane 4). In contrast, the treatment of platelets with scrRIAD-Arg_{11} failed to significantly influence PGI_2-induced phosphorylation of PKA substrates (Figure 4.11 A, top panel, lane 7). We

next compared this to the effects of established PKA inhibitors KT5270 and H89. Unlike RIAD-Arg_{11}, these inhibitors had a more profound effect on the phospho-PKA profile (Figure 4.11 A, top panel, lane 5). This highlights the difference between conventional PKA inhibitors which unspecifically block PKA activity and RIAD-Arg_{11}, which only targets PKA I and inhibits its AKAP-dependent activity (Carlson et al., 2006).

Furthermore, we looked at the effect of RIAD-Arg_{11} on individual PKA substrates. Treatment of platelets with PGI_2 (50nM) induced the phosphorylation of the well-established PKA substrate $VASP^{ser157}$, which was only slightly reduced by RIAD-Arg_{11} (1µM), and unaffected by scrRIAD-Arg_{11} (1µM) (Figure 4.11, second panel from top). Unpublished data from our lab showed that PKA also phosphorylates GSK3α on ser21 and RhoA on ser188. RIAD-Arg_{11} reduced the phosphorylation of $GSK3\alpha^{21}$ and to a lesser extent $RhoA^{188}$ with the scrambled peptide not having any effect (Figure 4.11, third and fourth panel from top). Observations made on phospho- $GSK3\alpha^{21}$ and $RhoA^{188}$ need further investigation to be confirmed. In all these samples the other unspecific PKA-AKAP inhibitor st-Ht31 did not have a significant effect on any of these PKA activity markers.

Together these data suggest that RIAD-Arg_{11} decreases platelet sensitivity to PGI_2, by preventing PKA-mediated phosphorylation of substrate proteins, but not cAMP formation, and that PKA-AKAP interactions may play an important role in allowing PKA to induce efficient phosphorylation events.

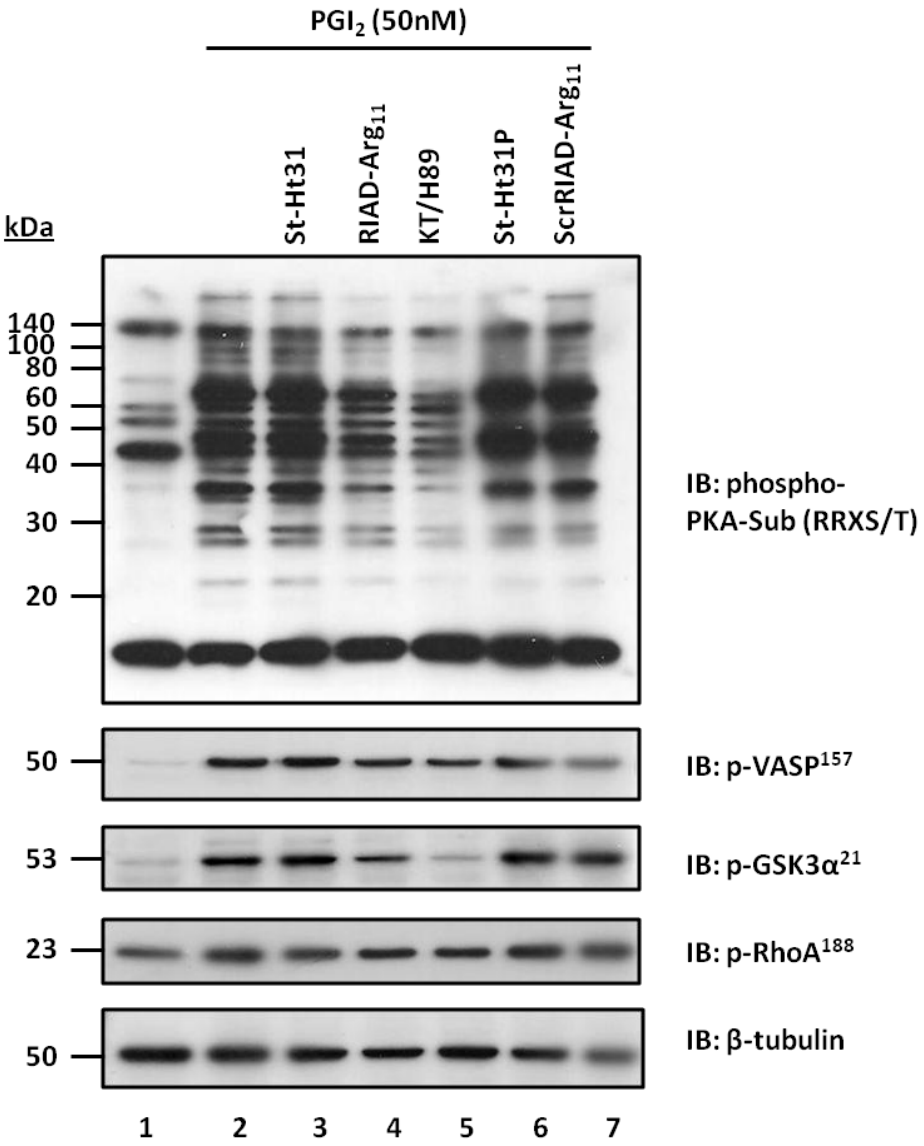

Figure 4. 11: RIAD-Arg11 reverses PGI2-mediated signaling events in platelets.

WP ($2.5x10^8$ platelets/mL) were preincubated with RIAD-Arg11 (1µM), ScrRIAD (1µM), St-Ht31 (2.5µM) or vehicle for 1 hour at 37°C before they were stimulated with PGI_2 (50nM) for 1 min. Platelet lysates (20µg/well) were then loaded onto a 10-18% gradient polyacrylamide gel and then resolved by SDS-PAGE for 2.5h at 120V. Proteins were then transferred onto a PVDF membrane using the Turbo™ Blotting System (Bio-Rad). Membranes were then blocked and immunoblotted with anti-phospho-PKA substrate rabbit antibody (1:1000), phospho-VASP^{ser157} rabbit antibody (1:1000), phospho-GSK3α^{ser21} rabbit (1:1000) or phospho-RhoA^{ser188} (1:1000) overnight at 4°C. Membranes were then stripped and reprobed with anti-β-Tubulin mouse antibody (1:1000) overnight at 4°C to check for equal loading. The top two blots are representative of three independent experiments with three separate donors whereas the rest are representative of 1 experiment.

4.9 Disruption of AKAP-PKA I interactions prevents PKA I translocation into platelet lipid rafts

A major function of AKAPs is to aid in the localisation of PKA into different subcellular compartments through their unique targeting domain (Pidoux and Tasken, 2010, Tasken and Aandahl, 2004). Data from figure 4.3 suggest that a significant amount of PKA I, but not PKA II, tranlocates into platelet lipid rafts upon stimulation with PGI_2. Therefore, we wanted to investigate a potential role for AKAPs in mediating this translocation. This was achieved by treating platelets with RIAD-Arg_{11} under different conditions and examining whether the previously observed redistribution of PKA I into rafts was affected.

In the first instance the ability of RIAD-Arg_{11} to delocalise the small pool of PKA I found in lipid rafts under basal conditions was determined. Platelet lipid rafts were isolated by sucrose gradient ultracentrifugation and fractions were analysed by SDS-PAGE and immunoblotting. High levels of LAT can be observed in fractions 5 and 6 which represent detergent-resistant fractions (Figure 4.12, Ai, LAT). Consistent with data from figure 4.3, we observed a small amount of PKA-RI in detergent-resistant fractions with the majority localised in the soluble fractions (figure 4.12, Ai, RI). Treatment of platelets with RIAD-Arg_{11} (10μM) for 1 hour had no significant effect on the basally raft-localised RI (Figure 4.12, Aii and Aiii, RI). Importantly, RIAD also did not alter the distribution of LAT or β3 which indicates that the peptide is not affecting the fractionation process or raft stability (Figure 4.12, Aii, LAT). These data suggest that RIAD-Arg_{11} is unable to delocalise PKA-RI that is present in platelet lipid rafts under basal conditions.

After that the effect of RIAD-Arg_{11} on PGI_2-mediated PKA I redistribution into lipid rafts was investigated. Consistent with data from figure 4.3, treatment with PGI_2 (100nM) led to a significant redistribution of PKA-RI into the detergent-resistant fractions, but had no effect on PKA-RII (figure 4.13, Aii). However, pre-incubation with RIAD-Arg_{11} (10μM) for 1 hour blocked any redistribution of PKA-RI into lipid rafts ($p \leq 0.05$), but had no effect on PKA-RII distribution (Figure 4.13, Aiii). In contrast, pre-incubating similar concentrations of ScrRIAD-Arg_{11} (10μM) with platelets under similar PGI_2 stimulatory conditions failed to block the redistribution of PKA-RI into lipid rafts. Data from these experiments suggest a significant role for AKAP-PKA I interactions to facilitate PKA-I redistribution into platelet lipid rafts in response to PGI_2.

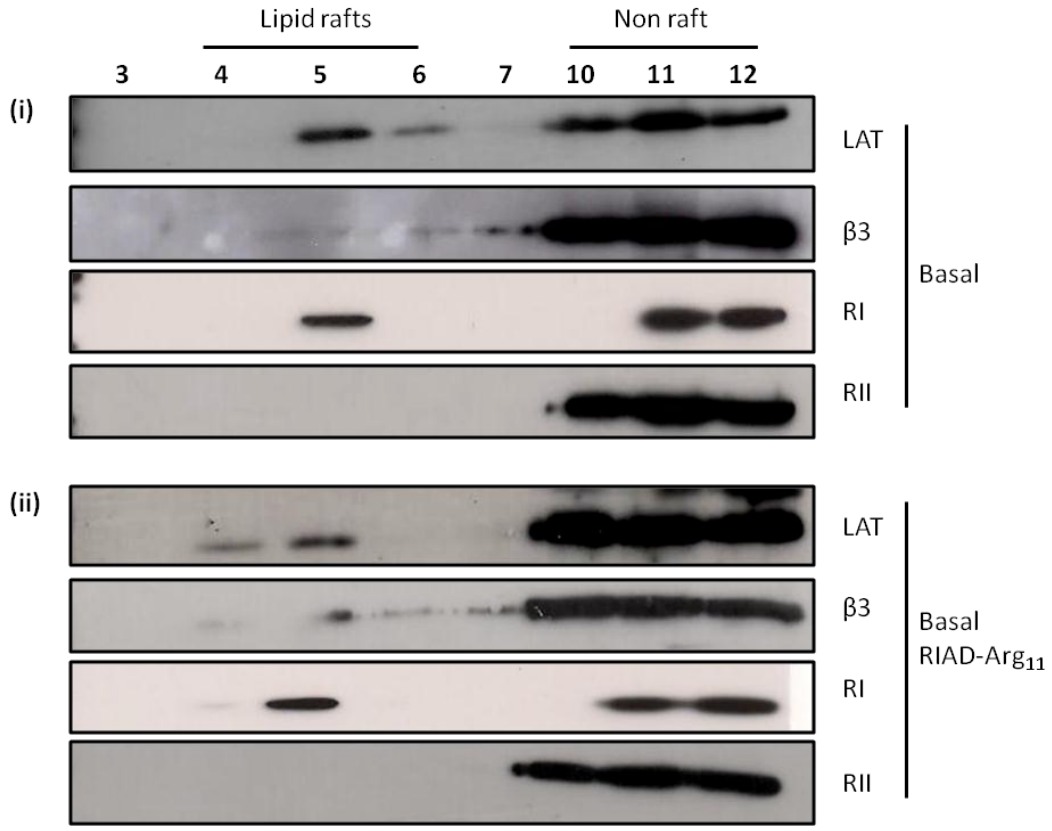

Figure 4. 12: RIAD is unable to delocalise PKA-RI from rafts under basal conditions. WP ($1x10^9$ platelets/mL) were either pre-incubated with RIAD-Arg_{11} (10µM) for 1 hour at 37°C or were left untreated. Platelets were then lysed with lipid raft lysis buffer containing 0.065% Triton X-100 for 30 min on ice. Lipid raft and non-raft fractions were then separated by sucrose gradient ultracentrifugation. Aliquots of fractions (45µl) were then analysed by 10% SDS-PAGE for 1.5h at 120V followed by immunoblotting for 2.5h at 100V. Membranes were then blocked and firstly probed with LAT (1:1000 rabbit) and integrin β3 (1:1000 rabbit) to identify raft and non-raft fractions, respectively. Membranes were then probed with either PKA-RI (1:1000 mouse) or PKA-RII (1:1000 mouse). Blots are representative of 2 independent experiments with separate donors.

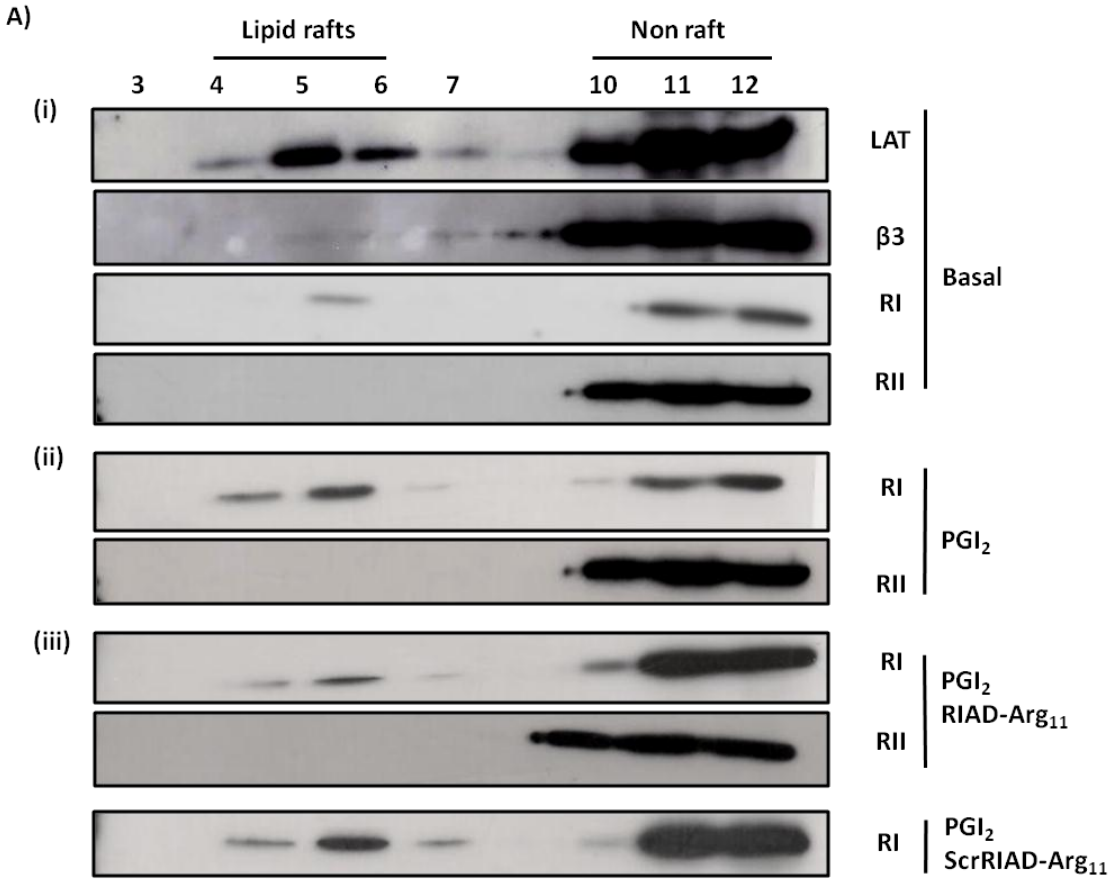
A)
Lipid rafts
Non raft
3
4
5
6
7
10
11
12
(i)
LAT
β3
RI
RII
Basal
(ii)
RI
RII
PGI2
(iii)
RI
RII
PGI2
RIAD-Arg11
RI
PGI2
ScrRIAD-Arg11

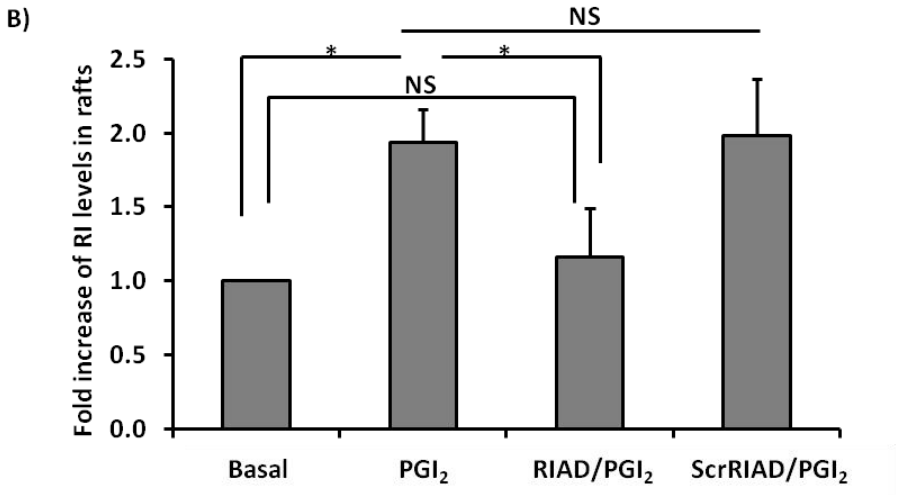
B)
NS
*
*
NS
Fold increase of RI levels in rafts
2.5
2.0
1.5
1.0
0.5
0.0
Basal
PGI2
RIAD/PGI2
ScrRIAD/PGI2

Figure 4. 13: RIAD blocks PGI2-mediated PKA I redistribution into lipid rafts.

(A) WP ($1x10^9$ platelets/mL) were pre-incubated with RIAD-Arg_{11} (10µM), scrRIAD-Arg_{11} (10µM) or vehicle for 1 hour at 37^oC before they were stimulated with PGI_2 for 1 min. Platelets were then lysed with lipid raft lysis buffer containing 0.065% Triton X-100 for 30 min on ice. Lipid raft and non-raft fractions were then separated by sucrose gradient ultracentrifugation. Aliquots of fractions (45µl) were then analysed by 10% SDS-PAGE for 1.5h at 120V followed by immunoblotting for 2.5h at 100V. Membranes were then blocked and firstly probed with LAT (1:1000 rabbit) and integrin β3 (1:1000 rabbit) to identify raft and non-raft fractions, respectively. Membranes were then probed with either PKA-RI (1:1000 mouse) or PKA-RII (1:1000 mouse). Blots are representative of 4 independent experiments. **(B)** Fold increase of RI levels in lipid rafts in response to different treatments normalised against basal levels. Data are from 4 independent experiments with 4 separate blood donors and are expressed as means ± SEM (*: $p \leq 0.05$).

4.10 PKA I targets several substrates in platelet lipid rafts

It has been established in other cell types that AKAP-mediated PKA translocation into a specific subcellular compartment has a functional relevance. This involves targeting substrates that reside in that compartment (Tasken and Aandahl, 2004). In the light of this and after establishing platelet lipid rafts as a PKA spatial compartment we wanted to determine whether or not PKA I targets any substrates in lipid rafts.

Platelets were either left untreated or stimulated with PGI_2 (100nM) with or without RIAD-Arg_{11} (10µM). Relatively low exposure time of PVDF membranes showed that a protein with an apparent molecular weight of 66kDa is basally phosphorylated by PKA in platelet lipid rafts (Figure 4.14 B). In response to PGI_2, the phosphorylation of this protein increased and three different bands with apparent molecular weights of 16, 130 and 200kDa were detected (Figure 4.14 C). Pre-incubation with RIAD-Arg_{11} (10µM) significantly decreased the phosphorylation of these proteins (Figure 4.14 D). Higher exposure time (15 min) of those membranes revealed more bands suggesting that more PKA I phosphorylation events might occur in rafts. In addition to the fore-mentioned 66kDa protein, overexposure revealed that proteins with apparent molecular weight of 130, 55, 35 and 16kDa might be basally phosphorylated in rafts by PKA I. Expectedly, overexposure showed more potential PKA I targets in lipid rafts compared with low exposure such as proteins with apparent molecular weights of 22, 27, 48kDa in addition to an increase in phosphorylation of the basally phosphorylated proteins. Similarly a decrease in the phosphorylation profile in rafts can be observed as a result of RIAD-

Arg_{11} treatment on the overexposed membranes. Taken together these data suggest that the relocation of an active form of PKA I to lipid rafts is mediated by an AKAP dependent-mechanism.

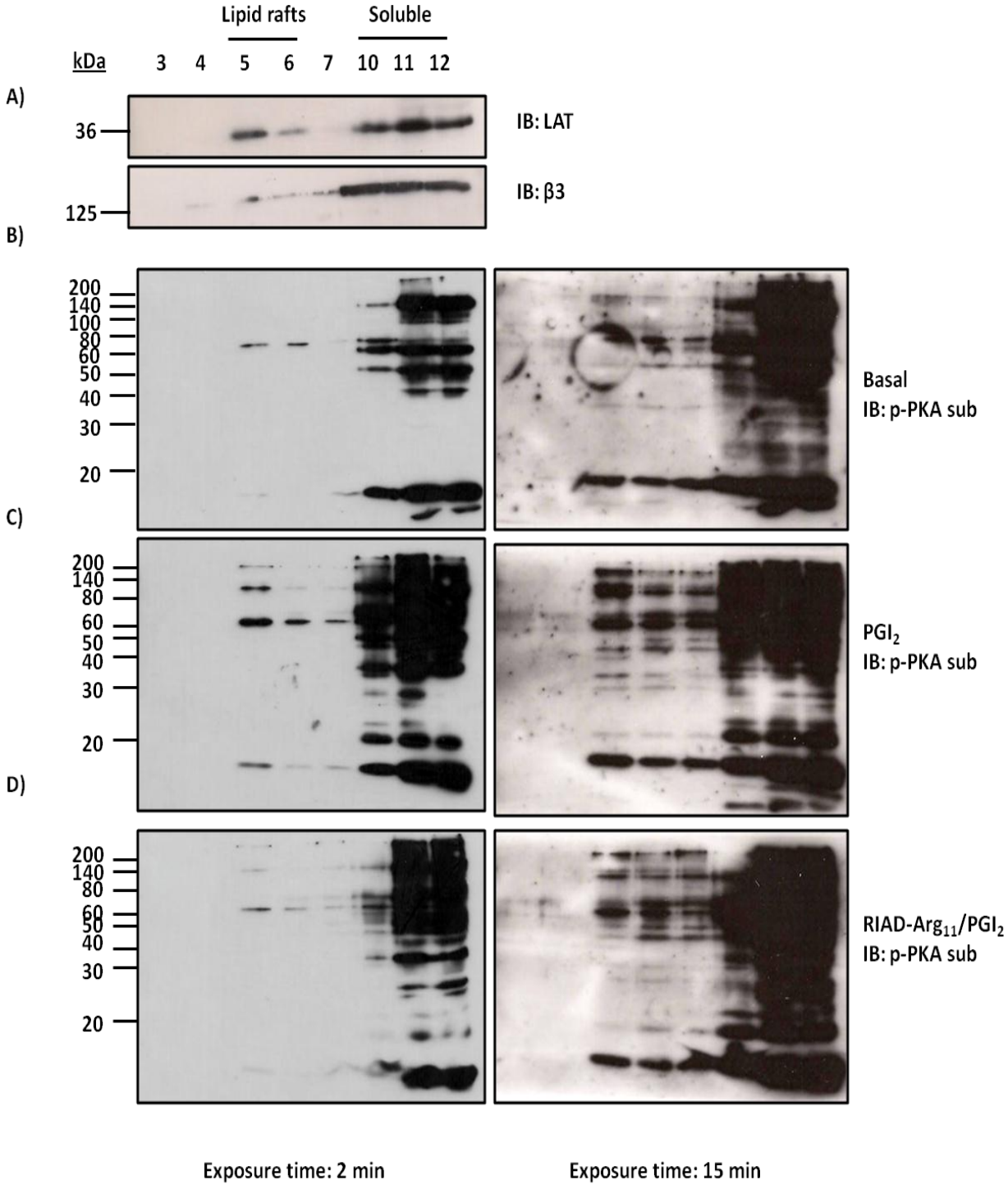
Lipid rafts
Soluble
kDa
3 4 5 6 7 10 11 12
A)
36
IB: LAT
125
IB: β3
B)
200
140
100
80
60
50
40
30
20
C)
Basal
IB: p-PKA sub
200
140
80
60
50
40
30
20
D)
PGI2
IB: p-PKA sub
200
140
80
60
50
40
30
20
RIAD-Arg11/PGI2
IB: p-PKA sub
Exposure time: 2 min
Exposure time: 15 min

Figure 4. 14: PKA I targets several substrates in lipid rafts in an AKAP-dependent mechanism.

WP ($1x10^9$ platelets/mL) were pre-incubated with RIAD-Arg_{11} (10μM), or vehicle for 1 hour at 37^oC before they were stimulated with PGI_2 for 1 min. Platelets were then lysed with lipid raft lysis buffer containing 0.065% Triton X-100 for 30 min on ice. Lipid raft and non-raft fractions were then separated by sucrose gradient ultracentrifugation. Fractions were then analysed by 10-18% gradient SDS-PAGE for 2.5h at 120V followed by immunoblotting for 2.5h at 100V. Membranes were then blocked and firstly probed with LAT (1:1000 rabbit) and integrin β3 (1:1000 rabbit) to identify raft and non-raft fractions, respectively. Membranes were then stripped and re-probed with p-PKA substrate antibody (1:1000 rabbit). Blots are representative of 3 independent experiments.

4.11 The role of PKA I-AKAP interaction in regulating platelet activation by vWF

The phosphorylation of GPIbβ at ser^{166} by PKA has been shown to result in reduced platelet adhesion to immobilised vWF, platelet agglutination and collagen-induced actin plymerisation (Wardell *et al*., 1989, Bodnar *et al*., 2002). The following set of experiments aims to investigate whether PKA I-AKAP interactions play any role in the phosphorylation of GPIbβ and whether or not this event regulates platelet activation by vWF.

4.11.1 PKA I-AKAP interactions are required for PGI_2-mediated inhibition of vWF-induced platelet aggregation

In the first instance we wanted to investigate the effect of RIAD-Arg_{11} on PGI_2-mediated inhibition of vWF-induced platelet aggregation. Washed platelets were stimulated with vWF (20µg/mL) in the presence of ristocetin (0.75mg/mL), which is a bacterial glycopeptide that activates the A1 domain of vWF and allows it to bind to GPIb (Andrews and Berndt, 2008). This induced an 81±2% aggregation response. Preincubation of platelets with PGI_2 (50nM) caused an inhibition response of 59±4% ($P<0.0001$). Interestingly, pre-incubating platelets with RIAD-Arg_{11} (1µM) reduced the inhibitory effect of PGI_2 to 28±9% ($P<0.05$, Figure 4.15). Similar treatment with scrRIAD-Arg_{11} (1µM) had no significant effect on PGI_2-mediated inhibition of vWF-induced aggregation. In control experiments, RIAD-Arg_{11} (1µM) did not potentiate vWF-induced aggregation when platelets were stimulated with a low dose (10µg/mL) (Figure 4.15 A, right traces). Data from this experiment suggest that PKA I-AKAP interactions are required to modulate vWF-induced aggregation by PGI_2.

A)

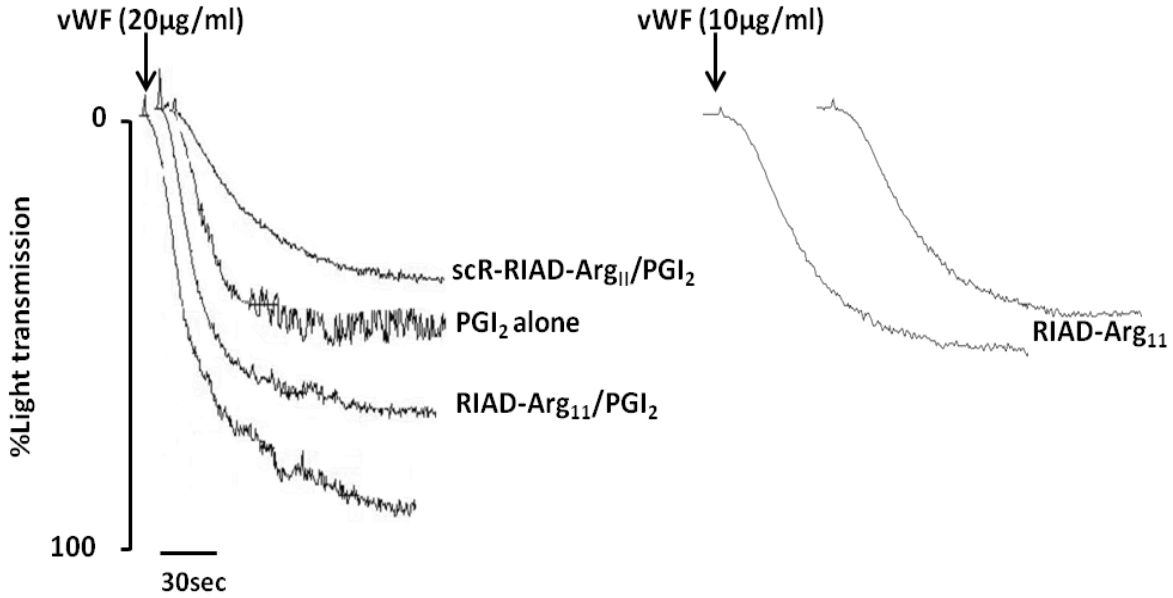
vWF (20µg/ml)
vWF (10µg/ml)
0
%Light transmission
scR-RIAD-Arg11/PGI2
PGI2 alone
RIAD-Arg11/PGI2
RIAD-Arg11
100
30sec

B)

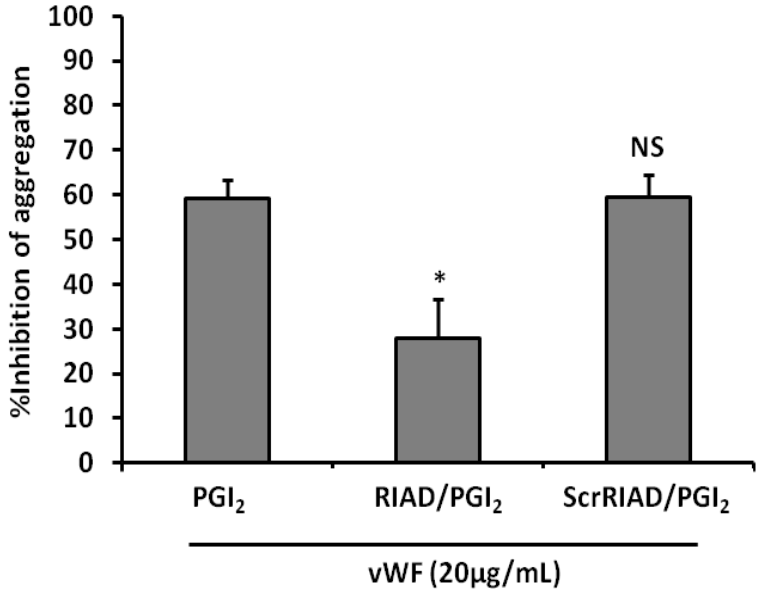
100
90
80
70
60
50
40
30
20
10
0
%Inhibition of aggregation
NS
*
PGI2
RIAD/PGI2
ScrRIAD/PGI2
vWF (20µg/mL)

Figure 4. 15: RIAD reverses the inhibitory effect of PGI2 on vWF-mediated platelet aggregation.

(A) WP ($2.5x10^8$ platelets/mL) were either stimulated with vWF(20µg/mL)/Ristocetin(0.75mg/mL) or pre-incubated with RIAD-Arg_{11} (1µM), ScrRIAD-Arg_{11} (1µM) or vehicle for 1 hour at 37°C. Platelets were then treated with PGI_2 (50nM) for 1 min before stimulating with vWF/Ristocetin. Traces on the right represent control samples treated only with RIAD-Arg_{11} (1µM) and low dose of vWF (10µg/mL)/Risto (0.75mg/mL). Aggregation was monitored for 4 min under constant stirring (1000rpm) at 37°C using a chrono-log dual channel light transmission aggregometer and aggregation traces were generated by aggreo/link computer software (chrono-log, USA). **(B)** Data expressed as means ± SEM of %inhibition of aggregation represent 4 independent experiments from separate donors (* : $p \leq 0.05$ when compared with PGI_2 alone).

4.11.2 PKA I-AKAP interactions are required for inhibition of platelets by PGI_2 under flow

The interaction of platelet GPIb complex with vWF is critical to the capture of platelets at sites of vascular injury (Ruggeri and Mendolicchio, 2007). Moreover, localization of GPIb-IX-V complex into platelet lipid rafts has been proposed to be critical for platelet capture by vWF under shear stress (Shrimpton *et al*., 2002). In addition, $GPIb\beta^{ser166}$ phosphorylation by PKA was reported to diminish vWF binding to GPIb-IX under flow in genetically modified cell lines (Bodnar *et al*., 2002). Having shown that PKA I-AKAPs interaction play a significant role in $GPIB\beta^{ser166}$ phosphorylation in lipid raft, we wanted to determine whether these interactions play any role in regulating platelet accrual under physiological conditions by examining platelet aggregation under flow.

Under arterial shear ($1000s^{-1}$), immobilized vWF (100µg/mL) supported adhesion of numerous small aggregates that covered 27.4±4% of the vWF-coated surface. This was reduced to 16±4% ($p<0.05$) by the presence of PGI_2 (100nM), demonstrating for the first time that PGI_2 inhibits platelet aggregation under physiological conditions of flow (Figure 4.16, compare control with PGI_2). Treatment of platelets with RIAD-Arg_{11} (10µM) alone did not influence platelet adhesion and accrual under flow. Incubation of platelets with the same concentration of RIAD-Arg_{11} for 60min prior to PGI_2, conditions that caused maximal effects in aggregation experiments, reversed the inhibitory effects of PGI_2, with the level of surface coverage increasing to 20.0±2.8% ($p<0.05$ compared to PGI_2 alone) similar to that of control. In contrast, pretreatment with scrRIAD-Arg_{11}, surface area coverage remained at 13±5%, no

different form PGI_2 alone (Figure 4.16). These data indicate that uncoupling of PKA-RI from platelet AKAPs can increase platelet adhesion and aggregation under flow by modulating the inhibitory actions of PGI_2.

A)

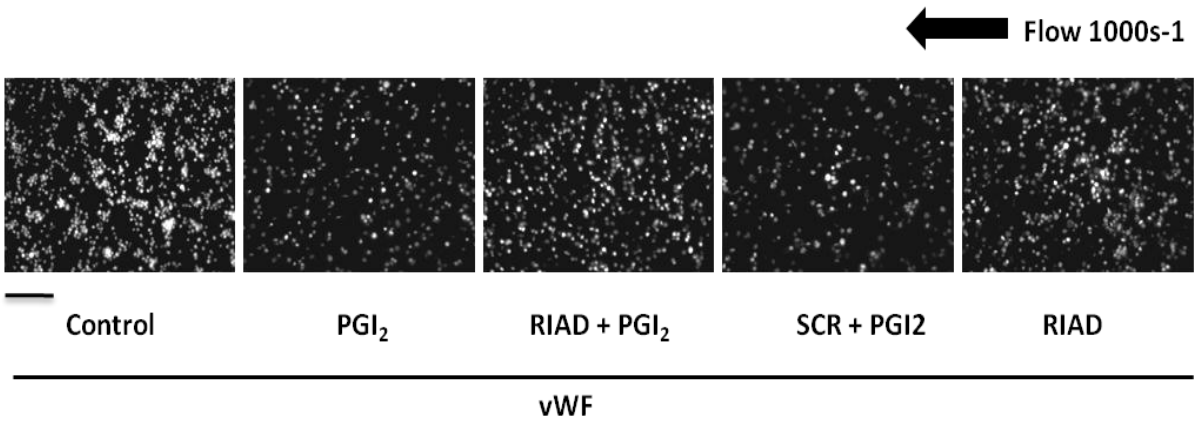
Flow 1000s-1
Control
PGI2
RIAD + PGI2
SCR + PGI2
RIAD
vWF

B)

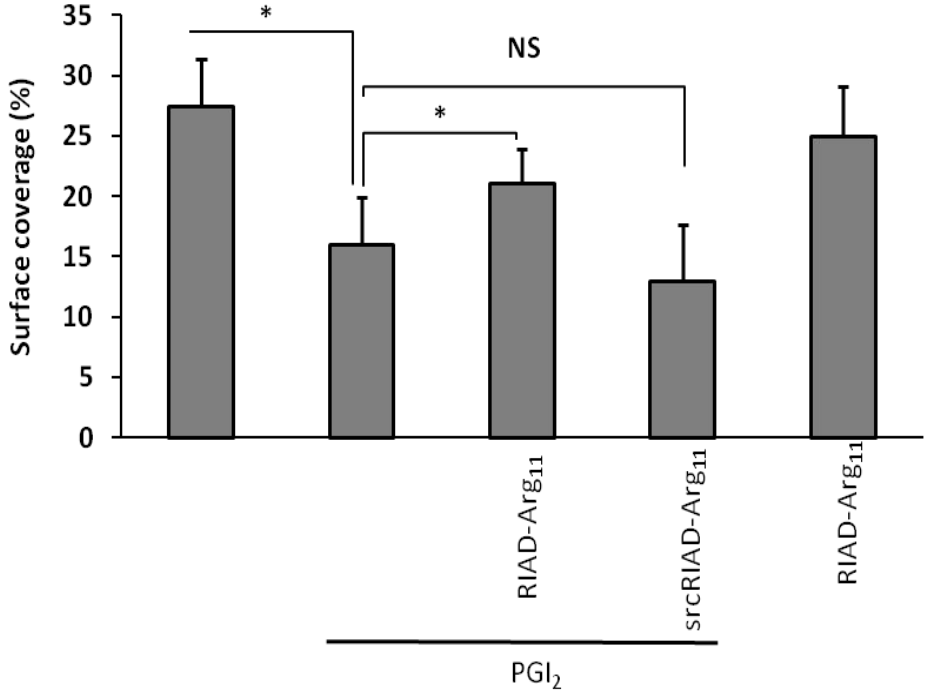
Surface coverage (%)
35
30
25
20
15
10
5
0
*
NS
*
RIAD-Arg11
srcRIAD-Arg11
RIAD-Arg11
PGI2

Figure 4. 16: RIAD-Arg11 modulates PGI2-mediated inhibition of platelet arrest under conditions of flow.

Glass microslide capillary tubes were coated for 12 hours at 4°C with vWF (100µg/mL) and uncoated surfaces blocked with BSA (10mg/mL) for 1h at 20°C. Washed platelets were left untreated (control) or incubated with either RIAD-Arg_{11} or scrRIAD-Arg_{11} (10µM) for 1h at 37^{o}C and treated with PGI_2 (100nM) for 1 min then stained with $DiOC_6$ (1µmol/L) and reconstituted with autologous red blood cells to final concentrations of (2×10^8 platelets/mL) and 50% (v/v) respectively. Reconstituted blood was then perfused through coated tubes for 4 minutes at a shear rate of $1000s^{-1}$. Platelet deposition was viewed by fluorescence microscopy. **(A)** Representative images from random fields of view stretching over a total area of $0.1mm^2$. Scale bar = 20µm. **(B)** Data are shown as percentage area coverage and are means ± SD of 4 independent experiments with separate blood donors. *: $P<0.05$. Experiment was carried out in collaboration with Dr. Simbarashe Magwenzi.

4.11.3 PKA I causes phosphorylation of GPIbβ in platelet lipid rafts in an AKAP-dependent mechanism

We have shown that PGI_2 inhibits vWF-induced platelet activation and that this inhibitory effect of PGI_2 is partially mediated by PKA I-AKAP interactions. Next we sought to investigate whether the phosphorylation of GPIbβ at ser^{166}, which is an event associated with platelet inhibition by cAMP increasing agents (Bodnar *et al*., 2002), is also regulated by PKA I-AKAP interactions.

4.11.3.1 Optimisation of anti p-GPIbβ antibody in blood platelets

In the first instance we wanted to determine the optimal conditions for the p-GPIbβ antibody (A gift from Professor Xiaoping Du). We observed heavy phosphorylation at basal levels when the antibody was used at 1:500 and 1:1000 (Figure 4.17 A, top blot). The heavy basal phosphorylation made it difficult to monitor any changes in phosphorylation even in response to treatment with high concentrations of PGI_2 (0.1-10μM) (Figure 4.17 A). Therefore, we tried different dilutions of the antibody and we found that 1:20000 was the optimal dilution of the antibody (Figure 4.17 B). The basal phosphorylation of $GPIb\beta^{166}$ was reported by Bodnar and colleagues who used the same antibody (Bodnar *et al*., 2002). We observed a clear increase in phosphorylation of $GPIb\beta^{166}$ in response to PGI_2 (100nM). Importantly, treatment of platelets with the PKA inhibitors KT/H89 (10μM/20μM) prior to addition of PGI_2 maintained GPIbβ phosphorylation at basal levels, highlighting that the phosphorylation is PKA-dependent (Figure 4.17 B).

Having confirmed that PGI_2-induced phosphorylation of GPIbβ was a PKA mediated event, we examined the potential role of AKAPs in this process. When we examined the effects of RIAD-Arg_{11} (1μM) in whole cell lysates we observed a modest reduction in the phosphorylation of GPIbβ[166]. This effect of RIAD-Arg_{11} was modest when compared with the effect of PKA inhibitors (KT5270: 10μM/H89: 20μM) which reduced the phosphorylation to basal levels. However, the scrambled version of the peptide had no effect (Figure 4.17 C). Since this modest effect of RIAD-Arg_{11} on GPIbβ phosphorylation was difficult to reproduce and hence quantify, when examined in the context of whole cell lysate, we decided to look at this phosphorylation event in a specific subcellular compartment.

4.11.3.2 GPIbβ is a target for PKA I-mediated phosphorylation in platelet lipid rafts

Given the critical importance of GPIbβ to platelet function, and the fact that it has been found in lipid rafts (Shrimpton *et al*., 2002), we examined this receptor as a potential target of PKA I signaling in these nanodomains. To investigate the importance of PKA localization to platelet-vWF interactions further, we examined the phosphorylation of GPIbβ in response to PGI_2 in lipid rafts. Under basal conditions we found phospho-GPIbβ present in the non-raft fraction, but little evidence of phospho-GPIbβ in the lipid raft fractions (Figure 4.18 Ai). However, treatment of platelets with PGI_2 (100nM) led to a 4.3±0.17 fold increase in phosphorylated GPIbβ in raft fractions ($P<0.0001$). Using matched samples we found that this phosphorylation of GPIbβ was associated with the redistribution of a pool of PKA-RI into raft fractions (Figure 4.18 Aii).

Having confirmed that an active PKA was required for the phosphorylation of GPIbβ in these microdomains, we next examined whether PKA-AKAP interactions contributed to this event. The experiments were repeated in the presence of RIAD-Arg_{11} (10μM) or its scrambled partner. Preincubation of platelets with RIAD-Arg_{11} reduced the phosphorylation of $GPIb\beta^{166}$ in the lipid raft fraction (3±0.19 fold over basal, P≤0.05, Figure 4.16 Aiii) whereas the scrambled partner had a less significant effect (Figure 4.18 Aiv). In the same samples this was associated with the loss of PKA I in the same fraction, suggesting the two events are intimately linked.

To highlight the difference between RIAD-Arg_{11} which indirectly reduce PKA activity as a result of blocking its translocation into rafts and conventional PKA inhibitors which directly block PKA activity, we repeated the same experiment but platelets were pretreated with a combination of KT5270 (10μM) and H89 (20μM) before stimulation with PGI_2 (100nM). As expected the PKA inhibitors completely blocked GPIbβ phosphorylation in lipid rafts, confirming again that phosphphorylation required an active PKA. However, the PKA inhibitors did not affect the PGI_2-induced PKA I translocation into these nanodomains (Figure 4.18 Av). These data indicate that phosphorylation of GPIbβ in lipid rafts is a target for type I PKA that requires the translocation of PKA-RI into the same cellular compartment.

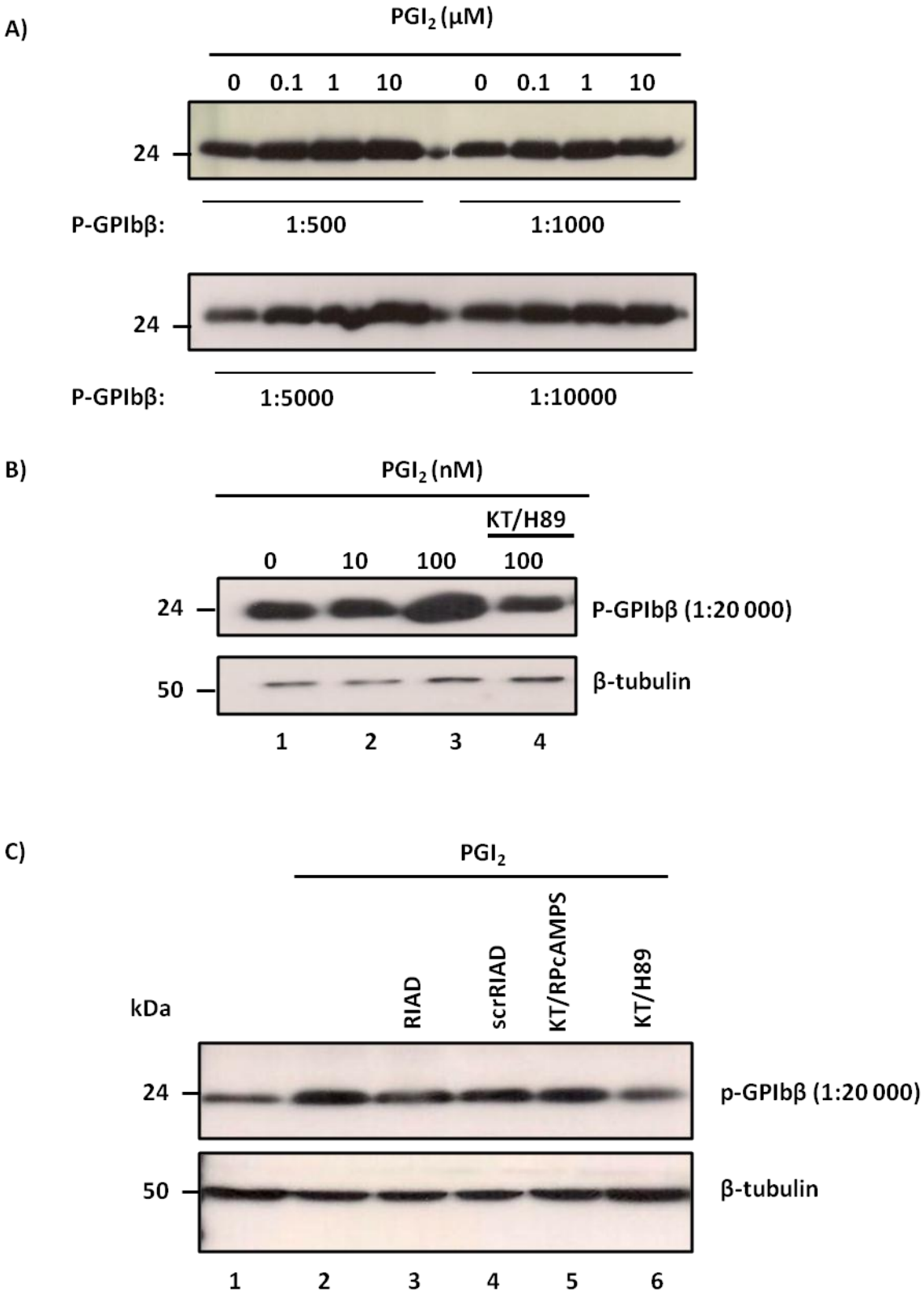
A)
PGI2 (μM)
0 0.1 1 10 0 0.1 1 10
24
P-GPIbβ:
1:500
1:1000
24
P-GPIbβ:
1:5000
1:10000
B)
PGI2 (nM)
KT/H89
0 10 100 100
24
P-GPIbβ (1:20 000)
50
β-tubulin
1 2 3 4
C)
PGI2
RIAD
scrRIAD
KT/RPcAMPS
KT/H89
kDa
24
p-GPIbβ (1:20 000)
50
β-tubulin
1 2 3 4 5 6

Figure 4. 17: Phosphorylation of GPIbβ by PKA is partially dependent on PKA I-AKAP interactions in whole cell lysates.

(A) WP ($2.5x10^8$ platelets/mL) were stimulated with increasing concentrations of PGI_2 (0.1-10μM) for 1 min. **(B)** WP ($2.5x10^8$ platelets/mL) were either stimulated with PGI_2 (10, 100nM) alone for 1 min or following incubation with PKA inhibitors (KT5270: 10μM/ H89: 20μM) for 20 min. **(C)** WP ($2.5x10^8$ platelets/mL) were pre-incubated with RIAD-Arg_{11} (1μM), scrRIAD-Arg_{11} (1μM) or vehicle for 1 hour then stimulated with PGI_2 (50nM) for 1 min. PKA inhibitors (KT5270: 10μM/ H89: 20μM or KT5270: 10μM/RPcAMPS: 500μM) were incubated with platelets for 20 min before stimulating with PGI_2 (50nM) for 1 min. Platelet lysates (20μg/well) were loaded onto a 10% polyacrylamide gel and then resolved by SDS-PAGE for 1.5h at 120V. Proteins were then transferred onto a PVDF membrane for 2.5h at 100V. Membranes were then blocked and probed with the indicated dilution of anti p-GPIbβ antibody (Rabbit) overnight at 4^oC. Membranes were probed with anti β-tubulin antibody (1:1000, mouse) to check for equal loading. Blots are representative of 2 independent experiments.

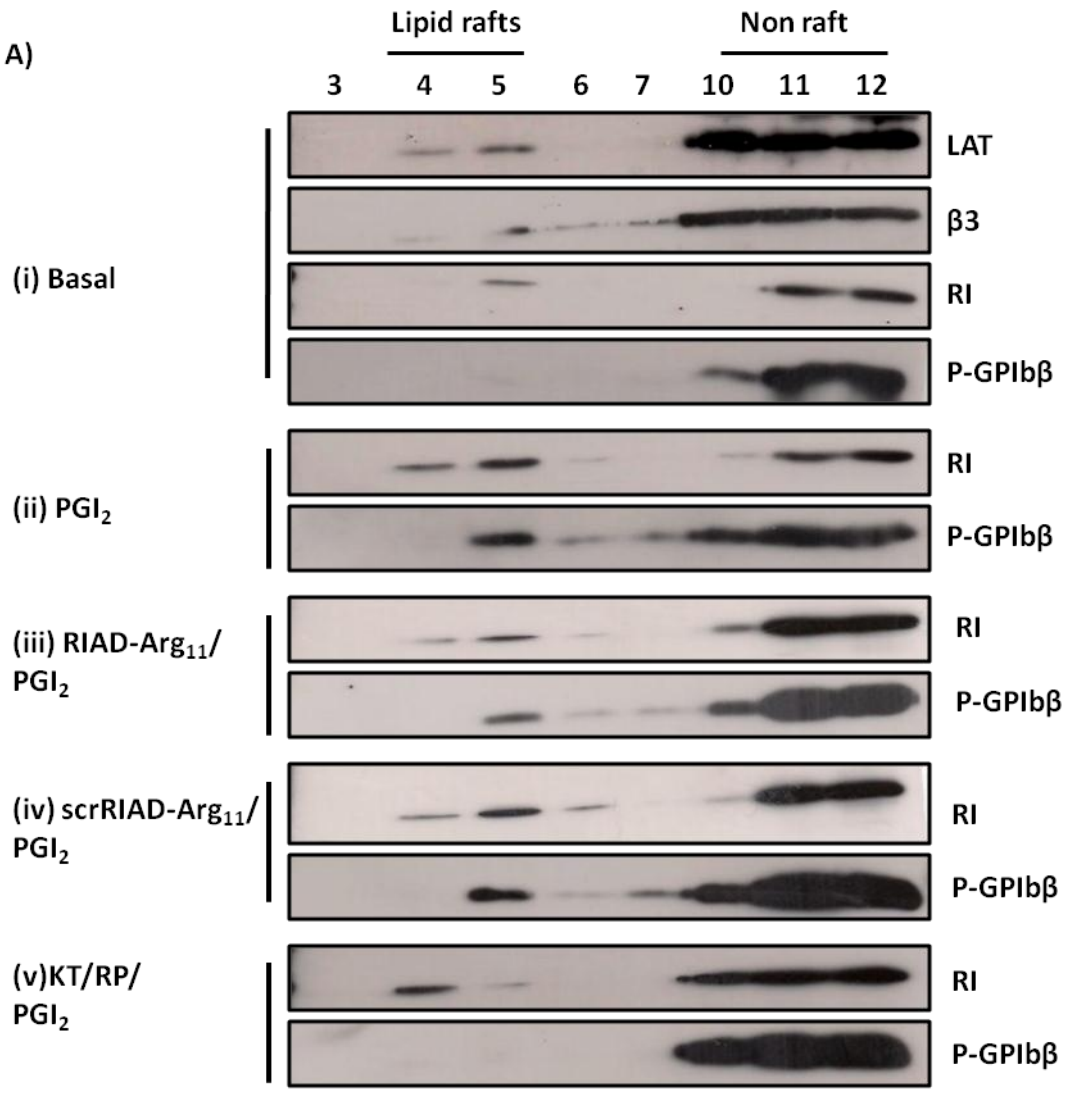
A)
Lipid rafts
Non raft
3
4
5
6
7
10
11
12
(i) Basal
LAT
β3
RI
P-GPIbβ
(ii) PGI2
RI
P-GPIbβ
(iii) RIAD-Arg11/ PGI2
RI
P-GPIbβ
(iv) scrRIAD-Arg11/ PGI2
RI
P-GPIbβ
(v)KT/RP/ PGI2
RI
P-GPIbβ

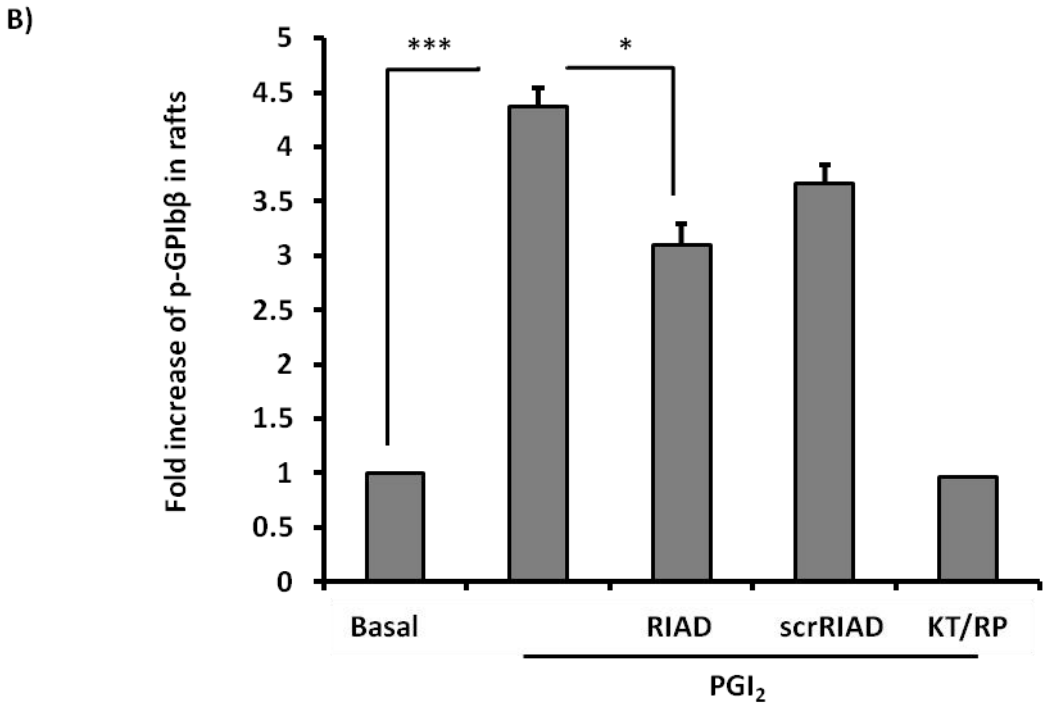
B)
Fold increase of p-GPIbβ in rafts
***
*
5
4.5
4
3.5
3
2.5
2
1.5
1
0.5
0
Basal
RIAD
scrRIAD
KT/RP
PGI2

Figure 4. 18: RIAD inhibits PKA I phosphorylation of GPIbβ in platelets lipid rafts.

(A) WP ($1x10^9$ platelets/mL) were pre-incubated with RIAD-Arg_{11} (10µM), scrRIAD-Arg_{11} (10µM) or vehicle for 1 hour at 37^oC before they were stimulated with PGI_2 for 1 min in the presence or absence of PKA inhibitors (KT5270: 10µM/ H89: 20µM) for 20 min. Platelets were then lysed with lipid raft lysis buffer containing 0.065% Triton X-100 for 30 min on ice. Lipid raft and non-raft fractions were then separated by sucrose gradient ultracentrifugation. Aliquots of fractions (45µl) were then analysed by 10% SDS-PAGE for 1.5h at 120V followed by immunoblotting for 2.5h at 100V. Membranes were then blocked and firstly probed with LAT (1:1000 rabbit) and integrin β3 (1:1000 rabbit) to identify raft and non-raft fractions, respectively. Membranes were then probed with either PKA-RI (1:1000, mouse) or p-GPIbβ (1:10000, rabbit). Blots are representative of 3 independent experiments. **(B)** Fold increase of p-GPIbβ levels in lipid rafts in response to different treatments normalised against basal levels. Data are from 3 independent experiments with 3 separate blood donors and are expressed as means ± SEM (*: $P<0.05$, ***; $P<0.0001$).

4.12 Discussion:

The cAMP signaling cascade regulates several platelet responses including Ca^{2+} mobilisation, (Imai *et al*., 1983, Feinstein *et al*., 1983, Geiger *et al*., 1992) shape change (Aktas *et al*., 2002) and secretion (Feijge *et al*., 2004), which are associated with reduced agonist-induced platelet aggregation (Horstrup *et al*., 1994) and the accumulation of platelets at sites of vascular injury (Sim *et al*., 2004). These events are thought to be regulated through PKA mediated phosphorylation of target proteins, although the identity of these proteins remains obscure. Elegant studies by El-Daher and colleagues demonstrated the phosphorylation of a number of PKA substrates in different cellular compartments (El-Daher *et al*., 1996). However, it is unclear in this report whether these targets are phosphorylated in a PKA-isoform specific manner. Furthermore, while PKA is known to induce protein phosphorylation in platelets, the physiological importance of its protein targets is still unclear. *In vitro* the enzyme phosphorylates G_{13}, inositol trisphosphate receptor (IP_3R), vasodilator stimulated phosphoprotein (VASP), actin-binding protein and caldesmon, with other potential substrates identified including heat shock protein27 (HSP27), myosin light chain kinase (MLCK), phosphodiesterase 3A (PDE3A), TxA_2 receptor and RhoA (Schwarz *et al*., 2001). Much of the data regarding the role of PKA in platelet function has been gained from *in vitro* studies, using cAMP mimetics that act as global cAMP modulators and bypass receptor mediated activation of AC. Therefore, it is still unclear the extent to which the currently identified PKA substrates are differentially phosphorylated by each PKA isozyme and whether the phosphorylation of the putative substrates are of physiological

relevance to platelet function. Here, we present evidence of a potentially new mechanism by which platelets regulate cAMP-dependent signaling. We show differential localization of PKA isoforms into lipid raft fractions, a process that maybe mediated by the coupling of PKA to AKAPs. Lipid raft-associated PKA I specifically targets and phosphorylates GPIbβ leading to reduced recruitment of platelets on to immobilized vWF.

The present data support a model for the potential compartmentalization of PKA signaling. While PKA I and PKA II are both expressed in platelets (Figure 4.1), there is evidence of differential localization of these isoforms. Since RIα, RIβ and RIIβ are the isoforms that has been reported to be present in platelets (Rowley *et al*., 2011), we used an antibody that can identify both RI isoforms and another one specific for RIIβ. We demonstrated the presence of a discrete population of PKA I, but not PKA II, in lipid raft fractions (Figure 4.3). Stimulation of adenylyl cyclase with physiological concentrations of PGI_2 led to the translocation of more PKA I into rafts in response to cAMP, observations that are consistent with previous work showing that in T cells PKA I is localized to lipid rafts in response to forskolin and increased cAMP (Carlson *et al*., 2006). Analysis of lipid raft fractions in platelets with an antibody that recognizes phosphorylated PKA substrates demonstrated the phosphorylation of a number of bands clearly highlighting that this pool of PKA was active and that the translocation of PKA I into the rafts may have functional implications (Figure 4.14). However, these data raised some important questions, firstly, what was mechanism that facilitated the translocation of PKA I to rafts in the absence of a palmitoylation sequence in PKA I, and secondly, what was the identity

of the PKA substrates in rafts and finally what role did their PKA phosphorylation play in platelet inhibition by PGI_2.

We began by focusing on the first question which addresses the potential translocation mechanism of PKA I. It is now well established in many cell types that A-kinase anchoring proteins (AKAPs), a group of structurally diverse, but functionally related proteins, can direct PKA to numerous cellular compartments (Tasken and Aandahl, 2004). We used a well-established approach that relies on cell permeable peptides that can compete with AKAPs for the binding of PKA. This tool has been used consistently by the field experts in order to determine the functional relevance of PKA-AKAP interactions in different cellular functions. Since our data indicated that PKA I was more dynamic than PKA II in platelets we concentrated on this isoform and used RIAD-Arg_{11} to specifically uncouple PKA I from potential AKAPs. We showed that optimal inhibition of several platelet functions such as aggregation, secretion and aggregation under flow by the physiological platelet inhibitor PGI_2 require PKA I-AKAP interactions (Figures 4.5, 9 and 16). Some of these data were reproduced with St-Ht31 (Figure 4.5) which is a dual-specific AKAP inhibitor. This is an important control because most PKA I-specific AKAPs are, in fact, dual-specifc (Tasken and Aandahl, 2004, Pidoux and Tasken, 2010).

RIAD was developed to specifically target type 1 specific AKAPs (Carlson *et al*., 2006) and has been used in numerous studies for this effect (Di Benedetto *et al*., 2008, Schillace *et al*., 2011, Means *et al*., 2011). An arginine tail was attached to the C-terminus of this peptide to facilitate its internalization into the cell. The role of

poly-arginine tails in delivering impermeable cargo into the cytoplasm is well established in the literature (Duchardt *et al*., 2007, Nakase *et al*., 2008). Using other poly-arginine tails such as the HIV-1 Tat peptide to increase cell permeability of other PKA-AKAP disruptors has also been reported (Patel *et al*., 2010). The commercially available dual-specific PKA-AKAP inhibitor St-Ht31 relies on the presence of a hydrophobic stearated moiety which enhances its cellular internalization (Futaki *et al*., 2001, Fernandez-Carneado *et al*., 2005). Despite having a poly-arginine tail, a significant amount of time was spent to determine the optimal conditions to ensure specificity and internalization of RIAD-Arg_{11}. We used fluorescence microscopy after the production of fluorecien-conjugated RIAD-Arg_{11} which was used to confirm peptide internalization and determine optimal incubation time. Data obtained from these experiments demonstrated that 1 hour was the optimal incubation time for the peptide (Figure 4.4 A). These conditions are consistent with conditions reported by other groups who used either the same peptide (Schillace *et al*., 2011) or other peptide with similar cellular carriers (Faruque *et al*., 2009). Moreover, consistent data with Fsk, a cell diffusible AC activator, confirmed that the effect of RIAD-Arg_{11} is neither specific to PGI_2 nor attributable to nonspecific extracellular effects such as competitive binding to the IP receptor.

In order to prove that the effect of RIAD-Arg_{11} on PGI_2-mediated inhibition of platelet functions was due to a specific effect on PKA, we carried out a series of experiments. Firstly we showed that the peptide did not potentiate platelet aggregation induced by collagen, thrombin or vWF (Figures 4.7 and 15) suggesting

that the enhanced platelet aggregation we observed occurred through modulation of the inhibitory effects of the cAMP/PKA signaling cascade. To further explore which part of the signaling pathway was affected we examined cAMP levels and phosphorylation events downstream of PKA. Consistent with the proposed mechanism of action of these inhibitory peptides of modulating PKA-AKAP interactions, RIAD-Arg_{11} had no effect on basal cAMP or elevation of cAMP levels in response to PGI_2 in the presence or absence of a PDE3 inhibitor (Figure 4.10). In contrast, phosphorylation of multiple PKA substrates was diminished by RIAD-Arg_{11} (Figure 4.11). Among the substrates was GSK3α and to a lesser extent RhoA. Unpublished data from our lab showed that these two proteins are targeted by PKA in platelets. Interestingly, the phosphorylation of the well-established PKA substrate VASP (Halbrugge *et al*., 1990) was not significantly affected by treatment with RIAD-Arg_{11} suggesting that phosphorylation of VASP by PKA is maybe independent of PKA I-AKAP interactions. Data were reproduced with st-Ht31 which diminished $VASP^{ser157}$ phosphorylation in a dose dependent manner (Figure 4.11). Importantly, the uncoupling of PKA I-AKAPs only reduces, but does not abolish phosphorylation of multiple PKA substrates, which is on contrast to the general PKA inhibitors KT/H-89 which reduced PGI_2-stimulation phosphorylation back to near basal levels (Figure 3.11). Consistent with these data, we never observed complete reversal of PGI_2 mediated inhibition of aggregation by RIAD-Arg_{11}. Thus, numerous substrates are targeted by PKA I in an AKAP-dependent manner, but that many PKA substrates are phosphorylated independently of this mechanism resulting in reduced but not abolished sensitivity to PGI_2. Similar observations have been made

in cardiomyocytes by another group using the same phospho-PKA substrate antibody and a poly-arginine conjugated PKA-AKAP disruptor where they showed only a reduction rather than a blockage in PKA signaling events after treatment with their peptide (Patel *et al*., 2010). The remaining phosphorylation events in the presence of RIAD-Arg_{11} , that are presumably sufficient to cause partial inhibition of aggregation, maybe be targets for non-AKAP associated PKA I or substrates of PKA II. These two possibilities are an important area of cAMP/PKA-platelet biology that requires further study.

The role of lipid raft in cAMP/PKA signaling in general is well established in the literature (Chini and Parenti, 2004, Willoughby and Cooper, 2007). Work by other groups showed the presence of AKAP-dependent redistribution of PKA isofroms into lipid rafts (Ruppelt *et al*., 2007, Schillace *et al*., 2011). Furthermore, unpublished data produced by our group showed differential distribution of PKA isoforms into platelet membrane and cytoplasm fractions. These observations along with the demonstration that the disruption of PKA I-AKAP influences PGI_2 mediated modulation of PKA activity, it seemed logical that PKA translocation into a sub-cellular compartment underpinned many of these observations. Our data throughout this study showed for the first time the differential localization of PKA isoforms into platelet lipid rafts under basal conditions in addition to further recruitment of PKA I into these microdomains in response to stimulation with PGI_2 (Figure 4.3). This PGI_2-stimulated redistribution of PKA I into platelet lipid rafts was almost completely blocked by RIAD-Arg_{11} suggesting a role for type 1 AKAPs in this translocation (Figure 4.13). In addition, we observed that this PGI_2-induced RI

translocation into lipid rafts was reversed after 10 minutes (data not shown). Therefore, from these data we concluded that redistribution of PKA I into lipid rafts in response to increased cAMP was AKAP-dependent.

Critical to the concept of compartmentalization of PKA signaling is the identification of potential specific substrates for PKA isoforms within distinct cellular locations. While a number of PKA substrates have been identified in platelets, their physiological importance is unclear because the experimental procedures are often not representative of the physiological situation and the potential specificity for PKA isoforms has never been tested. This latter issue is exacerbated by the lack of isoform specific inhibitors. However, by using RIAD to prevent AKAP coupling to type I PKA, it provided a tool to partially isolate PKA I signaling. Since only PKA I was present and active in lipid rafts, we hypothesized that proteins phosphorylated in response to PGI_2 in rafts were specific PKA I targets. Overexposure of membranes probed with the phospho-PKA substrate antibody showed a range of bands between 16 and 240kDa presumably representing proteins phosphorylated either basally or in response to strong stimulation with PGI_2 in platelet lipid rafts (Figure 4.14). We chose GPIbβ as a potential target for PKA I in lipid rafts for several reasons. Firstly the translocation of GPIb-IX-V complex into platelet lipid raft and the significance of this translocation to platelet function have been reported (Shrimpton *et al*., 2002). Secondly, phosphorylation of GPIbβ at ser^{166} has been reported to be PKA-mediated (Bodnar *et al*., 2002). Consistent with previous data we found basally phosphorylated GPIbβ in whole cell lysates (Bodnar *et al*., 2002). Phosphorylation was increased by PGI_2 treatment and reduced to basal level by PKA

inhibitors. Phosphorylation of GPIbβ was diminished slightly after RIAD-Arg_{11} treatment (Figure 4.15), although the heavy basal phosphorylation of GPIbβ in WCL made it difficult to see a significant effect. However, novel data produced during this study provides a new understanding of how phosphorylation of GPIbβ is regulated. While GPIbβ is basally phosphorylated in whole cell lysates, this phosphorylated form is absent from lipid rafts. However treatment of platelets with PGI_2 increased the presence of PKA I and an associated increase in phosphorylation of raft GPIbβ. This phosphorylation event was partially yet significantly reversed in response to treatment with RIAD suggesting a role for AKAPs in this phosphorylation event (Figure 4.16). The remaining phosphorylation can be attributed to the basally localized PKA I, which consistently could not be removed from rafts by RIAD (figure 4.12). These data showed that preventing PKA I translocation to the raft fraction was associated with diminished PKA activity represented by reduced phosphorylation of an array of PKA substrates including GPIbβ which reside in these nanodomains. Here we report for the first time that GPIbβ is phosphorylated in platelet lipid rafts by PKA I. We also suggest for the first time a non-redundant PKA I-specific phosphorylation event, which takes place in platelet lipid rafts and is dependent on AKAPs. Moreover, we suggest for the first time the potential presence of PKA I-AKAP macromolecule that resides in these platelet microdomains. Further work needs to be done to identify the AKAP and other components of this macromolecule. Similar observations were made in T-cells where CSK was identified as a PKA I-specific substrate in rafts whose phosphorylation was dependent on the AKAP Ezrin. Knocking down this AKAP in T-

cells resulted in disrupted cAMP-mediated modulation of immune function (Ruppelt *et al*., 2007). Unpublished data in our lab obtained from carrying out far Western blotting experiments suggest the presence of several putative AKAPs in platelets. Furthermore, an elegant platelet transcriptome study by Rowley *et al* suggest the presence of significant RNA levels for several AKAPs such as Ezrin, AKAP2, AKAP8, AKAP9, AKAP11, AKAP13, Pericentrin, WAVE-1 and AKAP8L (Rowley *et al*., 2011). A chemical proteomic study by Margarucci suggested the presence of AKAP2, AKAP7 and AKAP9 (Margarucci *et al*., 2011).

In the light of reports showing the role of PKA phosphorylation of GPIbβ^{ser166} in the modulation of platelet agglutination and GPIb-IX-V binding to vWF under flow (Bodnar *et al*., 2002), we wanted to see whether PKA I-AKAPs interactions played any part in these functional regulatory effects. We showed that inhibition of platelet vWF-induced aggregation by PGI_2 was partially and significantly reversed after treatment with RIAD (Figure 4.17). We also showed that incubation of platelets with PGI_2 reduced their ability to tether and adhere to vWF under arterial flow conditions, an effect that was reversed by uncoupling of PKA I from its AKAPs (Figure 4.18). These results demonstrated the physiological relevance of this AKAP-regulated phosphorylation event.

Collectively, data presented in this chapter demonstrate that the loss of PKA I from lipid rafts is associated with diminished sensitivity of platelets to its physiological inhibitor PGI_2 as evidenced by the reduced capacity of the prostanoid to inhibit

platelet functions and that these effects may be mediated through the interaction of PKA with AKAPs.

Chapter 5: The role of lipid rafts and actin filaments in cAMP-dependent platelet inhibition

5.1 Introduction

Cholesterol- and sphingolipid-enriched membrane microdomains, known as lipid rafts, play an equivocally important yet poorly understood role in signal transduction, protein trafficking, endocytosis and exocytosis in various cell types (Simons and Toomre, 2000). They are dynamic membrane assemblies that are separated from the rest of the membrane phospholipids thanks to the long acyl chains of their **sphingolipids**, which pack together forming membrane-embedded gel-like structures. The inclusion of **cholesterol** in these gel-like structures ensures great mobility and rather dynamic characteristics resulting in a liquid-ordered phase. Lipid rafts are known to play an enhancing role in a cellular signal by concentrating signalling components such as kinases and adaptor proteins downstream a specific receptor. This is particularly achieved through clustering of receptors located in highly mobile raft microdomains and consequently concentrating signalling molecules in a close proximity (Simons and Toomre, 2000, Patel *et al*., 2008).

In platelets several physiological receptors including GPVI/FcRγ and GPIb-IX-V have been reported to reside in lipid rafts, where they may form signalling complexes (Bodin *et al*., 2003, Lopez *et al*., 2005). It has been suggested that platelet lipid rafts play a positive role in different stages of haemostasis and thrombosis such as the initial adhesion stage, calcium influx and the generation of thrombogenic

microvisicles (Lopez *et al*., 2005, Bodin *et al*., 2003). However, the presence of inhibitory signalling complexes in lipid rafts is unclear. It could be hypothesised that in order to regulate positive signalling events emanating from lipid rafts, inhibitory signalling elements must have access to these same compartments.

In the previous chapter data were presented showing that some elements of the cAMP/PKA signalling cascade are recruited to lipid rafts to regulate platelet function. Upstream components of the PKA signalling cascade such as several AC isoforms, G-proteins and G-protein coupled receptors have also been found to localise differentially into lipid rafts (Chini and Parenti, 2004). But, in contrast to their proposed signal enhancing role, a rather constraining role has been proposed for these liquid-ordered microdomains in G-protein coupled receptor (GPCR) signal transduction in several cell types such as cardiomyocytes and HEK293 (Head *et al*., 2006, Patel *et al*., 2008, Pontier *et al*., 2008). In these reports, disruption of lipid rafts with methyl beta cyclodextrin (MβCD) enhanced cAMP synthesis as a result of increased association between β_2-AR, Gs and AC. However, the role of lipid rafts in cAMP synthesis in platelets is unclear.

Aims and objectives

In this chapter we sought to investigate the role of platelet lipid rafts as the potential first step in the compartmentalisation of cAMP generation as well as signalling. Using MβCD as a well-established tool to study the functional relevance of lipid rafts, work presented in this chapter aimed to determine how lipid raft disruption would:

1. Affect platelet inhibition by several PKA activating agents
2. Affect cAMP synthesis in platelets
3. Affect PGI_2-induced PKA signalling events
4. Affect the localisation of components of the cAMP/PKA signalling cascade.

5.2 Determination of optimal MβCD concentration for aggregation studies

The most established tool to study the role of lipid rafts in any cellular process is the use of β-cyclodextrins such as methyl β-cyclodextrin (MβCD). Cyclodextrins are water-soluble cyclic oligosaccharides, which have a hydrophobic cavity capable of dissolving hydrophobic molecules and render them hydrophilic (Pitha *et al*., 1988). The ability of β-cyclodextrins to lower membrane cholesterol levels is well established yet the mechanism is still unclear. In platelets, it is well documented that cholesterol depletion with MβCD reduces platelet aggregation induced by CRP, thrombin and collagen (van Lier *et al*., 2008, Lee *et al*., 2006). Therefore, a critical first step in understanding how lipid rafts affected cAMP signalling, was to establish a concentration of MβCD that could disrupt lipid rafts, with minimal effect on platelet aggregation in order to retain the ability to monitor the inhibitory effects induced by different cAMP/PKA-mediated platelet inhibitors.

Washed platelets were pre-incubated with increasing concentrations of MβCD (1-5mM) for 30 min at 37^{o}C and aggregation response was monitored (Figure 5.1). In the absence of the cholesterol depleting agent collagen (5µg/mL) induced an aggregation response of 80±2%. We observed that high dose of MβCD (5mM) had a dramatic effect on collagen-induced aggregation, which was reduced to 12±3% ($p<0.0001$) at which the effect of PKA-mediated platelet inhibitors would be difficult to monitor. A lower concentration of MβCD (2.5mM) caused only a small reduction in collagen-induced platelet aggregation, where the response was 67±3% ($p<0.05$). Although the reduction in aggregation response was significant, pre-treating

platelets with MβCD at 2.5mM still provided a sufficiently robust aggregation response to evaluate inhibition by cAMP signalling.

Having established an optimal dose of MβCD that can only partially inhibits platelet aggregation by collagen, it was important to us to confirm that this dose of the cholesterol depleting agent is sufficient to disrupt platelet lipid rafts and lower membrane cholesterol levels. Therefore, we isolated platelet lipid rafts by sucrose-gradient ultracentrifugation. The integrity of lipid rafts was determined by assessing the presence of the lipid raft marker LAT in its corresponding fractions. In the absence of MβCD (2.5mM) a distinct population of LAT located in fractions 4 and 5 (Figure 5.2A), consistent with intact lipid rafts. However, treatment of platelets with MβCD (2.5mM) disrupted the integrity of these fractions, as evidenced by the loss of LAT from lipid raft fractions (Figure 5.2 A). In order to confirm this finding, cholesterol concentrations were measured in each of the fractions. In untreated samples, fraction 5 showed a high cholesterol concentration, 13µM, consistent with it being considered the peak raft fraction. Incubation with MβCD reduced the cholesterol concentration in fraction 5 to 7µM, indicating that the used concentration of MβCD (2.5mM) is sufficient to disrupt platelet lipid rafts. Not only did this treatment affect cholesterol concentrations in lipid rafts but also had an effect on all the other fractions (Figure 5.2 B).

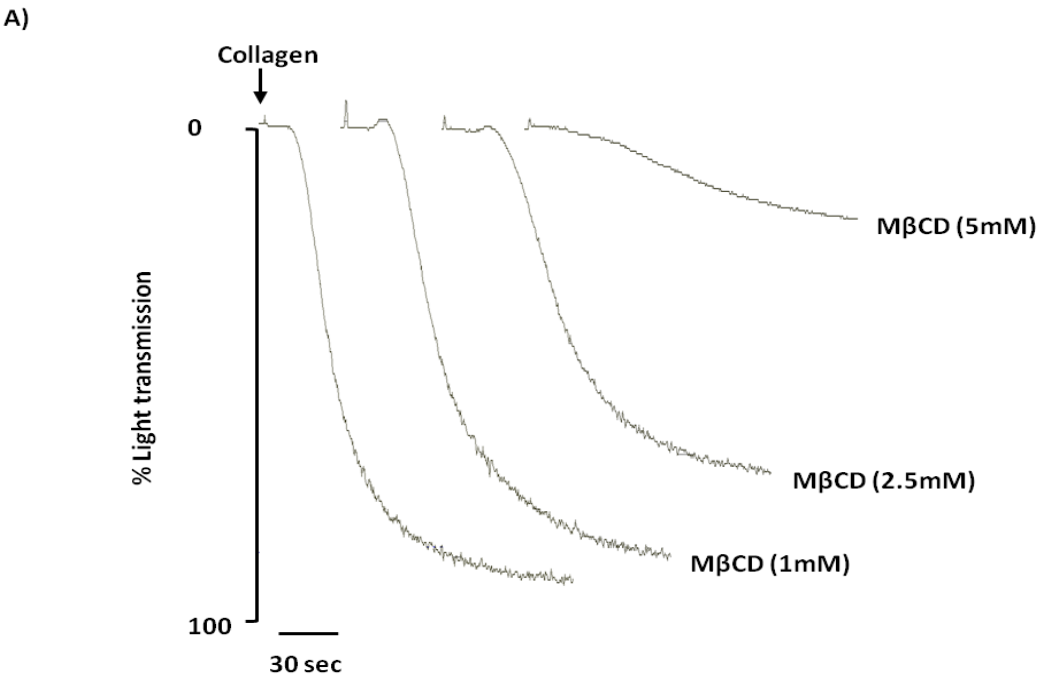
A)
Collagen
0
100
% Light transmission
30 sec
MβCD (5mM)
MβCD (2.5mM)
MβCD (1mM)

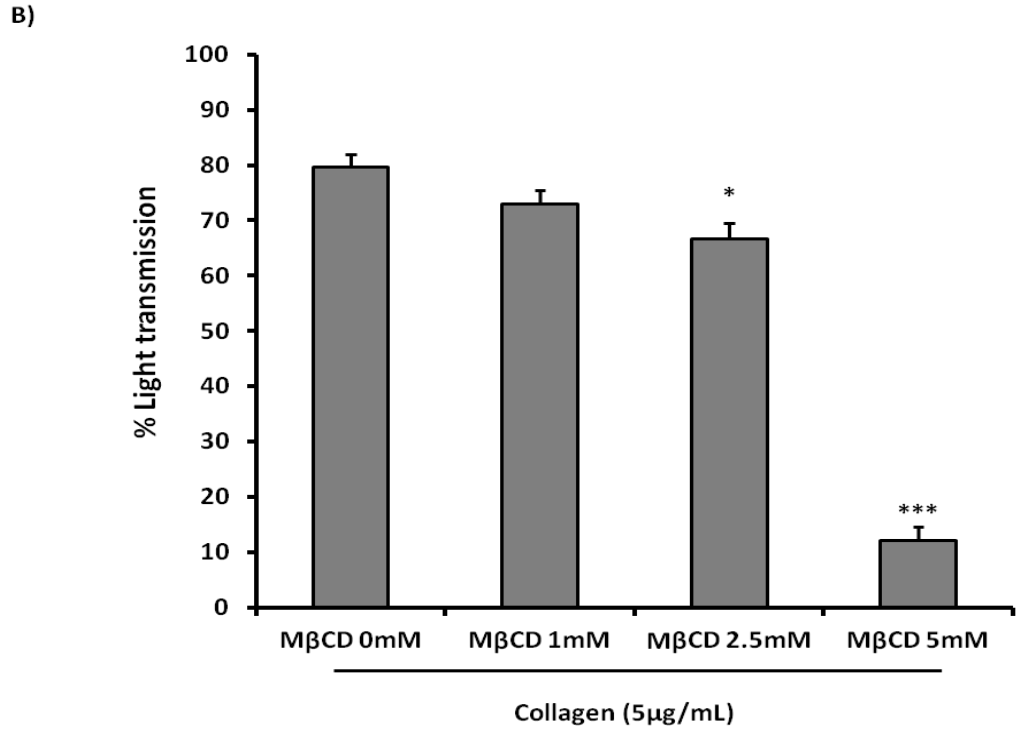
B)
% Light transmission
100
90
80
70
60
50
40
30
20
10
0
*
***
MβCD 0mM
MβCD 1mM
MβCD 2.5mM
MβCD 5mM
Collagen (5µg/mL)

Figure 5. 1: Optimisation of MβCD conditions with platelet aggregation.

WP ($2.5x10^8$ platelets/mL) were treated with increasing doses of MβCD (1-5mM) or with vehicle for 30 min at 37^oC then stimulated with collagen (5µg/mL). Aggregation was monitored for 4 min under constant stirring (1000rpm) at 37^oC using a chrono-log dual channel light transmission aggregometer and aggregation traces were generated by aggreo/link computer software (chrono-log, USA). **(A)** Shows representative traces. **(B)** Data expressed as means ± SEM of %light transmission of aggregation are from 3 independent experiments with different donors (* : $p \leq 0.05$, *** : $p \leq 0.0001$ when compared with collagen alone).

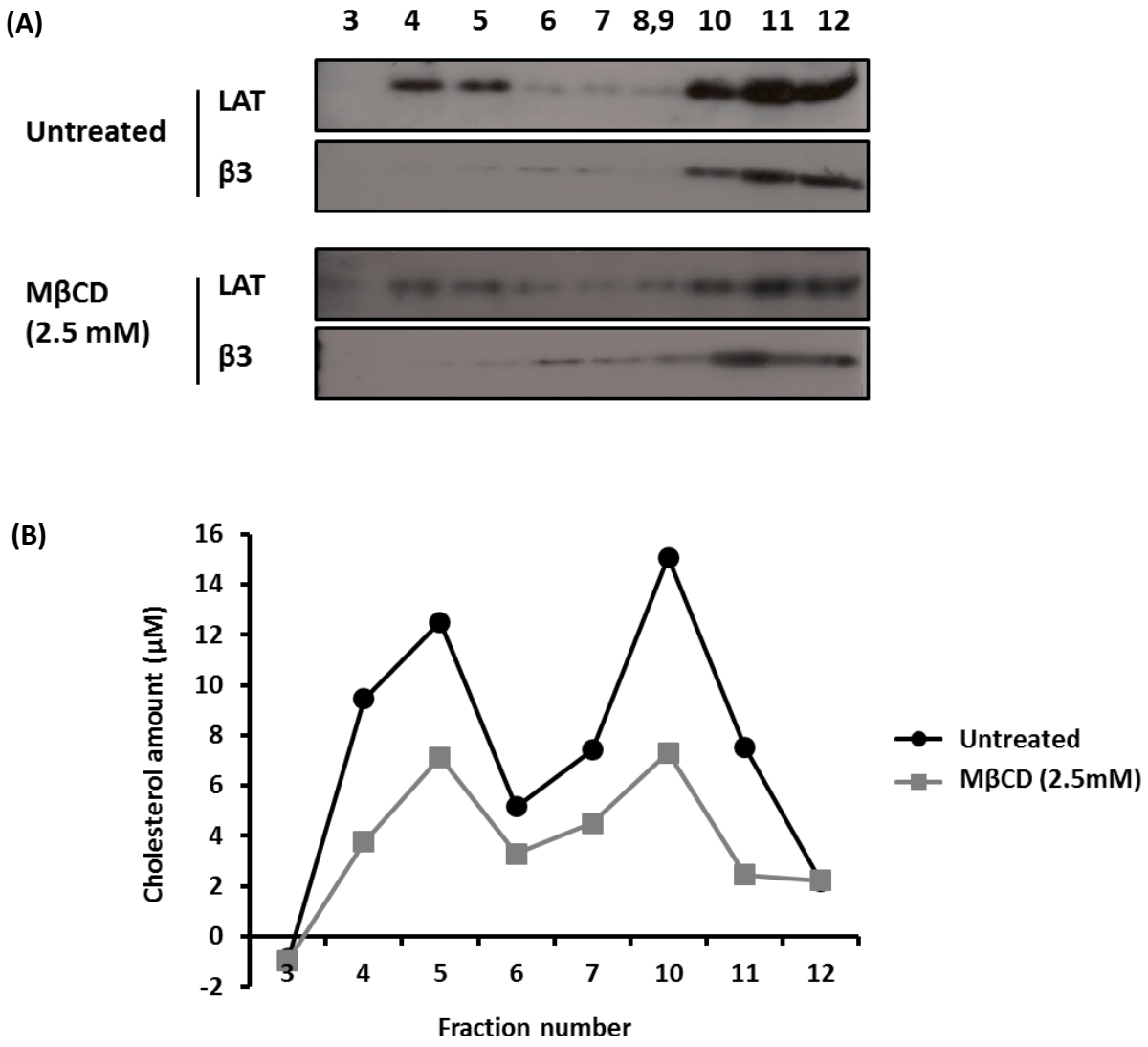

Figure 5. 2: Treatment of platelets with MβCD (2.5mM) disrupts lipid rafts and lower cholesterol levels.

Platelets ($1x10^9$platelets/mL) were either left untreated or incubated with MβCD (2.5mM) for 30 min at 37^oC. Platelets were then lysed with lipid raft lysis buffer containing 0.065% Triton X-100 for 30 min on ice. Lipid raft and non-raft fractions were then separated by sucrose gradient ultracentrifugation. **(A)** Aliquots of fractions (45µl) were then analysed by 10% SDS-PAGE for 1.5h at 120V followed by immunoblotting for 2.5h at 100V. Membranes were then blocked and firstly probed with LAT (1:1000 rabbit) and integrin β3 (1:1000 rabbit) to identify raft and non-raft fractions, respectively. **(B)** Cholesterol content of the loaded fractions was determined using a fluorescence assay as described in methods. Data are representative of 1 independent experiment.

5.3 Lipid raft disruption increases platelet sensitivity to cAMP elevating agents

Having established conditions that could modulate signalling events that relied on intact lipid rafts, we examined whether these conditions influenced platelet responses to cAMP/PKA. For these experiments, we used a number of different tools to trigger different parts of the cAMP/PKA signalling pathway.

5.3.1 Lipid raft disruption potentiates PGI_2-mediated inhibition of platelet aggregation

In the first instance, the integrity of these membrane microdomains on PGI_2-mediated inhibition of platelet aggregation was tested. WP were treated with either MβCD (2.5mM) or left untreated and then incubated with PGI_2 (1 - 100nM) before stimulation with collagen (5µg/ml). PGI_2 caused a concentration-dependent inhibition of platelet aggregation with 50% inhibition achieved using 49±10nM. To our surprise pre-treatment of washed platelets with MβCD (2.5mM) for 30 min at 37^{o}C significantly increased their sensitivity to PGI_2 as shown by a significant reduction in the concentration needed to achieve 50% inhibition, which was equal to 13±11nM ($p<0.05$) (Figure 5.3). To determine whether the effect that we observed was due to cholesterol depletion and not any nonspecific effects MβCD might have on platelets, we used a MβCD inactive analogue that is α-cyclodextrin (α-CD). Under similar conditions, this compound did not cause any increase in the inhibitory effect of PGI_2. These data suggest that disruption of platelet lipid rafts leads to a significant increase in platelet sensitivity to PGI_2.

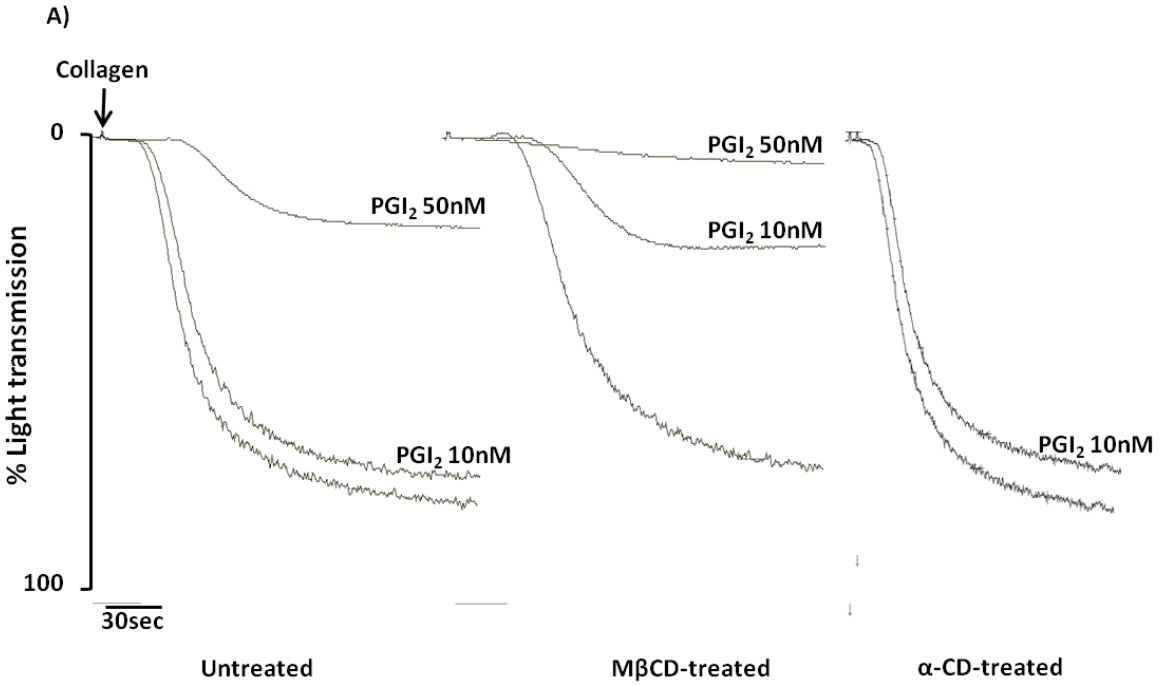
A)
Collagen
0
100
% Light transmission
30sec
PGI2 50nM
PGI2 10nM
PGI2 50nM
PGI2 10nM
PGI2 10nM
Untreated
MβCD-treated
α-CD-treated

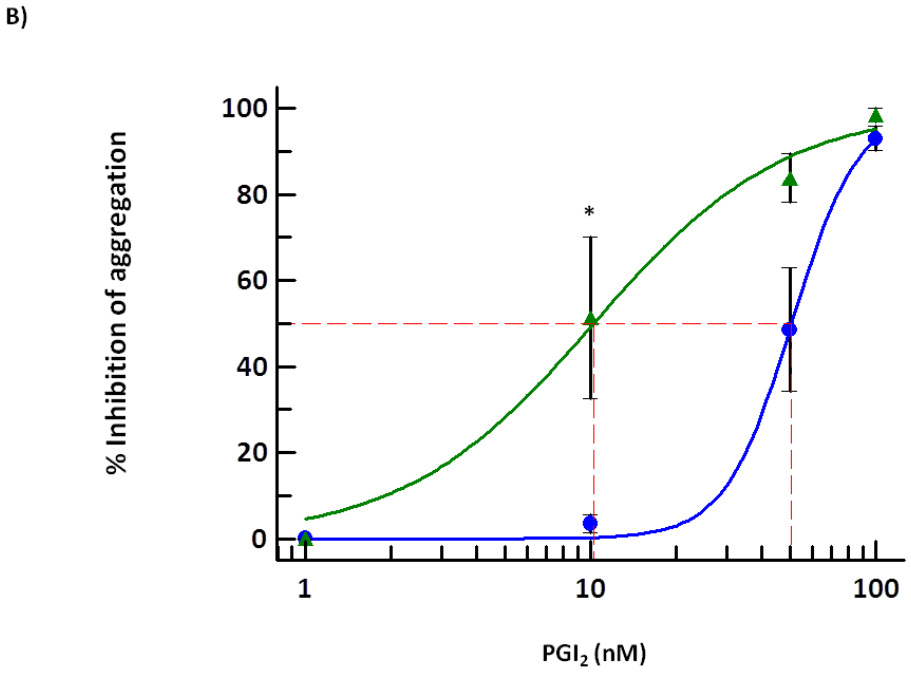
B)
% Inhibition of aggregation
100
80
60
40
20
0
1
10
100
*
PGI2 (nM)

Figure 5. 3: MβCD potentiates the inhibitory effect of PGI2 on platelet aggregation.

WP ($2.5x10^8$ platelets/mL) were pre-treated with vehicle, MβCD (2.5mM) or α-CD (2.5mM) for 30 min at 37^oC. Platelets were then either treated with PGI_2 (10 or 50nM) for 1 min followed by stimulation with collagen (5µg/mL) or were directly stimulated with the same concentration of collagen. Aggregation was monitored for 4 min under constant stirring (1000rpm) at 37^oC using a chrono-log dual channel light transmission aggregometer and aggregation traces were generated by aggreo/link computer software (chrono-log, USA). **(A)** Shows representative traces. **(B)** Shows data plotted as best fits for dose response vs % inhibition of aggregation for untreated (blue line) and MβCD-treated (green line). Data are representative of 4 independent experiments with different donors and are expressed as mean of % inhibition of aggregation ± SEM (* : $p \leq 0.05$ when compared with untreated samples).

5.3.2 Lipid raft disruption potentiates forskolin-mediated, but not cAMP analogue-mediated inhibition of platelet aggregation

Having demonstrated that lowering cholesterol levels in platelets increases their sensitivity to inhibition by PGI_2, we investigated whether the effect was specific to PGI_2. This was achieved by repeating the experiments with forskolin (Fsk) a direct activator of AC that bypasses the IP receptor. A low concentration of Fsk (2μM) caused only a threshold inhibitory effect (6±3%) on collagen-induced aggregation. This inhibitory effect was enhanced significantly after treatment with MβCD (2.5mM) reaching 32±2% ($p<0.001$). Similarly, treatment of platelets with a higher concentration of Fsk (10μM) caused a 39±10% inhibition of aggregation, which was increased significantly up to 90±9% ($p<0.01$) in the presence of MβCD (2.5mM) (Figure 5.4 A and B).

Next the experiments were repeated using 8-CPT-6-Phe-cAMP a cAMP analogue and a direct PKA activator, which bypasses AC completely. 8-CPT-6-Phe-cAMP, used at two concentrations 12.5μM and 25μM, inhibited aggregation by 34±9% and 68±3%, respectively. In contrast to the earlier findings with PGI_2 and forskolin, in the presence of MβCD the levels of inhibition in response to the two concentrations of the cAMP analogue remained unchanged at 38±8% ($p=0.7$) and 74±9% ($p=0.5$) (Figure 5.4 C). Taken together these data could suggest that cholesterol depletion affects the cAMP/PKA signalling pathway upstream of PKA and potentially at the level of the IPR-Gs-AC complex.

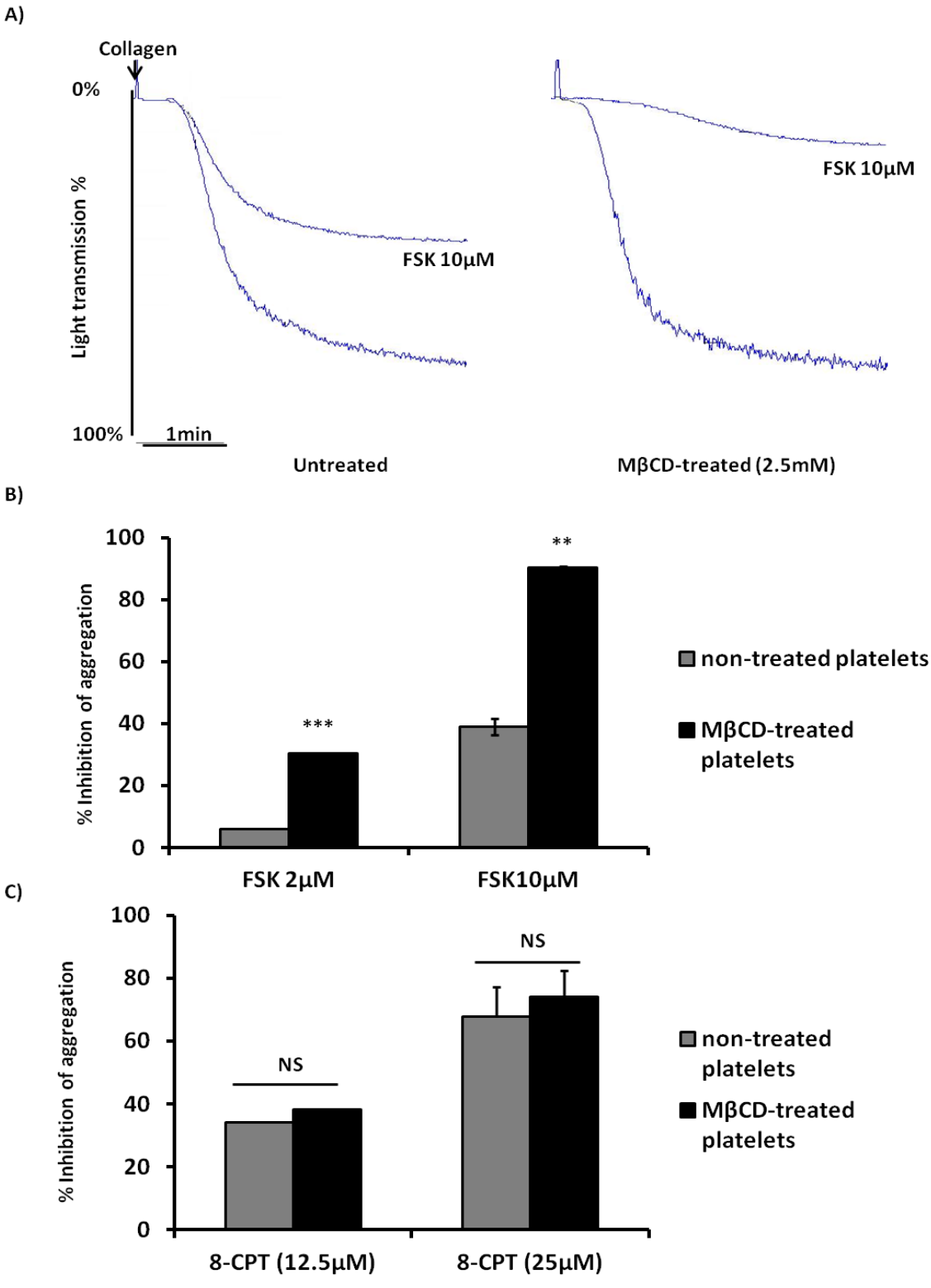
A)
Collagen
0%
Light transmission %
100%
1min
FSK 10µM
FSK 10µM
Untreated
MβCD-treated (2.5mM)
B)
% Inhibition of aggregation
100
80
60
40
20
0
***
**
FSK 2µM
FSK10µM
non-treated platelets
MβCD-treated platelets
C)
% Inhibition of aggregation
100
80
60
40
20
0
NS
NS
8-CPT (12.5µM)
8-CPT (25µM)
non-treated platelets
MβCD-treated platelets

Figure 5. 4: MβCD potentiates the inhibitory effect of Fsk on platelet aggregation but not 8-CPT-6-Phe-cAMP.

WP ($2.5x10^8$ platelets/mL) were pre-treated with vehicle or MβCD (2.5mM) for 30 min at 37^oC. Platelets were then either treated with Fsk (2 or 10µM) for 5 min followed by stimulation with collagen (5µg/mL) or were directly stimulated with the same concentration of collagen. Aggregation was monitored for 4 min under constant stirring (1000rpm) at 37^oC using a chrono-log dual channel light transmission aggregometer and aggregation traces were generated by aggreo/link computer software (chrono-log, USA). **(A)** Shows representative traces for Fsk with and without MβCD treatment. **(B)** and **(C)** Show data for Fsk and 8-CPT-cAMP, respectively. Data are from 5 independent experiments with different donors and expressed as %inhibition of platelet aggregation±SEM (**: $p<0.01$, ***: $p<0.001$ when compared with MβCD-untreated samples).

5.4 Lipid raft disruption enhances PGI_2-mediated cAMP synthesis in blood platelets

PGI_2 and forskolin exert their anti-platelet effects through the activation of adenylyl cyclase and elevations in cAMP levels(Feinstein et al., 1983)(Feinstein et al., 1983). cAMP molecules bind to cAMP-dependent protein kinase (PKA) in a cooperative manner leading to its activation, which in turn blunts platelet function through the phosphorylation of several key proteins. Having shown that lipid rafts potentially play an important regulatory role in platelet inhibition by cAMP-elevating agents, we then began to dissect the underlying mechanisms by examining the effects of MβCD on the activation of the cAMP-signalling cascade.

We started by examining the effect of MβCD on cAMP synthesis under basal and stimulatory conditions. Basal cAMP levels were equivalent to 177±42 fmol/10^7platelets. Treatment with MβCD (2.5mM) did not significantly change basal cAMP levels, which remained at 125±40 fmol/10^7platelets ($p=0.42$, Figure 5.5 A). Stimulating platelets with PGI_2 (50nM) raised cAMP levels up to 293±60 fmol/10^7platelets ($p<0.05$). This is equivalent to 74±39% increase in AC activity over basal levels. Interestingly, pre-treating platelets with MβCD (2.5mM) before stimulating with PGI_2 (50nM) raised cAMP levels up to 703±65 fmol/10^7platelets ($p<0.01$ compared with the absence of MβCD) which is equivalent to a 575±198% increase over MβCD-treated levels.

It is possible that the increase in cAMP levels in response to lipid raft disruption might be due to dislocation of PDE3 from lipid rafts. To investigate this, we

therefore repeated the experiment in the presence of the PDE3-specific inhibitor milrinone (10μM). Stimulating platelets with PGI_2 (50nM), in the presence of milrinone, increased cAMP concentrations from 173±36 to 715±138 fmol/10^7platelets ($p<0.001$). On the other hand, stimulating platelets with the same concentration of PGI_2 in the presence of MβCD (2.5mM) had a more profound effect on cAMP production ($p<0.001$ compared with the absence of MβCD) raising it from 172±27 up to 1780±73 fmol/10^7platelets ($p<0.0001$ compared with nonstimulated). Data in Figure 5.5 B shows a similar trend as the one observed in the absence of milrinone ruling out a PDE3-specific effect for cholesterol depletion. These data suggest that cholesterol depletion by MβCD significantly enhanced PGI_2-mediated AC activity.

To our surprise these observations could not be replicated with Fsk. cAMP levels in response to Fsk (2μM) were 595±195 and 609±105 fmol/10^7platelets ($p=0.47$) in the presence and absence of MβCD (2.5mM), respectively (Figure 5.5 C).

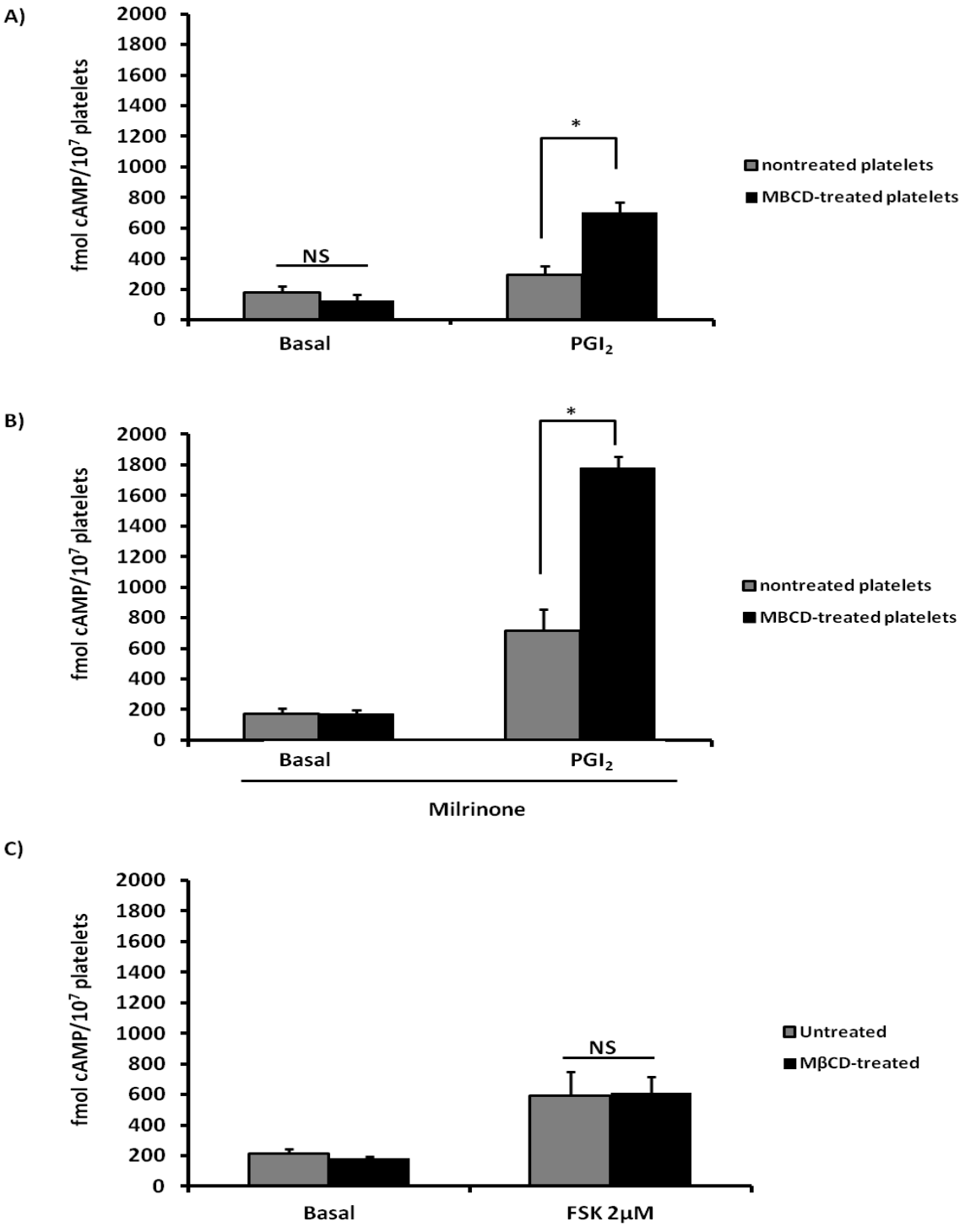
A)
fmol cAMP/10^7 platelets
2000
1800
1600
1400
1200
1000
800
600
400
200
0
*
NS
Basal
PGI2
nontreated platelets
MBCD-treated platelets
B)
fmol cAMP/10^7 platelets
*
Basal
PGI2
Milrinone
nontreated platelets
MBCD-treated platelets
C)
fmol cAMP/10^7 platelets
NS
Basal
FSK 2µM
Untreated
MβCD-treated

Figure 5. 5: MβCD potentiates the inhibitory effect of Fsk on platelet aggregation but not 8-CPT-6-Phe-cAMP.

(A) WP ($2x10^8$ platelets/mL) were assayed for their content of cAMP in the absence (grey bars) or presence (black bars) of MβCD (2.5mM for 30 min at 37^oC) either under non-stimulatory conditions or after stimulation with PGI_2 (50nM) for 30 sec. **(B)** As in A but in the presence of milrinone (10µM for 20 min). **(C)** As in A but platelets were stimulated with Fsk (2µM) for 5 min. Data are from 3 independent experiments with different donors and are expressed as means ± SEM. (*:$p<0.05$, NS: not significant).

5.5 Lipid raft disruption enhances PKA-mediated signalling events induced by PGI_2

Having established that cholesterol depletion increased AC activity in response to PGI_2, we sought to determine whether this resulted in enhanced PKA activity as evidenced by increased phosphorylation of PKA substrates in whole cell lysates. Using an antibody that recognises phosphorylated PKA substrates we found that proteins with apparent molecular weights of 55, 90 and 130kDa were mildly phosphorylated, while proteins of 44 and 16kDa were heavily phosphorylated under basal conditions (Figure 5.6, lane 1, top panel). Treatment of platelets with PGI_2 (1nM) led to a slight increase in phosphorylation of PKA substrates (Figure 5.6 A, lane 2, top panel). Robust phosphorylation can be observed with a higher dose of PGI_2 (50nM) with increased phosphorylation of proteins with apparent molecular weights of 44 and 70 and newly phosphorylated bands at 32, 38 and 66kDa (Figure 5.6, lane 3, top panel). Treatment of platelets with MβCD (2.5mM) alone caused a minor increase in phosphorylation of bands 55 and 38kDa compared to untreated cells (Figure 5.6, compare lane 4 and 1, top panel). When MβCD-treated platelets were stimulated with PGI_2, we observed that phosphorylation of numerous bands occurred with lower concentrations of the prostanoid. For example, when using PGI_2 (1nM), a significantly stronger phosphorylation was observed at 32 and 38kDa compared with MβCD-untreated cells. We also observed the phosphoryaltion of the band at 66kDa, which was absent at such a low concentration in the absence of MβCD (Figure 5.6, compare lane 5 and 2, top panel). In fact the level of phosphorylation induced by 1nM of PGI_2 in the presence of MβCD was comparable to the one observed with 50nM of PGI_2 in the absence of the cholesterol depleting

agent. A more obvious effect was observed at a higher concentration of PGI_2 (50nM) where treatment with the cholesterol-depleting agent caused a robust increase in phosphorylation of 32, 38, 44, 66, 70 and 150 kDa (Figure 5.6, compare lane 6 and 3, top panel). Consistent with these data we found that the presence of MβCD increased PGI_2-mediated $VASP^{157}$ phosphorylation at all concentrations of PGI_2 tested (Figure 5.6, middle panel). Data from these experiments suggest that MβCD-mediated enhanced platelet inhibition by PGI_2 is associated with enhanced AC and PKA activity.

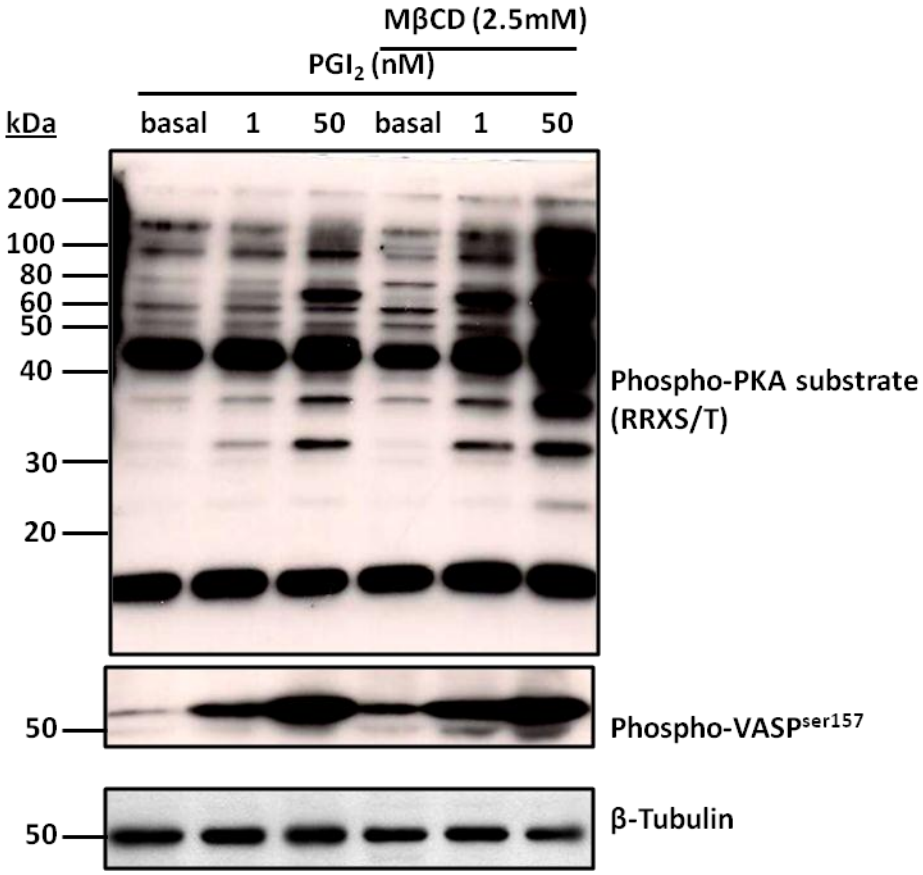

Figure 5. 6: MβCD enhances PGI2-mediated signalling events in blood platelets.

WP ($2.5x10^8$ platelets/mL) were treated either with vehicle or MβCD (2.5mM) for 30 min at 37°C. Platelets were then either lysed directly or stimulated with PGI_2 (10 or 50nM) for 1 min before they were lysed with x2 Laemmli buffer. Platelet lysates (20µg/well) were then loaded onto a 10-18% gradient polyacrylamide gel and then resolved by SDS-PAGE for 2.5h at 120V. Proteins were then transferred onto a PVDF membrane for 2.5h at 100V. Membranes were then blocked with 10% w/v BSA in TBSTand immunoblotted with anti-phospho-PKA substrate rabbit antibody (1:1000) overnight at 4°C (top panel). Membranes were then stripped and reprobed with anti phospho-$VASP^{ser157}$ rabbit antibody overnight at 4°C (middle panel). Membranes were finally immunoblotted for anti-β-Tubulin mouse antibody (1:1000) overnight at 4°C to check for equal loading. Blots are representative of three independent experiments with three separate donors.

5.6 Disruption of lipid rafts does not affect PKA signalling events induced by other PKA activating agents

Having shown that disruption of lipid rafts enhances PGI_2-mediated PKA signalling events in platelets we wanted to investigate the effect of MβCD on PKA signalling events induced by the direct AC activator Fsk.

We showed that Fsk-mediated inhibition of platelet aggregation was enhanced after cholesterol depletion with MβCD (Figure 5.4). However, we did not observe any potentiation in AC activity with Fsk under the same cholesterol lowering conditions (Figure 5.5). We next tested the effect of MβCD on Fsk-mediated phosphorylation events. Treatment of washed platelets with Fsk (2 and 10μM) induced the phosphorylation of proteins with apparent molecular weights of 35, 48, 66 and 240kDa, which was detected by the p-PKA substrate antibody. Pre-incubation of platelets with MβCD (2.5mM) showed no increase in the phosphorylation events mediated by PKA but rather a decrease in the intensity of phosphorylation with most of the proteins except proteins with apparent molecular weight of 16 and 55kDa whose phosphorylation was enhanced upon cholesterol depletion (Figure 5.7 A, top panel). Phosphorylation of $VASP^{ser157}$ was also unaffected by treatment with MβCD. Therefore, consistent with the AC data, these data suggest that disruption of lipid rafts has no significant effects on PKA signalling events induced by Fsk. Incubation of platelets with the direct PKA activator 8-CPT-6-Phe-cAMP (12.5 μM) increased the phosphorylation of $VASP^{ser157}$ and several other proteins (Figure 5.7 B, lane 1, 2). Consistent with the aggregation data, pretreatment with MβCD (2.5mM) did not enhance the phosphorylation events

induced by 8-CPT-6-Phe-cAMP but rather decreased the intensity of the phosphorylation of VASP[157] and phospho-PKA substrate profile (Figure 5.7 B, lane 3, 4). These data suggest that the enhanced sensitivity to PGI_2 in response to lipid raft disruption is not due to a direct effect on PKA but rather can be attributed to an effect on the IP receptor, Gs proteins or AC.

A)

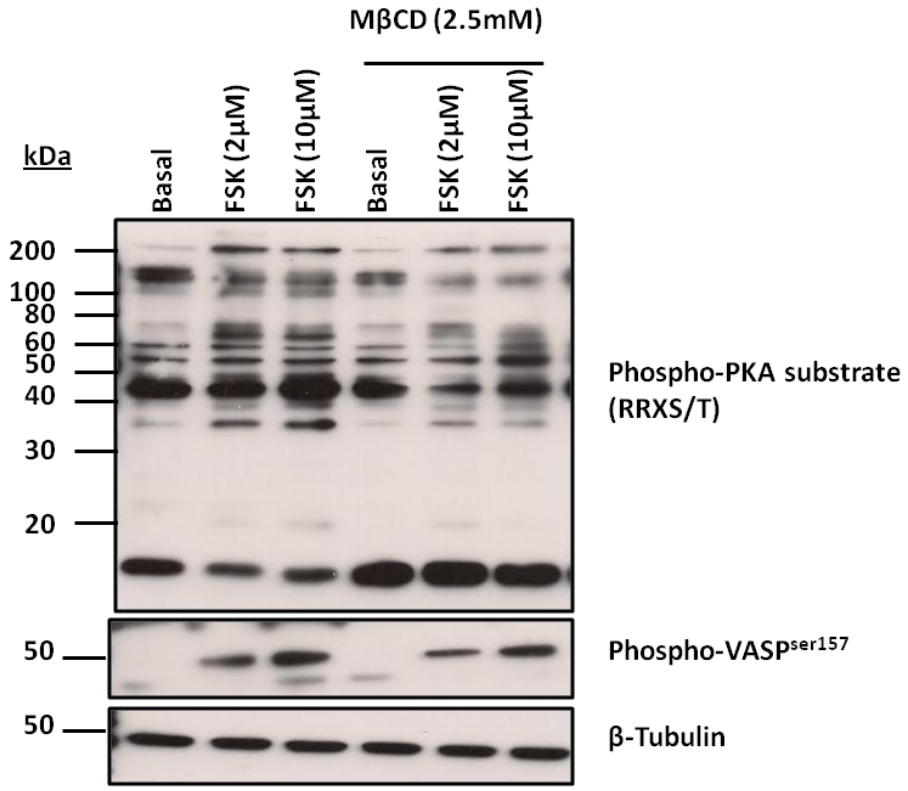
MβCD (2.5mM)
kDa
Basal
FSK (2μM)
FSK (10μM)
Basal
FSK (2μM)
FSK (10μM)
200
100
80
60
50
40
30
20
Phospho-PKA substrate (RRXS/T)
50
Phospho-VASPser157
50
β-Tubulin

B)

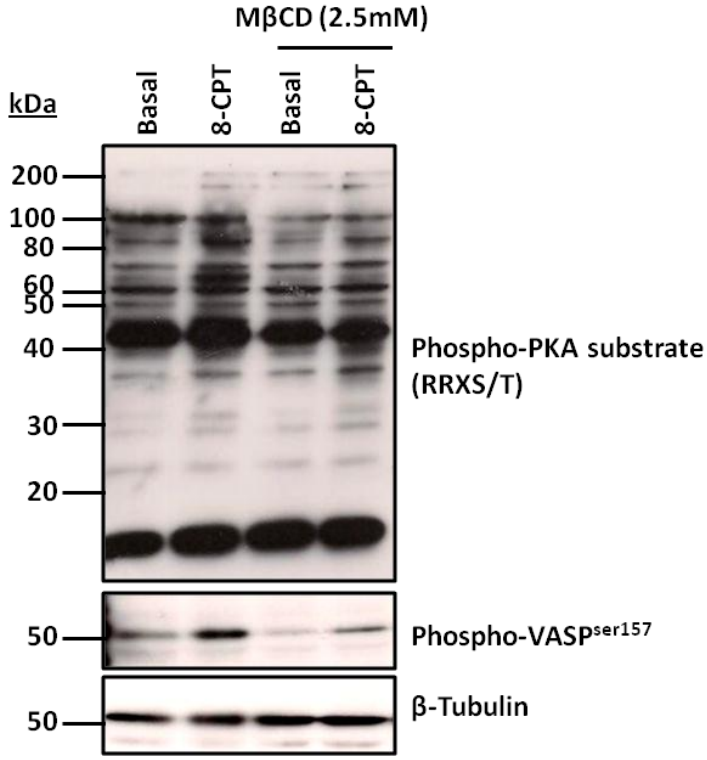
MβCD (2.5mM)
kDa
Basal
8-CPT
Basal
8-CPT
200
100
80
60
50
40
30
20
Phospho-PKA substrate (RRXS/T)
50
Phospho-VASPser157
50
β-Tubulin

Figure 5. 7: MβCD does not affect PKA-mediated signalling events induced by Fsk or 8-CPT-6-Phe-cAMP.

WP ($2.5x10^8$ platelets/mL) were treated either with vehicle or MβCD (2.5mM) for 30 min at 37^oC. Platelets were then either lysed directly or stimulated with **(A)** Fsk (2 or 10µM) for 5 min or **(B)** 8-CPT-cAMP (12.5µM) for 5 min before they were lysed with x2 Laemmli buffer. Platelet lysates (20µg/well) were then loaded onto a 10-18% gradient polyacrylamide gel and then resolved by SDS-PAGE for 2.5h at 120V. Proteins were then transferred onto a PVDF membrane for 2.5h at 100V. Membranes were then blocked with 10% w/v BSA in TBS-T and immunoblotted with anti-phospho-PKA substrate rabbit antibody (1:1000) overnight at 4^oC (top panel). Membranes were then stripped and reprobed with anti phospho-VASP^{ser157} rabbit antibody overnight at 4^oC (middle panel). Membranes were finally immunoblotted for anti-β-Tubulin mouse antibody (1:1000) overnight at 4^oC to check for equal loading. Blots are representative of two independent experiments with separate donors.

5.7 Disruption of actin filaments potentiates PGI_2-mediated inhibition of platelet aggregation

Components of the cytoskeleton such as actin filaments play an important role in membrane topology, exocytosis, shape change and cellular motility (Chang and Goldman, 2004, Revenu *et al*., 2004). There is a strong connection between several cytoskeleton components and lipid rafts, which can serve as sites for actin tail formation (Pelkmans *et al*., 2002). The actin cytoskeleton plays a role in maintaining the morphology of lipid rafts as well as the localisation of protein signalling complexes into these microdomains (Head *et al*., 2006). In addition, in cardiomyocytes, it has been shown that cytoskeleton inhibiting agents such as actin filament inhibitors enhance G protein-coupled receptor signalling (Head *et al*., 2006). All of these established findings encouraged us to investigate whether actin filament disruption would have similar effects on cAMP/PKA signalling in blood platelets.

To explore the role of the actin cytoskeleton we used cytochalasin D as a well-established inhibitor of actin polymerisation. Pretreatment of washed platelets with Cytochalasin D (10μM) caused a significant increase in PGI_2-mediated inhibition of collagen-induced platelet aggregation. The 50% inhibition was achieved using 51±10nM of PGI_2, which was reduced to 22±7nM ($p<0.05$) in the presence of the actin polymerization inhibitor (Figure 5.8 A and B).

To determine whether the observed sensitisation of platelets to cAMP signalling was specific to PGI_2, the aggregation experiment was repeated in the presence of

forskolin, a direct activator of AC and 8-CPT-6-Phe-cAMP. Fsk (2µM) caused 14±8% inhibition of platelet aggregation whereas pretreatment with Cytochalasin D increased this inhibitory effect to 61±17% ($p<0.05$). A higher concentration of Fsk (10µM) caused a 46±6% inhibition response which increased after treatment with Cytochalasin D up to 81±10% ($p<0.05$, Figure 5.8 C). The presence of Cytochalasin D did not potentiate the inhibitory effect of the direct PKA activator 8-CPT-6-Phe-cAMP (Figure 5.8 D). These data suggest that disruption of actin polymerization enhances the inhibitory effect of cAMP elevating agents on platelet aggregation, but had no effect on platelet inhibition induced by direct PKA activating agents.

A)

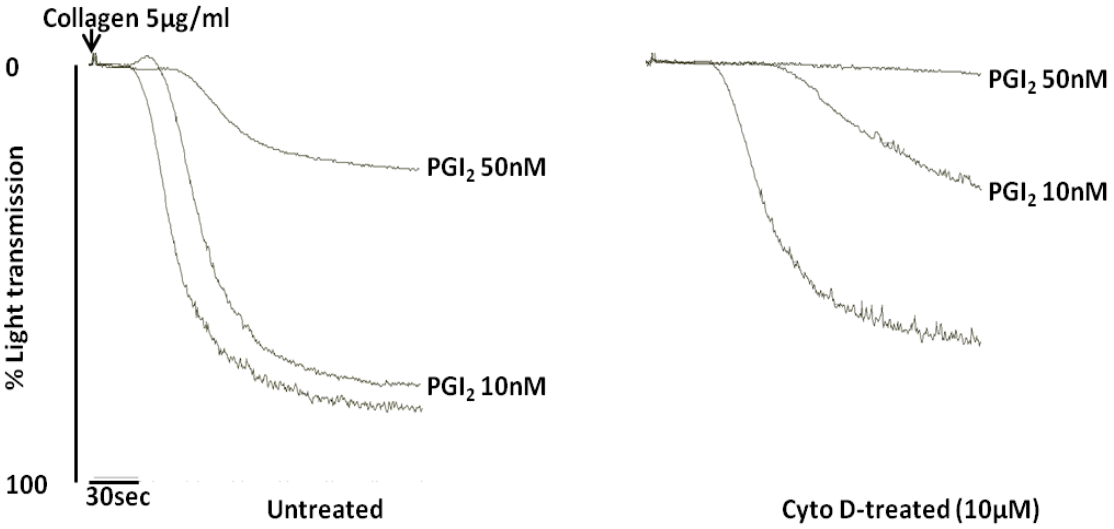
Collagen 5µg/ml
0
100
% Light transmission
30sec
PGI2 50nM
PGI2 10nM
Untreated
PGI2 50nM
PGI2 10nM
Cyto D-treated (10µM)

B)

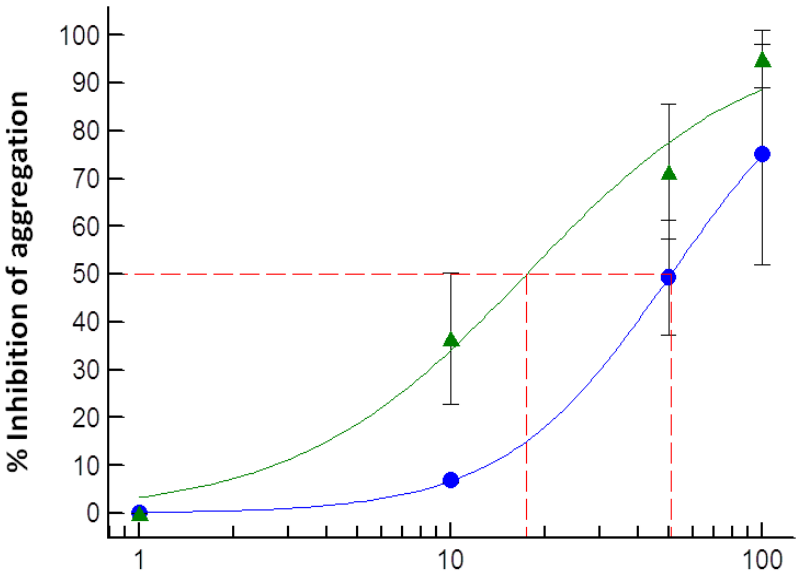
% Inhibition of aggregation
100
90
80
70
60
50
40
30
20
10
0
1
10
100

C)

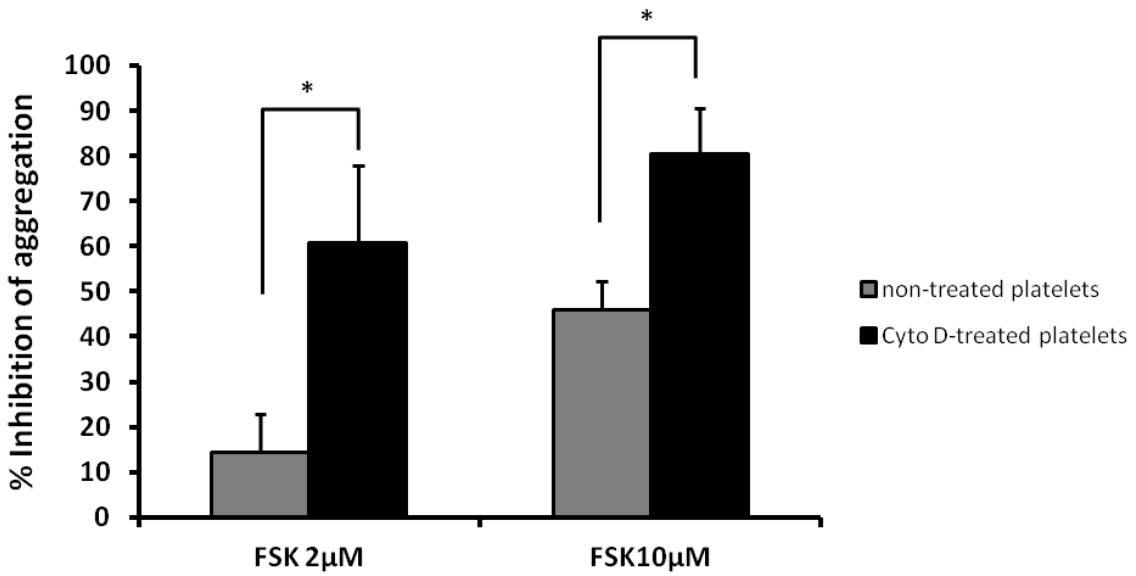
% Inhibition of aggregation
100
90
80
70
60
50
40
30
20
10
0
*
*
FSK 2µM
FSK10µM
non-treated platelets
Cyto D-treated platelets

D)

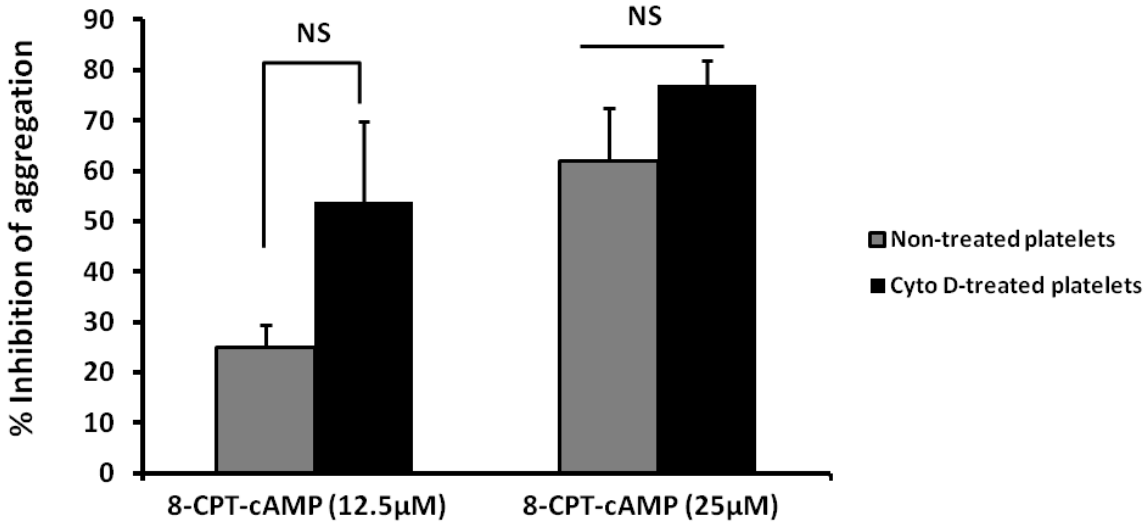
% Inhibition of aggregation
90
80
70
60
50
40
30
20
10
0
NS
NS
8-CPT-cAMP (12.5µM)
8-CPT-cAMP (25µM)
Non-treated platelets
Cyto D-treated platelets

Figure 5. 8: The effect of cytochalasin D on inhibition of platelet aggregation by PKA activating agents.

WP ($2.5x10^8$ platelets/mL) were pre-treated with vehicle or cytochalasinD (10µM) for 10 min at 37°C. Platelets were then either treated with PGI_2 (1-100nM) for 1 min **(A and B)**, Fsk (2 or 10µM) for 5 min **(C)** or with 8-CPT-6-Phe-cAMP (12.5 or 25µM) for 5 min **(D)** followed by stimulation with collagen (5µg/mL) or were directly stimulated with the same concentration of collagen. Aggregation was monitored for 4 min under constant stirring (1000rpm) at 37°C using a chrono-log dual channel light transmission aggregometer and aggregation traces were generated by aggreo/link computer software (chrono-log, USA). **(A)** Shows representative traces for PGI_2 in the presence or absence of CytochalasinD. **(B), (C) and (D)** Show data and stats for PGI_2, Fsk and 8-CPT-6-Phe-cAMP, respectively. Data are from 4 independent experiments with different donors and expressed as %inhibition of platelet aggregation±SEM (*: $p<0.05$, when compared with Cytochalasin D-untreated samples).

5.8 Disruption of actin filaments enhances PGI_2-mediated cAMP synthesis

The integrity of the actin cytoskeleton seemed to play a role in determining the inhibitory potency of cAMP elevating agents on platelet aggregation. To further explore the mechanism underpinning these functional effects, the outcome of actin filament disruption on AC activity was examined. In the absence of cytochalasin D, PGI_2 (50nM) increased basal cAMP levels from 159±15 to 209±25 fmol/10^7platelets ($p=0.07$, Data not shown). In the presence of cytochalasin D (10µM), PGI_2 (50nM) increased cAMP levels from 125±14 up to 229±18 fmol/10^7platelets, respectively ($p\leq0.01$, figure 5.9 A, black bars). Examining the concentrations of cAMP under these conditions suggested that cyto D had no real effect on cAMP formation in response to PGI_2. However, this could be slightly misleading because of the variability in the basal levels of cAMP between individual donors. To take this into account the data was normalised and also analysed as % increase over the basal levels. Using these criteria, PGI_2 (50nM) caused a 31±4% ($p<0.05$ compared to basal) increase in cAMP over basal levels in the absence of cytochalasin D. However, in the presence of the actin filament disruptor, the same concentration of PGI_2 induced an 89±24% increase in cAMP levels over basal ($p<0.05$ when compared with PGI_2 in the absence of cytoD, (Figure 5.9 A).

In the presence of the PDE3 inhibitor milrinone (10µM) no difference in basal cAMP levels between Cyto D-treated and untreated samples was observed, with 263±49 and 267±29 fmol/10^7platelets, respectively (Figure 5.9 B). Stimulation of these platelets with PGI_2 (50nM) led to a comparable increase in cAMP levels with

753±111 and 740±110 fmol/10^7platelets in the presence and the absence of Cyto D, respectively.

Unsurprisingly, actin filament disruption with Cyto D (10μM) had a very marginal effect on PKA signalling events induced by PGI_2. These effects can only be observed as a mild increase in $VASP^{ser157}$ phosphorylation whereas no clear effect on phosphorylation of other PKA substrates was observed (Figure 5.10).

These data suggest that actin filament disruption with Cytochalasin D result in a slight increase in AC activity and PKA phosphorylation events in response to PGI_2.

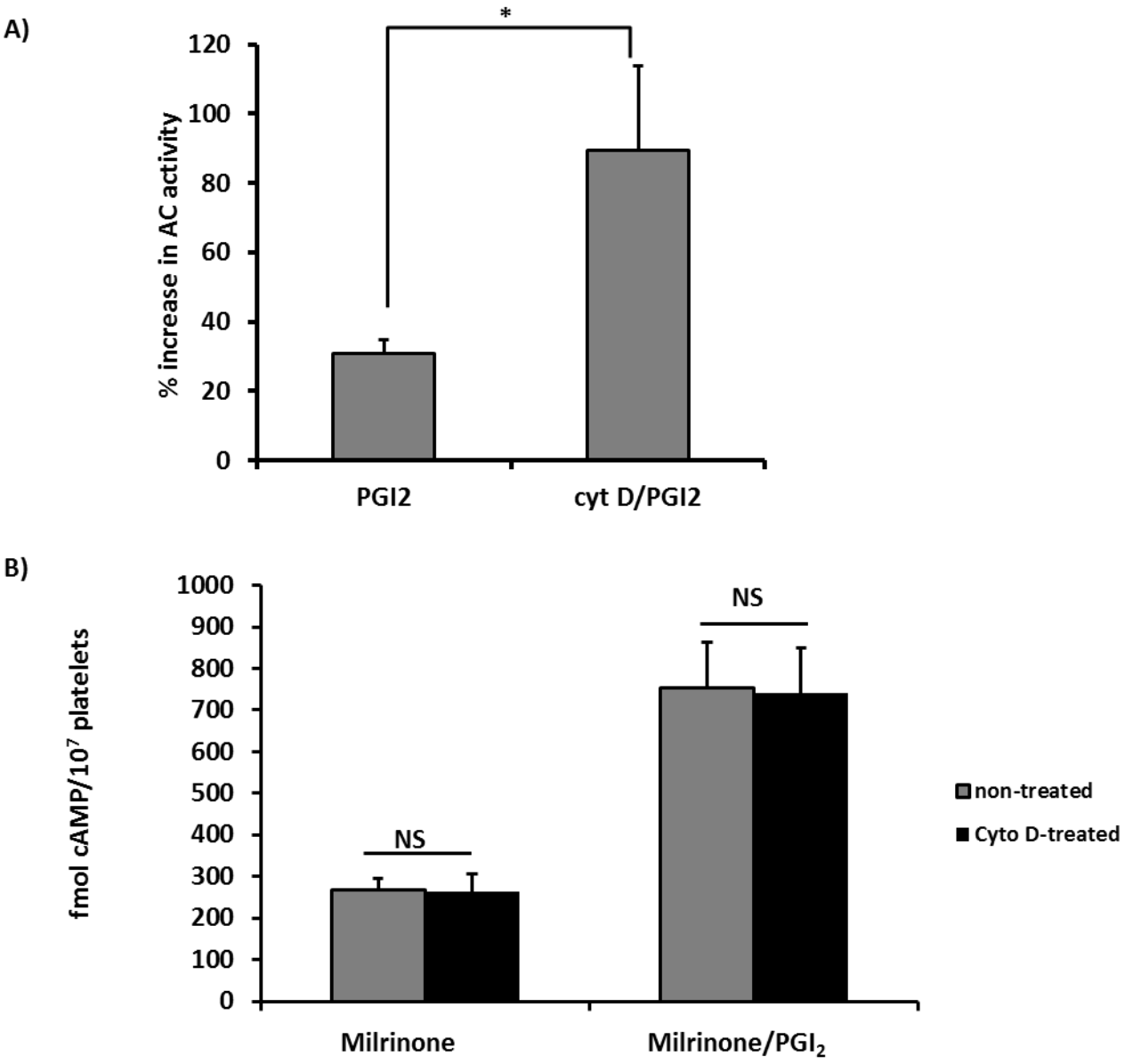

Figure 5. 9: The effect of cytochalasin D on PGI_2-mediated AC activity.

(A) WP ($2x10^8$ platelets/mL) were assayed for their content of cAMP in the absence or presence of Cyto D (10µM for 10 min at 37°C) either under non-stimulatory conditions or after stimulation with PGI_2 (50nM) for 30 sec. Data are presented as means ± SEM of %increase of cAMP levels over basal. **(B)** As in A but in the presence of milrinone (10µM for 20 min) and here data are expressed as means ± SEM of cAMP levels. Data are from 4 independent experiments with different donors (*:$p<0.05$, NS: not significant).

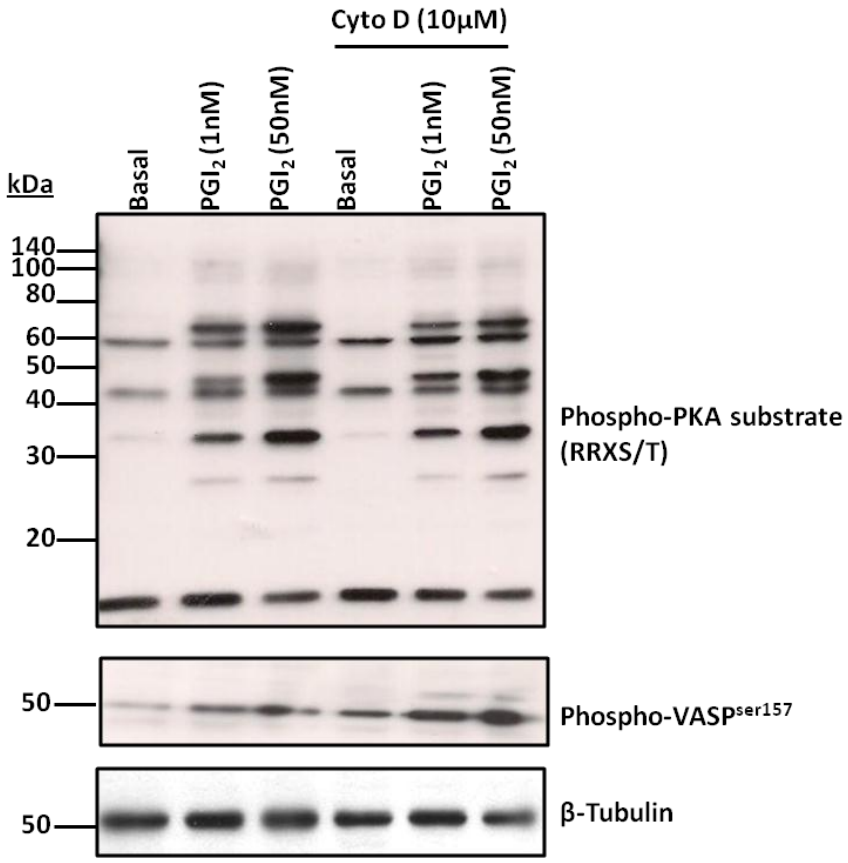

Figure 5. 10: Cyto D does not affect PKA-mediated signalling events induced by PGI_2.

WP ($2.5x10^8$ platelets/mL) were treated either with vehicle or Cyto D (10µM) for 10 min at 37°C. Platelets were then either lysed directly or stimulated with PGI_2 (1 or 50nM) for 1 min before they were lysed with x2 Laemmli buffer. Platelet lysates (20µg/well) were then loaded onto a 10-18% gradient polyacrylamide gel and then resolved by SDS-PAGE for 2.5h at 120V. Proteins were then transferred onto a PVDF membrane for 2.5h at 100V. Membranes were then blocked with 10% w/v BSA in TBST and immunoblotted with anti-phospho-PKA substrate rabbit antibody (1:1000) overnight at 4°C (top panel). Membranes were then stripped and reprobed with anti phospho-$VASP^{ser157}$ rabbit antibody overnight at 4°C (middle panel). Membranes were finally immunoblotted for anti-β-Tubulin mouse antibody (1:1000) overnight at 4°C to check for equal loading. Blots are representative of 3 independent experiments with separate donors.

5.9 Localisation of IP receptor, AC5/6 and $G\alpha_s$

The data presented suggested that disruption of lipid raft and actin filaments enhance the inhibitory effect of PGI_2 on platelet aggregation induced by collagen. This increased effectiveness of PGI_2 is associated with elevated AC activity, which resulted in increased PKA phosphorylation events. Since no increase in response to cAMP analogues was observed it suggested that our observations may occur at the IP receptor-Gs-AC level. Therefore, we wanted to investigate the localisation of these components and use that to interpret our observations.

To achieve this aim, platelet lipid rafts were isolated and the localisation of these components using antibodies against the IP receptor (A gift from Dr. Lucie Clapp), $G\alpha_s$ and AC5/6 (both from Santa Cruz Biotechnology) was determined. However, before the experiments could be performed the optimal conditions for each of these antibodies were determined. This was particularly important for the AC and IP antibodies as this had not been used in platelets previously.

5.9.1 Immuno-chemical characterisation of the $G\alpha_s$ antibody

Increasing amounts of whole cell lysates from untreated platelets were used to detect $G\alpha_s$ by immunoblotting. We observed a band with an apparent molecular weight of approximately 45kDa with only 5µg of protein. The intensity of this band increased proportionally with increased protein loading, which also was associated with the emergence of other non-specific bands (Figure 5.11 A). Subsequently, immunoprecipitation of $G\alpha_s$ from platelet WCL was performed. Pre-cleared platelet WCL (500µg protein) was incubated with 1, 2 and 5µg of $G\alpha_s$ antibody attached to

protein A-immobilised beads. A small band with apparent molecular weight of 45kDa could be observed with 5µg of the antibody, but not with lower amounts of the antibody or with 5µg of the IgG control (Figure 5.11 B). Data from this experiment confirmed the identity of the band detected earlier with immunoblotting and also confirmed the presence of $G\alpha_s$ protein in platelets.

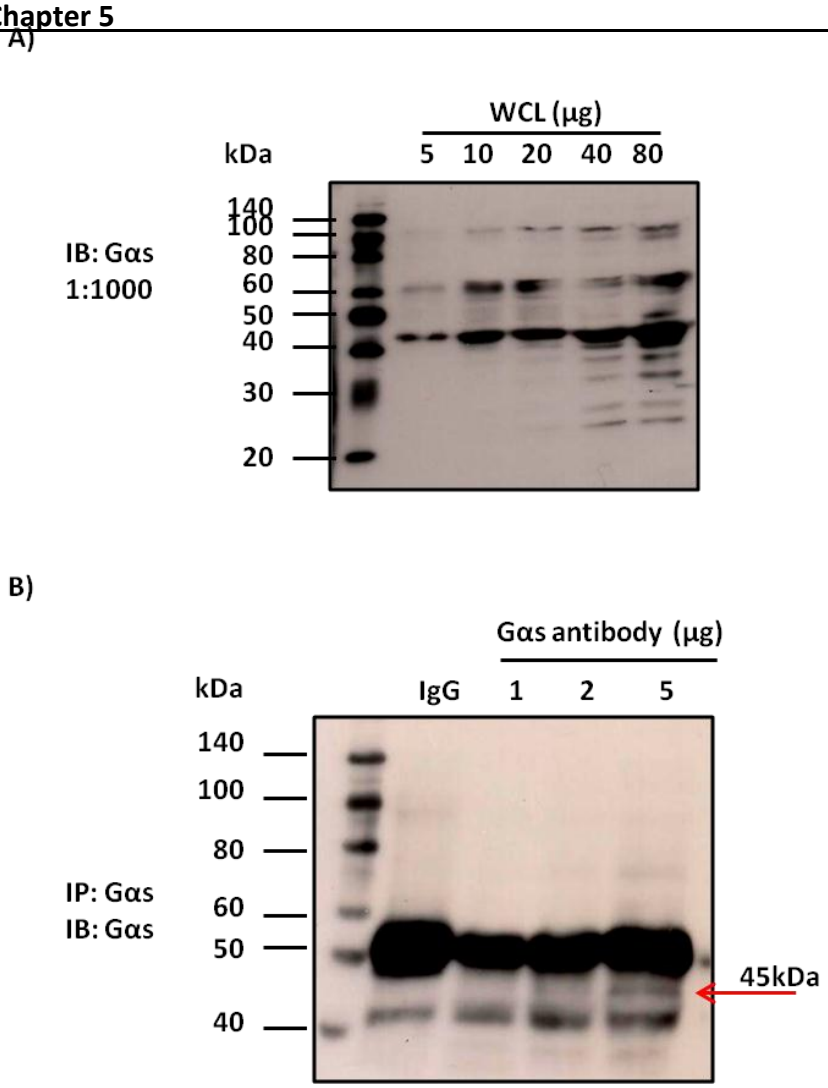

Figure 5. 11: Characterisation of the $G\alpha_s$ antibody.

(A) Untreated washed platelets ($1x10^9$ platelets/mL) were lysed with x2 Laemmli buffer. Platelet lysates (5-80µg) were loaded on a 10% polyacrylamide gel and then resolved by SDS-PAGE for 2.5h at 120V. Proteins were then transferred onto a PVDF membrane for 2.5h at 100V. Membranes were then blocked with 10% w/v BSA in TBST and immunoblotted with anti-$G\alpha_s$ rabbit antibody (1:1000) overnight at 4^oC with shaking. **(B)** WP ($9x10^8$ platelets/mL) were lysed using the IP lysis buffer (see appendix I). Lysates (500µg from 300µL) were precleared with protein A sepherose beads. Precleared lysates were then incubated with increasing amounts (1-5µg) of anti $G\alpha_s$ rabbit antibody (Santa Cruz, see appendix I) and one sample was incubated with rabbit IgG control (5µg). Samples were then treated as described in 2.4.1.1. Immunoprecipitates were then loaded on a 7.5% polacrylamide gel and were resolved by SDS-PAGE for 2.5h at 120V. Proteins were then transferred onto a PVDF membrane for 2.5h at 100V. Membranes were then blocked with 10% w/v BSA in TBST and immunoblotted with anti-$G\alpha_s$ rabbit antibody (1:1000) overnight at 4^oC with shaking. Blots are representative of one experiment.

5.9.2 Immuno-chemical characterisation of the AC5/6 antibody

In contrast to the $G\alpha_s$ antibody, the AC5/6 antibody was very nonspecific (Figure 5.12). The suggested apparent molecular weight of the AC5/6 by the manufacturer is approximately 132kDa. In the initial immunoblotting experiments using the AC5/6 antibody at a concentration of 1:1000 showed only one band with apparent molecular weight of about 40kDa (Figure 5.12 Ai). Overexposing these blots resulted in the emergence of a number of nonspecific bands and we were unable to observe any band at 132kDa even with 80µg of protein. Using a higher concentration of the antibody (1:200), we did observe a band at around the suggested molecular weight (Figure 5.12, Aiv, band indicated by a red arrow). We then repeated the same experiment, but this time PVDF membranes were blocked with 5% (w/v) skimmed dried milk in TBS-T. Figure 5.12 B shows a significant improvement represented by the loss of most of the nonspecific bands. A clear band at approximately 140kDa can be observed with different protein loading amounts (Figure 5.12 B). It was very important to confirm that this band was correspondent to AC5/6 therefore immunoprecipitation of platelet AC5/6 using increasing amount of the antibody (1-5µg) was performed.

Pre-cleared platelet WCL (500µg) was incubated with 1, 2 and 5µg of the AC5/6 antibody attached to protein A-immobilised beads. Immunoblotting of this immunoprecipitate a band with apparent molecular weight of 140kDa could be observed with 5µg of the antibody, but not with lower concentrations of the antibody or with 5µg of the IgG control (Figure 5.12 C). Data from this experiment

showed that AC5/6 is expressed in platelets and can be detected after SDS-PAGE and Western blotting at about 140kDa.

5.9.3 Immuno-blotting characterisation of the IPR antibody

The IP receptor antibody was a gift from Dr. Lucie Clapp. We characterised the antibody with our washed platelets using guidelines that were recommended.

Platelet whole cell lysate (10-70µg) were separated by SDS-PAGE followed by immune-blotting. After probing the PVDF membranes with two different dilutions of the antibody (1:500 and 1:200) we observed a band at around 53kDa corresponding to the IP receptor (Figure 5.13).

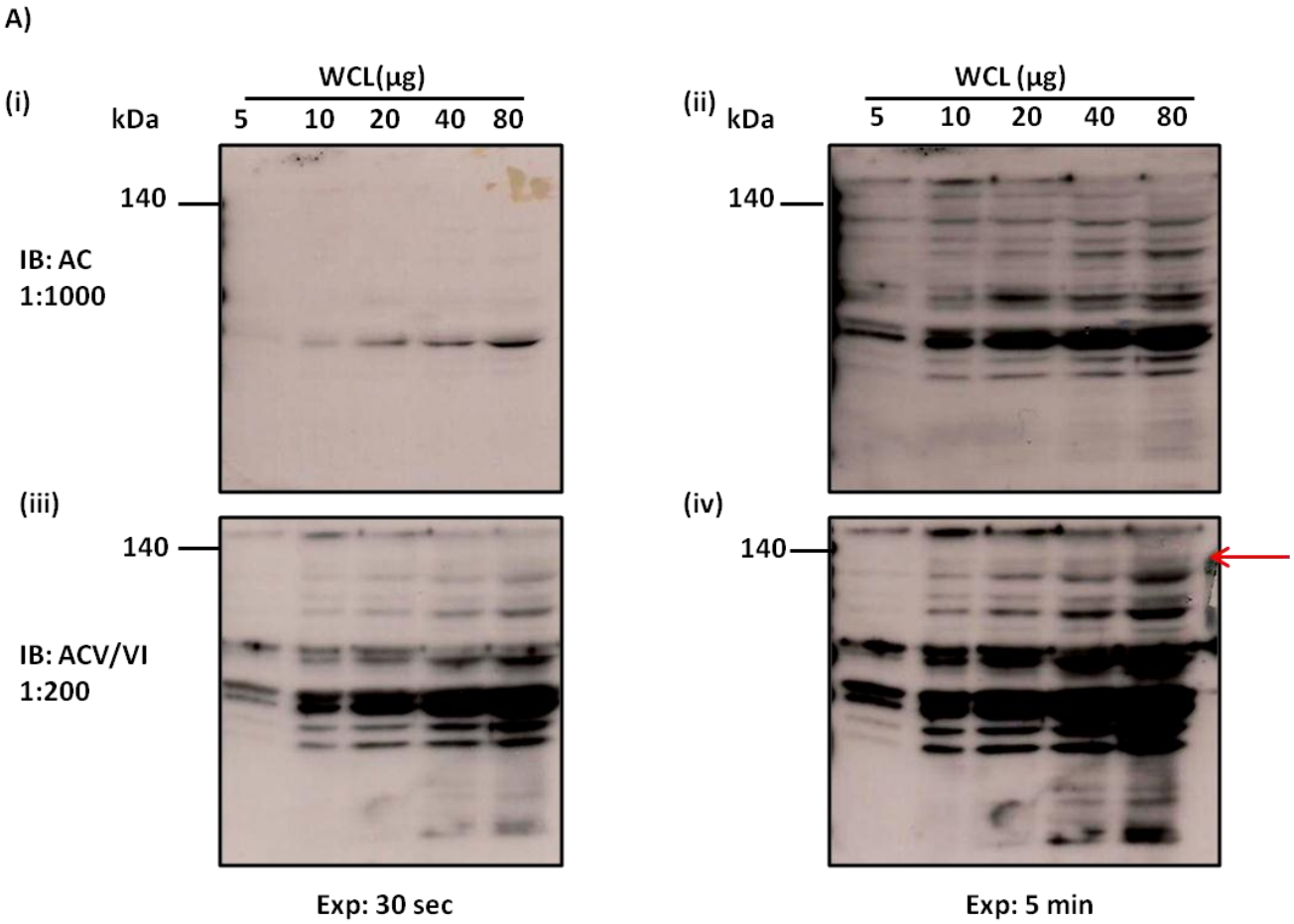
A)
(i)
WCL(µg)
kDa
5 10 20 40 80
140
IB: AC
1:1000
(ii)
WCL (µg)
kDa
5 10 20 40 80
140
(iii)
140
IB: ACV/VI
1:200
(iv)
140
Exp: 30 sec
Exp: 5 min

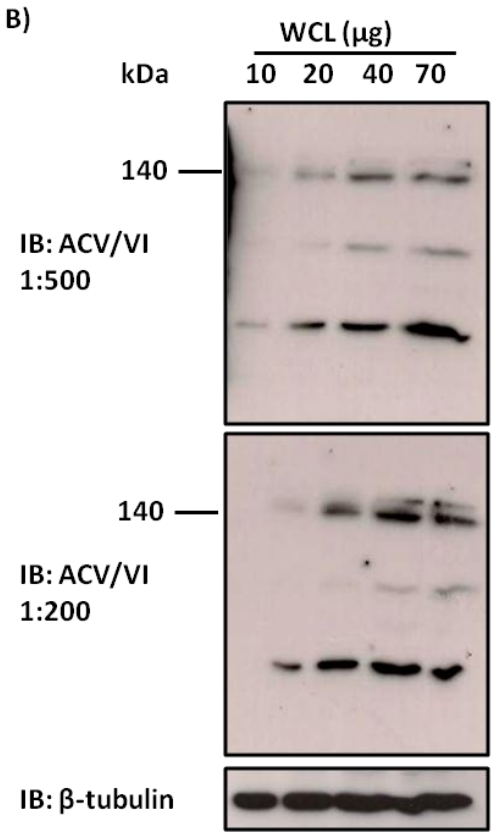
B)
WCL (µg)
kDa
10 20 40 70
140
IB: ACV/VI
1:500
140
IB: ACV/VI
1:200
IB: β-tubulin

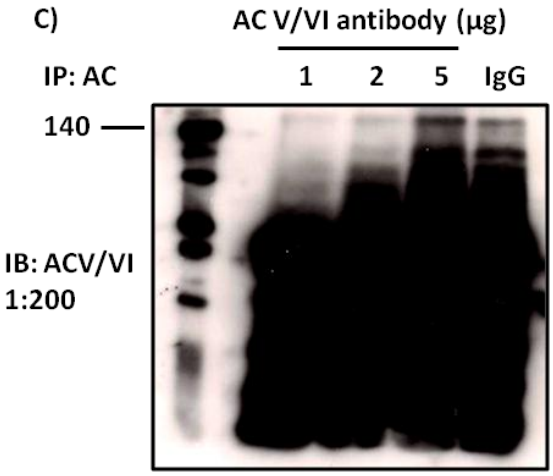
C)
AC V/VI antibody (µg)
IP: AC
1 2 5 IgG
140
IB: ACV/VI
1:200

Figure 5. 12: Characterization of the anti AC5/6 antibody.

(A) Untreated washed platelets ($1x10^9$ platelets/mL) were lysed with x2 Laemmli buffer. Platelet lysates were loaded on a 10% polyacrylamide gel and then resolved by SDS-PAGE for 2.5h at 120V. Proteins were then transferred onto a PVDF membrane for 2.5h at 100V. Membranes were then blocked with 10% w/v BSA in TBS-T and immunoblotted with anti-$G\alpha_s$ rabbit antibody (1:1000) overnight at 4^oC with shaking. Films were exposed **(EXP)** to the membranes in the cassette for either 30 sec or 5 min. **(B)** As in A but blocking buffer and antibody dilutions were made with 5% w/v and 1% w/v skimmed dried milk in TBS-T, respectively. Membranes were finally immunoblotted for anti-β-Tubulin mouse antibody (1:1000) overnight at 4^oC. **(C)** WP ($6x10^8$ platelets/mL) were lysed using the IP lysis buffer (see appendix I). Lysates (500µg from 240µL) were precleared with protein A sepherose beads. Precleared lysates were then incubated with increasing amounts (1-5µg) of anti AC5/6 rabbit antibody (Santa Cruz, see appendix III) and one sample was incubated with rabbit IgG control (5µg). Samples were then treated as described in 2.4.1.1. Immunoprecipitates were then loaded on a 10% polacrylamide gel and were resolved by SDS-PAGE for 2.5h at 120V. Proteins were then transferred onto a PVDF membrane for 2.5h at 100V. Membranes were then blocked with 5% w/v skimmed dried milk in TBS-T and immunoblotted with anti-AC5/6 rabbit antibody (1:200 made with 1% skimmed dried milk in TBS-T) overnight at 4^oC with shaking. Blots are representative of one experiment.

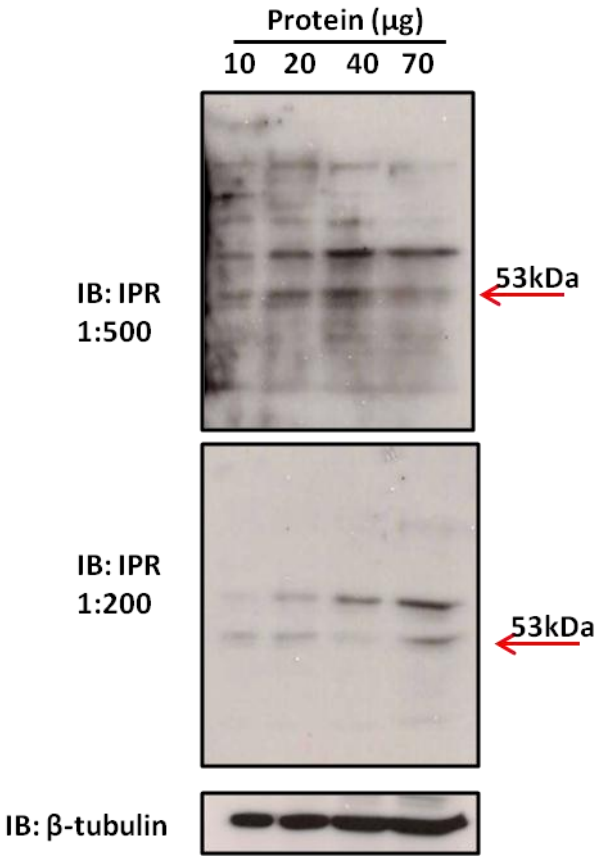

Figure 5. 13: Characterization of the anti IP receptor antibody.

(A) Untreated washed platelets ($6x10^8$ platelets/mL) were lysed with x2 Laemmli buffer. Platelet lysates (10-70µg) were loaded on a 10% polyacrylamide gel and then resolved by SDS-PAGE for 2.5h at 120V. Proteins were then transferred onto a PVDF membrane for 2.5h at 100V. Membranes were then blocked with 5% w/v skimmed dried milk in TBS-T and immunoblotted with anti-IP receptor rabbit antibody (1:500 and 1:200 dilutions made with 1% skimmed dried milk in TBS-T) overnight at 4^oC with shaking. Membranes were also washed with the same blocking buffer. Membranes were finally immunoblotted for anti-β-Tubulin mouse antibody (1:1000) overnight at 4^oC. Blots are representative of one experiment.

5.9.4 AC5/6, but not $G\alpha_s$ or IP receptor, is partially localised into platelet lipid rafts

Our data suggested that lipid rafts played a key role in the regulation of AC activity in platelets. To investigate this in more detail we isolated lipid raft fractions using sucrose density ultracentrifugation and the presence of components of the cAMP signalling cascade including the IP receptor, $G\alpha_s$ and AC5/6 were examined by immunoblotting. Lipid raft fractions were determined using LAT as a well-established lipid raft marker (Figure 5.14 A, fractions 4 and 5) whereas non-raft fractions were identified using the non-raft marker β3 (Figure 5.14 A, fractions 10, 11 and 12). In order to allow direct comparison on the same gel for different treatments, raft fractions were pooled together and run in one lane whereas non-raft fractions, from the same treatment, were pooled and run in the lane next to it.

In the first instance we looked at the localisation of AC5/6 in relation to lipid rafts (Figure 5.14 B, top panel). Under basal levels we observed a small pool of AC5/6 partitions in rafts and a larger pool in non-raft fractions. Upon treatment with a high concentration of PGI_2 (100nM), a smaller amount of AC5/6 was observed in raft fractions. No AC5/6 was observed in raft corresponding fractions when WP were pretreated with MβCD (2.5mM) mimicking the effects observed with a high dose of PGI_2.

After that we looked at the partition of $G\alpha_s$ in lipid rafts (Figure 5.14 B, middle panel). Surprisingly, no $G\alpha_s$ was found co-localizing with AC5/6 in platelet lipid rafts. Similarly we found no trace of the IP receptor in platelet lipid rafts. We postulate a

model where a population of AC5/6, but not $G\alpha_s$ or IP receptor, might be sequestered in platelet lipid rafts restricting from participating in the signal induced by a low or medium dose of PGI_2. And stimulation of platelets with a high dose of PGI_2 or treating them with MβCD could result in the release of this sequestered pool of AC5/6 allowing it to join the other components of the signal outside the rafts leading to the enhancement of the signal. These are preliminary observations that need to be confirmed using different antibodies.

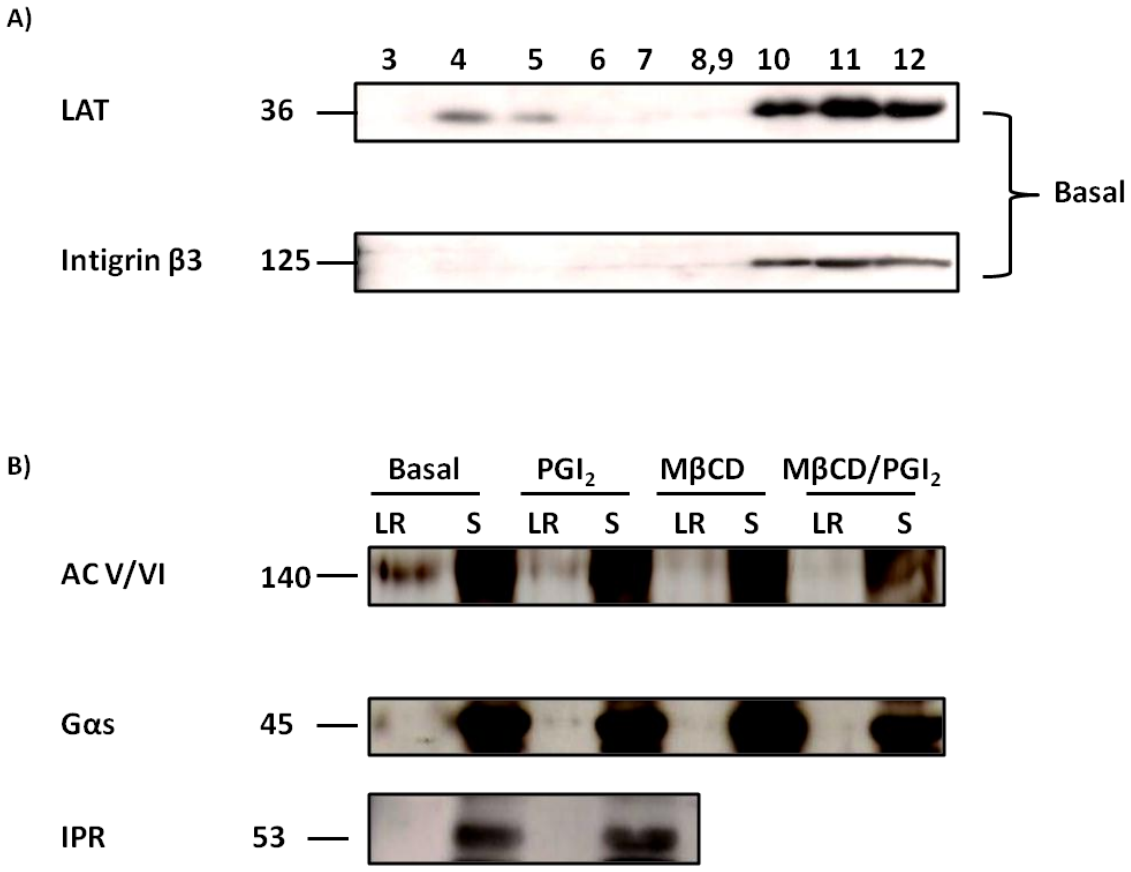

Figure 5. 14: AC5/6 but not $G\alpha_s$ or IP receptor is partially localised in platelet lipid rafts.

WP ($1x10^9$ platelets/mL) were either left untreated or stimulated with PGI_2 (100nM) for 30 sec in the presence or absence of MβCD (2.5mM) for 30 min at 37°C. Platelets were then lysed with lipid raft lysis buffer containing 0.065% Triton X-100 for 30 min on ice. Lipid raft and non-raft fractions were then separated by sucrose gradient ultracentrifugation. **(A)** Aliquots of fractions (45µl) were then analysed by 10% SDS-PAGE for 1.5h at 120V followed by immunoblotting for 2.5h at 100V. Membranes were then blocked and firstly probed with LAT (1:1000 rabbit) and integrin β3 (1:1000 rabbit) to identify raft and non-raft fractions, respectively. **(B)** Lipid raft fractions (LR) and soluble fractions (S) from different treatments were pooled together and loaded on a 7.5% polyacrylamide gel and were analysed by SDS-PAGE for 2.5h at 120V followed by immunoblotting for 2.5h at 100V. Membranes were blocked with 5% (w/v) skimmed dried milk in TBS-T and were then probed with either AC5/6 rabbit antibody (1:200), $G\alpha_s$ rabbit antibody or IP receptor rabbit antibody (1:500). Blots are representative of 3 independent experiments.

5.10 Discussion

Lipid rafts are important membrane nanodomains whose role in platelet activation has become a very attractive area of research (Lopez *et al*., 2005, Bodin *et al*., 2003). While a plethora of work in other cell types, focused on the role of lipid rafts in G protein-coupled receptors (GPCR) (Patel *et al*., 2008, Pontier *et al*., 2008), only few studies addressed the role of lipid rafts in the signalling of these ubiquitously expressed seven-transmembrane spanning receptors in platelets. The main focus of these few studies was their role in P2Y1 and P2Y12 receptor signalling (Vial *et al*., 2006, Quinton *et al*., 2005). In the present study, we address for the first time the role of platelet lipid rafts downstream the activation of an inhibitory GPCR that is the prostacyclin receptor (IP receptor).

We used methyl *β*-cyclodextrin (MβCD) as a well-established tool to lower cellular cholesterol levels (Zidovetzki and Levitan, 2007). Since we (Figure 5.1), and others (Lee *et al*., 2006, Pollitt *et al*., 2010), observed that lipid raft disruption abolishes platelet aggregation induced by GPVI and GPCR activation in a concentration-dependent manner, we used MβCD at a concentration that only partially inhibits platelet aggregation (2.5mM). This partial inhibition allowed us to examine the inhibitory effect of cAMP/PKA-dependent platelet inhibitors. This concentration still partially displaced our lipid raft marker LAT from the raft-corresponding fractions as shown through Western blotting and lowered cholesterol levels in these fractions (Figure 5.2). Throughout this study platelets were incubated with the indicated concentration of MβCD for 30 min at 37^{o}C. Concentrations and treatment

conditions of MβCD that we used are consistent with those used by others in platelets (Quinton *et al*., 2005) (Pollitt *et al*., 2010, Lee *et al*., 2006).

In this study we report for the first time that disruption of lipid rafts by MβCD enhances the inhibitory effect of PGI_2 and Fsk on platelet aggregation (Figure 5.3 and 5.4). As a negative control we chose to use an inactive analogue of MβCD, α-cyclodextrin (α-CD) (Hinzpeter *et al*., 2007, Agarwal *et al*., 2011). We chose the use of a MβCD inactive analogue as a control as an alternative to cholesterol repletion because the latter is likely to increase cholesterol levels above normal, which might affect cellular functions (Zidovetzki and Levitan, 2007). We also showed that when platelet cytoskeleton was disrupted with cytochalasin D, the inhibitory effect of PGI_2 was enhanced (Figure 5.8). This outcome of cytoskeleton disruption on cAMP/PKA signalling was reported by Head *et al* in cardiomyocytes and was then attributed to a role for the cytoskeleton in localising different elements of the cAMP/PKA signalling pathway into lipid rafts (Head *et al*., 2006). The conditions under which cytochalasin D was used in our experiments were consistent with those used by others in platelets (Pollitt *et al*., 2010). Since we could not reproduce any of these observations with the direct PKA activator 8-CPT-6-Phe-cAMP, we speculated that the disruption of lipid rafts and the cytoskeleton was affecting the signalling pathway at the level of the IP receptor-$G\alpha_s$-AC.

In the first instance we wanted to confirm the involvement of AC by looking at the effect of MβCD and cytochalasin D on its activity by measuring cAMP levels. The increased sensitivity of platelets to PGI_2 after lipid raft disruption was associated

with a significant increase in AC activity (Figure 5.5). The increased AC activity upon lipid raft disruption was maintained in the presence of the PDE3 inhibitor milrinone. Consistent with our observations, an enhanced AC activity after lipid raft disruption has been reported downstream of β_1AR and β_2AR in adult rat ventricular myocytes and in HEK293, respectively (Agarwal *et al*., 2011, Pontier *et al*., 2008). To our surprise the enhanced inhibitory effect of Fsk on platelet aggregation was not associated with an increase in AC activity. There are some conflicting reports as to whether disruption of lipid rafts increase Fsk-mediated cAMP synthesis. One report suggested that in HEK-293 disruption of lipid rafts increased AC activity induced by FsK (Pontier *et al*., 2008). Conversely, another group suggests that in the same cell type, the enhancement of AC activity as a result of lipid raft disruption is receptor-specific and hence no significant increase in AC activity was observed with Fsk in the presence of MβCD (DiPilato and Zhang, 2009). The fact that MβCD, by itself, did not affect basal cAMP levels under our conditions suggest that an activation of the receptor is required in order to see an enhancement in the AC activity, which could explain why we did not observe any enhancement in AC with Fsk as opposed to PGI_2. Although this is consistent with a report published by Allen *et al* (Allen *et al*., 2009), it is in disagreement with another report by Pontier, where they showed a significant increase in basal AC activity in response to cholesterol depletion by cyclodextrins (Pontier *et al*., 2008). Therefore, our data suggest that the effect of cholesterol depletion on AC activity in platelets is specific to the IP receptor. But, the mechanism by which lipid raft disruption enhances Fsk-mediated platelet inhibition still requires further investigation.

We also observed similar effects on AC activity when the cytoskeleton was disrupted with cytochalasin D (Figure 5.9), an effect that was consistent with work published by Head *et al* (Head *et al*., 2006). This effect on AC activity, however, was less pronounced when compared with that observed when platelet lipid rafts were disrupted by MβCD. And unlike the MβCD data, the potentiation effect was wiped out in the presence of milrinone. We also observed no effect on AC activity when Fsk was used in the presence cytochalsin D. This is consistent with Head's report, who also showed no significant increase in cAMP synthesis in response to Fsk in the presence of cytochalasin D unlike isoproterenol, which acts through the βAR (Head *et al*., 2006).

The enhanced PGI_2-induced AC activity mediated by cholesterol depletion was accompanied by a robust potentiation in PKA-mediated signalling events as represented by the phosphorylation of PKA substrate profile and $VASP^{ser157}$ (Figure 5.6). The effect of the cytoskeleton disruption on PKA signalling events however, was only observed with phosphorylated $VASP^{ser157}$ and was less profound than that observed with lipid raft disruption (Figure 5.10). The increased PKA activity as a result of MβCD treatment was reported before by Calaghan and colleagues, where the phosphorylation of two PKA substrates, phospholamban (PLB) and troponin I (TnI), in cardiomyocytes was enhanced as a result of treatment with MβCD (Calaghan *et al*., 2008). Another report addressing the effect of cholesterol depletion on PKA activity was published by Depry and colleagues where PKA activity was measured by Fluorescence Resonance Energy Transfer (FRET) techniques in

HEK293 cells was found to be enhanced in response to lipid raft disruption (Depry *et al*., 2011).

We confirmed throughout this study that disruption of platelet lipid raft with MβCD enhances the sensitivity of platelets to PGI_2 which was evident with aggregation, AC activity and PKA phosphorylation events. We then wanted to further explore the mechanism underlying all these interesting observations. Therefore, in the first instance the localisation of the IP receptor, $G\alpha_s$ and AC in relation to lipid rafts was determined. The lack of reports about specific AC isoforms in platelets in addition to the ubiquitousness of AC5 and AC6 (Willoughby and Cooper, 2007) and their established localisation in rafts (Ostrom *et al*., 2002, Ostrom *et al*., 2000), were the reasons why we chose to investigate the localisation of AC5/6 over other AC isoforms. The unreliability of commercially available AC antibodies has been a major issue that hindered numerous efforts in the AC field and resulted in numerous contradictory findings regarding the distribution of AC isoforms, expression levels and cellular localisation (Hanoune and Defer, 2001, Willoughby and Cooper, 2007, Liu *et al*., 2008). Under our conditions, we observed a band at about 140kDa along with several nonspecific bands when the AC antibody was used at a dilution of 1:200 (Figure 5.12). The nonspecificity issue and the need of using a high concentration of the same antibody have been addressed by Liu *et al* (Liu *et al*., 2008). We managed to reduce the number of nonspecific bands significantly when membranes were blocked and washed with 5% (w/v) nonfat dry milk in TBS-T.

The inability of commercially available IP receptor antibodies to recognise endogenous IP receptor has also been reported (Liu *et al*., 2008). Therefore, in this study we used a non-commercial antibody that was a gift from Dr. Luccie Clapp. By using this antibody we identified a band at 53kDa (Figure 5.13) that was similar to the one reported by Clapp *et al* (Falcetti *et al*., 2010).

Consistent with numerous reports in other cell types (Ostrom *et al*., 2002, Liu *et al*., 2008, Head *et al*., 2006), we observed a pool of AC5/6 in platelet lipid rafts and another pool in nonraft fractions. However, we were unable to detect any $G\alpha_s$ in platelet lipid rafts unlike what has been reported in last two reports referenced above. Furthermore, the IP receptor was also absent from these membrane domains under our conditions. This is in disagreement with Liu's report where they suggest the presence of a small pool of IP receptor in lipid rafts. However, these experiments were performed on exogenous hIP receptor expressed in COS-7 cells. Our findings about the absence of IP receptor from lipid rafts are consistent with reports confirming the absence of other prostanoid receptors from lipid rafts (Ostrom *et al*., 2002). Further work using different antibodies is required to confirm these observations.

Preliminary data showed dynamic properties for the raft-residing AC5/6 as lower levels were noticed in rafts upon IP receptor stimulation with high concentration of PGI_2. Our data does not explain the functional significance of this movement. But data in other cell types report the existence of functional AC6 homodimers as well as AC2 and 5 heterodimers (Ding *et al*., 2005, Baragli *et al*., 2008). Another possible

explanation would be the need of deploying more AC into nonraft membrane domains, where we exclusively found the IP receptor and $G\alpha_s$ proteins, in order to help producing more cAMP when it is required. It is possible that disruption of lipid rafts with MβCD helps mimic this scenario (Figure 5.15).

The involvement of other AC isoforms such as AC3 in the observations reported in this chapter will be the focus of future work. This is supported by reports showing its exclusive localisation in lipid rafts in other cell types (Ostrom *et al*., 2002, Liu *et al*., 2008) and its predominance over other AC isoforms as found in platelet trancriptosomes (Rowley *et al*., 2011). Also remains to be established is the mechanism by which cytochalasin D potentiates the inhibitory effect of PGI_2 on platelet activity.

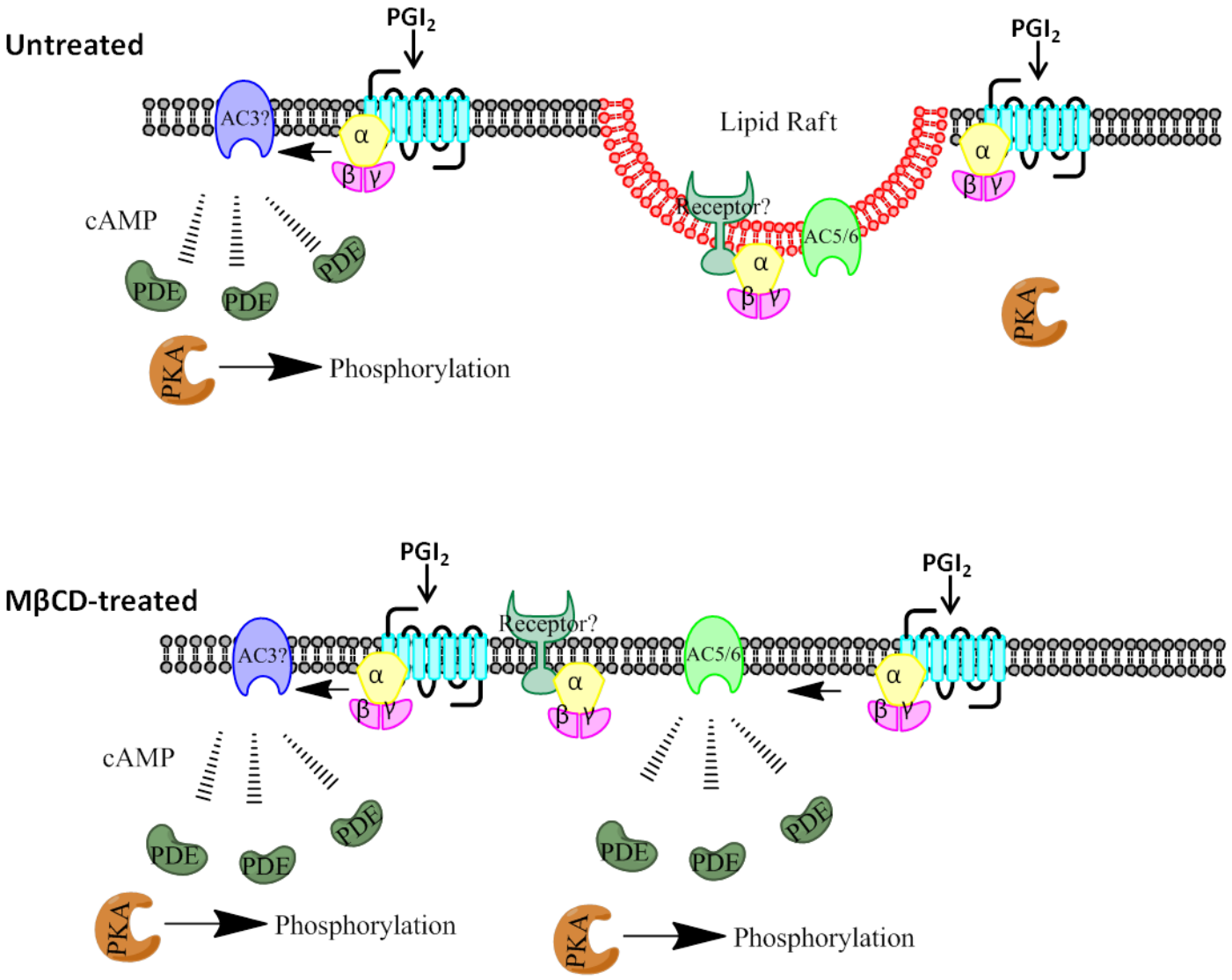

Figure 5. 15: A schematic figure showing a model of the effect of lipid raft disruption on cAMP/PKA signaling in blood platelets.

Chapter 6: Conclusions and future directions

Understanding the molecular basis of the cAMP/PKA signalling pathway has great potential to the development of new therapeutic approaches for the treatment of Arterial thrombosis. Patients with cardiovascular diseases have shown diminished responsiveness to PGI_2 leading to platelet hyperactivity (Mueller *et al*., 1986). Furthermore, the great potential of prostacyclin analogues, as vasodilators and antiplatelet agents, has been hampered by issues, such as bioavailability and receptor desensitisation (2000, Vane and Corin, 2003). Therefore, the dissection of the cAMP/PKA signalling cascade in blood platelets and in VSMCs could be of great clinical potential as it will help identifying novel therapeutic strategies that can more effectively target this pathway and oppose thrombosis.

The aim of this project was to identify new mechanisms that regulate cAMP and PKA signalling networks in blood platelets. We shed a light on the spatiotemporal regulation of the cAMP/PKA signalling pathway both at the level of cAMP production (signal initiation) and PKA activity (signal propagation). The experimental data suggest the presence of two mechanisms for spatiotemporal regulation of cAMP signalling in blood platelets. Critical to both of these mechanisms are membrane lipid rafts, which might work as physical barriers that sequester a population of AC5/6 regulating signal initiation, and at the same time are targets for PKA anchoring by A-kinase anchoring proteins (AKAPs), which aids signal propagation. It is possible that these mechanisms are actually integrated although there is currently insufficient data to make this conclusion.

In other cell types, it has been established that the spatiotemporal regulation of the cAMP/PKA signalling cascade takes place at both the lateral and the medial part of the cell with both parts being compartmentalised into distinct domains (Willoughby and Cooper, 2007, Pidoux and Tasken, 2010, Stangherlin and Zaccolo, 2012). This system helps isolate distinct cAMP signalling networks which, even if triggered simultaneously, can mediate distinct biological responses depending on the stimuli. In this project our hypothesis postulates the presence of multiple spatiotemporal regulatory mechanisms of cAMP/PKA signalling in platelets.

Platelets contain several isoforms of AC, although the role of these individual isoforms is unclear. To begin to investigate this we concentrated on AC6 as a ubiquitously expressed AC form of the enzyme. The loss of AC6 leads to reduced PKA activity in murine platelets (Aburima and Naseem – unpublished observations), suggesting its importance to platelet function. We provide evidence that platelet lipid rafts play a restraining role in cAMP/PKA signalling cascade triggered by PGI_2. We report for the first time that disruption of lipid rafts by MβCD enhances the inhibitory effect of PGI_2 and Fsk on platelet aggregation (Figure 5.3 and 5.4). This effect was the outcome of enhanced cAMP production and downstream PKA activity. We attribute this restraining effect of platelet lipid raft to a physical sequestration of a population of AC5/6 such that it is physically delocalised from the IP receptor and $G\alpha_s$ thereby controlling cAMP production (Figure 5.15). Our findings that lipid raft disruption enhances cAMP/PKA signalling are novel in platelets and are in agreement with those reported by others in other cell types (Pontier *et al*., 2008, Agarwal *et al*., 2011). In their report, Pontier and colleagues,

suggest that a pool of both AC6 and $G\alpha_s$ is sequestered in HEK293 lipid rafts away from the β_2AR. Agarwal, on the other hand, suggest a different mechanism, where a subpopulation of not only $G\alpha_s$ and AC but also the β_1AR receptor are all in rafts but the cAMP signal generated from their interaction is contained within these microdomains.

Disruption of the cytoskeleton, which is also thought to be important to lipid raft architecture, with cytochalasin D also increased platelet sensitivity to PGI_2 although to a lesser degree than observed after lipid raft disruption. To some degree these findings are consistent with the observations of Head and colleagues, who observed that cytoskeleton plays an important role cardiomyocytes by maintaining the integrity of lipid rafts. The loss of cytoskeleton integrity increased cAMP signalling by allowing unrestrained interaction between AC6 and the β-adrenergic receptor (Head *et al*., 2006). The complex interactions of IP, $G\alpha_s$ and AC6 in rafts require a more detailed characterisation.

The role of PDE in the compartmentalisation of cAMP signalling was not investigated during this project. However, one of the interesting observations was that PGI_2, (physiological AC agonist) can achieve the same level of inhibition of platelet aggregation as Fsk (nonphysiological AC agonist) with lower cAMP concentrations. We speculate that PGI_2 triggers its cAMP signal through a specific network, potentially through specific AC isoforms, that is efficiently directed towards effective targets that are important to platelet activity. In contrast, Fsk is a global activator of AC and therefore may produce a more diffuse pattern of cAMP

synthesis in the platelet. This lack of localised response may require more cAMP to be produced globally to target substrates that are required for platelets inhibition. More work need to be done to validate this possibility, potentially through isoform specific AC knockout mice. We observed a unique temporal pattern for PKA activity in response to PGI_2, compared to Fsk, when investigated by an antibody that can recognise multiple PKA substrates. Such an observation might be attributable to the presence of a fine temporal regulation mechanism of PDE activity in platelets. The compartmentalisation of cAMP pools in cardiomyocytes has been the main focus of Zaccolo and colleagues for about a decade and a significant progress has been achieved and helped improve our understanding of the wider context of cAMP compartmentalisation. By using FRET techniques this group managed to dissect the individual contribution of specific PDEs in shaping gradients of distinct cAMP pools. These pools inhibit the free diffusion of cAMP and help ensuring the specificity of a cAMP signal generated by a specific stimulus (Zaccolo, 2011). Data from cardiomyocytes suggested a small PDE2A activity (1% of total PDE activity) is present near the plasma membrane (Mongillo *et al*., 2006) whereas PDE3A activity was suggested to be more widespread and localised intracellularly on internal membranes (Mongillo *et al*., 2004). Since these two PDE isoforms are expressed in platelets, it is very tempting to speculate that similar mechanisms occur in platelets. Manns and colleagues observed that PDE2 inhibition caused a greater increase in cAMP levels when compared with the inhibition of PDE3, but only the inhibition of PDE3 enhanced the phosphorylation of $VASP^{157}$ (Manns *et al*., 2002). This might suggest that, by an unknown mechanism, VASP could be localised with PKA and

PDE3 in one distinct cellular compartment. A similar theory was postulated by Jensen and colleagues as they provided strong evidence that NO-induced inhibition of platelet shape change is mediated by blocking PDE3, but not PDE2 (Jensen *et al*., 2004). From their data, they speculate that by inhibiting PDE3, cGMP raises cAMP levels in a distinct compartment where PKA and VASP colocalise (Jensen *et al*., 2004) and is in agreement with data obtained from cardiac myocytes using FRET. It is possible that cGMP production enhances PDE2 activity in a PKA II-containing compartment but blocks PDE3 activity in a PKA I-containing compartment (Stangherlin *et al*., 2011). The assignment of a specific PDE isoform to a specific PKA isoform is yet to be reported in platelets, but is an attractive area of research.

It is clear from data presented in this thesis and the work of others that multiple PKA isoforms exist in platelets. Until now the locations, activity and molecular control of these isozymes have remained elusive. We, here, provide strong evidence that PKA isoforms have non-redundant roles and that their differential activity in platelets is spatially and temporally regulated by A-kinase anchoring proteins (AKAPs). Our evidence can be supported by both early and recent reports by others. El-Daher and colleagues reported that PKA substrates are differentially distributed in platelets and hence PKA activity is present in different subcellular compartments (El-Daher *et al*., 1996). However, these reports did not address the mechanism of PKA localisation or the specific localisation of an individual isoform to these domains. To the best of our knowledge, the differential contribution of PKA isoforms in platelet inhibition is unidentified. Experimental evidence from this project indicates that PKA isoforms are differentially localised to platelet lipid rafts

where PKA II is excluded under both basal and PGI_2-stimulating conditions whereas a population of PKA I is recruited. Moreover, our data suggest that PKA isoforms may have specific substrates since a population of GPIbβ, a well-established PKA target in platelets, is specifically targeted by PKA I, but not PKA II, in platelet lipid rafts in an AKAP-dependent manner. Further we have shown that such an event is important for the optimal inhibitory effect of PGI_2 on platelets as determined by vWF-mediated platelet aggregation and adhesion to vWF under flow. A similar scenario has been suggested in T-cells where the AKAP ezrin has been shown to mediate the redistribution of PKA I into lipid rafts where it phosphorylates C-terminal Src kinase (Csk); an event that is required for optimal inhibition of T-cell activation (Ruppelt *et al*., 2007). Although we have not identified a specific AKAP in platelets mediating this effect, we have evidence of the presence of three AKAPs (Raslan, Tasken and Naseem – unpublished observations). This is consistent with recent work published by Rowley and colleagues who reported the presence of significant RNA levels of many AKAPs in platelet trancriptomes (Rowley *et al*., 2011). Furthermore, chemical proteomic studies undertaken by Margarucci and colleagues reported the potential presence of cAMP scaffolds in platelets. Within these scaffolds they identified multiple AKAPs most of which are consistent with those reported by Rowley in platelet transcriptomes (Margarucci *et al*., 2011).

Herein, we provide strong evidence that at least two spatial regulatory mechanisms simultaneously govern cAMP/PKA signalling in platelets. We suggest that the signal starts from the IP receptor and $G\alpha_s$, which activates unknown isoforms of AC that have been made available by exclusion from lipid rafts. We then postulate that PKA

target different substrates in different subcellular compartments in an isoform- and AKAP-dependent manner. We identified platelet lipid raft as one of those compartments PKA I redistributes to, and GPIbβ as a PKA I-specific target residing in that compartment. This happens in response to platelet stimulation with PGI_2 and in a mechanism dependent on an interaction between PKA I and an unknown AKAP (Figure 6.1).

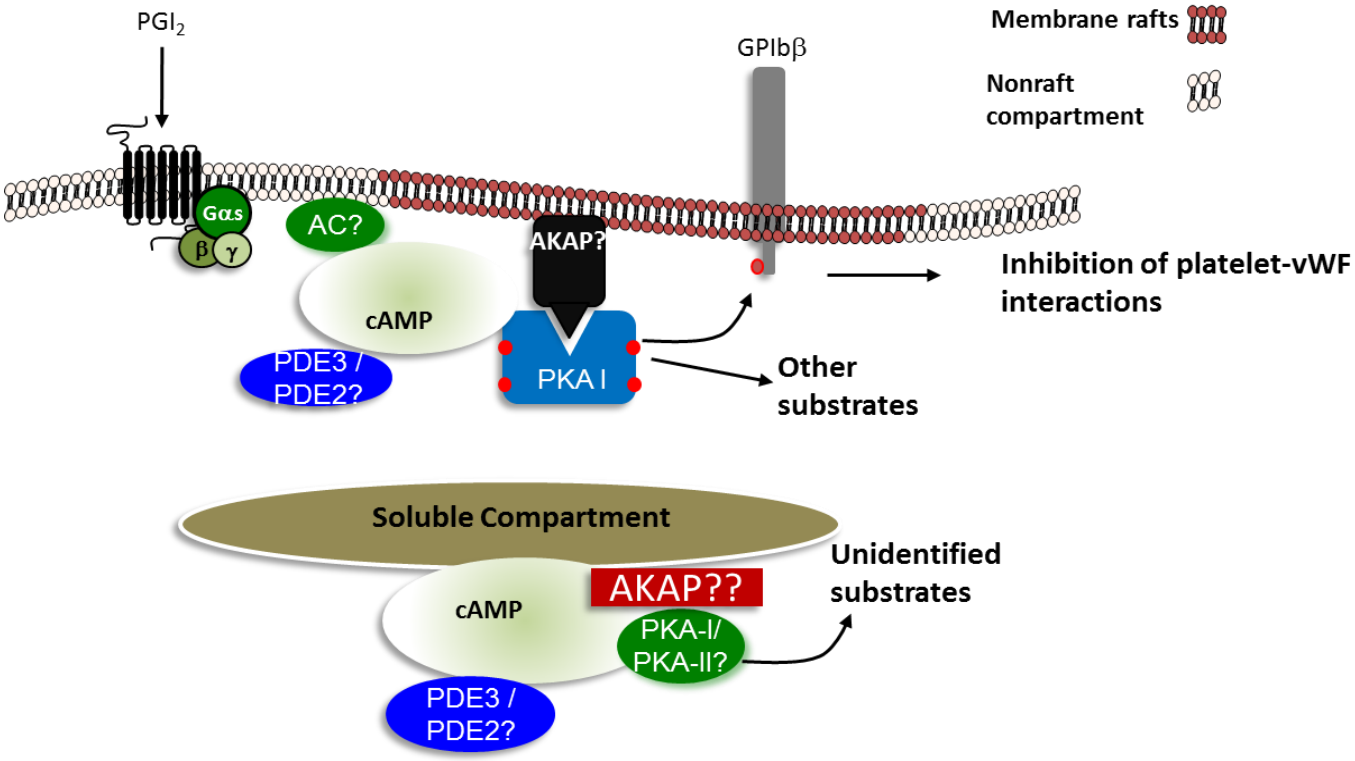

Figure 6. 1: A revised model of cAMP signalling in platelets as established by findings presented in this study.

PGI_2 binds the IP receptor activating an unknown isoform of AC. With the help of unidentified and compartmentelised PDEs, cAMP is subsequently formed in specific subcellular compartments activating either PKA I or PKA II and phosphorylating substrates residing in that compartment. In this study, lipid rafts were identified as one of these compartments, where only PKA I was found to be localised in an AKAP-dependent manner. AKAP-tethered PKA I Phosphorylates GPIbβ, which resides in the same compartment along with other unidentified substrates. The AKAP-dependent PKA I phosphorylation of GPIbβ in platelet lipid rafts regulates a specific biological function that is vWF-mediated platelet activation. More work is still needed to identify the other compartments and their components.

Future work

Our understanding of cAMP signalling in platelets is still in its infancy and significantly more work is required to understand these processes. While this study has provided a small insight into potential compartmentalisation of AC isoforms, clear questions still remain including:

- To determine whether other AC isoforms reside in lipid rafts such as AC3.
- To verify Rowley's findings which suggest the expression of AC isoform 3, 6 and 7 in platelets (Rowley *et al*., 2011) and determine the differential contribution to platelet inhibition by different cAMP elevating agents.
- To clarify the role of lipid raft in the localisation of AC5/6 and its regulators.
- To investigate whether compartmentalisation of PDEs plays a role in shaping cAMP gradients in platelets.

There is also a considerable amount of knowledge to be gained in the understanding of how different PKA isoforms are regulated in platelets. Using peptide disruptors of AKAP-PKA interactions as a tool to partially differentiate the role of these isoforms was successful to some degree by showing non-redundant actions. Using RIAD-Arg_{11} we tested the hypothesis that is redistribution of PKA I to lipid rafts is critical for PGI_2-mediated inhibition of platelet activation through phosphorylation of GPIbβ. However, at this point the identification of the AKAP(s) responsible remains elusive. Furthermore, the contribution of both anchored and

nonanchored PKA II to platelet inhibition by PGI_2 needs to be dissected. This may be achieved using the other AKAP-PKA II specific disruptor superAKAP-*IS* (Gold *et al*., 2006).

Having provided strong evidence that AKAP-PKA interactions are important to optimally inhibit platelets by various cAMP-elevating agents, the next step must be aimed towards the identification of individual AKAPs in platelets. Many approaches can be employed to achieve this aim.

1. **RI/RII overlay assay.** This simple far Western blotting method is a well-established procedure that has been routinely used in other cell types to identify potential AKAPs (Carr and Scott, 1992). It depends on the fact that AKAPs retain their ability to bind recombinant RI or RII after transfer to nitrocellulose membrane under denaturing conditions.
2. **Affinity chromatography and mass spectrometry**. Platelet whole cell lysate will be passed through cAMP-agarose columns, which after elution with RIAD or SuperAKAP-*IS* will be analysed by mass spectrometry to identify potential AKAPs.
3. **Immunoprecipitation of both PKA isoforms**. This will be followed by mass spectrometrical analysis of the coimmunoprecipitated proteins. This approach can also be utilised to identify other AKAP binding proteins.

AKAPs are multienzyme scaffolding proteins, which not only anchor PKA but also bind other proteins such as PKC, PDE and some phosphatases forming macromolecules that can regulate specific cellular functions (Tasken and Aandahl,

2004, Pidoux and Tasken, 2010). The presence of such macromolecules and their functional relevance will be determined with the help of mass spectrometry-based techniques.

MEG-01 cell line will be used to implement powerful molecular biology techniques such as gene silencing in order to confirm all findings obtained from platelets.

References

2000. Two randomised and placebo-controlled studies of an oral prostacyclin analogue (Iloprost) in severe leg ischaemia. The Oral Iloprost in severe Leg Ischaemia Study Group. *European journal of vascular and endovascular surgery : the official journal of the European Society for Vascular Surgery,* 20**,** 358-62.

AGARWAL, S. R., MACDOUGALL, D. A., TYSER, R., PUGH, S. D., CALAGHAN, S. C. & HARVEY, R. D. 2011. Effects of cholesterol depletion on compartmentalized cAMP responses in adult cardiac myocytes. *J Mol Cell Cardiol,* 50**,** 500-9.

AKTAS, B., HONIG-LIEDL, P., WALTER, U. & GEIGER, J. 2002. Inhibition of platelet P2Y12 and alpha2A receptor signaling by cGMP-dependent protein kinase. *Biochem Pharmacol,* 64**,** 433-9.

ALLEN, J. A., YU, J. Z., DAVE, R. H., BHATNAGAR, A., ROTH, B. L. & RASENICK, M. M. 2009. Caveolin-1 and lipid microdomains regulate Gs trafficking and attenuate Gs/adenylyl cyclase signaling. *Mol Pharmacol,* 76**,** 1082-93.

ALTSCHULER, D. & LAPETINA, E. G. 1993. Mutational analysis of the cAMP-dependent protein kinase-mediated phosphorylation site of Rap1b. *J Biol Chem,* 268**,** 7527-31.

AMUNDSON, D. M. & ZHOU, M. 1999. Fluorometric method for the enzymatic determination of cholesterol. *J Biochem Biophys Methods,* 38**,** 43-52.

ANDREWS, R. K. & BERNDT, M. C. 2008. Platelet adhesion: a game of catch and release. *J Clin Invest,* 118**,** 3009-11.

ANJA RUPPELT, N. G. O., GEORGE MAGKLARAS AND KJETIL TASKEN 2010. Physiological Substrates of PKA and PKG. *In:* DENNIS, R. A. B. A. E. A. (ed.) *Handbook of Cell Signalling.* 2 ed.

ANTL, M., VON BRUHL, M. L., EIGLSPERGER, C., WERNER, M., KONRAD, I., KOCHER, T., WILM, M., HOFMANN, F., MASSBERG, S. & SCHLOSSMANN, J. 2007. IRAG mediates NO/cGMP-dependent inhibition of platelet aggregation and thrombus formation. *Blood,* 109**,** 552-9.

ARMSTRONG, R. A. 1996. Platelet prostanoid receptors. *Pharmacol Ther,* 72**,** 171-91.

ARMSTRONG, R. A., LAWRENCE, R. A., JONES, R. L., WILSON, N. H. & COLLIER, A. 1989. Functional and ligand binding studies suggest heterogeneity of platelet prostacyclin receptors. *British journal of pharmacology,* 97**,** 657-68.

BARAGLI, A., GRIECO, M. L., TRIEU, P., VILLENEUVE, L. R. & HEBERT, T. E. 2008. Heterodimers of adenylyl cyclases 2 and 5 show enhanced functional responses in the presence of Galpha s. *Cell Signal,* 20**,** 480-92.

BARRY, F. A. & GIBBINS, J. M. 2002. Protein kinase B is regulated in platelets by the collagen receptor glycoprotein VI. *J Biol Chem,* 277**,** 12874-8.

BARRY, O. P., KAZANIETZ, M. G., PRATICO, D. & FITZGERALD, G. A. 1999. Arachidonic acid in platelet microparticles up-regulates cyclooxygenase-2-dependent prostaglandin formation via a protein kinase C/mitogen-activated protein kinase-dependent pathway. *The Journal of biological chemistry,* 274**,** 7545-56.

BELLUCCI, S. & CAEN, J. 2002. Molecular basis of Glanzmann's Thrombasthenia and current strategies in treatment. *Blood Rev,* 16**,** 193-202.

BITON, S. & ASHKENAZI, A. 2011. NEMO and RIP1 control cell fate in response to extensive DNA damage via TNF-alpha feedforward signaling. *Cell,* 145**,** 92-103.

BLAIR, I. A., BARROW, S. E., WADDELL, K. A., LEWIS, P. J. & DOLLERY, C. T. 1982. Prostacyclin is not a circulating hormone in man. *Prostaglandins,* 23**,** 579-89.

BODIN, S., TRONCHERE, H. & PAYRASTRE, B. 2003. Lipid rafts are critical membrane domains in blood platelet activation processes. *Biochim Biophys Acta,* 1610**,** 247-57.

BODNAR, R. J., XI, X., LI, Z., BERNDT, M. C. & DU, X. 2002. Regulation of glycoprotein Ib-IX-von Willebrand factor interaction by cAMP-dependent protein kinase-mediated phosphorylation at Ser 166 of glycoprotein Ib(beta). *J Biol Chem,* 277**,** 47080-7.

BOIE, Y., RUSHMORE, T. H., DARMON-GOODWIN, A., GRYGORCZYK, R., SLIPETZ, D. M., METTERS, K. M. & ABRAMOVITZ, M. 1994. Cloning and expression of a cDNA for the human prostanoid IP receptor. *The Journal of biological chemistry,* 269**,** 12173-8.

BORN, G. V. 1962. Aggregation of blood platelets by adenosine diphosphate and its reversal. *Nature,* 194**,** 927-9.

BRASS, L. F. 2003. Thrombin and platelet activation. *Chest,* 124**,** 18S-25S.

BRASS, L. F., ZHU, L. & STALKER, T. J. 2005. Minding the gaps to promote thrombus growth and stability. *J Clin Invest,* 115**,** 3385-92.

BRIDDON, S. J. & WATSON, S. P. 1999. Evidence for the involvement of p59fyn and p53/56lyn in collagen receptor signalling in human platelets. *Biochem J,* 338 (Pt 1)**,** 203-9.

BRILL, A., FUCHS, T. A., CHAUHAN, A. K., YANG, J. J., DE MEYER, S. F., KOLLNBERGER, M., WAKEFIELD, T. W., LAMMLE, B., MASSBERG, S. & WAGNER, D. D. 2011. von Willebrand factor-mediated platelet adhesion is critical for deep vein thrombosis in mouse models. *Blood,* 117**,** 1400-7.

BROOS, K., FEYS, H. B., DE MEYER, S. F., VANHOORELBEKE, K. & DECKMYN, H. 2011. Platelets at work in primary hemostasis. *Blood Rev,* 25**,** 155-67.

BRUCKDORFER, R. 2005. The basics about nitric oxide. *Mol Aspects Med,* 26**,** 3-31.

BRUNTON, L. L., HAYES, J. S. & MAYER, S. E. 1981. Functional compartmentation of cyclic AMP and protein kinase in heart. *Adv Cyclic Nucleotide Res,* 14**,** 391-7.

BUTT, E., ABEL, K., KRIEGER, M., PALM, D., HOPPE, V., HOPPE, J. & WALTER, U. 1994. cAMP- and cGMP-dependent protein kinase phosphorylation sites of the focal adhesion vasodilator-stimulated phosphoprotein (VASP) in vitro and in intact human platelets. *J Biol Chem,* 269**,** 14509-17.

BUTT, E., GAMBARYAN, S., GOTTFERT, N., GALLER, A., MARCUS, K. & MEYER, H. E. 2003. Actin binding of human LIM and SH3 protein is regulated by cGMP- and cAMP-dependent protein kinase phosphorylation on serine 146. *J Biol Chem,* 278**,** 15601-7.

BUTT, E., IMMLER, D., MEYER, H. E., KOTLYAROV, A., LAASS, K. & GAESTEL, M. 2001. Heat shock protein 27 is a substrate of cGMP-dependent protein kinase in

intact human platelets: phosphorylation-induced actin polymerization caused by HSP27 mutants. *J Biol Chem,* 276**,** 7108-13.

BUXTON, I. L. & BRUNTON, L. L. 1986. Compartmentation of hormone action in adult mammalian cardiomyocytes. *Adv Exp Med Biol,* 194**,** 117-27.

CADD, G. G., UHLER, M. D. & MCKNIGHT, G. S. 1990. Holoenzymes of cAMP-dependent protein kinase containing the neural form of type I regulatory subunit have an increased sensitivity to cyclic nucleotides. *The Journal of biological chemistry,* 265**,** 19502-6.

CALAGHAN, S., KOZERA, L. & WHITE, E. 2008. Compartmentalisation of cAMP-dependent signalling by caveolae in the adult cardiac myocyte. *J Mol Cell Cardiol,* 45**,** 88-92.

CANAVES, J. M. & TAYLOR, S. S. 2002. Classification and phylogenetic analysis of the cAMP-dependent protein kinase regulatory subunit family. *Journal of molecular evolution,* 54**,** 17-29.

CARLIER, M. F. 1993. Cytoskeleton: dynamic actin. *Curr Biol,* 3**,** 321-3.

CARLSON, C. R., LYGREN, B., BERGE, T., HOSHI, N., WONG, W., TASKEN, K. & SCOTT, J. D. 2006. Delineation of type I protein kinase A-selective signaling events using an RI anchoring disruptor. *J Biol Chem,* 281**,** 21535-45.

CARR, D. W. & SCOTT, J. D. 1992. Blotting and band-shifting: techniques for studying protein-protein interactions. *Trends Biochem Sci,* 17**,** 246-9.

CARR, D. W., STOFKO-HAHN, R. E., FRASER, I. D., BISHOP, S. M., ACOTT, T. S., BRENNAN, R. G. & SCOTT, J. D. 1991. Interaction of the regulatory subunit (RII) of cAMP-dependent protein kinase with RII-anchoring proteins occurs through an amphipathic helix binding motif. *J Biol Chem,* 266**,** 14188-92.

CAVALLINI, L., COASSIN, M., BOREAN, A. & ALEXANDRE, A. 1996. Prostacyclin and sodium nitroprusside inhibit the activity of the platelet inositol 1,4,5-trisphosphate receptor and promote its phosphorylation. *J Biol Chem,* 271**,** 5545-51.

CHANG, L. & GOLDMAN, R. D. 2004. Intermediate filaments mediate cytoskeletal crosstalk. *Nat Rev Mol Cell Biol,* 5**,** 601-13.

CHEN, D., BERNSTEIN, A. M., LEMONS, P. P. & WHITEHEART, S. W. 2000. Molecular mechanisms of platelet exocytosis: role of SNAP-23 and syntaxin 2 in dense core granule release. *Blood,* 95**,** 921-9.

CHEN, M. & STRACHER, A. 1989. In situ phosphorylation of platelet actin-binding protein by cAMP-dependent protein kinase stabilizes it against proteolysis by calpain. *J Biol Chem,* 264**,** 14282-9.

CHINI, B. & PARENTI, M. 2004. G-protein coupled receptors in lipid rafts and caveolae: how, when and why do they go there? *J Mol Endocrinol,* 32**,** 325-38.

CHIRKOV, Y. Y. & HOROWITZ, J. D. 2007. Impaired tissue responsiveness to organic nitrates and nitric oxide: a new therapeutic frontier? *Pharmacol Ther,* 116**,** 287-305.

CHRISTENSEN, A. E., SELHEIM, F., DE ROOIJ, J., DREMIER, S., SCHWEDE, F., DAO, K. K., MARTINEZ, A., MAENHAUT, C., BOS, J. L., GENIESER, H. G. & DOSKELAND, S. O. 2003. cAMP analog mapping of Epac1 and cAMP kinase. Discriminating

analogs demonstrate that Epac and cAMP kinase act synergistically to promote PC-12 cell neurite extension. *J Biol Chem,* 278**,** 35394-402.

COGHLAN, V. M., PERRINO, B. A., HOWARD, M., LANGEBERG, L. K., HICKS, J. B., GALLATIN, W. M. & SCOTT, J. D. 1995. Association of protein kinase A and protein phosphatase 2B with a common anchoring protein. *Science,* 267**,** 108-11.

COOPER, D. M. & CROSSTHWAITE, A. J. 2006. Higher-order organization and regulation of adenylyl cyclases. *Trends in pharmacological sciences,* 27**,** 426-31.

CORBIN, J. D., KEELY, S. L. & PARK, C. R. 1975a. The distribution and dissociation of cyclic adenosine 3':5'-monophosphate-dependent protein kinases in adipose, cardiac, and other tissues. *J Biol Chem,* 250**,** 218-25.

CORBIN, J. D., KEELY, S. L. & PARK, C. R. 1975b. The distribution and dissociation of cyclic adenosine 3':5'-monophosphate-dependent protein kinases in adipose, cardiac, and other tissues. *The Journal of biological chemistry,* 250**,** 218-25.

DANIEL, J. L., MOLISH, I. R., RIGMAIDEN, M. & STEWART, G. 1984. Evidence for a role of myosin phosphorylation in the initiation of the platelet shape change response. *J Biol Chem,* 259**,** 9826-31.

DANIELEWSKI, O., SCHULTESS, J. & SMOLENSKI, A. 2005. The NO/cGMP pathway inhibits Rap 1 activation in human platelets via cGMP-dependent protein kinase I. *Thromb Haemost,* 93**,** 319-25.

DE MEYER, S. F., DECKMYN, H. & VANHOORELBEKE, K. 2009. von Willebrand factor to the rescue. *Blood,* 113**,** 5049-57.

DE NUCCI, G., GRYGLEWSKI, R. J., WARNER, T. D. & VANE, J. R. 1988. Receptor-mediated release of endothelium-derived relaxing factor and prostacyclin from bovine aortic endothelial cells is coupled. *Proc Natl Acad Sci U S A,* 85**,** 2334-8.

DE ROOIJ, J., ZWARTKRUIS, F. J., VERHEIJEN, M. H., COOL, R. H., NIJMAN, S. M., WITTINGHOFER, A. & BOS, J. L. 1998. Epac is a Rap1 guanine-nucleotide-exchange factor directly activated by cyclic AMP. *Nature,* 396**,** 474-7.

DE WIT, R. J., HEKSTRA, D., JASTORFF, B., STEC, W. J., BARANIAK, J., VAN DRIEL, R. & VAN HAASTERT, P. J. 1984. Inhibitory action of certain cyclophosphate derivatives of cAMP on cAMP-dependent protein kinases. *Eur J Biochem,* 142**,** 255-60.

DEGERMAN, E., BELFRAGE, P. & MANGANIELLO, V. C. 1997. Structure, localization, and regulation of cGMP-inhibited phosphodiesterase (PDE3). *J Biol Chem,* 272**,** 6823-6.

DENIS, C., METHIA, N., FRENETTE, P. S., RAYBURN, H., ULLMAN-CULLERE, M., HYNES, R. O. & WAGNER, D. D. 1998. A mouse model of severe von Willebrand disease: defects in hemostasis and thrombosis. *Proc Natl Acad Sci U S A,* 95**,** 9524-9.

DEPRY, C., ALLEN, M. D. & ZHANG, J. 2011. Visualization of PKA activity in plasma membrane microdomains. *Mol Biosyst,* 7**,** 52-8.

DEUTSCH, V. R. & TOMER, A. 2006. Megakaryocyte development and platelet production. *Br J Haematol,* 134**,** 453-66.

DHANJAL, T. S., ROSS, E. A., AUGER, J. M., MCCARTY, O. J., HUGHES, C. E., SENIS, Y. A., BUCKLEY, C. D. & WATSON, S. P. 2007. Minimal regulation of platelet activity by PECAM-1. *Platelets,* 18**,** 56-67.

DI BENEDETTO, G., ZOCCARATO, A., LISSANDRON, V., TERRIN, A., LI, X., HOUSLAY, M. D., BAILLIE, G. S. & ZACCOLO, M. 2008. Protein kinase A type I and type II define distinct intracellular signaling compartments. *Circ Res,* 103**,** 836-44.

DICKINSON, N. T., JANG, E. K. & HASLAM, R. J. 1997. Activation of cGMP-stimulated phosphodiesterase by nitroprusside limits cAMP accumulation in human platelets: effects on platelet aggregation. *Biochem J,* 323 (Pt 2)**,** 371-7.

DING, Q., GROS, R., CHORAZYCZEWSKI, J., FERGUSON, S. S. & FELDMAN, R. D. 2005. Isoform-specific regulation of adenylyl cyclase function by disruption of membrane trafficking. *Mol Pharmacol,* 67**,** 564-71.

DIPILATO, L. M. & ZHANG, J. 2009. The role of membrane microdomains in shaping beta2-adrenergic receptor-mediated cAMP dynamics. *Mol Biosyst,* 5**,** 832-7.

DISKAR, M., ZENN, H. M., KAUPISCH, A., PRINZ, A. & HERBERG, F. W. 2007. Molecular basis for isoform-specific autoregulation of protein kinase A. *Cellular signalling,* 19**,** 2024-34.

DODGE, K. L., KHOUANGSATHIENE, S., KAPILOFF, M. S., MOUTON, R., HILL, E. V., HOUSLAY, M. D., LANGEBERG, L. K. & SCOTT, J. D. 2001. mAKAP assembles a protein kinase A/PDE4 phosphodiesterase cAMP signaling module. *Embo J,* 20**,** 1921-30.

DORSAM, R. T. & KUNAPULI, S. P. 2004. Central role of the P2Y12 receptor in platelet activation. *J Clin Invest,* 113**,** 340-5.

DOSTMANN, W. R. & TAYLOR, S. S. 1991. Identifying the molecular switches that determine whether (Rp)-cAMPS functions as an antagonist or an agonist in the activation of cAMP-dependent protein kinase I. *Biochemistry,* 30**,** 8710-6.

DU, X. 2007. Signaling and regulation of the platelet glycoprotein Ib-IX-V complex. *Curr Opin Hematol,* 14**,** 262-9.

DUCHARDT, F., FOTIN-MLECZEK, M., SCHWARZ, H., FISCHER, R. & BROCK, R. 2007. A comprehensive model for the cellular uptake of cationic cell-penetrating peptides. *Traffic,* 8**,** 848-66.

DUNKERN, T. R. & HATZELMANN, A. 2005. The effect of Sildenafil on human platelet secretory function is controlled by a complex interplay between phosphodiesterases 2, 3 and 5. *Cellular signalling,* 17**,** 331-9.

DUSTING, G. J., MONCADA, S. & VANE, J. R. 1978. Disappearance of prostacyclin (PGI2) in the circulation of the dog [proceedings]. *Br J Pharmacol,* 62**,** 414P-415P.

DUTTA-ROY, A. K. & SINHA, A. K. 1987. Purification and properties of prostaglandin E1/prostacyclin receptor of human blood platelets. *J Biol Chem,* 262**,** 12685-91.

EL-DAHER, S. S., EIGENTHALER, M., WALTER, U., FURUICHI, T., MIYAWAKI, A., MIKOSHIBA, K., KAKKAR, V. V. & AUTHI, K. S. 1996. Distribution and activation of cAMP- and cGMP-dependent protein kinases in highly purified human platelet plasma and intracellular membranes. *Thromb Haemost,* 76**,** 1063-71.

EL-DAHER, S. S., PATEL, Y., SIDDIQUA, A., HASSOCK, S., EDMUNDS, S., MADDISON, B., PATEL, G., GOULDING, D., LUPU, F., WOJCIKIEWICZ, R. J. & AUTHI, K. S. 2000. Distinct localization and function of (1,4,5)IP(3) receptor subtypes and the (1,3,4,5)IP(4) receptor GAP1(IP4BP) in highly purified human platelet membranes. *Blood,* 95**,** 3412-22.

ENGH, R. A., GIROD, A., KINZEL, V., HUBER, R. & BOSSEMEYER, D. 1996. Crystal structures of catalytic subunit of cAMP-dependent protein kinase in complex with isoquinolinesulfonyl protein kinase inhibitors H7, H8, and H89. Structural implications for selectivity. *J Biol Chem,* 271**,** 26157-64.

FALCETTI, E., HALL, S. M., PHILLIPS, P. G., PATEL, J., MORRELL, N. W., HAWORTH, S. G. & CLAPP, L. H. 2010. Smooth muscle proliferation and role of the prostacyclin (IP) receptor in idiopathic pulmonary arterial hypertension. *Am J Respir Crit Care Med,* 182**,** 1161-70.

FARUQUE, O. M., LE-NGUYEN, D., LAJOIX, A. D., VIVES, E., PETIT, P., BATAILLE, D. & HANI EL, H. 2009. Cell-permeable peptide-based disruption of endogenous PKA-AKAP complexes: a tool for studying the molecular roles of AKAP-mediated PKA subcellular anchoring. *Am J Physiol Cell Physiol,* 296**,** C306-16.

FEIJGE, M. A., ANSINK, K., VANSCHOONBEEK, K. & HEEMSKERK, J. W. 2004. Control of platelet activation by cyclic AMP turnover and cyclic nucleotide phosphodiesterase type-3. *Biochem Pharmacol,* 67**,** 1559-67.

FEINMAN, R. D., LUBOWSKY, J., CHARO, I. & ZABINSKI, M. P. 1977. The lumi-aggregometer: a new instrument for simultaneous measurement of secretion and aggregation by platelets. *J Lab Clin Med,* 90**,** 125-9.

FEINSTEIN, M. B., EGAN, J. J., SHA'AFI, R. I. & WHITE, J. 1983. The cytoplasmic concentration of free calcium in platelets is controlled by stimulators of cyclic AMP production (PGD2, PGE1, forskolin). *Biochem Biophys Res Commun,* 113**,** 598-604.

FEINSTEIN, M. B. & FRASER, C. 1975. Human platelet secretion and aggregation induced by calcium ionophores. Inhibition by PGE1 and dibutyryl cyclic AMP. *J Gen Physiol,* 66**,** 561-81.

FERNANDEZ-CARNEADO, J., KOGAN, M. J., VAN MAU, N., PUJALS, S., LOPEZ-IGLESIAS, C., HEITZ, F. & GIRALT, E. 2005. Fatty acyl moieties: improving Pro-rich peptide uptake inside HeLa cells. *J Pept Res,* 65**,** 580-90.

FETALVERO, K. M., MARTIN, K. A. & HWA, J. 2007. Cardioprotective prostacyclin signaling in vascular smooth muscle. *Prostaglandins & other lipid mediators,* 82**,** 109-18.

FISCH, A., TOBUSCH, K., VEIT, K., MEYER, J. & DARIUS, H. 1997. Prostacyclin receptor desensitization is a reversible phenomenon in human platelets. *Circulation,* 96**,** 756-60.

FISHER, C. A., KAPPA, J. R., SINHA, A. K., COTTRELL, E. D., REISER, H. J. & ADDONIZIO, V. P. 1987. Comparison of equimolar concentrations of iloprost, prostacyclin, and prostaglandin E1 on human platelet function. *J Lab Clin Med,* 109**,** 184-90.

FLAUMENHAFT, R., CROCE, K., CHEN, E., FURIE, B. & FURIE, B. C. 1999. Proteins of the exocytotic core complex mediate platelet alpha-granule secretion. Roles

of vesicle-associated membrane protein, SNAP-23, and syntaxin 4. *J Biol Chem,* 274**,** 2492-501.

FOSTER, C. J., PROSSER, D. M., AGANS, J. M., ZHAI, Y., SMITH, M. D., LACHOWICZ, J. E., ZHANG, F. L., GUSTAFSON, E., MONSMA, F. J., JR., WIEKOWSKI, M. T., ABBONDANZO, S. J., COOK, D. N., BAYNE, M. L., LIRA, S. A. & CHINTALA, M. S. 2001. Molecular identification and characterization of the platelet ADP receptor targeted by thienopyridine antithrombotic drugs. *J Clin Invest,* 107**,** 1591-8.

FOX, J. E. 1985. Identification of actin-binding protein as the protein linking the membrane skeleton to glycoproteins on platelet plasma membranes. *The Journal of biological chemistry,* 260**,** 11970-7.

FOX, J. E., REYNOLDS, C. C. & JOHNSON, M. M. 1987. Identification of glycoprotein Ib beta as one of the major proteins phosphorylated during exposure of intact platelets to agents that activate cyclic AMP-dependent protein kinase. *J Biol Chem,* 262**,** 12627-31.

FRANGOS, J. A., ESKIN, S. G., MCINTIRE, L. V. & IVES, C. L. 1985. Flow effects on prostacyclin production by cultured human endothelial cells. *Science,* 227**,** 1477-9.

FURCHGOTT, R. F., CHERRY, P. D., ZAWADZKI, J. V. & JOTHIANANDAN, D. 1984. Endothelial cells as mediators of vasodilation of arteries. *J Cardiovasc Pharmacol,* 6 Suppl 2**,** S336-43.

FUTAKI, S., OHASHI, W., SUZUKI, T., NIWA, M., TANAKA, S., UEDA, K., HARASHIMA, H. & SUGIURA, Y. 2001. Stearylated arginine-rich peptides: a new class of transfection systems. *Bioconjug Chem,* 12**,** 1005-11.

GACHET, C., LEON, C. & HECHLER, B. 2006. The platelet P2 receptors in arterial thrombosis. *Blood Cells Mol Dis,* 36**,** 223-7.

GAMBARYAN, S., KOBSAR, A., RUKOYATKINA, N., HERTERICH, S., GEIGER, J., SMOLENSKI, A., LOHMANN, S. M. & WALTER, U. 2010. Thrombin and collagen induce a feedback inhibitory signaling pathway in platelets involving dissociation of the catalytic subunit of protein kinase A from an NFkappaB-IkappaB complex. *The Journal of biological chemistry,* 285**,** 18352-63.

GAMM, D. M., BAUDE, E. J. & UHLER, M. D. 1996. The major catalytic subunit isoforms of cAMP-dependent protein kinase have distinct biochemical properties in vitro and in vivo. *The Journal of biological chemistry,* 271**,** 15736-42.

GARCIA, A., KIM, S., BHAVARAJU, K., SCHOENWAELDER, S. M. & KUNAPULI, S. P. 2010. Role of phosphoinositide 3-kinase beta in platelet aggregation and thromboxane A2 generation mediated by Gi signalling pathways. *Biochem J,* 429**,** 369-77.

GEIGER, J., NOLTE, C., BUTT, E., SAGE, S. O. & WALTER, U. 1992. Role of cGMP and cGMP-dependent protein kinase in nitrovasodilator inhibition of agonist-evoked calcium elevation in human platelets. *Proc Natl Acad Sci U S A,* 89**,** 1031-5.

GIBBINS, J., ASSELIN, J., FARNDALE, R., BARNES, M., LAW, C. L. & WATSON, S. P. 1996. Tyrosine phosphorylation of the Fc receptor gamma-chain in collagen-stimulated platelets. *J Biol Chem,* 271**,** 18095-9.

GIBBINS, J. M. 2004a. Platelet adhesion signalling and the regulation of thrombus formation. *J Cell Sci,* 117**,** 3415-25.

GIBBINS, J. M. 2004b. *Platelets and megakaryocytes*, Springer.

GIBBINS, J. M., BRIDDON, S., SHUTES, A., VAN VUGT, M. J., VAN DE WINKEL, J. G., SAITO, T. & WATSON, S. P. 1998. The p85 subunit of phosphatidylinositol 3-kinase associates with the Fc receptor gamma-chain and linker for activitor of T cells (LAT) in platelets stimulated by collagen and convulxin. *J Biol Chem,* 273**,** 34437-43.

GIBBINS, J. M., OKUMA, M., FARNDALE, R., BARNES, M. & WATSON, S. P. 1997. Glycoprotein VI is the collagen receptor in platelets which underlies tyrosine phosphorylation of the Fc receptor gamma-chain. *FEBS Lett,* 413**,** 255-9.

GIOVANAZZI, S., ACCOMAZZO, M. R., LETARI, O., OLIVA, D. & NICOSIA, S. 1997. Internalization and down-regulation of the prostacyclin receptor in human platelets. *The Biochemical journal,* 325 (Pt 1)**,** 71-7.

GOLD, M. G., LYGREN, B., DOKURNO, P., HOSHI, N., MCCONNACHIE, G., TASKEN, K., CARLSON, C. R., SCOTT, J. D. & BARFORD, D. 2006. Molecular basis of AKAP specificity for PKA regulatory subunits. *Mol Cell,* 24**,** 383-95.

GOPALAKRISHNA, R., CHEN, Z. H. & GUNDIMEDA, U. 1993. Nitric oxide and nitric oxide-generating agents induce a reversible inactivation of protein kinase C activity and phorbol ester binding. *J Biol Chem,* 268**,** 27180-5.

GORMAN, R. R., BUNTING, S. & MILLER, O. V. 1977. Modulation of human platelet adenylate cyclase by prostacyclin (PGX). *Prostaglandins,* 13**,** 377-88.

GRABER, S. E. & HAWIGER, J. 1982. Evidence that changes in platelet cyclic AMP levels regulate the fibrinogen receptor on human platelets. *J Biol Chem,* 257**,** 14606-9.

GRANT, P. G., MANNARINO, A. F. & COLMAN, R. W. 1988. cAMP-mediated phosphorylation of the low-Km cAMP phosphodiesterase markedly stimulates its catalytic activity. *Proc Natl Acad Sci U S A,* 85**,** 9071-5.

GROSS, B. S., MELFORD, S. K. & WATSON, S. P. 1999. Evidence that phospholipase C-gamma2 interacts with SLP-76, Syk, Lyn, LAT and the Fc receptor gamma-chain after stimulation of the collagen receptor glycoprotein VI in human platelets. *Eur J Biochem,* 263**,** 612-23.

GROUP, S. L. I. S. 2000. Two randomised and placebo-controlled studies of an oral prostacyclin analogue (Iloprost) in severe leg ischaemia. The Oral Iloprost in severe Leg Ischaemia Study Group. *European journal of vascular and endovascular surgery : the official journal of the European Society for Vascular Surgery,* 20**,** 358-62.

GRYGLEWSKI, R. J. 2008. Prostacyclin among prostanoids. *Pharmacol Rep,* 60**,** 3-11.

HAGIWARA, M., ENDO, T., KANAYAMA, T. & HIDAKA, H. 1984. Effect of 1-(3-chloroanilino)-4-phenylphthalazine (MY-5445), a specific inhibitor of cyclic GMP phosphodiesterase, on human platelet aggregation. *J Pharmacol Exp Ther,* 228**,** 467-71.

HALBRUGGE, M., FRIEDRICH, C., EIGENTHALER, M., SCHANZENBACHER, P. & WALTER, U. 1990. Stoichiometric and reversible phosphorylation of a 46-kDa protein in human platelets in response to cGMP- and cAMP-elevating vasodilators. *J Biol Chem,* 265**,** 3088-93.

HALBRUGGE, M. & WALTER, U. 1989. Purification of a vasodilator-regulated phosphoprotein from human platelets. *Eur J Biochem,* 185**,** 41-50.

HANOUNE, J. & DEFER, N. 2001. Regulation and role of adenylyl cyclase isoforms. *Annu Rev Pharmacol Toxicol,* 41**,** 145-74.

HARBECK, B., HUTTELMAIER, S., SCHLUTER, K., JOCKUSCH, B. M. & ILLENBERGER, S. 2000. Phosphorylation of the vasodilator-stimulated phosphoprotein regulates its interaction with actin. *J Biol Chem,* 275**,** 30817-25.

HARRISON, P. & CRAMER, E. M. 1993. Platelet alpha-granules. *Blood Rev,* 7**,** 52-62.

HARRISON, P., WILBOURN, B., DEBILI, N., VAINCHENKER, W., BRETON-GORIUS, J., LAWRIE, A. S., MASSE, J. M., SAVIDGE, G. F. & CRAMER, E. M. 1989. Uptake of plasma fibrinogen into the alpha granules of human megakaryocytes and platelets. *J Clin Invest,* 84**,** 1320-4.

HARTWIG, J. H. 2006. The platelet: form and function. *Semin Hematol,* 43**,** S94-100.

HARTWIG, J. H. & DESISTO, M. 1991. The cytoskeleton of the resting human blood platelet: structure of the membrane skeleton and its attachment to actin filaments. *J Cell Biol,* 112**,** 407-25.

HARTWIG, J. H. & STOSSEL, T. P. 1979. Cytochalasin B and the structure of actin gels. *J Mol Biol,* 134**,** 539-53.

HASLAM, R. J., DICKINSON, N. T. & JANG, E. K. 1999. Cyclic nucleotides and phosphodiesterases in platelets. *Thromb Haemost,* 82**,** 412-23.

HASSOCK, S. R., ZHU, M. X., TROST, C., FLOCKERZI, V. & AUTHI, K. S. 2002. Expression and role of TRPC proteins in human platelets: evidence that TRPC6 forms the store-independent calcium entry channel. *Blood,* 100**,** 2801-11.

HATHAWAY, D. R. & ADELSTEIN, R. S. 1979. Human platelet myosin light chain kinase requires the calcium-binding protein calmodulin for activity. *Proc Natl Acad Sci U S A,* 76**,** 1653-7.

HATHAWAY, D. R., EATON, C. R. & ADELSTEIN, R. S. 1981. Regulation of human platelet myosin light chain kinase by the catalytic subunit of cyclic AMP-dependent protein kinase. *Nature,* 291**,** 252-6.

HAYES, J. S., BRUNTON, L. L., BROWN, J. H., REESE, J. B. & MAYER, S. E. 1979. Hormonally specific expression of cardiac protein kinase activity. *Proc Natl Acad Sci U S A,* 76**,** 1570-4.

HAYES, J. S., LAWLER, O. A., WALSH, M. T. & KINSELLA, B. T. 1999. The prostacyclin receptor is isoprenylated. Isoprenylation is required for efficient receptor-effector coupling. *The Journal of biological chemistry,* 274**,** 23707-18.

HEAD, B. P., PATEL, H. H., ROTH, D. M., MURRAY, F., SWANEY, J. S., NIESMAN, I. R., FARQUHAR, M. G. & INSEL, P. A. 2006. Microtubules and actin microfilaments regulate lipid raft/caveolae localization of adenylyl cyclase signaling components. *J Biol Chem,* 281**,** 26391-9.

HEMRIC, M. E., TRACY, P. B. & HAEBERLE, J. R. 1994. Caldesmon enhances the binding of myosin to the cytoskeleton during platelet activation. *J Biol Chem,* 269**,** 4125-8.

HERBERG, F. W., MALESZKA, A., EIDE, T., VOSSEBEIN, L. & TASKEN, K. 2000. Analysis of A-kinase anchoring protein (AKAP) interaction with protein kinase A (PKA) regulatory subunits: PKA isoform specificity in AKAP binding. *J Mol Biol,* 298**,** 329-39.

HERBERG, F. W. & TAYLOR, S. S. 1993. Physiological inhibitors of the catalytic subunit of cAMP-dependent protein kinase: effect of MgATP on protein-protein interactions. *Biochemistry,* 32**,** 14015-22.

HERMANS, E. 2003. Biochemical and pharmacological control of the multiplicity of coupling at G-protein-coupled receptors. *Pharmacol Ther,* 99**,** 25-44.

HERS, I., BERLANGA, O., TIEKSTRA, M. J., KAMIGUTI, A. S., THEAKSTON, R. D. & WATSON, S. P. 2000. Evidence against a direct role of the integrin alpha2beta1 in collagen-induced tyrosine phosphorylation in human platelets. *Eur J Biochem,* 267**,** 2088-97.

HETTASCH, J. M. & SELLERS, J. R. 1991. Caldesmon phosphorylation in intact human platelets by cAMP-dependent protein kinase and protein kinase C. *J Biol Chem,* 266**,** 11876-81.

HINDRIKS, G., IJSSELDIJK, M. J., SONNENBERG, A., SIXMA, J. J. & DE GROOT, P. G. 1992. Platelet adhesion to laminin: role of Ca2+ and Mg2+ ions, shear rate, and platelet membrane glycoproteins. *Blood,* 79**,** 928-35.

HINZPETER, A., FRITSCH, J., BOROT, F., TRUDEL, S., VIEU, D. L., BROUILLARD, F., BAUDOUIN-LEGROS, M., CLAIN, J., EDELMAN, A. & OLLERO, M. 2007. Membrane cholesterol content modulates ClC-2 gating and sensitivity to oxidative stress. *J Biol Chem,* 282**,** 2423-32.

HOFFMEISTER, M., RIHA, P., NEUMULLER, O., DANIELEWSKI, O., SCHULTESS, J. & SMOLENSKI, A. P. 2008. Cyclic nucleotide-dependent protein kinases inhibit binding of 14-3-3 to the GTPase-activating protein Rap1GAP2 in platelets. *J Biol Chem,* 283**,** 2297-306.

HOOPER, N. M. 1999. Detergent-insoluble glycosphingolipid/cholesterol-rich membrane domains, lipid rafts and caveolae (review). *Mol Membr Biol,* 16**,** 145-56.

HORSTRUP, K., JABLONKA, B., HONIG-LIEDL, P., JUST, M., KOCHSIEK, K. & WALTER, U. 1994. Phosphorylation of focal adhesion vasodilator-stimulated phosphoprotein at Ser157 in intact human platelets correlates with fibrinogen receptor inhibition. *Eur J Biochem,* 225**,** 21-7.

HUANG, P. L., HUANG, Z., MASHIMO, H., BLOCH, K. D., MOSKOWITZ, M. A., BEVAN, J. A. & FISHMAN, M. C. 1995. Hypertension in mice lacking the gene for endothelial nitric oxide synthase. *Nature,* 377**,** 239-42.

HUIZINGA, E. G., TSUJI, S., ROMIJN, R. A., SCHIPHORST, M. E., DE GROOT, P. G., SIXMA, J. J. & GROS, P. 2002. Structures of glycoprotein Ibalpha and its complex with von Willebrand factor A1 domain. *Science,* 297**,** 1176-9.

HUNTER, R. W., MACKINTOSH, C. & HERS, I. 2009. Protein kinase C-mediated phosphorylation and activation of PDE3A regulate cAMP levels in human platelets. *J Biol Chem,* 284**,** 12339-48.

HURLEY, J. H. 1999. Structure, mechanism, and regulation of mammalian adenylyl cyclase. *J Biol Chem,* 274**,** 7599-602.

IGNARRO, L. J., BUGA, G. M., WOOD, K. S., BYRNS, R. E. & CHAUDHURI, G. 1987. Endothelium-derived relaxing factor produced and released from artery and vein is nitric oxide. *Proc Natl Acad Sci U S A,* 84**,** 9265-9.

IMAI, A., HATTORI, H., TAKAHASHI, M. & NOZAWA, Y. 1983. Evidence that cyclic AMP may regulate Ca2+-mobilization and phospholipases in thrombin-stimulated human platelets. *Biochem Biophys Res Commun,* 112**,** 693-700.

ITALIANO, J. E., JR., LECINE, P., SHIVDASANI, R. A. & HARTWIG, J. H. 1999. Blood platelets are assembled principally at the ends of proplatelet processes produced by differentiated megakaryocytes. *J Cell Biol,* 147**,** 1299-312.

ITO, M., NISHIKAWA, M., FUJIOKA, M., MIYAHARA, M., ISAKA, N., SHIKU, H. & NAKANO, T. 1996. Characterization of the isoenzymes of cyclic nucleotide phosphodiesterase in human platelets and the effects of E4021. *Cell Signal,* 8**,** 575-81.

JACKSON, S. P. 2007. The growing complexity of platelet aggregation. *Blood,* 109**,** 5087-95.

JANG, E. K., AZZAM, J. E., DICKINSON, N. T., DAVIDSON, M. M. & HASLAM, R. J. 2002. Roles for both cyclic GMP and cyclic AMP in the inhibition of collagen-induced platelet aggregation by nitroprusside. *Br J Haematol,* 117**,** 664-75.

JENSEN, B. O., SELHEIM, F., DOSKELAND, S. O., GEAR, A. R. & HOLMSEN, H. 2004. Protein kinase A mediates inhibition of the thrombin-induced platelet shape change by nitric oxide. *Blood,* 104**,** 2775-82.

JIN, J. & KUNAPULI, S. P. 1998. Coactivation of two different G protein-coupled receptors is essential for ADP-induced platelet aggregation. *Proc Natl Acad Sci U S A,* 95**,** 8070-4.

JOHNSTON-COX, H. A., YANG, D. & RAVID, K. 2011. Physiological implications of adenosine receptor-mediated platelet aggregation. *Journal of cellular physiology,* 226**,** 46-51.

JURK, K., CLEMETSON, K. J., DE GROOT, P. G., BRODDE, M. F., STEINER, M., SAVION, N., VARON, D., SIXMA, J. J., VAN AKEN, H. & KEHREL, B. E. 2003. Thrombospondin-1 mediates platelet adhesion at high shear via glycoprotein Ib (GPIb): an alternative/backup mechanism to von Willebrand factor. *Faseb J,* 17**,** 1490-2.

KASE, H., IWAHASHI, K., NAKANISHI, S., MATSUDA, Y., YAMADA, K., TAKAHASHI, M., MURAKATA, C., SATO, A. & KANEKO, M. 1987. K-252 compounds, novel and potent inhibitors of protein kinase C and cyclic nucleotide-dependent protein kinases. *Biochem Biophys Res Commun,* 142**,** 436-40.

KATO, K., KANAJI, T., RUSSELL, S., KUNICKI, T. J., FURIHATA, K., KANAJI, S., MARCHESE, P., REININGER, A., RUGGERI, Z. M. & WARE, J. 2003. The contribution of glycoprotein VI to stable platelet adhesion and thrombus formation illustrated by targeted gene deletion. *Blood,* 102**,** 1701-7.

KAUSHANSKY, K. 2005. The molecular mechanisms that control thrombopoiesis. *J Clin Invest,* 115**,** 3339-47.

KENNEDY, I., COLEMAN, R. A., HUMPHREY, P. P., LEVY, G. P. & LUMLEY, P. 1982. Studies on the characterisation of prostanoid receptors: a proposed classification. *Prostaglandins,* 24**,** 667-89.

KINSELLA, B. T., O'MAHONY, D. J. & FITZGERALD, G. A. 1997. The human thromboxane A2 receptor alpha isoform (TP alpha) functionally couples to the G proteins Gq and G11 in vivo and is activated by the isoprostane 8-epi prostaglandin F2 alpha. *J Pharmacol Exp Ther,* 281**,** 957-64.

KLAGES, B., BRANDT, U., SIMON, M. I., SCHULTZ, G. & OFFERMANNS, S. 1999. Activation of G12/G13 results in shape change and Rho/Rho-kinase-mediated myosin light chain phosphorylation in mouse platelets. *J Cell Biol,* 144**,** 745-54.

KLAUCK, T. M., FAUX, M. C., LABUDDA, K., LANGEBERG, L. K., JAKEN, S. & SCOTT, J. D. 1996. Coordination of three signaling enzymes by AKAP79, a mammalian scaffold protein. *Science,* 271**,** 1589-92.

KLOEZE, J. 1970. Prostaglandins and platelet aggregation in vivo. II. Influence of PGE1 and PGF1 alpha on platelet thrombus formation induced by an electric stimulus in veins on the rat brain surface. *Thromb Diath Haemorrh,* 23**,** 293-8.

KOBAYASHI, T., KIRIYAMA, M., HIRATA, T., HIRATA, M., USHIKUBI, F. & NARUMIYA, S. 1997. Identification of domains conferring ligand binding specificity to the prostanoid receptor. Studies on chimeric prostacyclin/prostaglandin D receptors. *The Journal of biological chemistry,* 272**,** 15154-60.

KOBAYASHI, T., USHIKUBI, F. & NARUMIYA, S. 2000. Amino acid residues conferring ligand binding properties of prostaglandin I and prostaglandin D receptors. Identification by site-directed mutagenesis. *The Journal of biological chemistry,* 275**,** 24294-303.

KOHLER, D., STRAUB, A., WEISSMULLER, T., FAIGLE, M., BENDER, S., LEHMANN, R., WENDEL, H. P., KURZ, J., WALTER, U., ZACHAROWSKI, K. & ROSENBERGER, P. 2011. Phosphorylation of vasodilator-stimulated phosphoprotein prevents platelet-neutrophil complex formation and dampens myocardial ischemia-reperfusion injury. *Circulation,* 123**,** 2579-90.

KRUPINSKI, J., COUSSEN, F., BAKALYAR, H. A., TANG, W. J., FEINSTEIN, P. G., ORTH, K., SLAUGHTER, C., REED, R. R. & GILMAN, A. G. 1989. Adenylyl cyclase amino acid sequence: possible channel- or transporter-like structure. *Science,* 244**,** 1558-64.

KULKARNI, S., DOPHEIDE, S. M., YAP, C. L., RAVANAT, C., FREUND, M., MANGIN, P., HEEL, K. A., STREET, A., HARPER, I. S., LANZA, F. & JACKSON, S. P. 2000. A revised model of platelet aggregation. *J Clin Invest,* 105**,** 783-91.

KULKARNI, S., WOOLLARD, K. J., THOMAS, S., OXLEY, D. & JACKSON, S. P. 2007. Conversion of platelets from a proaggregatory to a proinflammatory adhesive phenotype: role of PAF in spatially regulating neutrophil adhesion and spreading. *Blood,* 110**,** 1879-86.

LAEMMLI, U. K. 1970. Cleavage of structural proteins during the assembly of the head of bacteriophage T4. *Nature,* 227**,** 680-5.

LAPETINA, E. G., LACAL, J. C., REEP, B. R. & MOLINA Y VEDIA, L. 1989. A ras-related protein is phosphorylated and translocated by agonists that increase cAMP levels in human platelets. *Proc Natl Acad Sci U S A,* 86**,** 3131-4.

LAVOIE, J. N., HICKEY, E., WEBER, L. A. & LANDRY, J. 1993. Modulation of actin microfilament dynamics and fluid phase pinocytosis by phosphorylation of heat shock protein 27. *J Biol Chem,* 268**,** 24210-4.

LEE, F. A., VAN LIER, M., RELOU, I. A., FOLEY, L., AKKERMAN, J. W., HEIJNEN, H. F. & FARNDALE, R. W. 2006. Lipid rafts facilitate the interaction of PECAM-1 with the glycoprotein VI-FcR gamma-chain complex in human platelets. *J Biol Chem,* 281**,** 39330-8.

LEON, C., HECHLER, B., FREUND, M., ECKLY, A., VIAL, C., OHLMANN, P., DIERICH, A., LEMEUR, M., CAZENAVE, J. P. & GACHET, C. 1999. Defective platelet aggregation and increased resistance to thrombosis in purinergic P2Y(1) receptor-null mice. *J Clin Invest,* 104**,** 1731-7.

LEON, D. A., HERBERG, F. W., BANKY, P. & TAYLOR, S. S. 1997. A stable alpha-helical domain at the N terminus of the RIalpha subunits of cAMP-dependent protein kinase is a novel dimerization/docking motif. *J Biol Chem,* 272**,** 28431-7.

LI, Z., AJDIC, J., EIGENTHALER, M. & DU, X. 2003. A predominant role for cAMP-dependent protein kinase in the cGMP-induced phosphorylation of vasodilator-stimulated phosphoprotein and platelet inhibition in humans. *Blood,* 101**,** 4423-9.

LIOU, J. Y., SHYUE, S. K., TSAI, M. J., CHUNG, C. L., CHU, K. Y. & WU, K. K. 2000. Colocalization of prostacyclin synthase with prostaglandin H synthase-1 (PGHS-1) but not phorbol ester-induced PGHS-2 in cultured endothelial cells. *The Journal of biological chemistry,* 275**,** 15314-20.

LIU, X., THANGAVEL, M., SUN, S. Q., KAMINSKY, J., MAHAUTMR, P., STITHAM, J., HWA, J. & OSTROM, R. S. 2008. Adenylyl cyclase type 6 overexpression selectively enhances beta-adrenergic and prostacyclin receptor-mediated inhibition of cardiac fibroblast function because of colocalization in lipid rafts. *Naunyn Schmiedebergs Arch Pharmacol,* 377**,** 359-69.

LIU, Y., RUOHO, A. E., RAO, V. D. & HURLEY, J. H. 1997a. Catalytic mechanism of the adenylyl and guanylyl cyclases: modeling and mutational analysis. *Proc Natl Acad Sci U S A,* 94**,** 13414-9.

LIU, Y., RUOHO, A. E., RAO, V. D. & HURLEY, J. H. 1997b. Catalytic mechanism of the adenylyl and guanylyl cyclases: modeling and mutational analysis. *Proceedings of the National Academy of Sciences of the United States of America,* 94**,** 13414-9.

LOHMANN, S. M. & WALTER, U. 2005. Tracking functions of cGMP-dependent protein kinases (cGK). *Front Biosci,* 10**,** 1313-28.

LONG, M. W. 1998. Megakaryocyte differentiation events. *Semin Hematol,* 35**,** 192-9.

LOPEZ, J. A., DEL CONDE, I. & SHRIMPTON, C. N. 2005. Receptors, rafts, and microvesicles in thrombosis and inflammation. *J Thromb Haemost,* 3**,** 1737-44.

LOWRY, O. H., ROSEBROUGH, N. J., FARR, A. L. & RANDALL, R. J. 1951. Protein measurement with the Folin phenol reagent. *J Biol Chem,* 193**,** 265-75.

LUO, B. H., CARMAN, C. V. & SPRINGER, T. A. 2007. Structural basis of integrin regulation and signaling. *Annu Rev Immunol,* 25**,** 619-47.

MA, Y. Q., QIN, J. & PLOW, E. F. 2007. Platelet integrin alpha(IIb)beta(3): activation mechanisms. *J Thromb Haemost,* 5**,** 1345-52.

MACPHEE, C. H., REIFSNYDER, D. H., MOORE, T. A., LEREA, K. M. & BEAVO, J. A. 1988. Phosphorylation results in activation of a cAMP phosphodiesterase in human platelets. *J Biol Chem,* 263**,** 10353-8.

MALININ, N. L., ZHANG, L., CHOI, J., CIOCEA, A., RAZORENOVA, O., MA, Y. Q., PODREZ, E. A., TOSI, M., LENNON, D. P., CAPLAN, A. I., SHURIN, S. B., PLOW, E. F. & BYZOVA, T. V. 2009. A point mutation in KINDLIN3 ablates activation of three integrin subfamilies in humans. *Nat Med,* 15**,** 313-8.

MANGANELLO, J. M., DJELLAS, Y., BORG, C., ANTONAKIS, K. & LE BRETON, G. C. 1999. Cyclic AMP-dependent phosphorylation of thromboxane A(2) receptor-associated Galpha(13). *J Biol Chem,* 274**,** 28003-10.

MANNS, J. M., BRENNA, K. J., COLMAN, R. W. & SHETH, S. B. 2002. Differential regulation of human platelet responses by cGMP inhibited and stimulated cAMP phosphodiesterases. *Thromb Haemost,* 87**,** 873-9.

MARCUS, A. J. & SAFIER, L. B. 1993. Thromboregulation: multicellular modulation of platelet reactivity in hemostasis and thrombosis. *Faseb J,* 7**,** 516-22.

MARGARUCCI, L., ROEST, M., PREISINGER, C., BLEIJERVELD, O. B., VAN HOLTEN, T. C., HECK, A. J. & SCHOLTEN, A. 2011. Collagen stimulation of platelets induces a rapid spatial response of cAMP and cGMP signaling scaffolds. *Mol Biosyst,* 7**,** 2311-9.

MARGUET, D., LENNE, P. F., RIGNEAULT, H. & HE, H. T. 2006. Dynamics in the plasma membrane: how to combine fluidity and order. *Embo J,* 25**,** 3446-57.

MARQUIS, N. R., VIGDAHL, R. L. & TAVORMINA, P. A. 1969. Platelet aggregation. I. Regulation by cyclic AMP and prostaglandin E1. *Biochem Biophys Res Commun,* 36**,** 965-72.

MARTIN, B. R., DEERINCK, T. J., ELLISMAN, M. H., TAYLOR, S. S. & TSIEN, R. Y. 2007. Isoform-specific PKA dynamics revealed by dye-triggered aggregation and DAKAP1alpha-mediated localization in living cells. *Chemistry & biology,* 14**,** 1031-42.

MASSBERG, S., GAWAZ, M., GRUNER, S., SCHULTE, V., KONRAD, I., ZOHLNHOFER, D., HEINZMANN, U. & NIESWANDT, B. 2003. A crucial role of glycoprotein VI for platelet recruitment to the injured arterial wall in vivo. *J Exp Med,* 197**,** 41-9.

MASSBERG, S., GRUNER, S., KONRAD, I., GARCIA ARGUINZONIS, M. I., EIGENTHALER, M., HEMLER, K., KERSTING, J., SCHULZ, C., MULLER, I., BESTA, F., NIESWANDT, B., HEINZMANN, U., WALTER, U. & GAWAZ, M. 2004. Enhanced in vivo platelet adhesion in vasodilator-stimulated phosphoprotein (VASP)-deficient mice. *Blood,* 103**,** 136-42.

MASSBERG, S., SAUSBIER, M., KLATT, P., BAUER, M., PFEIFER, A., SIESS, W., FASSLER, R., RUTH, P., KROMBACH, F. & HOFMANN, F. 1999. Increased

adhesion and aggregation of platelets lacking cyclic guanosine 3',5'-monophosphate kinase I. *J Exp Med,* 189**,** 1255-64.

MAURICE, D. H. & HASLAM, R. J. 1990. Molecular basis of the synergistic inhibition of platelet function by nitrovasodilators and activators of adenylate cyclase: inhibition of cyclic AMP breakdown by cyclic GMP. *Mol Pharmacol,* 37**,** 671-81.

MCADAM, B. F., CATELLA-LAWSON, F., MARDINI, I. A., KAPOOR, S., LAWSON, J. A. & FITZGERALD, G. A. 1999. Systemic biosynthesis of prostacyclin by cyclooxygenase (COX)-2: the human pharmacology of a selective inhibitor of COX-2. *Proceedings of the National Academy of Sciences of the United States of America,* 96**,** 272-7.

MCNICOL, A. & ISRAELS, S. J. 1999. Platelet dense granules: structure, function and implications for haemostasis. *Thromb Res,* 95**,** 1-18.

MEANS, C. K., LYGREN, B., LANGEBERG, L. K., JAIN, A., DIXON, R. E., VEGA, A. L., GOLD, M. G., PETROSYAN, S., TAYLOR, S. S., MURPHY, A. N., HA, T., SANTANA, L. F., TASKEN, K. & SCOTT, J. D. 2011. An entirely specific type I A-kinase anchoring protein that can sequester two molecules of protein kinase A at mitochondria. *Proc Natl Acad Sci U S A,* 108**,** E1227-35.

MELLION, B. T., IGNARRO, L. J., OHLSTEIN, E. H., PONTECORVO, E. G., HYMAN, A. L. & KADOWITZ, P. J. 1981. Evidence for the inhibitory role of guanosine 3', 5'-monophosphate in ADP-induced human platelet aggregation in the presence of nitric oxide and related vasodilators. *Blood,* 57**,** 946-55.

MITCHELL, J. A., ALI, F., BAILEY, L., MORENO, L. & HARRINGTON, L. S. 2008. Role of nitric oxide and prostacyclin as vasoactive hormones released by the endothelium. *Exp Physiol,* 93**,** 141-7.

MITCHELL, J. A. & WARNER, T. D. 2006a. COX isoforms in the cardiovascular system: understanding the activities of non-steroidal anti-inflammatory drugs. *Nat Rev Drug Discov,* 5**,** 75-86.

MITCHELL, J. A. & WARNER, T. D. 2006b. COX isoforms in the cardiovascular system: understanding the activities of non-steroidal anti-inflammatory drugs. *Nature reviews. Drug discovery,* 5**,** 75-86.

MOIR, R. D., LEE, J., HAEUSLER, R. A., DESAI, N., ENGELKE, D. R. & WILLIS, I. M. 2006. Protein kinase A regulates RNA polymerase III transcription through the nuclear localization of Maf1. *Proc Natl Acad Sci U S A,* 103**,** 15044-9.

MONCADA, S. 1982a. Eighth Gaddum Memorial Lecture. University of London Institute of Education, December 1980. Biological importance of prostacyclin. *Br J Pharmacol,* 76**,** 3-31.

MONCADA, S. 1982b. Prostacyclin and arterial wall biology. *Arteriosclerosis,* 2**,** 193-207.

MONCADA, S., GRYGLEWSKI, R., BUNTING, S. & VANE, J. R. 1976. An enzyme isolated from arteries transforms prostaglandin endoperoxides to an unstable substance that inhibits platelet aggregation. *Nature,* 263**,** 663-5.

MONGILLO, M., MCSORLEY, T., EVELLIN, S., SOOD, A., LISSANDRON, V., TERRIN, A., HUSTON, E., HANNAWACKER, A., LOHSE, M. J., POZZAN, T., HOUSLAY, M. D. & ZACCOLO, M. 2004. Fluorescence resonance energy transfer-based analysis of cAMP dynamics in live neonatal rat cardiac myocytes reveals

distinct functions of compartmentalized phosphodiesterases. *Circ Res,* 95**,** 67-75.

MONGILLO, M., TOCCHETTI, C. G., TERRIN, A., LISSANDRON, V., CHEUNG, Y. F., DOSTMANN, W. R., POZZAN, T., KASS, D. A., PAOLOCCI, N., HOUSLAY, M. D. & ZACCOLO, M. 2006. Compartmentalized phosphodiesterase-2 activity blunts beta-adrenergic cardiac inotropy via an NO/cGMP-dependent pathway. *Circ Res,* 98**,** 226-34.

MOORTHY, B. S., GAO, Y. & ANAND, G. S. 2011. Phosphodiesterases catalyze hydrolysis of cAMP-bound to regulatory subunit of protein kinase A and mediate signal termination. *Molecular & cellular proteomics : MCP,* 10**,** M110 002295.

MOROI, M., JUNG, S. M., OKUMA, M. & SHINMYOZU, K. 1989. A patient with platelets deficient in glycoprotein VI that lack both collagen-induced aggregation and adhesion. *J Clin Invest,* 84**,** 1440-5.

MOROI, M., ONITSUKA, I., IMAIZUMI, T. & JUNG, S. M. 2000. Involvement of activated integrin alpha2beta1 in the firm adhesion of platelets onto a surface of immobilized collagen under flow conditions. *Thromb Haemost,* 83**,** 769-76.

MOSER, M., NIESWANDT, B., USSAR, S., POZGAJOVA, M. & FASSLER, R. 2008. Kindlin-3 is essential for integrin activation and platelet aggregation. *Nat Med,* 14**,** 325-30.

MUELLER, H. S., RAO, P. S., GREENBERG, M. A., BUTTRICK, P. M., SUSSMAN, II, LEVITE, H. A., GROSE, R. M., PEREZ-DAVILA, V., STRAIN, J. E. & SPAET, T. H. 1986. Platelet hyperactivity in acute myocardial infarction in man--effects of prostacyclin. *Herz,* 11**,** 116-26.

MUNZEL, T., DAIBER, A., ULLRICH, V. & MULSCH, A. 2005. Vascular consequences of endothelial nitric oxide synthase uncoupling for the activity and expression of the soluble guanylyl cyclase and the cGMP-dependent protein kinase. *Arterioscler Thromb Vasc Biol,* 25**,** 1551-7.

MURATA, T., USHIKUBI, F., MATSUOKA, T., HIRATA, M., YAMASAKI, A., SUGIMOTO, Y., ICHIKAWA, A., AZE, Y., TANAKA, T., YOSHIDA, N., UENO, A., OH-ISHI, S. & NARUMIYA, S. 1997. Altered pain perception and inflammatory response in mice lacking prostacyclin receptor. *Nature,* 388**,** 678-82.

MURRAY, A. J. 2008. Pharmacological PKA inhibition: all may not be what it seems. *Sci Signal,* 1**,** re4.

MURUGAPPAN, S., SHANKAR, H. & KUNAPULI, S. P. 2004. Platelet receptors for adenine nucleotides and thromboxane A2. *Semin Thromb Hemost,* 30**,** 411-8.

MUSTARD, J. F., KINLOUGH-RATHBONE, R. L. & PACKHAM, M. A. 1989. Isolation of human platelets from plasma by centrifugation and washing. *Methods Enzymol,* 169**,** 3-11.

NAGALLA, S., SHAW, C., KONG, X., KONDKAR, A. A., EDELSTEIN, L. C., MA, L., CHEN, J., MCKNIGHT, G. S., LOPEZ, J. A., YANG, L., JIN, Y., BRAY, M. S., LEAL, S. M., DONG, J. F. & BRAY, P. F. 2011. Platelet microRNA-mRNA coexpression profiles correlate with platelet reactivity. *Blood,* 117**,** 5189-97.

NAKADE, S., RHEE, S. K., HAMANAKA, H. & MIKOSHIBA, K. 1994. Cyclic AMP-dependent phosphorylation of an immunoaffinity-purified homotetrameric inositol 1,4,5-trisphosphate receptor (type I) increases Ca2+ flux in reconstituted lipid vesicles. *J Biol Chem,* 269**,** 6735-42.

NAKAGAWA, O., TANAKA, I., USUI, T., HARADA, M., SASAKI, Y., ITOH, H., YOSHIMASA, T., NAMBA, T., NARUMIYA, S. & NAKAO, K. 1994. Molecular cloning of human prostacyclin receptor cDNA and its gene expression in the cardiovascular system. *Circulation,* 90**,** 1643-7.

NAKAMURA, T. & GOLD, G. H. 1987. A cyclic nucleotide-gated conductance in olfactory receptor cilia. *Nature,* 325**,** 442-4.

NAKASE, I., TAKEUCHI, T., TANAKA, G. & FUTAKI, S. 2008. Methodological and cellular aspects that govern the internalization mechanisms of arginine-rich cell-penetrating peptides. *Adv Drug Deliv Rev,* 60**,** 598-607.

NASEEM, K. M. 2005. The role of nitric oxide in cardiovascular diseases. *Mol Aspects Med,* 26**,** 33-65.

NASEEM, K. M. & ROBERTS, W. 2011. Nitric oxide at a glance. *Platelets,* 22**,** 148-52.

NEEDLEMAN, P., MONCADA, S., BUNTING, S., VANE, J. R., HAMBERG, M. & SAMUELSSON, B. 1976. Identification of an enzyme in platelet microsomes which generates thromboxane A2 from prostaglandin endoperoxides. *Nature,* 261**,** 558-60.

NEVES, S. R., RAM, P. T. & IYENGAR, R. 2002. G protein pathways. *Science,* 296**,** 1636-9.

NEWLON, M. G., ROY, M., MORIKIS, D., CARR, D. W., WESTPHAL, R., SCOTT, J. D. & JENNINGS, P. A. 2001. A novel mechanism of PKA anchoring revealed by solution structures of anchoring complexes. *Embo J,* 20**,** 1651-62.

NI, H., DENIS, C. V., SUBBARAO, S., DEGEN, J. L., SATO, T. N., HYNES, R. O. & WAGNER, D. D. 2000. Persistence of platelet thrombus formation in arterioles of mice lacking both von Willebrand factor and fibrinogen. *J Clin Invest,* 106**,** 385-92.

NIESWANDT, B., BRAKEBUSCH, C., BERGMEIER, W., SCHULTE, V., BOUVARD, D., MOKHTARI-NEJAD, R., LINDHOUT, T., HEEMSKERK, J. W., ZIRNGIBL, H. & FASSLER, R. 2001. Glycoprotein VI but not alpha2beta1 integrin is essential for platelet interaction with collagen. *Embo J,* 20**,** 2120-30.

NIESWANDT, B. & WATSON, S. P. 2003. Platelet-collagen interaction: is GPVI the central receptor? *Blood,* 102**,** 449-61.

NILIUS, S. M., HASSE, A., KUGER, P., SCHROR, K. & MEYER-KIRCHRATH, J. 2000. Agonist-induced long-term desensitization of the human prostacyclin receptor. *FEBS letters,* 484**,** 211-6.

NISHIKAWA, M., DE LANEROLLE, P., LINCOLN, T. M. & ADELSTEIN, R. S. 1984. Phosphorylation of mammalian myosin light chain kinases by the catalytic subunit of cyclic AMP-dependent protein kinase and by cyclic GMP-dependent protein kinase. *J Biol Chem,* 259**,** 8429-36.

NOE, L., DI MICHELE, M., GIETS, E., THYS, C., WITTEVRONGEL, C., DE VOS, R., OVERBERGH, L., WAELKENS, E., JAEKEN, J., VAN GEET, C. & FRESON, K. 2010. Platelet Gs hypofunction and abnormal morphology resulting from a

heterozygous RGS2 mutation. *Journal of thrombosis and haemostasis : JTH,* 8**,** 1594-603.

OBERPRIELER, N. G., ROBERTS, W., GRAHAM, A. M., HOMER-VANNIASINKAM, S. & NASEEM, K. M. 2007. Inhibition of ADP-induced platelet adhesion to immobilised fibrinogen by nitric oxide: evidence for cGMP-independent mechanisms. *Biochem Pharmacol,* 73**,** 1593-601.

ODA, A., IKEDA, Y., OCHS, H. D., DRUKER, B. J., OZAKI, K., HANDA, M., ARIGA, T., SAKIYAMA, Y., WITTE, O. N. & WAHL, M. I. 2000. Rapid tyrosine phosphorylation and activation of Bruton's tyrosine/Tec kinases in platelets induced by collagen binding or CD32 cross-linking. *Blood,* 95**,** 1663-70.

OFFERMANNS, S. 2006. Activation of platelet function through G protein-coupled receptors. *Circ Res,* 99**,** 1293-304.

OFFERMANNS, S., LAUGWITZ, K. L., SPICHER, K. & SCHULTZ, G. 1994. G proteins of the G12 family are activated via thromboxane A2 and thrombin receptors in human platelets. *Proc Natl Acad Sci U S A,* 91**,** 504-8.

OFFERMANNS, S., TOOMBS, C. F., HU, Y. H. & SIMON, M. I. 1997. Defective platelet activation in G alpha(q)-deficient mice. *Nature,* 389**,** 183-6.

OHLMANN, P., LAUGWITZ, K. L., NURNBERG, B., SPICHER, K., SCHULTZ, G., CAZENAVE, J. P. & GACHET, C. 1995. The human platelet ADP receptor activates Gi2 proteins. *Biochem J,* 312 (Pt 3)**,** 775-9.

OLIVERIA, S. F., DELL'ACQUA, M. L. & SATHER, W. A. 2007. AKAP79/150 anchoring of calcineurin controls neuronal L-type Ca2+ channel activity and nuclear signaling. *Neuron,* 55**,** 261-75.

OMORI, K. & KOTERA, J. 2007. Overview of PDEs and their regulation. *Circ Res,* 100**,** 309-27.

OSTROM, R. S., LIU, X., HEAD, B. P., GREGORIAN, C., SEASHOLTZ, T. M. & INSEL, P. A. 2002. Localization of adenylyl cyclase isoforms and G protein-coupled receptors in vascular smooth muscle cells: expression in caveolin-rich and noncaveolin domains. *Mol Pharmacol,* 62**,** 983-92.

OSTROM, R. S., VIOLIN, J. D., COLEMAN, S. & INSEL, P. A. 2000. Selective enhancement of beta-adrenergic receptor signaling by overexpression of adenylyl cyclase type 6: colocalization of receptor and adenylyl cyclase in caveolae of cardiac myocytes. *Mol Pharmacol,* 57**,** 1075-9.

PARENTE, L. & PERRETTI, M. 2003. Advances in the pathophysiology of constitutive and inducible cyclooxygenases: two enzymes in the spotlight. *Biochem Pharmacol,* 65**,** 153-9.

PATEL, H. H., HAMURO, L. L., CHUN, B. J., KAWARAGUCHI, Y., QUICK, A., REBOLLEDO, B., PENNYPACKER, J., THURSTON, J., RODRIGUEZ-PINTO, N., SELF, C., OLSON, G., INSEL, P. A., GILES, W. R., TAYLOR, S. S. & ROTH, D. M. 2010. Disruption of protein kinase A localization using a trans-activator of transcription (TAT)-conjugated A-kinase-anchoring peptide reduces cardiac function. *J Biol Chem,* 285**,** 27632-40.

PATEL, H. H., MURRAY, F. & INSEL, P. A. 2008. Caveolae as organizers of pharmacologically relevant signal transduction molecules. *Annu Rev Pharmacol Toxicol,* 48**,** 359-91.

PATEL, S. R., HARTWIG, J. H. & ITALIANO, J. E., JR. 2005. The biogenesis of platelets from megakaryocyte proplatelets. *J Clin Invest,* 115**,** 3348-54.

PELKMANS, L., PUNTENER, D. & HELENIUS, A. 2002. Local actin polymerization and dynamin recruitment in SV40-induced internalization of caveolae. *Science,* 296**,** 535-9.

PIDOUX, G. & TASKEN, K. 2010. Specificity and spatial dynamics of protein kinase A signaling organized by A-kinase-anchoring proteins. *J Mol Endocrinol,* 44**,** 271-84.

PIGAZZI, A., HEYDRICK, S., FOLLI, F., BENOIT, S., MICHELSON, A. & LOSCALZO, J. 1999. Nitric oxide inhibits thrombin receptor-activating peptide-induced phosphoinositide 3-kinase activity in human platelets. *J Biol Chem,* 274**,** 14368-75.

PITHA, J., IRIE, T., SKLAR, P. B. & NYE, J. S. 1988. Drug solubilizers to aid pharmacologists: amorphous cyclodextrin derivatives. *Life Sci,* 43**,** 493-502.

POLLITT, A. Y., GRYGIELSKA, B., LEBLOND, B., DESIRE, L., EBLE, J. A. & WATSON, S. P. 2010. Phosphorylation of CLEC-2 is dependent on lipid rafts, actin polymerization, secondary mediators, and Rac. *Blood,* 115**,** 2938-46.

PONTIER, S. M., PERCHERANCIER, Y., GALANDRIN, S., BREIT, A., GALES, C. & BOUVIER, M. 2008. Cholesterol-dependent separation of the beta2-adrenergic receptor from its partners determines signaling efficacy: insight into nanoscale organization of signal transduction. *J Biol Chem,* 283**,** 24659-72.

POTTER, R. L. & TAYLOR, S. S. 1979. Relationships between structural domains and function in the regulatory subunit of cAMP-dependent protein kinases I and II from porcine skeletal muscle. *The Journal of biological chemistry,* 254**,** 2413-8.

PUGH, N., SIMPSON, A. M., SMETHURST, P. A., DE GROOT, P. G., RAYNAL, N. & FARNDALE, R. W. 2010. Synergism between platelet collagen receptors defined using receptor-specific collagen-mimetic peptide substrata in flowing blood. *Blood,* 115**,** 5069-79.

QUEK, L. S., BOLEN, J. & WATSON, S. P. 1998. A role for Bruton's tyrosine kinase (Btk) in platelet activation by collagen. *Curr Biol,* 8**,** 1137-40.

QUINTON, T. M., KIM, S., JIN, J. & KUNAPULI, S. P. 2005. Lipid rafts are required in Galpha(i) signaling downstream of the P2Y12 receptor during ADP-mediated platelet activation. *J Thromb Haemost,* 3**,** 1036-41.

RADOMSKI, M. W., PALMER, R. M. & MONCADA, S. 1987a. Comparative pharmacology of endothelium-derived relaxing factor, nitric oxide and prostacyclin in platelets. *Br J Pharmacol,* 92**,** 181-7.

RADOMSKI, M. W., PALMER, R. M. & MONCADA, S. 1987b. Endogenous nitric oxide inhibits human platelet adhesion to vascular endothelium. *Lancet,* 2**,** 1057-8.

RADOMSKI, M. W., PALMER, R. M. & MONCADA, S. 1990. Characterization of the L-arginine:nitric oxide pathway in human platelets. *Br J Pharmacol,* 101**,** 325-8.

RANGEL-ALDAO, R. & ROSEN, O. M. 1976. Dissociation and reassociation of the phosphorylated and nonphosphorylated forms of adenosine 3':5' -

monophosphate-dependent protein kinase from bovine cardiac muscle. *The Journal of biological chemistry,* 251**,** 3375-80.

REED, G. L. 2004. Platelet secretory mechanisms. *Semin Thromb Hemost,* 30**,** 441-50.

REID, H. M. & KINSELLA, B. T. 2003. The alpha, but not the beta, isoform of the human thromboxane A2 receptor is a target for nitric oxide-mediated desensitization. Independent modulation of Tp alpha signaling by nitric oxide and prostacyclin. *J Biol Chem,* 278**,** 51190-202.

REINHARD, M., JARCHAU, T. & WALTER, U. 2001. Actin-based motility: stop and go with Ena/VASP proteins. *Trends Biochem Sci,* 26**,** 243-9.

REITER, R., RESCH, U. & SINZINGER, H. 2001. Do human platelets express COX-2? *Prostaglandins Leukot Essent Fatty Acids,* 64**,** 299-305.

REN, Q., YE, S. & WHITEHEART, S. W. 2008. The platelet release reaction: just when you thought platelet secretion was simple. *Curr Opin Hematol,* 15**,** 537-41.

REVENU, C., ATHMAN, R., ROBINE, S. & LOUVARD, D. 2004. The co-workers of actin filaments: from cell structures to signals. *Nat Rev Mol Cell Biol,* 5**,** 635-46.

ROSENMUND, C., CARR, D. W., BERGESON, S. E., NILAVER, G., SCOTT, J. D. & WESTBROOK, G. L. 1994. Anchoring of protein kinase A is required for modulation of AMPA/kainate receptors on hippocampal neurons. *Nature,* 368**,** 853-6.

ROWLEY, J. W., OLER, A. J., TOLLEY, N. D., HUNTER, B. N., LOW, E. N., NIX, D. A., YOST, C. C., ZIMMERMAN, G. A. & WEYRICH, A. S. 2011. Genome-wide RNA-seq analysis of human and mouse platelet transcriptomes. *Blood,* 118**,** e101-11.

RUGGERI, Z. M. 2002. Platelets in atherothrombosis. *Nat Med,* 8**,** 1227-34.

RUGGERI, Z. M. & MENDOLICCHIO, G. L. 2007. Adhesion mechanisms in platelet function. *Circ Res,* 100**,** 1673-85.

RUGGERI, Z. M., ORJE, J. N., HABERMANN, R., FEDERICI, A. B. & REININGER, A. J. 2006. Activation-independent platelet adhesion and aggregation under elevated shear stress. *Blood,* 108**,** 1903-10.

RUPPELT, A., MOSENDEN, R., GRONHOLM, M., AANDAHL, E. M., TOBIN, D., CARLSON, C. R., ABRAHAMSEN, H., HERBERG, F. W., CARPEN, O. & TASKEN, K. 2007. Inhibition of T cell activation by cyclic adenosine 5'-monophosphate requires lipid raft targeting of protein kinase A type I by the A-kinase anchoring protein ezrin. *J Immunol,* 179**,** 5159-68.

SALLES, II, FEYS, H. B., ISERBYT, B. F., DE MEYER, S. F., VANHOORELBEKE, K. & DECKMYN, H. 2008. Inherited traits affecting platelet function. *Blood Rev,* 22**,** 155-72.

SAMUELSSON, B., GOLDYNE, M., GRANSTROM, E., HAMBERG, M., HAMMARSTROM, S. & MALMSTEN, C. 1978. Prostaglandins and thromboxanes. *Annu Rev Biochem,* 47**,** 997-1029.

SANDBERG, M., BUTT, E., NOLTE, C., FISCHER, L., HALBRUGGE, M., BELTMAN, J., JAHNSEN, T., GENIESER, H. G., JASTORFF, B. & WALTER, U. 1991. Characterization of Sp-5,6-dichloro-1-beta-D-ribofuranosylbenzimidazole-3',5'-monophosphorothioate (Sp-5,6-DCl-cBiMPS) as a potent and specific

activator of cyclic-AMP-dependent protein kinase in cell extracts and intact cells. *Biochem J,* 279 (Pt 2)**,** 521-7.

SANTORO, S. A. 1986. Identification of a 160,000 dalton platelet membrane protein that mediates the initial divalent cation-dependent adhesion of platelets to collagen. *Cell,* 46**,** 913-20.

SAVAGE, B., ALMUS-JACOBS, F. & RUGGERI, Z. M. 1998. Specific synergy of multiple substrate-receptor interactions in platelet thrombus formation under flow. *Cell,* 94**,** 657-66.

SAVAGE, B., SALDIVAR, E. & RUGGERI, Z. M. 1996. Initiation of platelet adhesion by arrest onto fibrinogen or translocation on von Willebrand factor. *Cell,* 84**,** 289-97.

SCHAFER, A. I., COOPER, B., O'HARA, D. & HANDIN, R. I. 1979. Identification of platelet receptors for prostaglandin I2 and D2. *J Biol Chem,* 254**,** 2914-7.

SCHIEVELLA, A. R., REGIER, M. K., SMITH, W. L. & LIN, L. L. 1995. Calcium-mediated translocation of cytosolic phospholipase A2 to the nuclear envelope and endoplasmic reticulum. *The Journal of biological chemistry,* 270**,** 30749-54.

SCHILLACE, R. V., MILLER, C. L. & CARR, D. W. 2011. AKAPs in lipid rafts are required for optimal antigen presentation by dendritic cells. *Immunol Cell Biol,* 89**,** 650-8.

SCHOENWAELDER, S. M. & BURRIDGE, K. 1999. Bidirectional signaling between the cytoskeleton and integrins. *Curr Opin Cell Biol,* 11**,** 274-86.

SCHULTESS, J., DANIELEWSKI, O. & SMOLENSKI, A. P. 2005. Rap1GAP2 is a new GTPase-activating protein of Rap1 expressed in human platelets. *Blood,* 105**,** 3185-92.

SCHWARZ, U. R., WALTER, U. & EIGENTHALER, M. 2001. Taming platelets with cyclic nucleotides. *Biochem Pharmacol,* 62**,** 1153-61.

SCHWEDE, F., CHRISTENSEN, A., LIAUW, S., HIPPE, T., KOPPERUD, R., JASTORFF, B. & DOSKELAND, S. O. 2000. 8-Substituted cAMP analogues reveal marked differences in adaptability, hydrogen bonding, and charge accommodation between homologous binding sites (AI/AII and BI/BII) in cAMP kinase I and II. *Biochemistry,* 39**,** 8803-12.

SCOTT, J. D. 1991. Cyclic nucleotide-dependent protein kinases. *Pharmacology & therapeutics,* 50**,** 123-45.

SEAMON, K. B., PADGETT, W. & DALY, J. W. 1981. Forskolin: unique diterpene activator of adenylate cyclase in membranes and in intact cells. *Proc Natl Acad Sci U S A,* 78**,** 3363-7.

SHATTIL, S. J. & BRASS, L. F. 1987. Induction of the fibrinogen receptor on human platelets by intracellular mediators. *J Biol Chem,* 262**,** 992-1000.

SHATTIL, S. J. & NEWMAN, P. J. 2004. Integrins: dynamic scaffolds for adhesion and signaling in platelets. *Blood,* 104**,** 1606-15.

SHIUE, L., GREEN, J., GREEN, O. M., KARAS, J. L., MORGENSTERN, J. P., RAM, M. K., TAYLOR, M. K., ZOLLER, M. J., ZYDOWSKY, L. D., BOLEN, J. B. & ET AL. 1995. Interaction of p72syk with the gamma and beta subunits of the high-affinity receptor for immunoglobulin E, Fc epsilon RI. *Mol Cell Biol,* 15**,** 272-81.

SHRIMPTON, C. N., BORTHAKUR, G., LARRUCEA, S., CRUZ, M. A., DONG, J. F. & LOPEZ, J. A. 2002. Localization of the adhesion receptor glycoprotein Ib-IX-V

complex to lipid rafts is required for platelet adhesion and activation. *J Exp Med,* 196**,** 1057-66.

SIESS, W., WINEGAR, D. A. & LAPETINA, E. G. 1990. Rap1-B is phosphorylated by protein kinase A in intact human platelets. *Biochem Biophys Res Commun,* 170**,** 944-50.

SIM, D. S., MERRILL-SKOLOFF, G., FURIE, B. C., FURIE, B. & FLAUMENHAFT, R. 2004. Initial accumulation of platelets during arterial thrombus formation in vivo is inhibited by elevation of basal cAMP levels. *Blood,* 103**,** 2127-34.

SIMONS, K. & TOOMRE, D. 2000. Lipid rafts and signal transduction. *Nat Rev Mol Cell Biol,* 1**,** 31-9.

SKALHEGG, B. S. & TASKEN, K. 2000. Specificity in the cAMP/PKA signaling pathway. Differential expression,regulation, and subcellular localization of subunits of PKA. *Front Biosci,* 5**,** D678-93.

SMITH, F. D., LANGEBERG, L. K. & SCOTT, J. D. 2006. The where's and when's of kinase anchoring. *Trends Biochem Sci,* 31**,** 316-23.

SMOLENSKI, A. 2011. Novel roles of cAMP/cGMP dependent signaling in platelets. *J Thromb Haemost*.

SMYTH, E. M., LI, W. H. & FITZGERALD, G. A. 1998. Phosphorylation of the prostacyclin receptor during homologous desensitization. A critical role for protein kinase c. *The Journal of biological chemistry,* 273**,** 23258-66.

SMYTH, E. M., NESTOR, P. V. & FITZGERALD, G. A. 1996. Agonist-dependent phosphorylation of an epitope-tagged human prostacyclin receptor. *The Journal of biological chemistry,* 271**,** 33698-704.

STANGHERLIN, A., GESELLCHEN, F., ZOCCARATO, A., TERRIN, A., FIELDS, L. A., BERRERA, M., SURDO, N. C., CRAIG, M. A., SMITH, G., HAMILTON, G. & ZACCOLO, M. 2011. cGMP signals modulate cAMP levels in a compartment-specific manner to regulate catecholamine-dependent signaling in cardiac myocytes. *Circ Res,* 108**,** 929-39.

STANGHERLIN, A. & ZACCOLO, M. 2012. Phosphodiesterases and subcellular compartmentalized cAMP signaling in the cardiovascular system. *Am J Physiol Heart Circ Physiol,* 302**,** H379-90.

STEINBERG, S. F. & BRUNTON, L. L. 2001. Compartmentation of G protein-coupled signaling pathways in cardiac myocytes. *Annu Rev Pharmacol Toxicol,* 41**,** 751-73.

STROOP, S. D. & BEAVO, J. A. 1991. Structure and function studies of the cGMP-stimulated phosphodiesterase. *J Biol Chem,* 266**,** 23802-9.

SUH, T. T., HOLMBACK, K., JENSEN, N. J., DAUGHERTY, C. C., SMALL, K., SIMON, D. I., POTTER, S. & DEGEN, J. L. 1995. Resolution of spontaneous bleeding events but failure of pregnancy in fibrinogen-deficient mice. *Genes Dev,* 9**,** 2020-33.

SUNAHARA, R. K., BEUVE, A., TESMER, J. J., SPRANG, S. R., GARBERS, D. L. & GILMAN, A. G. 1998. Exchange of substrate and inhibitor specificities between adenylyl and guanylyl cyclases. *J Biol Chem,* 273**,** 16332-8.

SUPATTAPONE, S., DANOFF, S. K., THEIBERT, A., JOSEPH, S. K., STEINER, J. & SNYDER, S. H. 1988. Cyclic AMP-dependent phosphorylation of a brain inositol trisphosphate receptor decreases its release of calcium. *Proc Natl Acad Sci U S A,* 85**,** 8747-50.

SUTHERLAND, E. W. & RALL, T. W. 1958. Fractionation and characterization of a cyclic adenine ribonucleotide formed by tissue particles. *J Biol Chem,* 232**,** 1077-91.

SZCZEKLIK, A., GRYGLEWSKI, R. J., NIZANKOWSKI, R., SKAWINSKI, S., GLUSZKO, P. & KORBUT, R. 1980. Prostacyclin therapy in peripheral arterial disease. *Thrombosis research,* 19**,** 191-9.

TAKAGI, J., PETRE, B. M., WALZ, T. & SPRINGER, T. A. 2002. Global conformational rearrangements in integrin extracellular domains in outside-in and inside-out signaling. *Cell,* 110**,** 599-11.

TASKEN, K. & AANDAHL, E. M. 2004. Localized effects of cAMP mediated by distinct routes of protein kinase A. *Physiol Rev,* 84**,** 137-67.

TASKEN, K. & RUPPELT, A. 2006. Negative regulation of T-cell receptor activation by the cAMP-PKA-Csk signalling pathway in T-cell lipid rafts. *Front Biosci,* 11**,** 2929-39.

TATESON, J. E., MONCADA, S. & VANE, J. R. 1977. Effects of prostacyclin (PGX) on cyclic AMP concentrations in human platelets. *Prostaglandins,* 13**,** 389-97.

TAYLOR, S. S., KIM, C., CHENG, C. Y., BROWN, S. H., WU, J. & KANNAN, N. 2008. Signaling through cAMP and cAMP-dependent protein kinase: diverse strategies for drug design. *Biochim Biophys Acta,* 1784**,** 16-26.

TAYLOR, S. S., KIM, C., VIGIL, D., HASTE, N. M., YANG, J., WU, J. & ANAND, G. S. 2005. Dynamics of signaling by PKA. *Biochim Biophys Acta,* 1754**,** 25-37.

TESMER, J. J., SUNAHARA, R. K., GILMAN, A. G. & SPRANG, S. R. 1997. Crystal structure of the catalytic domains of adenylyl cyclase in a complex with Gsalpha.GTPgammaS. *Science,* 278**,** 1907-16.

THOMAS, D. W., MANNON, R. B., MANNON, P. J., LATOUR, A., OLIVER, J. A., HOFFMAN, M., SMITHIES, O., KOLLER, B. H. & COFFMAN, T. M. 1998. Coagulation defects and altered hemodynamic responses in mice lacking receptors for thromboxane A2. *J Clin Invest,* 102**,** 1994-2001.

TOMLINSON, M. G., CALAMINUS, S. D., BERLANGA, O., AUGER, J. M., BORI-SANZ, T., MEYAARD, L. & WATSON, S. P. 2007. Collagen promotes sustained glycoprotein VI signaling in platelets and cell lines. *J Thromb Haemost,* 5**,** 2274-83.

TOPPER, J. N., CAI, J., STAVRAKIS, G., ANDERSON, K. R., WOOLF, E. A., SAMPSON, B. A., SCHOEN, F. J., FALB, D. & GIMBRONE, M. A., JR. 1998. Human prostaglandin transporter gene (hPGT) is regulated by fluid mechanical stimuli in cultured endothelial cells and expressed in vascular endothelium in vivo. *Circulation,* 98**,** 2396-403.

TOWBIN, H., STAEHELIN, T. & GORDON, J. 1979. Electrophoretic transfer of proteins from polyacrylamide gels to nitrocellulose sheets: procedure and some applications. *Proc Natl Acad Sci U S A,* 76**,** 4350-4.

TSAI, A. L., HSU, M. J., PATSCH, W. & WU, K. K. 1991. Regulation of PGI2 activity by serum proteins: serum albumin but not high density lipoprotein is the PGI2 binding and stabilizing protein in human blood. *Biochim Biophys Acta,* 1115**,** 131-40.

TSIKAS, D., IKIC, M., TEWES, K. S., RAIDA, M. & FROLICH, J. C. 1999. Inhibition of platelet aggregation by S-nitroso-cysteine via cGMP-independent

mechanisms: evidence of inhibition of thromboxane A2 synthesis in human blood platelets. *FEBS Lett,* 442**,** 162-6.

VAN GEET, C., IZZI, B., LABARQUE, V. & FRESON, K. 2009. Human platelet pathology related to defects in the G-protein signaling cascade. *J Thromb Haemost,* 7 Suppl 1**,** 282-6.

VAN LIER, M., VERHOEF, S., CAUWENBERGHS, S., HEEMSKERK, J. W., AKKERMAN, J. W. & HEIJNEN, H. F. 2008. Role of membrane cholesterol in platelet calcium signalling in response to VWF and collagen under stasis and flow. *Thromb Haemost,* 99**,** 1068-78.

VANE, J. & CORIN, R. E. 2003. Prostacyclin: a vascular mediator. *European journal of vascular and endovascular surgery : the official journal of the European Society for Vascular Surgery,* 26**,** 571-8.

VANE, J. R., BAKHLE, Y. S. & BOTTING, R. M. 1998. Cyclooxygenases 1 and 2. *Annu Rev Pharmacol Toxicol,* 38**,** 97-120.

VARGA-SZABO, D., BRAUN, A. & NIESWANDT, B. 2009. Calcium signaling in platelets. *J Thromb Haemost,* 7**,** 1057-66.

VARGA-SZABO, D., PLEINES, I. & NIESWANDT, B. 2008. Cell adhesion mechanisms in platelets. *Arterioscler Thromb Vasc Biol,* 28**,** 403-12.

VARGAS, J. R., RADOMSKI, M. & MONCADA, S. 1982. The use of prostacyclin in the separation from plasma and washing of human platelets. *Prostaglandins,* 23**,** 929-45.

VERKLEIJ, M. W., MORTON, L. F., KNIGHT, C. G., DE GROOT, P. G., BARNES, M. J. & SIXMA, J. J. 1998. Simple collagen-like peptides support platelet adhesion under static but not under flow conditions: interaction via alpha2 beta1 and von Willebrand factor with specific sequences in native collagen is a requirement to resist shear forces. *Blood,* 91**,** 3808-16.

VIAL, C., FUNG, C. Y., GOODALL, A. H., MAHAUT-SMITH, M. P. & EVANS, R. J. 2006. Differential sensitivity of human platelet P2X1 and P2Y1 receptors to disruption of lipid rafts. *Biochem Biophys Res Commun,* 343**,** 415-9.

VIGIL, D., BLUMENTHAL, D. K., HELLER, W. T., BROWN, S., CANAVES, J. M., TAYLOR, S. S. & TREWHELLA, J. 2004. Conformational differences among solution structures of the type Ialpha, IIalpha and IIbeta protein kinase A regulatory subunit homodimers: role of the linker regions. *Journal of molecular biology,* 337**,** 1183-94.

WALDMANN, R., NIEBERDING, M. & WALTER, U. 1987. Vasodilator-stimulated protein phosphorylation in platelets is mediated by cAMP- and cGMP-dependent protein kinases. *Eur J Biochem,* 167**,** 441-8.

WALTER, U. & GAMBARYAN, S. 2009. cGMP and cGMP-dependent protein kinase in platelets and blood cells. *Handb Exp Pharmacol***,** 533-48.

WANG, D., WANG, M., CHENG, Y. & FITZGERALD, G. A. 2005. Cardiovascular hazard and non-steroidal anti-inflammatory drugs. *Current opinion in pharmacology,* 5**,** 204-10.

WARDELL, M. R., REYNOLDS, C. C., BERNDT, M. C., WALLACE, R. W. & FOX, J. E. 1989. Platelet glycoprotein Ib beta is phosphorylated on serine 166 by cyclic AMP-dependent protein kinase. *J Biol Chem,* 264**,** 15656-61.

WATSON, S., BERLANGA, O., BEST, D. & FRAMPTON, J. 2000. Update on collagen receptor interactions in platelets: is the two-state model still valid? *Platelets,* 11**,** 252-8.

WATSON, S. P., AUGER, J. M., MCCARTY, O. J. T. & PEARCE, A. C. 2005. GPVI and integrin Î±IIbÎ²3 signaling in platelets. *Journal of Thrombosis and Haemostasis,* 3**,** 1752-1762.

WATSON, S. P., HERBERT, J. M. & POLLITT, A. Y. 2010. GPVI and CLEC-2 in hemostasis and vascular integrity. *J Thromb Haemost,* 8**,** 1456-67.

WEISHAAR, R. E., BURROWS, S. D., KOBYLARZ, D. C., QUADE, M. M. & EVANS, D. B. 1986. Multiple molecular forms of cyclic nucleotide phosphodiesterase in cardiac and smooth muscle and in platelets. Isolation, characterization, and effects of various reference phosphodiesterase inhibitors and cardiotonic agents. *Biochem Pharmacol,* 35**,** 787-800.

WEKSLER, B. B., MARCUS, A. J. & JAFFE, E. A. 1977. Synthesis of prostaglandin I2 (prostacyclin) by cultured human and bovine endothelial cells. *Proc Natl Acad Sci U S A,* 74**,** 3922-6.

WENTWORTH, J. K., PULA, G. & POOLE, A. W. 2006. Vasodilator-stimulated phosphoprotein (VASP) is phosphorylated on Ser157 by protein kinase C-dependent and -independent mechanisms in thrombin-stimulated human platelets. *Biochem J,* 393**,** 555-64.

WHITE, J. G. 1987. An overview of platelet structural physiology. *Scanning Microsc,* 1**,** 1677-700.

WHITE, J. G. 1988. Platelet membrane ultrastructure and its changes during platelet activation. *Prog Clin Biol Res,* 283**,** 1-32.

WHITE, J. G. 2007. Platelet Structure. *In:* MICHELSON, A. D. (ed.) *Platelets Second Edition.*

WHITTLE, B. J. & MONCADA, S. 1985. Platelet actions of stable carbocyclic analogues of prostacyclin. *Circulation,* 72**,** 1219-25.

WILLIAMS, R. H. & NOLLERT, M. U. 2004. Platelet-derived NO slows thrombus growth on a collagen type III surface. *Thromb J,* 2**,** 11.

WILLIS, A. L., SMITH, D. L., VIGO, C. & KLUGE, A. F. 1986. Effects of prostacyclin and orally active stable mimetic agent RS-93427-007 on basic mechanisms of atherogenesis. *Lancet,* 2**,** 682-3.

WILLOUGHBY, D. & COOPER, D. M. 2007. Organization and Ca2+ regulation of adenylyl cyclases in cAMP microdomains. *Physiol Rev,* 87**,** 965-1010.

YAN, S. Z., HUANG, Z. H., RAO, V. D., HURLEY, J. H. & TANG, W. J. 1997. Three discrete regions of mammalian adenylyl cyclase form a site for Gsalpha activation. *The Journal of biological chemistry,* 272**,** 18849-54.

ZACCOLO, M. 2011. Spatial control of cAMP signalling in health and disease. *Current opinion in pharmacology,* 11**,** 649-55.

ZACCOLO, M. & POZZAN, T. 2002. Discrete microdomains with high concentration of cAMP in stimulated rat neonatal cardiac myocytes. *Science,* 295**,** 1711-5.

ZAHEDI, R. P., LEWANDROWSKI, U., WIESNER, J., WORTELKAMP, S., MOEBIUS, J., SCHUTZ, C., WALTER, U., GAMBARYAN, S. & SICKMANN, A. 2008. Phosphoproteome of resting human platelets. *J Proteome Res,* 7**,** 526-34.

ZHANG, G., LIU, Y., RUOHO, A. E. & HURLEY, J. H. 1997. Structure of the adenylyl cyclase catalytic core. *Nature,* 386**,** 247-53.

ZHANG, P., SMITH-NGUYEN, E. V., KESHWANI, M. M., DEAL, M. S., KORNEV, A. P. & TAYLOR, S. S. 2012. Structure and allostery of the PKA RIIbeta tetrameric holoenzyme. *Science,* 335**,** 712-6.

ZHANG, W. & COLMAN, R. W. 2007. Thrombin regulates intracellular cyclic AMP concentration in human platelets through phosphorylation/activation of phosphodiesterase 3A. *Blood,* 110**,** 1475-82.

ZHANG, W., SLOAN-LANCASTER, J., KITCHEN, J., TRIBLE, R. P. & SAMELSON, L. E. 1998a. LAT: the ZAP-70 tyrosine kinase substrate that links T cell receptor to cellular activation. *Cell,* 92**,** 83-92.

ZHANG, W., TRIBLE, R. P. & SAMELSON, L. E. 1998b. LAT palmitoylation: its essential role in membrane microdomain targeting and tyrosine phosphorylation during T cell activation. *Immunity,* 9**,** 239-46.

ZHANG, Z., AUSTIN, S. C. & SMYTH, E. M. 2001. Glycosylation of the human prostacyclin receptor: role in ligand binding and signal transduction. *Mol Pharmacol,* 60**,** 480-7.

ZIDOVETZKI, R. & LEVITAN, I. 2007. Use of cyclodextrins to manipulate plasma membrane cholesterol content: evidence, misconceptions and control strategies. *Biochim Biophys Acta,* 1768**,** 1311-24.

ZIMMERMANN, G., ZHOU, D. & TAUSSIG, R. 1998. Mutations uncover a role for two magnesium ions in the catalytic mechanism of adenylyl cyclase. *J Biol Chem,* 273**,** 19650-5.

Appendices

Appendix I

Buffer composition and equipment used for methods described in this study.

Isolation and preparation of human blood platelets by pH method

Buffers

- Acid-citrate dextrose (ACD): Glucose (113mM), Tri-sodium-citrate (29mM), NaCl (72mM), citric acid (3mM), pH 6.4
- Tyrode's buffer: NaCl (137mM), KCl (2.7mM), $MgCl_2$ (1mM), Glucose (5.6mM), NaH_2PO_4 (3.3mM), HEPES (20mM), pH 7.4
- 0.3M citric acid, pH 6.5
- Wash buffer: Citric acid (0.036M), EDTA (0.1M), Glucose (0.005M), KCl (0.005M), NaCl (0.09M)

Equipment

- Butterfly-21 Venisystems ..... Abbot Laboratories
- Falcon Tubes (15 and 50ml) ..... Falcon, Becton Dickinson
- Centrifuge……. Universal 320, Hettich

Determination of platelet concentration

Buffers

- Ammonium oxalate: Ammonium oxalate (1% w/v) in dH_2O

Equipment

- Improved Neubauer cell counter

  Inverted light microscope

Measurement of platelet aggregation

Buffers

- Tyrode's buffer: NaCl (137mM), KCl (2.7mM), $MgCl_2$ (1mM), Glucose (5.6mM), NaH_2PO_4 (3.3mM), HEPES (20mM), pH 7.4

Equipment

- Aggregation Module-Dual Channel..... Payton
- Aggregation cuvettes

Measurement of protein concentration

Assay kit

- DC protein assay kit..... Bio-Rad

Buffers

- Tyrode's buffer: NaCl (137mM), KCl (2.7mM), $MgCl_2$ (1mM), Glucose (5.6mM), NaH_2PO_4 (3.3mM), HEPES (20mM), pH 7.4
- lysis buffer (2x): Tris base (50mM), SDS (4% w/v), pH:6.8

Equipment

- Costar 96-well cell culture plate ..... Corning Incorporated
- Multiplate reader with 750nm filter

Measurement of cAMP concentration

Assay kit

- Enzymeimmuno Assay (EIA)..... Cayman Chemical Company.

Buffers

- EIA assay buffer: supplied by manufacturer and constituted with 90mL ultrapure water.
- cAMP Standard: supplied by manufacturer and constituted by addition of mL of constituted EIA buffer which gives a cAMP solution of 7500 pmol/mL.
- cAMP antibody: reconstituted by addition of 6mL of constituted EIA buffer.
- cAMP AChE tracer: constituted by addition of 6mL of constituted EIA buffer.
- Wash buffer: supplied by manufacturer and prepared by 400x dilution with ultrapure water and contains 0.05% (v/v) Tween-20.
- Elman's reagent: supplied by manufacturer and reconstituted by addition of 20mL of ultrapure water.
- cAMP Lysis buffer: 0.1M HcL
- Acetic anhydride
- KOH: 4M
- Microplate: 96 wells plate coated with mouse anti-rabbit IgG.

Equipment

- 1.5mL eppendorfs
- Glass aggregation cuvettes
- Microplate shaker
- Plate reader with 450nm filter

Isolation of platelet lipid rafts

Buffers

- Lysis buffer: Tris-base (20mM), NaCl (100mM), sodium pyrophosphate (60mM), sodium glycerophosphate (20mM), sodium azide (0.02% w/v), triton X-100 (0.065%), Protease Inhibitors cocktail, pH 8.0.

Equipment

- Thin wall tubes, ultraclear (ultracentrifuge tubes)….Beckman Coulter
- Ultracentrifuge…….Beckman Coulter

Analysis of platelet proteins

Sodium dodecyl sulphate -polyacrylamide gel electrophoresis (SDS-PAGE)

Sample preparation.

Buffers

- Laemmli sample buffer (2x): Tris base (50mM), SDS (4% w/v), Glycerol (20% v/v), bromophenol blue (trace), 2-mercaptoethanol (5% v/v) pH 6.8

Equipment

- Aggregation Module-Dual Channel..... Payton
- Aggregation cuvettes

Method

Buffers

- Buffer 1: Tris base (0.5M), SDS (0.4% w/v), pH 8.8
- Buffer 2: Tris base (1.5M), SDS (0.4% w/v), pH 6.8
- Ammonium persulphate (APS): APS (10% w/v) in dH_2O
- Running buffer: Tris base (25mM), Glycine (192mM), SDS (0.1% w/v)

Equipment

- Miniprotean 3 Cell..... Bio-Rad (UK)
- Gradient mixer ..... Bio-Rad (UK)
- Peristaltic pump
- Butterfly-21 Venisystems..... Abbot Laboratories
- Plastic tubing
- Biotin-protein ladder..... Cell Signaling Tech. (UK)

Immunochemical investigation of platelet proteins

Immunoprecipitation.

Buffers

- lysis buffer containing phosphatase and protease inhibitors: NaCl (150mM), Tris base (10mM), EDTA (1mM), EGTA (10mM), Igepal (1% v/v), PMSF (1mM), Aprotinin (5ug/ml), Leupeptin (5ug/ml), Pepstatin (0.5ug/ml), Na_3VO_4 (2.5 mM), pH 7.4
- Tris buffered saline containing Tween (0.1%): NaCl (100mM), Tris base (10mM), Tween 20 (0.1% v/v), pH 7.4
- Laemmli sample buffer (2x): Tris base (50mM), SDS (4% w/v), Glycerol (20% v/v), bromophenol blue (trace), 2-mercaptoethanol (5% v/v) pH 6.8

Equipment

- Rotator
- Microcentrifuge

Immunoblotting

Buffers

- Transfer buffer: Tris base (25mM), Glycine (192mM), methanol (20% v/v)
- Tris buffered saline containing Tween (0.1%): NaCl (100mM), Tris base (10mM), Tween 20 (0.1% v/v), pH 7.4
- Restore^{TM} Plus Wester Blot Stripping buffer: from Thermo Scientific
- ECL 1: Luminol (250mM), p-coumaric acid (90mM), Tris base (1M, pH 8.5), in 100ml using dH_20
- ECL 2: Tris base (1M, pH 8.5), 64µl of H_2O_2 (30%), in 100ml using dH_2O
- ECL 1 and ECL 2 were mixed fresh at a ratio of 1:1 before use.
- Developing solution: diluted 1:5 prior to use in dH_2O
- Fixing solution: diluted 1:5 prior to use in dH_2O

Equipment

- Hybond-P PVDF membrane ..... Amersham Pharmacia Biotech
- Mini Trans-Blot elctroph. transfer cell..... Bio-Rad (UK)
- Exposure cassette ..... Sigma Ltd (Poole, UK)
- Hyper film..... Amersham Biosciences (UK)
- Microplate shaker

Composition of polyacrylamide gels

Gradient gel compositions for 1.5mm casting plates.

Compound	3% stacking gel	10% resolving gel	18% resolving gel
dH_2O	4.87ml	1.418ml	0,708ml
Acrylamide 30%	0.75ml	1.182ml	1.961ml
Buffer I	---	0.886ml	0.886ml
Buffer II	1.87ml	---	---
APS 10%	75µl	18µl	18µl
TEMED	10µl	2µl	2µl

10% gel compositions for 1.5mm casting plates.

Compound	3% stacking gel	10% resolving gel
dH_2O	4.87ml	6.4ml
Acrylamide 30%	0.75ml	5.3ml
Buffer I	---	4ml
APS 10%	75µl	75µl
TEMED	10µl	5.3µl

7.5% gel compositions for 1.5mm casting plates.

Compound	3% stacking gel	7.5% resolving gel
dH_2O	4.87ml	9.9ml
Acrylamide 30%	0.75ml	6.25ml
Buffer I	---	6ml
50% (v/v) glycerol/water	---	1.6ml
APS 10%	75µl	90µl
TEMED	10µl	8µl

Appendix II

Main platelet agonists and inhibitors used in this study

Compound	Supplier	Solubility	Concentration	Preincubation
Indomethacin	Sigma Aldrich	Ethanol	10µM	20min
Apyrase	Sigma Aldrich	dH_2O	1U/ml	20min
EGTA	Sigma Aldrich	dH_2O	1mM	20min
Forsklin	Sigma Aldrich	Ethanol	10µM	5min
H89	Cayman Chemicals	DMSO	5µM	20min
PGE_1	Sigma Aldrich	Ethanol	1µM	1min
RIAD	A kind gift from Prof. K Tasken	dH_2O	1µM	60min
Super AKAP	A kind gift from Prof. K Tasken	dH_2O	1µM	6min
StHt-31	Promega	xxxx	5µM	60min
PGI_2	Cayman Chemicals	Ethanol	50nM	1min
KT 5720	Sigma Aldrich	Methanol	10µM	20min
MβCD	Sigma Aldrich	dH_2O	2.5mM	30min
Collagen	Nycomed (Alexix Sheild UK)	xxxx	5µg/ml	Not required
Thrombin	Sigma Aldrich	dH_2O	0.05U/ml	Not required
vWF (Fanhdi)	Grifols	dH_2O	20µg/ml	Not required
Ristocetin	Sigma Aldrich	dH_2O	0.75mg/ml	Not required

Antibody list

Antibody	Company
Goat Anti-rabbit IgG-HRP	**Amersham**
Anti-Biotin-protein ladder	**Cell signalling**
Anti-$G\alpha_s$ (Rabbit polyclonal)	**Santa Cruz**
Anti-integrin β3 (Rabbit polyclonal)	**Santa Cruz**
Anti-LAT (Rabbit monoclonal)	**Upstate**
Anti-mouse IgG-HRP	**Amersham**
Anti-PKA [RI] (Mouse monoclonal)	**BD Transduction Labs**
Anti-PKA [RIIβ] (Mouse monoclonal)	**BD Transduction Labs**
Anti-phospho-PKA substrate (RRXS/T) (Rabbit monoclonal)	**Cell Signaling**
Anti-phosphotyrosoine clone 4G10 (Mouse monoclonal)	**Upstate**
Anti-phospho-VASP (Ser 157) (Rabbit polyclonal)	**Cell Signalling**
A cyclase V/VI (Rabbit polyclonal)	**Santa Cruz**
Anti-β-Tubulin (Mouse monoclonal)	**Millipore**
Anti-phospho-RhoA (Ser 188) (Rabbit polyclonal)	**Santa Cruz**
Anti-Phospho-GPIbβ (Ser 166) (Rabbit monoclonal)	**A kind gift from Prof. Xiaoping Du**
Anti-Phospho-GSK3α (Ser 21) (Rabbit monoclonal)	**Cell signalling**
Anti-IP receptor (Mouse monoclonal)	**A kind gift from Dr. Lucie Clapp**